Treatment of metastatic colorectal cancer: A role for curcumin?

Thesis submitted for the degree of

Doctor of Philosophy at the University of Leicester

By

Mark I. James, BSc. MSc.

Department of Cancer Studies and Molecular Medicine

University of Leicester

September 2014

Abstract

Treatment of metastatic colorectal cancer: A role for Curcumin?

Mark I. James

Colorectal cancer remains the third largest cause of mortality from cancer related death, with approximately 90% of these deaths attributed to metastatic spread of the disease. There is a need to improve chemotherapy, with the dietary polyphenol curcumin, derived from turmeric, representing a potential candidate as it possess very few side effects and it has shown efficacy in mouse models. Recent advances in our understanding of tumour development have highlighted the existence of tumour initiating cells (TIC), which possess clonogenic potential, are essential for tumour growth, and represent an important therapeutic target. This study sought to determine whether curcumin in combination with oxaliplatin+5-Fluorouracil (OX+5-FU) represented a better combination for targeting TICs, using a variety of models consisting of cells derived directly from colorectal liver metastasis (CRLM). $ALDH^{High}$ activity, CD133 and CD26 were all found to mark a spheroid forming population, a method that tests for clonogenicity and selects for TICs. Curcumin significantly reduced the number of spheroids compared to DMSO, and enhanced efficacy of OX+5-FU. The only marker to decrease after treatment was $ALDH^{High}$ activity, which was also positively associated with spheroid growth. CD26 expressing cells were identified as a possible chemo-resistant population, however, this population remained unaffected by curcumin. *Ex vivo* analysis using explant cultures demonstrated that curcumin could significantly decrease ki67 and increase cleaved capase-3 expression, notably enhancing the effects of oxaliplatin in a proportion of patients. A pilot study was undertaken using non-obese diabetic/severe combined immunodeficient (NOD-SCID) mice to reflect a clinical regimen, and assess *in vivo* whether curcumin could enhance efficacy of OX+5-FU, but the results advocate the use of higher doses as little effect was seen. Overall this body of work contributes to knowledge on propagating CRLM TICs, their expression of known TIC markers, and response to curcumin.

Acknowledgements

First and primarily I would like to thank my supervisors, without whom I would not have been able to study for this PhD. I am very grateful for all of their help throughout my PhD, and will never forget it. I would also like to thank the pathology department, specifically Janine, Angie and Linda for cutting hundreds of slides for me. I would also like to thank Debbie and Trudi for help looking after my mice and teaching me how to handle/perform specific procedures I was required to learn. Hong also carried out some of the early mouse work, and injected the cells for my animal study, for which I am very grateful. I also owe Ankur a big thank you for all of his help with the animal work, collecting samples and teaching me certain techniques early on during my masters, and I also enjoyed our numerous cancer stem cell/general life discussions. I am very grateful to Jenny and Samita for collecting samples for me, and Jenny for helping out with the FACS which has been a massive help. Additionally, I am also very grateful for Gill's help with the immunohistochemistry, without whom I would have never finished it all, and Jen's help taking images. I would also like to thank Leonie for her help with HPLC, Peter for his help analysing my slides, and Maria for her help with statistics. Finally, but by no means least, I would like to thank Aida for all of her help, love and support.

List of Contents

List of Figures

Chapter 1

Chapter 2

Chapter 3

Chapter 4

Chapter 5

Appendix

List of Tables

Chapter 1

Chapter 2

Chapter 3

Chapter 4

Chapter 5

Appendix

List of Abbreviations

5,10-MTHF	5,10-methylenetetrahydrofolate
5-FU	5-Fluorouracil
15-PGDH	15-hydroxyprostaglandin dehydrogenase
ABCG2	ATP-binding cassette sub-family G member 2
ACF	Aberrant crypt foci
ADA	Adenosine deaminase
AFP	α-fetoprotein
AKT	Also called protein kinase B (PKB)
ALDH	Aldehyde dehydrogenase
AML	Acute myeloid leukaemia
APC	Adenomatous polyposis coli
ASCL2	Achaete-scute complex-like 2
Bcl-2	B-cell Lymphoma 2
BMP	Bone morphogenic protein
CAF	Cancer associated fibroblast
CamKII	Calmodulin-dependent protein kinase II
CBP	p300/CREB-Binding Protein
CDK	Cyclin dependant kinase
CIMP	CpG island methylator phenotype
CIN	Chromosome instability
CK1	Casein kinase 1
CN	Calcineurin
COX	Cyclooxygenase
CRC	Colorectal cancer
CRLM	Colorectal liver metastasis
CRUK	Cancer research UK

DAAM1	Dishevelled-associated activator of morphogenesis 1
DAG	1,2 diacylglycerol
DCC	Deleted in colorectal cancer
DEAB	Diethylaminobenzaldehyde
DKK	Dikkopf
DMEM	Dulbecco’s modified eagle media
DMSO	Dimethyl sulfoxide
DSH	Dishevelled
ECM	Extra cellular matrix
EGF	Epithelial growth factor
EGFR	Epithelial growth factor receptor
EMT	Epithelial-mesenchymal transition
EpB2	EPH receptor B2
EpCAM	Epithelial-cell adhesion molecule
ER	Endoplasmic reticulum
ERCC1	Excision repair cross-complementation group 1
ERK	Extracellular signal-regulated kinase
FAK	Focal adhesion kinase
FAP	Familial adenomatous polyposis
FCS	Foetal calf serum
FdUMP	Fluorodeoxyuridine monophosphate
FdUPT	Fluorodeoxyuridine triphosphate
FGF	Fibroblast growth factor
FUTP	Fluorouridine triphosphate
FZD	Frizzled
GATA6	GATA binding factor 6
GLI1	Glioma-associated oncogene homolog 1
GSC	Goosecoid

GSK-3β	Glycogen synthase kinase 3 beta
HCG	Human Chorionic Gonadotropin
HGF	Hepatocyte growth factor
HIF1α	Hypoxia inducible factor 1 alpha
HNF-3β/FoxA2	Hepatocyte nuclear factor 3 beta/Forkhead box A2
HNPCC	Hereditary non-polyposis colorectal cancer
IHC	Immunohistochemistry
IP3	1,4,5-triphosphate
JNK	Jun N-terminal protein kinase
KRAS	Kirsten ras
LC3	Light chain 3
LGR5	Leucine-rich repeat-containing G-protein coupled receptor 5
LRP5/6	Low-density lipoprotein receptor–related protein 5/6
LV	Leucovorin
M1G	3-(2-deoxy-beta-di-erythro-pentafuranosyl)-pyr[1,2-alpha]-purin-10(3H)one
MAML-1	Mastermind like-1
MAPK	Mitogen-activated protein kinase
mCRC	Metastatic colorectal cancer
MET	Mesenchymal to epithelial transition
MMP	Matrix metalloproteinase
MMR	Mismatch repair
MSI	Microsatellite instability
MTHF	methyltetrahydrofolate
MTHFR	Methylenetetrahydrofolate reductase
NAT-2	N-acetyltransferase
NEMO	NF-kappa B Essential Modulator
NFAT	Nuclear factor of activated T-cells

NICD	Notch intracellular domain
NLK	Nemo-like kinase
NOD-SCID	Non-obese diabetic/severe combined immunodeficiency
NSAIDs	Non-steroidal anti-inflammatory drugs
Otx2	Orthodenticle Homeobox 2
OX	Oxaliplatin
PDX-1/IPF1	Pancreatic and duodenal homeobox 1/ Insulin promoter factor 1
PGE2	Prostaglandin E2
PKC3	Protein kinase 3
PLC	Phospholipase C
PTK7	Protein tyrosine kinase 7
PUMA	p53 up-regulated modulator of apoptosis
RAC1	Ras-related c3 botulinum toxin substrate
RhoA	Ras homolog family member A
ROCK	Rho-associated coiled-coil containing protein kinase
ROS	Reactive oxygen species
SHH	Sonic hedgehog
SMAD	Mothers against decapentaplegic
SOX17	Sex determining region Y-box 17
SOX2	SRY-box containing gene 2
TCF/LEF	T-cell factor/lymphoid enhancer factor
TGF-β	Transforming growth factor-beta
TIC	Tumour initiating cell
TNFα	Tumour necrosis factor alpha
TNM	Tumour node metastases
TP63/TP73L	Tumour Protein P63/ Tumour Protein P73-Like
TS	Thymidylate synthase
UK	United Kingdom

u-PA	Urokinase plasminogen activator
VEGF	Vascular endothelial growth factor
XRCC1	X-ray repair cross-complementing protein

Chapter 1: Introduction

Colorectal cancer

1.1 Statistics and incidence

Cancer is the second biggest cause of disease related mortality in the United Kingdom (UK)[1], with the lifetime probability of being diagnosed with an invasive cancer at 45% for men and 38% for women[2]. Cancer incidence increases with age and on average 51% of patients will survive (defined by over ten year survival) (http://www.cancerresearchuk.org/cancer-info/cancerstats/survival/common-cancers/). Cancer can be categorised based on the site from which it originates. According to the latest statistics published by Cancer Research UK (CRUK) the top 5 most common malignancies are breast, lung, prostate, colorectal and malignant melanoma (Cancer Research UK, UK Cancer Incidence (2010) by Country Summary, April 2013). Colorectal cancer (CRC) is the third most common malignancy arising in both men and women. This is also true for mortality (Figure 1.1). The overall survival rates for colorectal cancer in the UK appear similar to the US, with an average 5-year survival of 54.8%, and 10-year survival of 50.5% in the UK. The results for rectal cancer are also similar with a 5 and 10 year average survival of 56.1% and 49.7% (http://www.cancerresearchuk.org/cancer-info/cancerstats/types/bowel/survival/bowel-cancer-survival-statistics). These statistics are dramatically altered depending on whether the patient presents with localised disease (5-year survival of 90.1%) or metastatic disease (5 year survival of 11.7%).

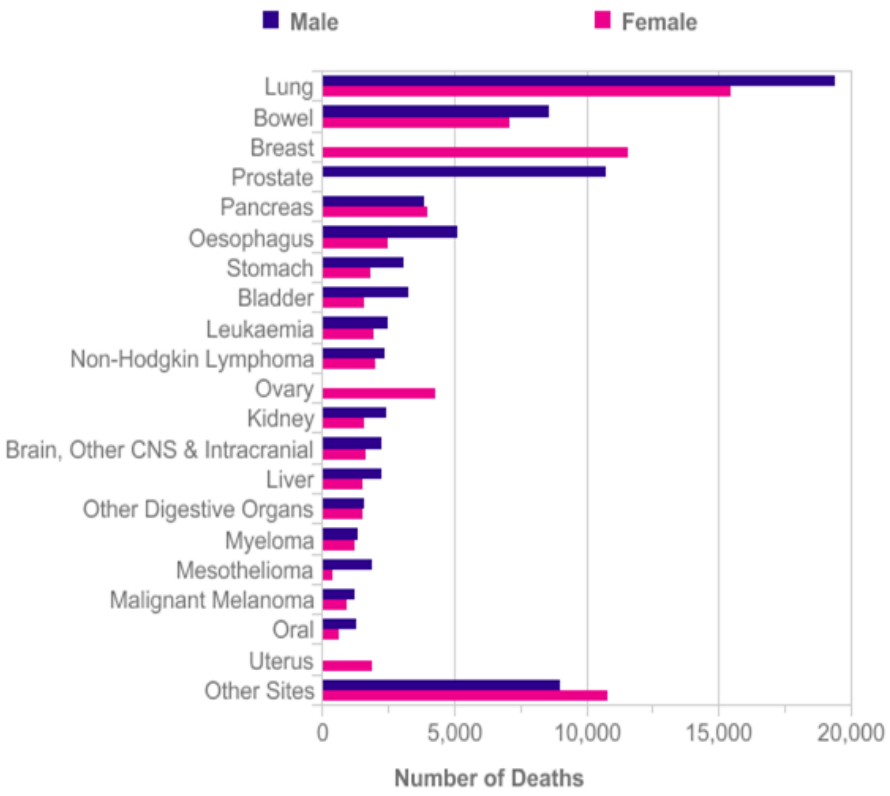

Figure 1.1 The 20 most common causes of cancer deaths in males and females
Taken from the Cancer Research UK website, (www.cancerresearchuk.org/cancerinfo/cancerstats/mortality/cancerdeaths/#Twenty). Bowel cancer refers to colorectal cancer.

Metastasis is the spread of the primary cancer to lymph nodes, and different organs of the body, and is the cause of 90% of cancer related deaths due to associated organ failure[3]. Surgery provides the best treatment option, with 38% and 26% of patients surviving 5 and 10 years respectively, following metastasectomy[4]. In comparison, patients who are unable to undergo surgical resection, will receive palliative chemotherapy with a 5 year survival probability of only 1.1%[5]. For CRC, surgery alone can improve survival, but only approximately 10-30% of patients present with an operable metastasis[4,6]. Pre-operative chemotherapy (conversion therapy) can sometimes be used to down-size tumours and render them operable, which can be achieved in approximately 12-30% of patients[6-8]. Patients that have to first undergo conversion therapy have been shown to have a similar survival compared to patients

who do not require this step[6,8]. These statistics highlight the negative impact metastasis has upon the chance of long term survival, and how current treatment for metastatic colorectal cancer (mCRC) is inadequate.

1.2 **Epidemiology**

The most common forms of cancer vary from country to country. More economically developed countries have a higher cancer burden than less economically developed countries, with non-communicable or environmentally-driven cancers such as lung, breast, prostate and cancers of the colorectum dominating[9]. This can be attributed to differences in exposures through diverse cultures, diet and the environment. More economically developed countries tend to have a diet that is higher in pro-carcinogens such as fat, salt and sugar, and when combined with a more sedentary lifestyle, this contributes to an increased cancer incidence[10]. However, the progress made in screening and early detection with improved treatment strategies have resulted in a decrease in incidence in some countries such as America, but other countries with fewer resources such as Mexico and Brazil in Central and South America, and Romania in Eastern Europe continue to show an increase in incidence[9,10]. Less developed countries typically have a higher rate of cancers such as stomach, liver, oral cavity, pharynx, and cervix, with a quarter of these thought to be attributable to chronic infection[11]. Tobacco related cancers are a cause of a large proportion of cancers in developed countries, but these are also increasing substantially in less developed countries (World Health Organisation world cancer report 2008)[11,12].

The highest cancer incidence is seen in countries such as America (40/100,000), and in European countries[13]. The countries that show the biggest increase in incidence are those transitioning from a low-income economy to a high-income economy, such as Japan. Countries with the lowest cancer incidence include African (5/100,000) and some Asian countries; however some of this is likely to be partly due to

underreporting[13]. Immigration studies have shown that a person's chance of developing cancer is altered to mirror the cancer incidence in the country of migration, demonstrating that the environment is a major factor in promoting different cancer types[14].

1.3 **Risk factors**

Risk factors for developing cancer can be divided in two broad groups, genetic pre-disposition and environmental causes which promote the appearance of sporadic cancer. For CRC, various risk factors have been identified, however approximately 35% of cases are attributed to genetics, demonstrated through twin studies[15]. Different hereditary genetic changes have been found to cause different polyposis syndromes. Hereditary non-polyposis colorectal cancer (HNPCC) and familial adenomatous polyposis (FAP) represent the two major genetic causes of CRC. The remaining are made up of rare inherited causes, including Peutz-Jeghers Syndrome and Juvenile Polyposis Coli[16]. The vast majority of CRC cases arise spontaneously, and many risk factors have been identified. Diets consisting of high saturated fat and/or animal fat have been correlated with an increased CRC incidence in human studies[17-19]. When these diets are replicated in an experimental setting and are given to rats, a promotional effect on CRC development is seen, confirming the human studies[20]. Red meat that has been well-done, resulting in formation of compounds such as heterocyclic amines has also been associated with an increased risk of colorectal cancer[21-23]. Some dietary factors have been associated with a reduced risk of adenoma formation and CRC such as a high intake of dietary fibre, eating fish, consumption of vegetables (particularly green vegetables) and fruit[19,24,25].

In addition, various lifestyle factors have been linked to increased adenoma occurrence such as: smoking, especially in individuals with the rapid N-acetyltransferase 2 (NAT2) genotype[26], lack of physical activity[27], obesity[28], and high alcohol intake, particularly when combined with low folate intake[29,30].

1.4 **The colon physiology, microenvironment and stem cells**

The colon (or large intestine) consists of the cecum, ascending colon, transverse colon, descending colon, sigmoid colon and rectum (Figure 1.2). The primary function of the colon is to absorb water and vitamins and to store/expel waste. The surface of the colon is formed from an epithelial sheet of cells with millions of invaginations (crypts) which form the principal functional unit of the colonic tract. Each crypt is formed from a hierarchy of approximately 2000 cells, starting with approximately 4-6 adult stem cells residing at the base of crypts[31,32]. The stem cells can indefinitely self-renew, preventing the stem cell population from depleting, but can also produce transit amplifying cells, which occupy the bottom half of the crypt. Transit amplifying cells divide rapidly before terminally differentiating into either mucus secreting goblet cells, absorptive enterocyte cells or hormone secreting endocrine cells, and are found in the top half of the crypt (Figure 1.2)[33].

Surrounding the crypts is a syncytium of myofibroblasts (pericryptal myofibroblasts), which are believed to be responsible for the control of stem cell division and differentiation through paracrine signalling[34,35]. They are distinct from the normal fibroblast, which form the majority of the lamina propria, as they display smooth muscle characteristics and as such can be distinguished by their expression of α-smooth muscle actin, and have been shown to be connected to the muscularis mucosae[36].

Figure 1.

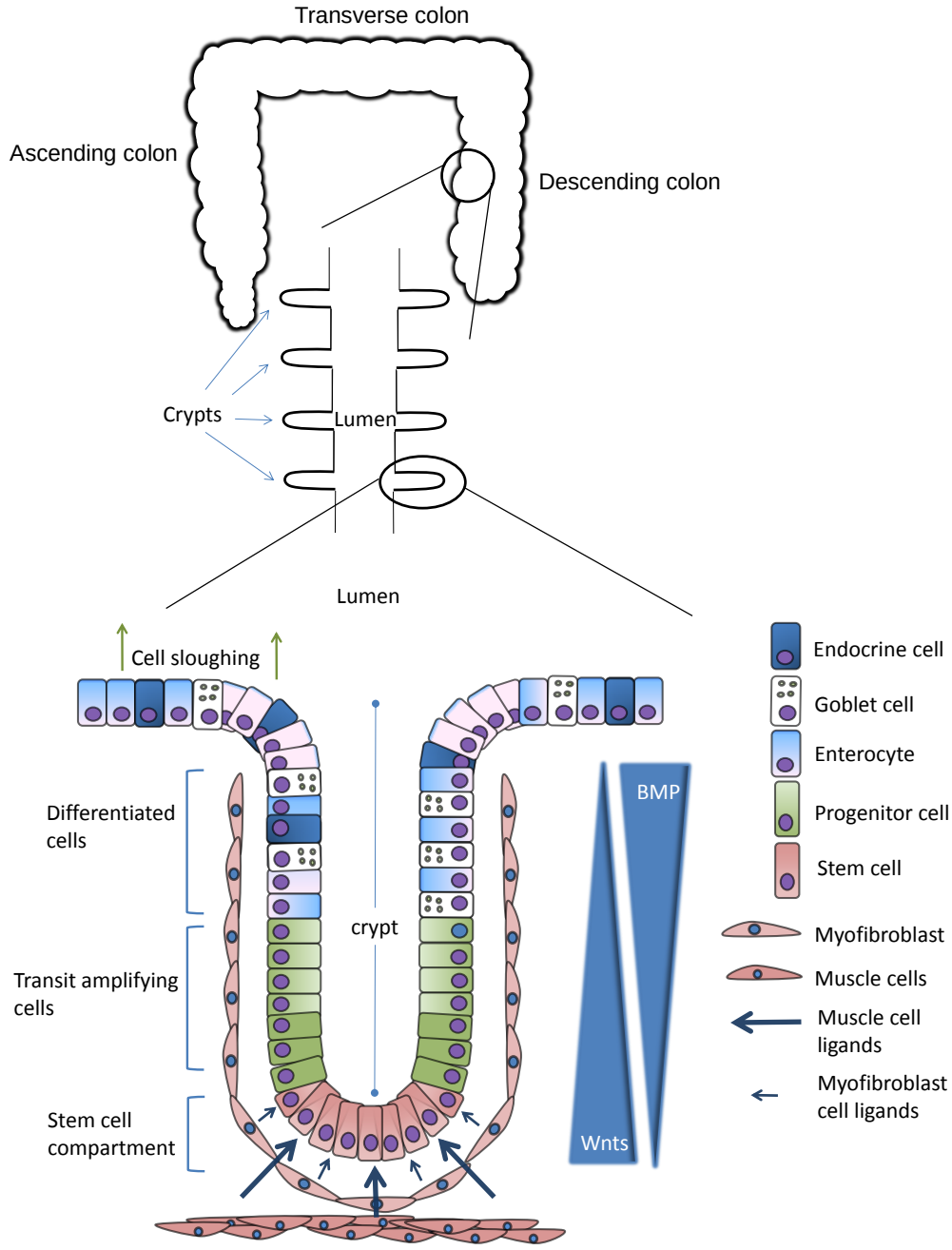

Figure 1.2 Structure and regulation of a normal colon crypt

Under normal physiological conditions crypts appear as an invagination of the colonic epithelial lining. The stem cells reside at the crypt base (red cells) where they are regulated through paracrine interaction between local myofibroblasts and muscle cells. As the cells divide and are pushed upwards out of the base of the crypt, known as the stem cell niche, they begin to differentiate. The first progenitors are called transit amplifying cells and they rapidly divide before terminally differentiating into one of three main lineages: endocrine cells, goblet cells or enterocyte cells. This differentiation process is controlled through a decreasing gradient of Wnt signalling towards the lumen, and increasing bone morphogenic protein (BMP) signalling. Secretion of

cytokines such as Noggin and WNT3a within the stem cell niche control stem cell division.

The Wnt signalling pathway has been demonstrated to be integral in the development and regulation of the colonic epithelium[37]. The Wnt signalling pathway is active throughout the crypt, but is differentially regulated. In the crypt base, signalling via the canonical Wnt pathway can be observed, whilst a range of different Wnt ligands are expressed at the top of the crypt, promoting non-canonical Wnt signalling and signalling independent from β-catenin[35,38]. The colonic stem cells are dependent on canonical Wnt signalling, which is mediated through nuclear β-catenin bound with T-cell factor 4/lymphoid enhancer factor (TCF4/LEF)[39,40], and controls crypt homeostasis and stem cell maintenance[41,42]. The Wnt signal cascade is initiated through binding of Wnt ligands to the membrane complex composed of frizzled (FZD) and low-density lipoprotein receptor–related protein 5/6 (LRP5/6)[43-45]. In the absence of Wnt ligands a complex called the 'the destruction complex' is formed by adenomatous polyposis coli (APC), casein kinase 1 (CK1), glycogen synthase kinase 3 beta (GSK3-β), and Axin2. The destruction complex binds to β-catenin and sequentially phosphorylates it, targeting β-catenin for degradation[46]. Upon stimulation of the receptor by FZD the destruction complex dissociates and releases β-catenin, subsequently making it available to translocate to the nucleus. This set of events results in a complex transcriptional program that directs cell fate, cell proliferation, and stem cell maintenance. The importance of regulating this pathway is highlighted by the observation that almost all CRCs contain a mutation within the Wnt signalling pathway, resulting in enhanced signalling and mice with a knock-out of the TCF4 gene, the main TCF involved in colon Wnt signalling, suffer from loss of crypts due to absent Wnt signalling[47]. A summary of canonical and non-canonical Wnt signalling is presented in figure 1.3

Normal stem cells are characterised by nuclear β-catenin, and as a result express Wnt target genes, some of which include cell surface markers that have been

used for isolating stem cells, such as leucine-rich repeat containing G protein-coupled receptor 5 (*LGR5*)[48,49] and *CD44*[42], crypt spatial organisers including EPH receptor B2 (*EphB2*) and B3 receptors (*EphB3*)[50], and other genes such as achaete-scute complex-like 2 (*ASCL2),* which codes for a transcription factor involved in regulating intestinal stem cell fate[51].

The reason for such an active Wnt signalling pathway within the stem cells is partially attributed to the pericryptal myofibroblasts surrounding the crypt base, and smooth muscle cells which create a stem cell niche providing Wnt ligands, in additional to Wnt ligands produced by the stem cells themselves (Wnts 3, 6 and 9B)[35,38]. The Wnt protein family is defined through sequence homology, all sharing sequences for secretion and glycosylation, with a characteristic distribution of 22 cysteine residues believed to occur for proper protein folding. Wnt proteins are also lipid modified through palmitoylation, which is necessary for canonical Wnt signlling[52].

Certain members of the frizzled family are also expressed more at the base of crypts (FZD2, FZD3, FZD7, and FZDB), and inhibitors of the non-canonical Wnt signalling pathway such as dikkopf (DKK) are believed to help promote the correct Wnt signalling required by stem cells[35,38]. The necessity for Wnt signalling in stem cells is demonstrated in mice that have Wnt signalling inhibited by Dickkopf-1 and show a complete loss of crypts in adult animals[37].

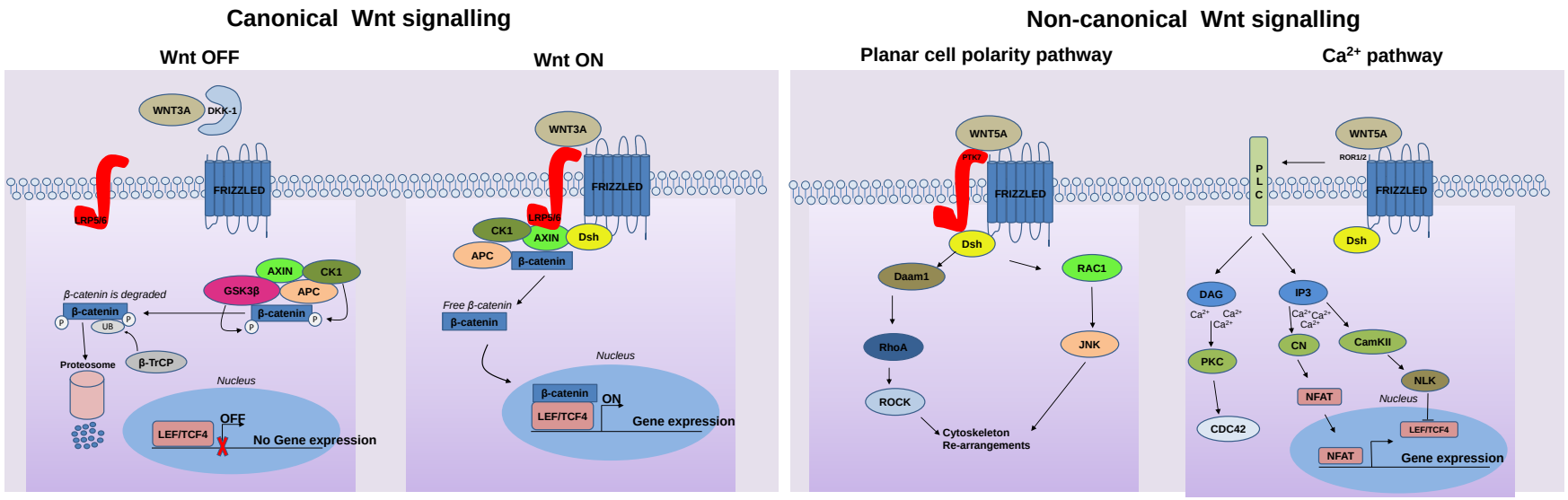

Figure 1.3 An overview of the canonical and non-canonical Wnt pathway

In the Wnt canonical pathway (left panel), when no Wnts are present, the 'destruction' complex formed by CK1, APC, GSK3-β and Axin phosphorylates β-catenin targeting it for ubiqutination and destruction, preventing gene expression of β-catenin target genes. Upon binding of a Wnts such as WNT3a to LRP5/6 and FZD, the 'destruction' complex dissociates and β-catenin is released and can translocate to the nucleus and form a complex with LEF/TCF4, initiating transcription of target genes. There are at least two well described non-canonical pathways (right panel). In the planar cell polarity pathway, which controls actin re-arrangements and cell polarisation, a different frizzled co-receptor is used such as protein tyrosine kinase 7 (PTK7). Binding of Wnts such as Wnt5a to PTK7 and FZD results in recruitment of dishevelled (DSH). Dishevelled-associated activator of morphogenesis 1 (DAAM1) binds to DSH by its carboxyl terminus, and Ras homolog family member A (RhoA) by its amino terminus, leading to the formation of DSH-RhoA complex. RhoA then activates rho-ssociated coiled-coil containing protein kinase (ROCK) which mediates cytoskeleton changes. DSH also binds to ras-related c3 botulinum toxin substrate 1 (RAC1) which activates c-Jun N-terminal protein kinases (JNK). A non-canonical pathway involving Ca^{2+} also exists to further control cell polarity. In the Ca^{2+} pathway, when non-canonical Wnts such as Wnt5a bind to FZD receptors, phospholipase C (PLC) is activated and inositol 1,4,5-triphosphate (IP3) and 1,2 diacylglycerol (DAG) are produced. These then interact with the calcium channels present on the membrane of endoplasmic reticulum (ER) resulting in release of Ca^{2+}. When Ca^{2+} is released it causes the activation of the Ca^{2+} sensitive protein kinase C proteins (PKC), calcineurin (CN) and calmodulin-dependent protein kinase II (CaMKII). CaMKII has also been shown to activate nemo-like kinase (NLK) which can antagonize β-catenin/TCF signalling, whereas CN can activate the transcription factor nuclear factor of activated T-cells (NFAT) to promote ventral cell fates in the Xenopus embryo. P=phosphorylation, and UB=ubiquitination by beta-transducin repeat containing protein (β-TrCP).

Wnt signalling has been described as essential, but not sufficient for maintenance of stem cell activation and self-renewal, implicating the need for signalling via other pathways in order to create the correct environment for normal stem cell maintenance. Bone morphogenic protein (BMP) ligands activate the transforming growth factor beta (TGF-β) signalling pathway by binding to TGF-β receptors, which then transduce the signal to the nucleus through phosphorylated mothers against decapentaplegic (SMAD) proteins 3 and 4, resulting in inhibition of proliferation through transcriptional repression of *c-Myc* and up-regulation of *p15Ink4b*, a cyclin-dependant kinase inhibitor[53-55]. Within the stem cell niche the TGF-β pathway is inhibited through BMP antagonists such as gremlin 1, 2 and chordin-like 1 which are secreted by pericryptal myofibroblasts located at the base of crypts[35]. This creates the correct stem cell niche required for the balance between self-renewal and differentiation. Additionally, GATA binding protein 6 (GATA6) has been found to prevent excessive BMP signalling in colon adenomas in the stem cell compartment though transcriptional repression. This highlights the need to prevent excessive BMP signalling for stem cell self-renewal, as excessive BMP signalling causes a reduction in adenoma growth and stem cell self-renewal[56]. Concordant with the view that BMP signalling inhibits stem cell self-renewal, preventing them from over proliferating, Bmpr1a (a BMP receptor) deficient mice, or mice overexpressing the BMP inhibitor Noggin, show an increase in stem cells, hyper-proliferation and increased crypt fission[57,58].

The Wnt signalling pathway is important for correct colon development and homeostasis, but it is by no means the sole regulator, albeit the best characterised, as interplay is required with additional pathways. The Notch pathway for example, has also been shown to be integral in maintaining the stem cell pool, and differentiation. Notch signalling is mediated by a ‘signalling cell’ that provides Notch ligands such as delta or jagged. These ligands bind to the Notch receptor and stimulate the formation of a γ-secretase protein complex which cleaves the transmembrane domain of the Notch receptor. This releases the Notch intracellular domain (NICD) which translocates to the

nucleus and binds to one of three transcriptional regulators: suppressor of hairless (also known as CSL, LAG-1 CBF-1 or RBP-J), mastermind like-1 (MAML-1) and p300/CREB-Binding Protein (CBP). This ultimately results in transcription of target genes such as *Hes-1* and Hes-related protein gene families, with *Hes-1* being the most abundant.[59]. Notch activity has been shown to decide the lineage fate between enterocyte and secretory cell types, with decreased Notch signalling favouring the goblet cell fate[60-62]. However, Notch activity in the presence of canonical Wnt signalling helps dictate proliferation speed and stem cell homeostasis, with Notch signalling required for maintenance of crypt progenitor cells[60-62]. The importance of Notch signalling was highlighted in a study using an inducible gut-specific Notch-mutant mouse model. The results showed that Notch signalling was involved in regulation of the cell cycle in crypt progenitor cells by transcriptionally repressing two cyclin-dependant kinases (CDKs) inhibitors allowing proliferation[63].

1.5 **CRC Tumourigenesis**

CRC has been the focus of a large amount of research which led to the development of the adenoma-carcinoma sequence by Vogelstein and Fearon (Figure 1.4)[64]. This model explains tumourigenesis as a series of mutational events in key genes including tumour suppressors and oncogenes over a long period of time. The first stage in colon tumourigenesis through the adenoma-carcinoma sequence is considered to be mutation of the tumour suppressor gene adenomatous polyposis coli (*APC*).

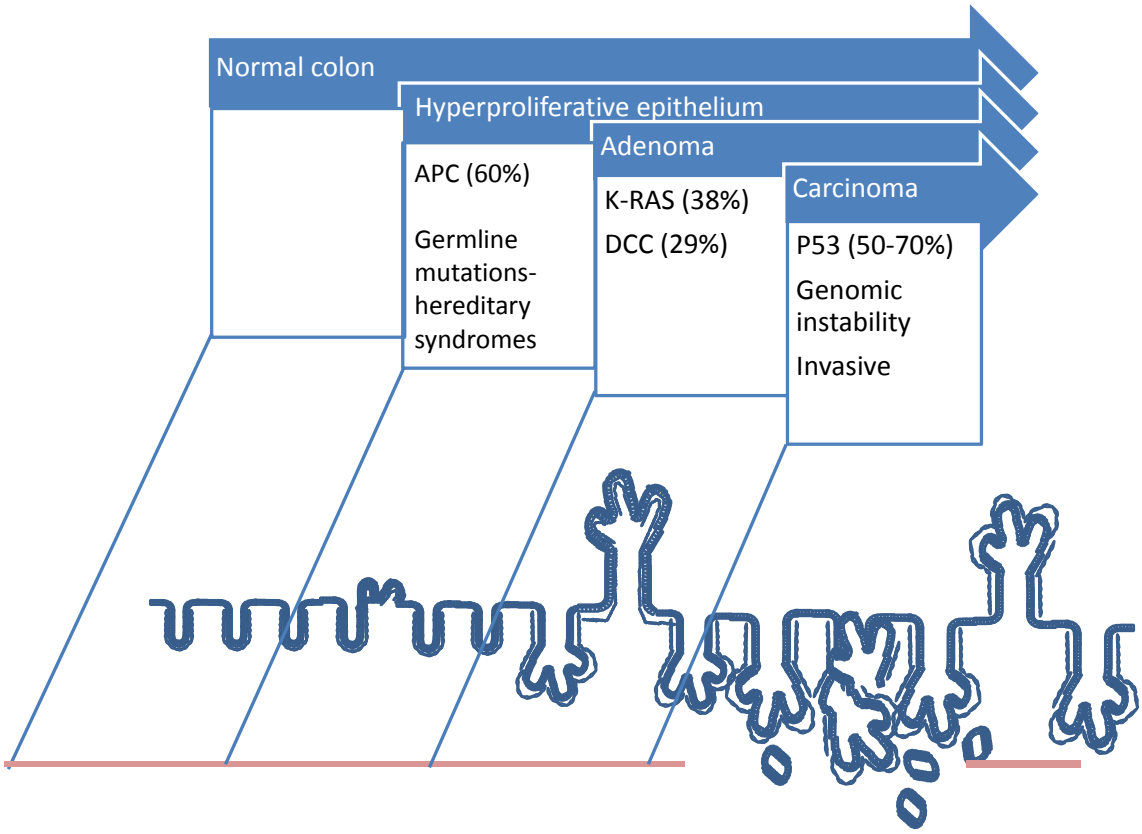

Figure 1.4 The adenoma-carcinoma sequence
A model of CRC progression was formulated in 1990 by Vogelstein and Fearon. In the first step when only normal colon can be histologically observed, germline mutations may be present that predispose an individual to further transformation. These mutations can also be acquired through sporadic mutation, but in both instances more mutations are required to continue tumourigenesis. Mutations in genes that promote proliferation such as *K-RAS* are required, but for carcinoma development mutations in genes that regulate the cell cycle are key, to prevent oncogene induced senescence. The mutation of *p53* is considered to mark the transition from an adenoma to a carcinoma. Once a carcinoma has developed, the tumour begins to invade the surrounding stroma and genomic instability promotes further mutations. Percentages represent the proportion of CRC cases with mutations[65-67]. Note the disordered crypt fibroblasts, representing cancer associated fibroblasts.

APC has multiple physiological functions, one of which is regulation of the canonical Wnt signalling pathway by controlling the amount of available β-catenin in the cytoplasm through formation of the destruction complex described earlier[68]. When *APC* is mutated the amount of free β-catenin increases; this is able to enter the nucleus[69] and ultimately activate the Wnt pathway, which includes proto-oncogenes *c-Myc* and *CCND1*[70,71], resulting in increased proliferation. A genetic predisposition to

form hundreds to thousands of benign polyps protruding from the lumen of the colon, as seen in patients with FAP, is due to a heterogeneous germline mutation in the *APC* gene[72-74]. After a second mutation in the remaining wild-type allele these polyps can become malignant, demonstrating the important role APC plays in CRC development. For this reason, APC has often been referred to as a gatekeeper gene to CRC. Wnt signalling has been shown to be up-regulated once APC is mutated; however, high Wnt signalling alone does not fully demarcate the tumourigenic population. Additional activating mutations in genes coding for proteins involved in the mitogen-activated protein kinase (MAPK) signalling pathway, such as mutations in kirsten ras (*KRAS*), and mutations in deleted in colorectal cancer (*DCC*) and *p53* are also required for tumourigenesis. This results in increased Wnt signalling and loss of cell cycle regulation[64,75,76].

Since the initial description of the adenoma-carcinoma sequence, alternative pathways involving different mutations have been found to cause colorectal cancer. For example, an alternative pathway believed to start with a *BRAF* mutation has been proposed with *BRAF* found mutated in 10% of patients[77].

Within colorectal tumours that contain mutations in *APC*, heterogeneity is observed in the number of cells with nuclear β-catenin, and therefore activation of the Wnt signalling pathway. It would be expected that all cells that possess a mutant APC should have an active Wnt signalling however this is not observed. Wnt signalling heterogeneity may be due to production of microenvironmental signalling factors such as c-met, the ligand for hepatocyte growth factor (HGF)[78]. Consistent with *APC* mutated cells still being responsive to Wnt ligands, a recent study into colorectal cell lines demonstrated that despite APC mutation cells still respond to WNT3A, a stimulator of the canonical pathway[79].

The adenoma-carcinoma sequence is an over-simplification, describing commonly mutated genes as a function of tumour stage. Since its development, several tumour types have been discovered in which tumour evolution is driven through

different mechanisms. For example, tumours can be grouped based on whether they display chromosome instability (CIN), microsatellite instability (MSI), or a CpG Island methylator phenotype (CIMP). To complicate matters, tumours can display characteristics of more than one group. Tumour development in FAP patients, and in approximately 85% of sporadic cancers, show chromosome instability, with loss of chromosome regions such as 5q and 18q, which contain the genes for *APC* and *DCC* respectively[64].

Mutation or hypermethylation of either of the mismatch repair (MMR) genes MSH2 and MLH1, results in widespread mutations in microsatellite regions of DNA (mono, di, or trinucleotide repeats) due to a decreased ability to repair mismatch mutations during DNA replication[80-82], producing the MSI phenotype. Humans have 12 genes relating to MMR[83], however in colorectal cancer the main genes reported to be involved with colorectal cancer include MLH1, MSH2, MSH6, PMS2. Microsatellite repeats can be found in the promoter of various genes, for example the TGF-β II gene contains microsatellite repeats within its promoter where mutations directly affect transcription[84]. Mutation and epigenetic transcriptional silencing of MMR genes represent two different pathways to produce the MSI phenotype. Mutations in MMR genes are found in familial cases where a germline mutation results in heterozygosity leading to a genetic predisposition to CRC, known as HNPCC or Lynch Syndrome[80]. These tumours also generally display chromosome instability[85].

Sporadic CRCs that display MSI and defective MMR are generally a result of hypermethylation of the MLH1 gene, and occur as part of a global change in methylation known as the CpG island methylator phenotype (CIMP) pathway[86]. With the advancement of new technologies such as RNA sequencing and microarray analysis, further analyses of subsets within patient cohorts has been facilitated, leading to the discovery of additional tumour sub-groups which respond differently to therapy. For example, recent investigations have identified a new subtype of CRC relating to sessile-serrated adenomas, which is largely microsatellite stable and has an

unfavourable prognosis and resistance to epithelial growth factor receptor (EGFR) therapy[87]. Another group has identified three tumour classifications based upon the levels of CIMP, which are characterised by the presence or absence of *BRAF*, *KRAS* or *p53* mutations[88]. Stratifying tumours by their underlying phenotypic and genotypic characterisation may help determine which patients should receive certain therapies, as *BRAF* and *KRAS* mutations are involved in insensitivity to monoclonal antibodies targeting EGFR, and MMR status has also been linked to response to 5-FU (as discussed later).

1.5.1 Tumour initiating cells (TICs)

Several models have been proposed to explain tumour development. The most predominant, the “stochastic model”, explains tumour development and progression through random mutational events, giving the mutated cell a growth or survival advantage. This creates the heterogeneity observed in cancers, with additional mutations driving cancer progression[89]. This model hypothesises that all cells are equally capable of causing cancer. However, the contrary has been demonstrated in a variety of cancers, which has led to an alternative hypothesis of cancer development, termed the hierarchical model (Figure 1.5).

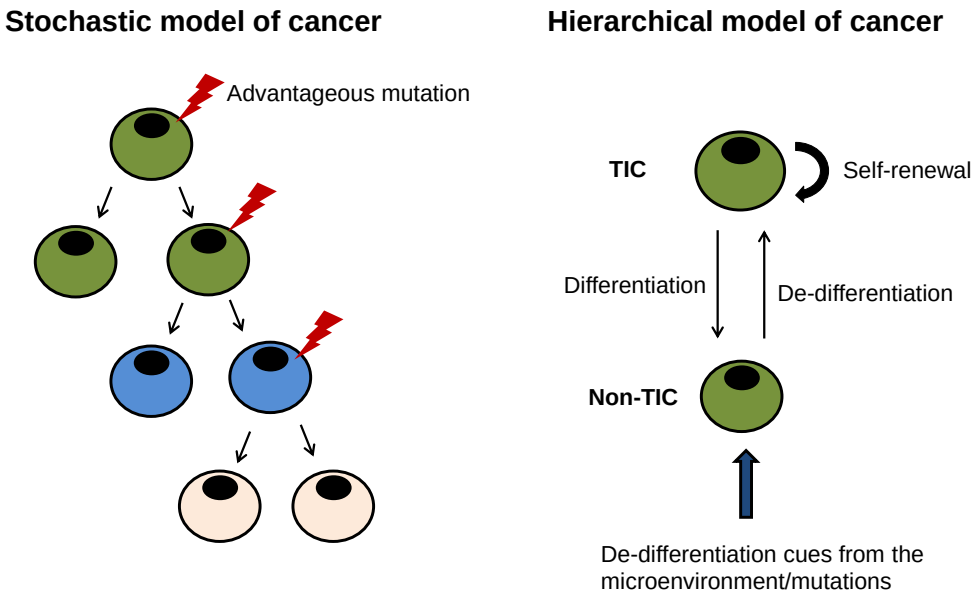

Figure 1.5 Stochastic theory compared with the hierarchical theory of cancer
The stochastic model of cancer believes that all cells have the equal ability to propagate cancer, and that tumour evolution is through random mutational events that give a cell an advantage (red symbol represents a mutational event). The cells with an advantage can then clonally expand, with further mutations causing further progression. In the stochastic model each cell colour represents a new generation of cells. The hierarchical model of cancer believes that a subset of cells, with similar properties to normal adult multipotent stem cells, propagate the tumour and are therefore referred to as tumour initiating cells (TICs). The TICs are believed to produce the tumour heterogeneity through differentiating in a similar manner observed during normal intestinal maintenance. De-differentiation is thought to possibly occur in tumours, with more differentiated tumour cells forming more TICs. A reconciliation between the two hypotheses is the agreed need for mutations to drive tumour progression.

The hierarchical model, more commonly known as the cancer stem cell theory, believes small subsets of cells with stem-like properties propagate cancer. These sub-sets are commonly referred to as cancer stem or stem-like cells as their properties reflect those seen in adult stem cells, in that they are; un-differentiated, slow dividing, self-renewing, and have the ability to produce differentiated progeny. However, in this thesis they shall be referred to as tumour initiating cells (TICs) due to their definition requiring them to be able to form tumours. This model is in contrast to the stochastic model, as in the hierarchical model only the stem-like cells have the ability to propagate cancer. The origin of these stem-like cells is yet to be definitively established. A likely

candidate is transformation of a normal adult stem cell due to their inherent longevity, which provides a sufficient time frame for the cells to be exposed to carcinogens, and acquire the necessary mutations for initiating and promoting tumourigenesis. In accordance with this, evidence from studying FAP patients has shown that tumour overpopulation begins from mutated cells at the base of crypts[90,91]. However, there is contrary evidence from patients with small sporadic adenomas demonstrating dysplastic differentiated cells found growing at the top of crypts, which were the first observable pre-neoplastic legions. However, the authors commented that they could not rule out the possibility of a mutated stem cell migrating upwards before proliferating[92], and so reconciling the notion that oncogenesis starts in the adult stem cell. Additional evidence that lends support to this hypothesis has been presented with the recent finding that mice harbouring the correct mutations in the villus compartment, but not in the crypt compartment, still form tumours. However it was noted that cells still re-formed stem cell populations and it was therefore concluded that cells were required to de-differentiate before they were capable of forming tumours, demonstrating the need for a stem cell population for initiation of tumourigenesis[93].

The hierarchical model and the concept of TICs was first proposed 150 years ago, but did not receive much interest until 1997 with the discovery of the cell surface markers CD34 and CD38 that could identify a sub-population of acute myeloid leukaemia (AML) cells with increased tumorigenic potential (CD34+CD38-)[94]. This subset of cells could consistently reconstitute the entire cancer heterogeneity in non-obese diabetic-severe combined immunodeficient (NOD-SCID) mice, and be maintained through serial transplantation[94]. TIC markers were also identified in breast cancer in 2003 after research showed a small population of CD44+CD24−/lineage(-) cells could form tumours when transplanted into NOD-SCID mice, and were able to recreate the heterogeneity of the original tumour[95]. This led to the discovery of a variety of markers in solid tumours that could be used to identify cells that fulfil the criteria of a TIC, consisting of the ability to self-renew and the ability to produce the other progeny

within the tumour. These two main traits are generally tested for in specific ways. For example, the ability to self-renewal can be assessed through spheroid formation *in vitro*, and the ability to form tumours which can be serially passaged *in vivo*. TICs are also described to be chemoresistant, a trait which explains tumour recurrence. Based on this set of criteria and using these methodologies, to date putative TIC markers have been identified in many cancers including brain, head and neck, pancreatic, melanoma, hepatic, lung, prostate, ovarian, breast and colorectal cancers[96-105].

The theory has gained substantial support through the use of genetically manipulated mouse models that enable lineage tracing of stem cell fate *in vivo*, avoiding the pitfalls of xenotransplantation. These models have shown that LGR5+ cells are able to generate all of the cells of the normal crypt, and that it is these cells which provide the cell of origin for adenoma formation. This is evidenced by specific deletion of APC in intestinal LGR5+ cells resulting in adenoma formation, which is rarely seen when deleted in LGR5- cells[49,106,107]. Additionally, a mouse model for glioblastoma multiforme has demonstrated that following challenge with the chemotherapy drug temozolomide, the tumour is repopulated by cells genetically marked by nestin-green fluorescent protein expression. Whereas when tumours are treated with systemic ganciclovir, which targets thymidine kinase (also under the control of the Nestin promoter) to cause cell death specifically in nestin positive cells, there was a significant increase in survival[108]. This study supports the view that a stem cell-like population re-populates tumour growth after therapy, and targeting this population results in a significant increase in efficacy of anti-tumour therapy. This provides further evidence that TICs are responsible for therapy relapse and there is a need to target them.

Initially the hierarchal model was believed to be rigid with only the TICs forming the apex from which all the other tumour cells were derived. However, this concept has recently been challenged, in that more differentiated cells may also have the capacity to form TICs under the correct setting, with the microenvironment playing an integral

part in regulating stem cell characteristics. For example, a study investigating intestinal adenoma formation in mice demonstrated that when mouse villus cells have β-catenin stabilised in conjunction with tumour necrosis factor α (TNFα) and microenvironment-induced NF-κB signalling, they form tumours[93]. Additionally, differentiated cells have also been shown to be reprogrammed to a stem-like cell state when localised next to a myofibroblast producing HGF[78]. Similar results have been published alluding to HGF regulating stemness in glioblastoma xenografts and in prostate cancer[109,110]. Furthermore, in breast cancer, *ZEB1* promoter de-methylation, and therefore expression, has been shown to be linked to a TIC phenotype. In this study, TICs marked by high CD44 expression exhibited decreased methylation of the *ZEB1* promoter, thus allowing *ZEB1* expression. In cells marked by $CD44^{Low}$ expression, *ZEB1* was in a bivalent state with both permissive and repressive histone H3 modification, so the gene is repressed but ready for quick activation when stimulated. It was demonstrated that TFG-β, which is found in the breast cancer microenvironment, can cause de-methylation of *ZEB1* and thus promote a TIC phenotype. These findings provide further evidence of the link between micro environmental factors and the stem cell phenotype[111]. Research by the Swanton group has demonstrated significant intratumoural heterogeneity in non–small cell lung cancer and clear cell renal carcinomas through sequencing multiple regions within the same tumour[112-114]. This research has highlighted that within a tumour there are many subclones that contain different mutation spectrums, with heterogeneity between clones observed for 73-75% of driver mutations in clear cell renal carcinomas. This may reconcile both the stochastic theory with the hierarchical theory, as subclones with different mutation spectrums will likely evolve in a stochastic manner driving tumour evolution as previously thought, while the TIC is still required as this represents the population which is likely to receive the mutation and then produce subclones as it fuels tumour growth.

1.5.2 Tumour initiating cell markers

To identify TICs many cell surface proteins have been investigated, as they represent markers which can be readily identified and used for sorting cells whilst retaining cell viability. Additionally, the 'side population' (a population that actively effluxes fluorescent dyes such as Hoechst), which is usually assessed by flow cytometry, has been shown to mark TICs. However, more recently, other intra-cellular markers have been investigated such as activity of the enzyme aldehyde dehydrogenase (ALDH).

Within the context of CRC no single, or set of markers, have been found to completely distinguish the TIC population. The first marker reported for CRC was CD133, a pentaspan-transmembrane glycoprotein (also called Prominin 1) with little known function. In a study by Ricci-Vitiani *et al*., CD133+ cells represented 2.5±1.4% of the primary colorectal cancer population in 16 patient samples, and importantly, CD133- cells lacked the tumour initiating ability that CD133+ cells possessed in NOD-SCID mice[101]. Simultaneously, O'Brien *et al*., also identified the tumour initiating ability of CD133+ cells[96]. Since the initial investigations into CD133, it has been the focus of a large proportion of the research on CRC TICs, and has been investigated in a variety of other cancers including brain, hepatocellular carcinoma and prostate cancer[98,99,115,116]. The use of CD133 as a TIC marker is controversial as in some studies it has identified a large population, which contrasts with the concept that TICs constitute a small subset of the tumour population. Additionally, CD133 negative cells have also since been reported to form tumours in NOD-SCID mice[117,118]. However, a specific epitope of CD133 may mark undifferentiated cells - the AC133 epitope (used throughout this thesis). CD133 is differently glycosylated as cells become differentiated which causes a change in protein conformation altering available epitopes[119]. Nonetheless, the tumorigenic potential of CD133+ cells has been proven in a variety of separate studies, and has also been shown to be a prognostic marker, with higher CD133 expression being associated with a significantly worse clinical outcome[108].

The precise function of CD133 is relatively unknown. Studies have shown that CD133 expression is associated with metastasis and chemo-resistance and is detected in the blood present on circulating cancer cells[120-122]. The embryonic stem cell genes, octamer binding transcription factor 3/4 (*OCT4*) and/or SRY-box containing gene 2 (*SOX2*), have been found to bind to the P1 promoter region of the CD133 gene. Furthermore, expression of SOX2 and OCT4 induce expression of CD133 after they themselves are up-regulated under hypoxic conditions by HIF1α and HIF2α[123]. Additionally, CD133 has also been demonstrated to be involved in autophagy, being located at the plasma memembrane under normal glucose conditions, but under low glucose conditions relocating to the cytoplasm and localising with the autophagy marker microtubule-associated protein light chain 3 (LC3)[124]. Transient reduction in CD133 expression has also been shown to reduce the number of autophagic LC3 puncta, with it's involvement in autophagy promoting cellular survival under nutrient starvation and hypoxia[124,125].

The ability of CD133+ cells to form tumours is enhanced when used in combination with other TIC markers, such as the enzyme activity of aldehyde dehydrogenase[118]. ALDH oxidises intracellular aldehydes, including the oxidation of retinol to retinoic acid, which is involved in haematopoietic stem cell differentiation[126]. ALDH also helps decrease DNA damage by providing protection against alkylating agents such as oxazaphosphorine and cyclophosphamide[127,128]. High ALDH1 activity ($ALDH1^{high}$) has been shown to mark TIC populations for breast cancer, lung cancer and acute myeloid leukaemia[129-132]. In normal colonic crypts ALDH1A1 protein expression is very specific to a small population of cells at the base of crypts, forming a sub-population of CD133+ cells[118]. In mice xenografts, $ALDH^{high}$ cells isolated from human colorectal tumours result in tumour formation in NOD-SCID mice, whereas $ALDH^{Low}$ fail to grow. This tumour forming ability is further increased in populations that are positive for both CD133+ and high ALDH activity[118].

Another TIC marker of interest is the transcription factor nanog, which is important during embryonic development and reprogramming of induced pluripotent stem cells, and has been shown to be associated with cancer progression. One study reported expression of nanog in 80% of colorectal liver metastases, with 75% expressing the nearly identical retrogene nanogp8. By utilising a unique restriction enzyme site on the nanogp8 transcript, RT-PCR analysis revealed 6 out of 8 samples expressed both forms of nanog, while only 2 expressed either nanog or nanogp8. In this study, spheroids highly expressed nanog, and when nanog expression was knocked down, spherogenicity was reduced, concurrent with reductions in the side-population and tumour forming ability[133]. Another group reported nanog expression to be higher in human CRC CD133+ cells compared to CD133- cells, with the degree of expression directly correlated with the occurrence of liver metastasis[134]. Similar findings in prostate cancer have been demonstrated, with nanog being highly expressed in CD44+ cells and occurring preferentially as the nanogp8 form[135]. Nanog provides a link between stem cell traits and *bona fide* embryonic stem cells.

The majority of investigations into TICs have focused on primary cancers, rather than the metastatic site. Markers which help to identify the metastatic TIC are less well characterised. Recently, a study identified the membrane marker CD26 as being able to predict metastasis, and that only CD26+ cells, not CD26- cells, could form metastases when injected into the cecal wall of NOD-SCID mice[136]. Additionally, the CD26+ cellular population was more chemo-resistant and showed increased invasiveness.

CD26 is a well characterised 110 kDa protein, which usually forms a homodimer in the plasma membrane, but research regarding its function as a TIC marker is lacking[137]. The CD26 extra-cellular domain contains a protease section capable of cleaving NH_2- terminal dipeptides from polypeptides with either L-proline or L-alanine at the penultimate position[137]. A cysteine rich region in the extra-cellular domain has been demonstrated to bind to collagen and fibronectin[138]. CD26 also has a

binding site for adenosine deaminase (ADA), and since ADA catalyses the irreversible deamination of adenosine to inosine, this reaction reduces the amount of adenosine in the microenvironment[139]. Adenosine has been shown to modulate several aspects of tumour biology, such as promoting immune tolerance, affecting tumour proliferation by either increasing or decreasing it depending on the tumour, and promoting apoptosis. The discrepancies between tumour types have been suggested to be due to the type of adenosine receptor activated[140]. Within colorectal cancer adenosine has been shown to both promote and reduce proliferation, again depending on the receptor stimulated, therefore, the role of adenosine metabolism by CD26 for tumour growth remains inconclusive. The A2B receptor has been described as being overexpressed in colorectal cancer tissue and in colorectal cancer cell lines compared to normal tissue, with inhibition of the receptor causing a decrease in cell proliferation, and hypoxia causing further up-regulation[141]. CD26 could therefore regulate tumour proliferation in colorectal cancer by altering the amount of available adenosine; through metabolising adenosine, CD26 would create local areas in which proliferation would be reduced through reduced A2B stimulation. This could represent an indirect way CD26 can promote chemo-resistance to drug regimens used in the treatment of CRC which target rapidly dividing cells, such as FOLFOX (composed of 5-FU, oxaliplatin and leucovorin). In the immune system CD26 expression is involved in T-cell activation, and it is also currently being investigated as a clinical target in type 2 diabetes [142]. Alternatively, stimulation of the A3 receptor reduces tumour growth, so CD26 can also enhance growth by reducing adenosine concentrations and therefore stimulation of the A3 receptor[143]. In cancers other than CRC, CD26 has been shown to have opposing effects in different tumour types. For example, in malignant melanoma CD26 expression is repressed during melanoma tumourigenesis and its loss is associated with specific chromosome defects. Upon re-expression of CD26, restricted tumour growth and migration ensue[144,145]. Conversely, in mesothelioma CD26 expression has been associated with TIC properties, and in T cell-acute lymphoblastic leukaemia cell

lines the proportion of CD26+ cells increased following treatment with 8-azaguanine, demonstrating that CD26+ cells may have chemo-resistant properties in this setting[146,147]. Recently, CD26 expression has also been shown to demarcate the leukemic stem cell in chronic myeloid leukaemia[148].

Many other markers have been investigated in CRC, including CD166, CD24, CD44 and Musashi homolog 1, yet no single or group of markers have been agreed upon or unequivocally demonstrated to be able to completely distinguish the TIC population in humans, with the markers tested usually identifying a larger population consisting of TICs and non-TICs[149-152]. Additionally, it is possible that different tumour types, and different populations within the same tumour, harbour TICs characterised by the presence of different surface markers, as has been found in breast cancer[153].

1.5.3 Clinical implications of TICs

The TIC cell population is believed to be the cause of cancer recurrence following chemotherapy, due to an increased resistance to current chemotherapy drugs such as oxaliplatin (OX) and 5-Fluorouracil (5-FU). CD133+ cells have demonstrated resistance to 5-FU and oxaliplatin in NOD-SCID xenograft studies using human CRC tissue, whereas CD133- cells showed an increased sensitivity[154]. Similarly, cells with $ALDH^{High}$ activity have been shown to be resistant to cyclophosphamide treatment. Small interfering (si) RNA knock down of ALDH1A1 in human CRC xenografts in NOD-SCID mice sensitised tumours to cyclophosphamide treatment, resulting in decreased tumour volumes compared to the control treatment[128]. The drug efflux membrane protein ATP-binding cassette sub-family G member 2 (ABCG2) is expressed by TICs, and represents one mechanism by which TICs can evade chemotherapy[155-157]. Another key factor is the nature of some of the current chemotherapy drugs which target cells that divide more frequently, interfering with DNA synthesis. A sub-population of TICs may divide less frequently, and as such would not be targeted[158]. As TICs can reconstitute the entire tumour population, failure to eliminate them would result in re-

population of the tumour, therefore targeting the TIC population may circumvent relapse as the tumour would be unable to sustain itself. If the TIC population was eradicated, the remaining bulk would consist of the differentiated cell component which is more successfully targeted by current chemotherapeutics (Figure 1.6).

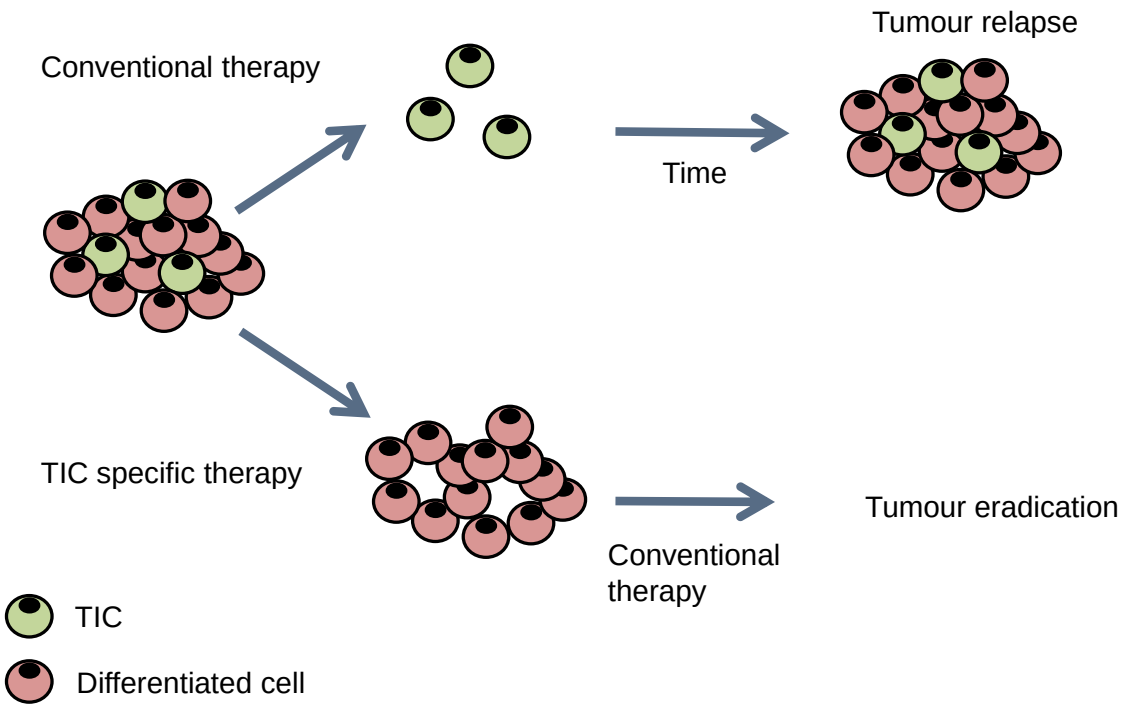

Figure 1.6 The potential effect of using a TIC targeted therapy on tumour response
Conventional chemotherapy spares the tumour initiating population (green) which results in tumour relapse. By targeting the tumour initiating cells the differentiated cells (red) are left which can be treated using conventional therapy resulting in tumour regression.

Making therapies that specifically target TICs is further hindered by the influence of the tumour microenvironment, signalling from which, potentially gives any cell the ability to de-differentiate and become a TIC[78]. This means an ideal agent or combination of agents should be able to target both the TICs and micro-environmental signals, preventing transition of residual tumour cells to TICs.

1.6 **Metastasis**

Metastasis is a complex process whereby cells gain a migratory phenotype, enter blood and lymphatic vessels, and travel around the body before colonising lymph nodes or distant organs. Figure 1.7 breaks this process into a simplified model, alluding to distinct obstacles that need to be overcome by the cell, in order to achieve distant colonisation. This involves cells having to acquire invasive properties, enter the circulation through intravasation, survive circulation, enter a distant organ through extravasation, and finally to colonise. The complexity of this process is reflected by the fact only approximately 0.01% of cells are able to overcome these barriers and form distant colonies[159].

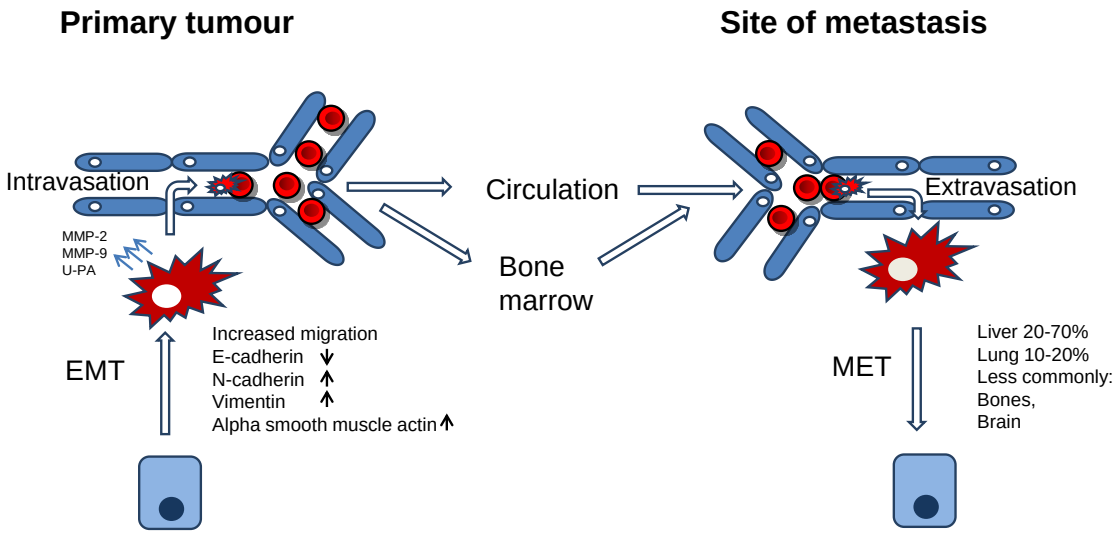

Figure 1.7 An overview of the metastatic process
The metastatic process begins with a tumour cell acquiring the ability to migrate by converting to a more fibroblast-like state. This is achieved by epithelial to mesenchymal transition (EMT) which is marked by a decrease in E-cadherin, and increases in N-cadherin, vimentin and alpha smooth muscle actin protein expression. To create a pathway through to the blood vessels, proteins which degrade the matrix, such as MMP-2 and MMP-9, are secreted. Once at the blood vessels, cells enter the organ through the process of intravasation. During circulation, tumour cells have been reported to reside in the bone marrow, possibly developing further metastatic traits before re-entering the circulation. At the metastatic site, cells leave the circulation through the process of extravasation, and go through a mesenchymal to epithelial transition (MET), reverting from a fibroblast-like state back into an epithelial state. In CRC, the most prevalent site of metastasis is the liver, followed by the lungs and brain.

The first step towards metastasis is generally considered to be the acquirement of a migratory phenotype. There have been two types of migration observed, single cell migration and group migration, which involves a small group of cells that remain connected through cell-cell junction molecules.

Single cell migration has been proposed to be orchestrated by epithelial-mesenchymal transition (EMT), which has been demonstrated *in vitro* and gives cells increased migration and invasion capabilities. The EMT programme is not unique to

cancer metastasis, as it is an essential process during embryonic development and wound healing[160,161]. Cells that have undergone EMT express fibroblast markers such as vimentin and N-cadherin, and repress epithelial markers such as E-cadherin. This is achieved via EMT 'master' genes such as *SNAIL*, *TWIST* and *ZEB1*, causing global changes in gene expression that promote cytoskeletal re-arrangements and a fibroblast-like phenotype[162-164]. Mutation and hypermethylation can also lead to repression of E-cadherin and help drive the EMT process[165-167]. N-cadherin promotes migration, and during EMT the repression of E-Cadherin and *de novo* expression of N-cadherin (called the cadherin switch) is an important step, as this allows cells to detach from neighbouring cells through loss of adherens junctions, and migrate to nearby vessels[168]. The decision for a cell to enter EMT is partially influenced by the tumour microenvironment. Production of cytokines HGF and TGF-β by cancer associated fibroblasts (CAFs) help to promote a migratory phenotype[78].

Once a cell has undergone EMT it is then able to migrate to nearby vessels and enter via the process of intravasation, where cells migrate between endothelial cells to enter blood and lymphatic vessels. Intravasation is not well defined in CRC, but studies indicate that urokinase plasminogen activator (u-PA) and other proteinases including matrix metalloproteinases 2 and 9 (MMP-2, and MMP-9) are expressed to degrade the extracellular matrix (ECM), aiding intravasation by providing direct access to vessels[169-174].

Focal adhesion kinase (FAK) may also act to help metastatic cells survive anoikis (programmed cell death due to loss of attachment to ECM) by promoting activation of the extracellular signal-regulated kinase (ERK) or protein kinase B (PKB also known as AKT) cell survival signalling pathways[174-176]. Once in the blood stream the mechanical pressure kills many cells, as the stress results in production of nitric oxide and reactive oxygen species (ROS) which trigger apoptosis[177-179]. This can be evaded via up-regulation of stress proteins such as heat shock protein 70, and by the metastasising cell associating with platelets and other circulating tumour cells which

provides further protection[180-182]. Expression of vascular endothelial growth factor -D (VEGF-D) and PGE2 in the primary tumour results in lymphatic vessel widening, aiding metastasis to local lymph nodes, which can be significantly reduced following treatment with non-steroidal anti-inflammatory drugs (NSAIDs)[183]. A recent study has shown that platelets activated by tumour cells release dense granules which contain the nucleotide adenine. Adenine is thought to promote extravasation and increase the opening between endothelial cells by causing loss of junction contacts mediated though activation of the purinergic receptor $P2Y_2$[184].

In some cancers such as breast, a long dormancy between dissemination and colonization is observable. Furthermore, it has also been demonstrated that cells are primed for specific organ colonisation. For example, in the pleural fluid from patients with breast cancer there were distinct sub-populations that metastasised to specific organs when injected into mice, and another study identified that cells expressing metadherin specifically metastasised to the lung[185,186]. It has also been seen that circulating tumour cells can move to the bone marrow where they act as a cell reservoir and potentially further adapt before colonisation[187-190].

At the site of colonisation, cells that have been through EMT are required to go through the process of mesenchymal-epithelial transition (MET) before colonisation. Cells that disseminate from the colon predominately travel via the portal vein to the liver, which is believed to be susceptible to the process of extravasation due to the presence of fenestrated endothelium which allows easier access into the organ[191,192].

One hypothesis to explain how certain cells acquire metastatic potential is that the TIC population acts as a reservoir for these cells which then require the correct signals in order to initiate the process of EMT and begin metastasis[193]. Recently this concept has gained some support by the identification of a TIC population that can cycle between two types of populations; migratory or proliferative, in squamous cell carcinoma[194]. Alternatively, it has been proposed that any tumour cell under the correct circumstances can undergo EMT. Furthermore, once the cell has been through EMT it

acquires TIC-like properties, which would then promote the colonising ability of the cells in distant organs. The association of EMT characteristics with TIC properties has been reported in human breast cancer cells that have been triggered to go through EMT by treatment with TGF-β, the cells display expression of TIC markers and have stem cell characteristics[195]. Therefore, if a clinical agent can target the TIC properties it may not only be able to inhibit tumour growth but could also concurrently disrupt the process of metastasis, due to the EMT-TIC association.

1.7 **Diagnosis and symptoms**

Staging is the process of determining how far a cancer has progressed and is used in deciding the appropriate treatment to give to patients. The most common system used is the TNM (**T**umour, **N**ode, **M**etastasis) staging system. Tumour size is ranked on a scale of 0-4 and similarly, lymph node involvement is ranked on a scale of 0-2. Metastasis is ranked on a two-step scale. The TNM staging system is the most widely used system and is superseding the use of older staging methods. However, the Dukes' staging system that ranks progression in stages from 0 to 4 is still commonly used. The TNM staging system is described in Table 1.1.

Stage Description	Stage	Tumour	Node	Metastasis	TNM Description
Carcinoma *in situ*	Stage 0	Tis	N0	M0	Carcinoma *in situ*
The tumour has grown into the colon wall or muscle layer without any node involvement	Stage 1	T1	N0	M0	Tumour has invaded the submucosa
	Stage 1	T2	N0	M0	Tumour invades muscularis propria
The tumour has grown through the colon wall with no node involvement	Stage 2a	T3	N0	M0	Tumour invades through the muscularis propria into pericolorectal tissues
The tumour has grown through the wall of the colon and into other surrounding tissue or organs, but there is no node involvement or metastasis	Stage 2b	T4	N0	M0	Tumour penetrates to the surface of the peritoneum and has grown into other parts of the bowel or surrounding organs
The tumour has either not grown out of the colon, or has grown through the muscle layer but there is up to 3 nodes involved	Stage 3a	T1	N1	M0	The Tumour has invaded the submucosa with metastases in 1-3 lymph nodes
	Stage 3a	T2	N1	M0	Tumour invades muscularis propria with metastases in 1-3 lymph nodes
The tumour has grown through the colon wall and into surrounding tissue and organs with up to 3 nodes involved	Stage 3b	T3	N1	M0	Tumour invades through the muscularis propria into pericolorectal tissues with metastases in 1-3 lymph nodes
	Stage 3b	T4	N1	M0	Tumour penetrates to the surface of the peritoneum and grown into other parts of the bowel or surrounding organs with metastases in 1-3 lymph nodes
The tumour is any size but 4 or more nodes are involved	Stage 3c	Any size	N2	M0	There is metastases in 4 or more local lymph nodes
The tumour is any size but 4 or more nodes are involved and there are distant metastases to another organ.	Stage 4	Any size	Any node involvement	M1	The tumour is any size, with any number of lymph nodes involved, and there are distant metastases to another organ.

Table 1.1 The different stages of the TNM staging system[196]

Tumour grading describes how aggressive a tumour is, and is divided into three grades: Grade 1 refers to slow growing tumours; Grade 2 refers to slightly faster and more abnormal looking (or moderately differentiated) tumours; Grade 3 refers to the most aggressive tumours which are often poorly differentiated.

Symptoms of CRC can mimic other diseases such as haemorrhoids and irritable bowel syndrome, and include blood loss in stools, changes in bowel habits, dizziness (caused by anaemia due to blood loss from the bowel) and unexplained weight loss. A GP may conduct a rectal examination, feeling for any lumps or swelling, and refer patients for further tests if there is any abnormality. If referred to a more specialist doctor, a sigmoidoscopy or colonoscopy may be carried out, and any polyps or abnormal areas can be biopsied and taken for further analysis by a pathologist. If cancerous tissue is detected, the stage is deduced using a computerised tomography or magnetic resonance imaging, and the best treatment plan established.

1.8 **Surgery and Chemotherapy**

For primary CRC tumours, treatment is largely dependent on the staging of the tumour. Generally, the treatment for stage 0 is local excision or polypectomy, but if the tumour is large then resection (surgical removal) may be performed. Treatment for stage I and II tumours is resection. Patients with a stage II tumour that displays features considered to be a high risk (over 12 lymph nodes involved, poorly differentiated, vascular or lymphatic invasion, tumour obstruction of colon lumen) and stage III tumours, will also receive adjuvant chemotherapy (chemotherapy post-surgery)[197]. The chemotherapy standard is a combination of oxaliplatin and 5-FU, plus leucovorin (LV, also called folinic acid), which when used in this combination is referred to as FOLFOX. In patients where it is not possible to take oxaliplatin due to unacceptable neuropathic side effects, then 5-FU and LV only, or capecitabine (an oral fluoropyrimidine) will be administered. When considering chemotherapy, several other

factors may also be taken into consideration such as MSI status, since MSI+ patients have been shown not to benefit from 5-FU chemotherapy[198].

For mCRC the most common site for metastasis is the liver. Resection of the metastatic site is the best treatment, but this is only feasible when the resection area is small enough such that it will still leave a functional liver. If the colorectal liver metastasis (CRLM) tumour is too large, chemotherapy prior to resection (neoadjuvant/conversion therapy) can be used to downsize the tumour. An additional benefit of conversion chemotherapy is the possible removal of micrometastases, and additionally, response to neoadjuvant chemotherapy may act as a further prognostic marker[199]. The pitfalls of neoadjuvant chemotherapy include; a complete response to the chemotherapy can disrupt surgical planning due to difficulties in visualising the tumour, side effects can cause liver damage, and chemotherapy is expensive[200]. The majority of chemotherapy administered in CRLM is for palliative care, to try and provide a better quality of life and longevity for patients who do not qualify for surgical resection. An overview of the treatment steps for CRLM is shown in figure 1.8.

After resection 30-50% of patients will have recurrent metastasis within 5-years, which is believed to occur from microscopic residual disease or micrometastases that could not be visualised, and therefore not removed during surgery[201,202].

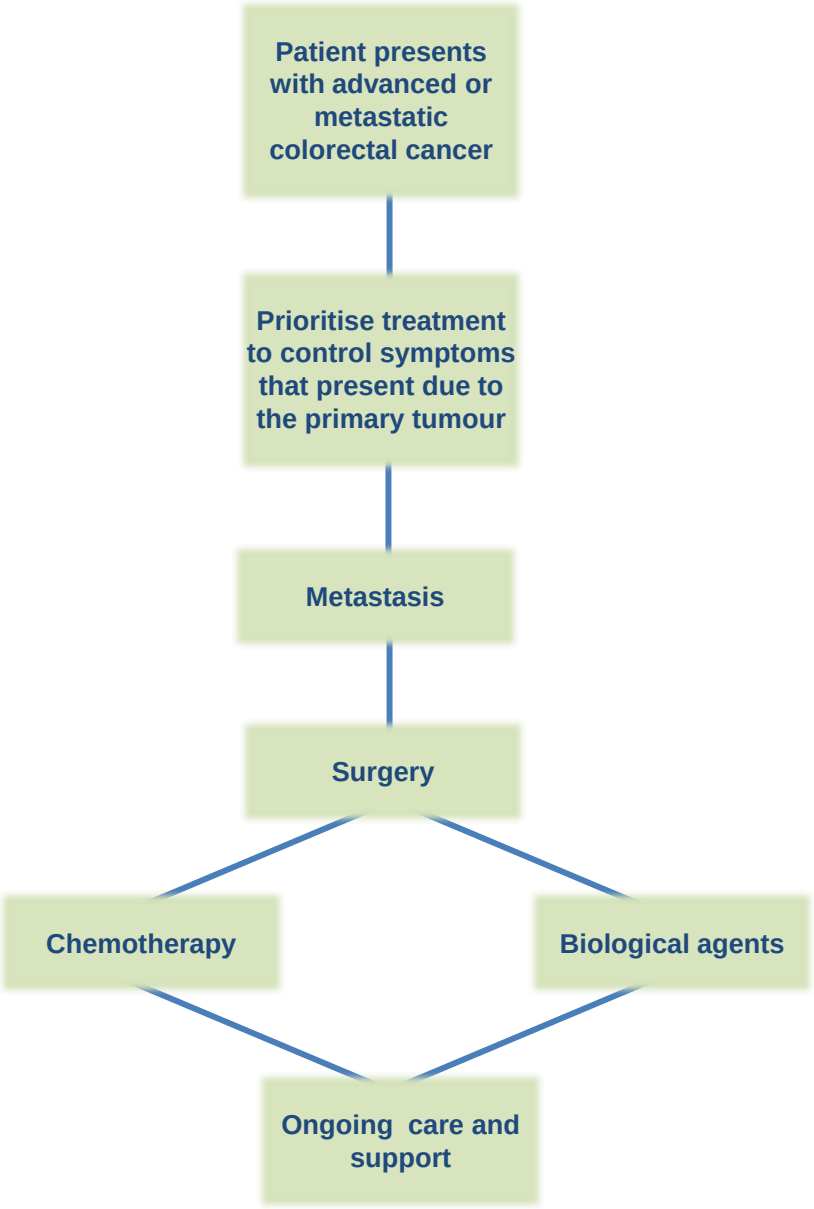

Figure 1.8 An overview of treatment for metastatic CRC.
An overview of the treatment decision process for management of metastatic CRC, adapted from the National Institute for Clinical Excellence (NICE) guidelines for the management of advanced and metastatic colorectal cancer (http://pathways.nice.org.uk/pathways/colorectal-cancer/colorectal-cancer-overview#content=view-node%3Anodes-extrahepatic-metastasis&path=view%3A/pathways/colorectal-cancer/managing-advanced-and-metastatic-colorectal-cancer.xml).

FOLFOX forms the frontline chemotherapy for most of the mCRC regimens, with additional agents recently approved for use in mCRC (but not primary CRC) including Irinotecan, Bevacizumab, Cetuximab and Panitumumab. Below is a description of the mechanisms of action, possible drug combinations and some of the major toxicities for oxaliplatin and 5-FU. The remaining drugs used for mCRC treatment are summarised in Table 1.2.

1.8.1 5-FU and oxaliplatin

5-FU is a fluoropyrimidine which is usually given intravenously in combination with leucovorin. 5-FU is extensively metabolised, producing three active metabolites called fluorouridine triphosphate (FUTP), fluorodeoxyuridine triphosphate (FdUPT) and fluorodeoxyuridine monophosphate (FdUMP)[203,204] (Figure 1.9). Mechanisms of action for 5-FU include blocking the enzyme thymidylate synthase (TS) from carrying out its normal physiological function of thymidine monophosphate production, which is a precursor to the DNA base thymidine and is essential for DNA replication[203]. LV stabilises binding of the 5-FU metabolite FdUMP to the TS active site[205]. As a pyrimidine analogue, an alternate pathway through which 5-FU promotes cell death is via miss-incorporation of its metabolites FUTP and FdUT into mRNA and DNA respectively[206]. Alternatively, 5-FU can be administered in an oral form called capecitabine which has a similar mechanism of action, efficacy and toxicity as 5-FU, existing as a pro-drug that undergoes enzymatic conversion to 5-FU[207,208].

Toxicity of chemotherapy regimens depend on the schedule of administration. The most common side effects following FOLFOX administration include diarrhoea, stomatitis (inflammation of the mucus lining in the mouth), neutropenia (low neutrophil number), palmar-plantar erythrodysesthesia (hand-foot syndrome), and neurotoxicity[209-211].

Oxaliplatin is a platinum-based agent that inhibits DNA replication and transcription by blocking DNA polymerase through formation of intra- and inter-strand DNA crosslinks[212]. Oxaliplatin was added to 5-FU and leucovorin to form the FOLFOX regimen following trials which demonstrated that patients who progressed whilst receiving 5-FU+LV achieved a 46% response rate when administered the triple combination OX+5-FU+LV. Subsequently, it was shown that treatment with OX+5-FU+LV afforded significantly longer progression-free survival (median, 9.0 v 6.2 months) and better response rates (50.7% v 22.3%) compared to patients who did not receive oxaliplatin[213-215]. Oxaliplatin is also combined with oral capecitabine to form the treatment called Xelox, which is usually used when patient cannot tolerate FOLFOX or prefer the Xelox regimen[216,217]. Toxicities include neutropenia, inflammation and necrosis at the site of injection, neurotoxicity and diarrhoea.

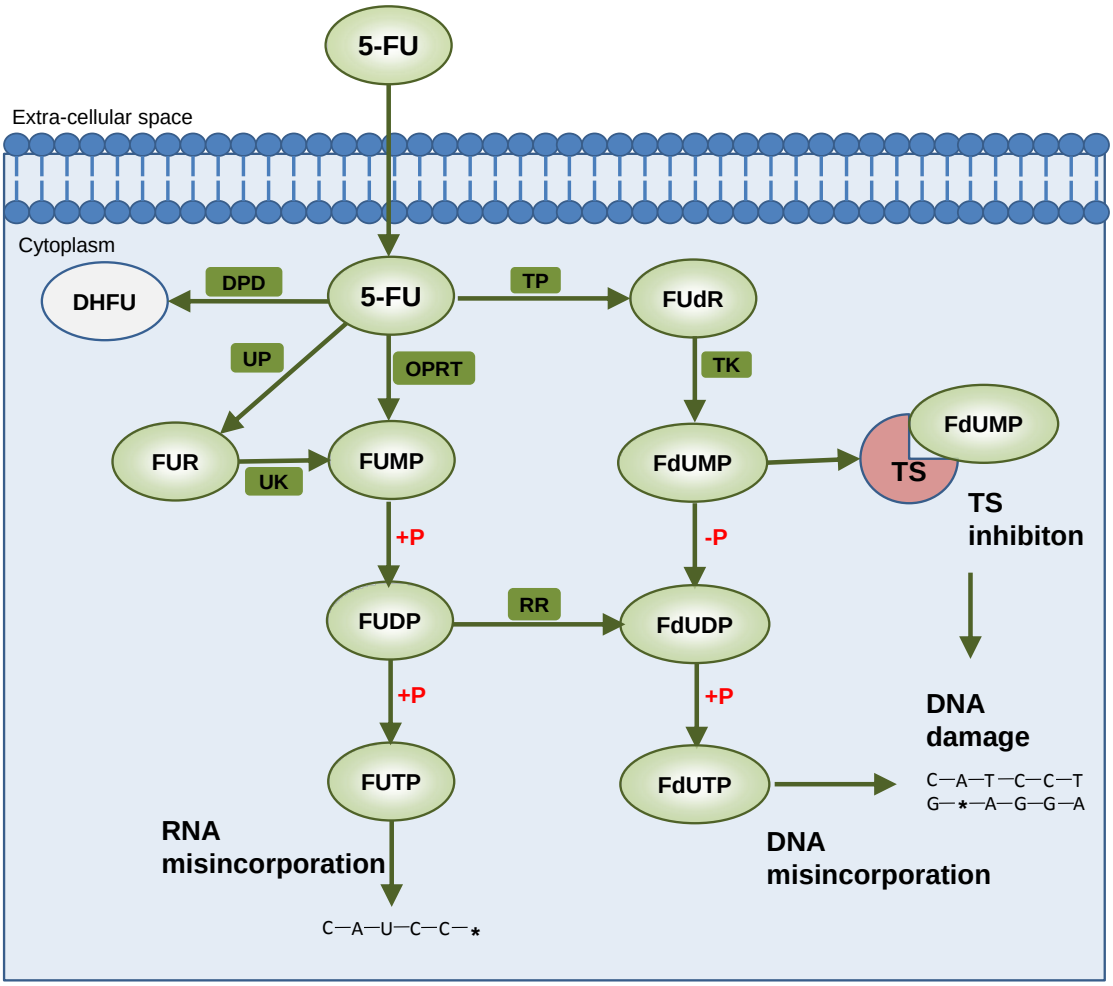

Figure 1.9 A summary of 5-FU metabolism effects
5-FU is converted in the cell into four main products; dihydrofluorouracil (DHFU), fluorouridine triphosphate (FUTP), fluorodeoxyuridine triphosphate (FdUPT) or fluorodeoxyuridine monophosphate (FdUMP). The conversion to DHFU by dihydropyrimidine dehydrogenase (DPD) is a catabolic step and is the rate limiting factor in 5-FU metabolism. FUTP, FdUPT and FdUMP represent the three active metabolites. 5-FU can be metabolised into fluorouridine monophosphate (FUMP) by orotate phosphoribosyltransferase (OPRT) or indirectly via fluorouridine (FUR) through uridine phosphorylase (UP) then uridine kinase (UK). FUMP is then phosphorylated to become FUDP, which can be further phosphorylated to produce FUTP. Alternatively, FUDP can be converted to fluorodeoxyuridine diphosphate (FdUDP) by ribonucleotide reductase (RR). The production of the active metabolites from FdUDP depends on either de-phosphorylation to produce FdUMP, or phosphorylation to produce FdUTP. Another route to FdUMP production also exists, with thymidine phosphorylase (TP) catalysing the conversion of 5-FU to fluorodeoxyuridine (FUdR). Thymidine kinase (TK) then phosphorylates FUdR to FdUMP. The solid green squares represent the enzymes, +P/-P represents phosphorylation/de-phosphorylation steps. Light green ovals represent metabolites. Asterisks indicate miss-incorporation of metabolites into RNA or DNA.

Drug	Mechanism of action
Irinotecan	A potent inhibitor of topoisomerase I, an enzyme required for DNA uncoiling and recoiling. It is administered either alone or in combination with 5-FU and LV (FOLFIRI), as a second line treatment if patients are unsuitable for FOLFOX[218,219].
Bevacizumab	This is a monoclonal antibody that targets vascular endothelial growth factor (VEGF) to inhibit angiogenesis. It is has been shown to be beneficial when added to the standard chemotherapy regimen, and so is usually combined with FOLFOX or FOLFIRI, but is not used as a single agent[220].
Cetuximab	Cetuximab represents a chimeric (human and mouse) monoclonal antibody that targets the epidermal growth factor receptor (EGFR) and can be used either in combination with Irinotecan or alone[221,222]. The expression status of EGFR has no effect upon its efficacy, however, K-Ras mutations have been shown to affect the efficacy of Cetuximab. Wild-type tumours for the K-Ras gene gain a benefit from Cetuximab, whereas tumours with a mutated K-Ras gene do not[223].
Panitumumab	In 2006 Panitumumab, a fully humanised monoclonal antibody against EGFR, was approved for use as a monotherapy in mCRC patients who have failed to respond to a treatment consisting of a fluoropyrimidine plus either oxaliplatin or irinotecan[224-226].

Table 1.2 NICE approved drugs for treatment of mCRC

1.8.2 Markers of chemoresistance

There is a current focus on the concept of personalised or precision medicine in an attempt to identify patients that will respond to specific chemotherapy regimens. This will allow patients who would not benefit to be spared drug side effects and other possible deleterious effects on tumour evolution, which may affect further treatment strategies, whilst also increasing the chances of efficacy.

5-FU

The majority of the literature suggests that tumours with deficient MMR/MSI are predicted to have a lack of response to 5-FU, which is supported by data from both *in vitro* and clinical studies[227-229]. However, some ambiguity still exists which thus far has

prevented further clinical utility of MMR testing. These ambiguities may possibly arise from the origin of the MMR deficiency; i.e., whether it is due to germline mutations or sporadic methylation in MMR genes[230], and requires further investigation before it could be considered whether to conduct clinical testing of MMR status.

The expression of TS has also been shown to correlate with tumour response. Patients that express higher levels due to a variable number of tandem repeats in the 5'-untranslated region show a poorer response to therapy and decreased rates of toxicity, as the higher expression levels result in less enzyme inhibition, allowing continued thymidine production, which ultimately leads to less inhibition of DNA synthesis. The binding of 5-FU to TS is stabilised by 5,10-methylenetetrahydrofolate (5,10-MTHF). Polymorphisms that affect the activity of the enzyme methylenetetrahydrofolate reductase (MTHFR), which catalyses the irreversible conversion of (MTHF) to 5-methyltetrahydrofolate have been shown to affect 5-FU metabolism. Two single nucleotide polymorphisms (SNPs), (677C>T and 1298A>C alleles), have been associated with reduced activity and a positive effect on survival due to an increase in TS inhibition[231,232]. However, other studies have failed to identify such a link[233,234]. Finally, DPD a rate limiting enzyme involved in the catabolism of 5-FU has been found to have polymorphisms that alters DPD activity. For example, the DPYD*2A allele can produce an enzyme with no activity[235,236], and this allele is believed to account for severe 5-FU-induced side effects as 5-FU is not broken down, which increases its half-life and prolongs toxicity.

Oxaliplatin

The expression of excision repair cross-complementation group 1 enzyme (ERCC1) assessed by immunohistochemistry (IHC), or the presence of a C to T SNP at codon -118 (with the C allele conferring a worse response) have been demonstrated to predict response to oxaliplatin treatment[237-239]. However, conflicting results as to which allele confers a better response have been published. Despite this, there is

agreement that lower expression of ERCC1 results in better overall survival, and this has been shown for both lower mRNA and protein expression[240,241]. This is presumably due to the role of ERCC1 in nucleotide excision repair and the removal of platinum DNA adducts/crosslinks[242]. For example, a recent study demonstrated that patients with over 5% of cells positive for ERCC1 which was assessed immunhistochemically, were shown to have a lower 5-year survival and overall survival compared to patients who were negative for the marker[237]. No effect was seen in patients who received 5-FU-based chemotherapy only, indicating ERCC1 may be specific for predicting resistance to oxaliplatin[237]. Additionally, *XRCC1* mutations such as G>A substitution leading to an Arg399Gln amino acid change has been shown to reduce the ability of X-ray repair cross-complementing protein 1 (XRCC1) to repair DNA strand breaks induced by oxaliplatin[243,244]. The combination of mutation status in both *ERCC1* and *XRCC1* has been demonstrated to better predict survival compared to the use of each marker alone[245].

Anti-EGFR antibodies

EGFR is a receptor with intrinsic tyrosine kinase activity, activation of which results in stimulation of intracellular signalling cascades which ultimately leads to cellular proliferation. There are two main axes through which EGFR signalling is transmitted through cells, namely the RAS/RAF/ERK and PIK3CA pathways[246]. It has been irrefutably demonstrated that patients with mutant *KRAS* have no benefit from anti-EGFR therapy, which has led to the incorporation of *KRAS* testing before the commencement of anti-EGFR treatment[247-249]. This has been confirmed independently in numerous trials[250,251]. A downstream serine/threonine-protein kinase called BRAF has also been found to be mutated in a large number of cancers, and may also account for anti-EGFR antibody resistance in *KRAS* WT patients[247,252].

Mutations in the *PIK3CA* gene, which encodes the catalytic subunit p110α of the class I PI3K, are also associated with anti-EGFR resistance[247,253]. These mutations

can present independently, or concomitantly, with mutations in the RAS/RAF/ERK pathway, thus analysis of both pathways presents a superior approach to identifying patients who have inherent resistance to anti-EGFR therapy. Indeed, one study analysed mutations in *KRAS*, *PIK3CA* and *PTEN*, and identified 70% of mCRC patients that did not respond to therapy[254].

1.9 **Curcumin**

1.9.1 Background

Curcumin (diferuloylmethane) is a hydrophobic polyphenol that constitutes the major curcuminoid and yellow pigment in the spice turmeric (77% curcumin, 17% demethoxycurcumin and 3% bis-demethoxycurcumin), and is derived from the rhizome of the herb *Curcuma longa*. Curcumin has long been known to possess anti-inflammatory properties, and was used in ancient traditional Indian and Chinese medicine. More recently, curcumin has been demonstrated *in vitro* and *in vivo* to possess chemopreventive and anti-cancer properties against several different cancers, acting through multiple cellular pathways (summarised in Figure 1.10). In support of this activity, epidemiological evidence shows a lower cancer incidence (including CRC) in India, a country which uses a large amount of turmeric in cooking[255]. Indians that migrate to countries with a higher incidence of CRC such as the UK or US, adopt a similar incidence to that of the host nation, indicating that changes in culture, lifestyle and environment can have a large impact on CRC incidence. A study conducted in Leicester, UK, on cancer incidence in the South Asian population (Indian, Pakistani and Bangladeshi) found there was a lower level of colorectal cancer incidence in older South Asians compared to younger South Asians[256]. This may be attributed to the older generations maintaining a more traditional lifestyle and diet as opposed to younger generations that have adopted a more Western lifestyle. Since curcumin is used in a lot of traditional Indian cooking, it may be that curcumin is one factor that could have contributed to this finding.

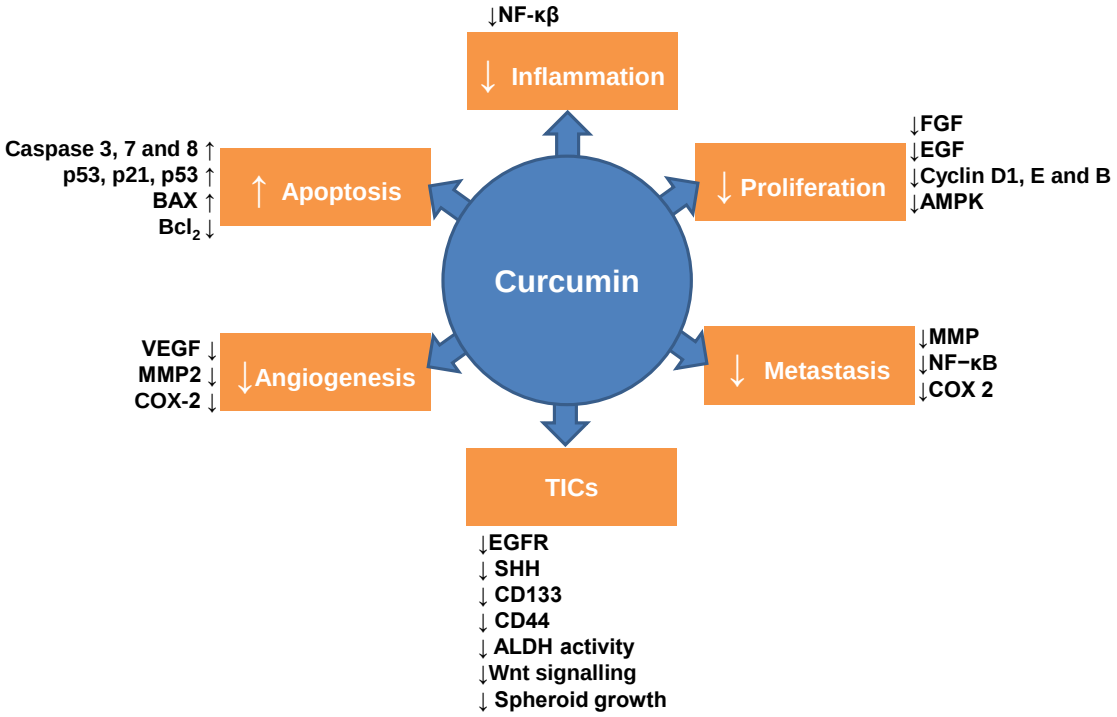

Figure 1.10 An overview of the multiple anticancer effects of curcumin
A summary of the published data relating to potential mechanisms through which curcumin may exhibit anti-tumourigenic properties (discussed in section 1.9.3 mechanisms of action).

1.9.2 Safety and Bioavailability

The bioavailability of curcumin is relatively poor with low serum levels being reported in both mice and humans after oral ingestion[257-259]. Increasing the dose in mice did not alter the fraction of curcumin absorbed (60-66%), resulting in an overall increase in absorbtion[260], with the majority of curcumin excreted in the faeces of both mice and humans[258,260,261]. Absorbed curcumin undergoes conjugation, primarily sulfation and glucuronidation in the liver, colonic mucosa and kidneys[262]. Metabolism produces a variety of curcumin metabolites with little known functional roles, with the exception of the reduced metabolite tetrahydrocurcumin which has been demonstrated to possess anti-inflammatory and anti-oxidant activity[263-265]. However, it is less potent

than curcumin at inhibiting the enzyme cyclooxygenase 2 (COX2), over-expression of which correlates with the advanced stages of CRC[266,267]. Another factor affecting the potential efficacy of curcumin *in vivo* is a short half-life. Administration of 36-180 mg of curcumin daily for up to 4 months produced no detectable levels of parent curcumin, or its metabolites, in blood or urine, but curcumin was recovered in the faeces[259]. Despite poor bioavailability curcumin has still reached efficacious levels in many organs and demonstrated the potential to prevent and reduce colorectal cancer burden in mouse models of carcinogenesis, and increased effects of gemcitabine treatment in a mouse orthotopic model of pancreatic cancer[268]. For example, a study by our group demonstrated adenoma reduction by 39 and 40% following dietary doses of 0.2 and 0.5% curcumin respectively, in a mouse model of familial adenomatous polyposis (*Apc*$^{Min+}$)[269]. Curcumin has also shown *in vivo* anti-cancer activity in rodent models of oesophageal cancer, oral cavity cancer, hepatocellular carcinoma and stomach cancer[270-273].

A variety of methods have now been described to overcome the poor bioavailability of oral curcumin. One approach is the use of an adjuvant which blocks metabolic pathways involved in curcumin metabolism. Piperine is a natural compound that blocks hepatic and intestinal glucuronidation, and in humans when given concomitantly, it improves curcumin bioavailability by 2000%[274]. Other methods improve the delivery by formulating curcumin with phospholipids. This can be undertaken by incorporating curcumin with phospholipids [275,276]. Several synthetic curcumin analogues have also been reported to overcome the issue of low bioavailability, while retaining potent anti-cancer potential[277,278].

The safety of curcumin is demonstrated by the fact it is approved for use as a food colouring agent by the food and drug administration (FDA) in the US, and by the European Food Safety Authority and is labelled as the E number E100. It can be found in a wide variety of foods including processed cheese, custard and curry.

1.9.3 Mechanisms of action

Many of the properties of curcumin have been attributed to its role as an anti-oxidant, an anti-inflammatory, or its ability to disrupt the cell cycle and pathways involved in proliferation/apoptosis. Curcumin can scavenge free radicals involved in lipid peroxidation (lipid degradation due to free radical attack) in addition to up-regulating antioxidant enzymes, including dismutase, catalase and glutathione peroxidise[279,280]. In this manner curcumin can protect the cell from DNA lesions that may cause mutations if not repaired, ultimately leading to tumour initiation. This may explain one mechanism contributing to the potential chemopreventive properties of curcumin. Conversely, curcumin has also been demonstrated to increase ROS, resulting in DNA damage and apoptosis[281]. Differences in the ability of curcumin to act as an anti-oxidant or pro-oxidant have been attributed to the concentration used, with higher concentrations favouring pro-oxidation.[282]

Apoptosis

The ability of curcumin to promote apoptosis has been demonstrated in a variety of cell types and in different manners, and has been shown to affect 104 of the 214 different genes involved in apoptosis in a breast cancer cell line[283]. Apoptosis can be divided into two main categories; intrinsic and extrinsic. Both pathways converge on activating the effector caspases 3, 6 and 7 which proceed through the “execution pathway” resulting in cell death[284].

Curcumin can activate both the intrinsic and extrinsic apoptotic pathways. Curcumin has been shown to cause an imbalance in Ca^{2+} ions, cause endoplasmic reticulum (ER) stress and generate ROS, resulting in caspase-3 activation and apoptosis[285]. Other studies have demonstrated the ability of curcumin to promote the expression of BAX and p53, and repress B-cell Lymphoma 2 (Bcl-2) and cause cytochrome c release[286,287]. In a model of colon carcinogenesis where mice were treated with the carcinogen azoxymethane to promote formation of aberrant crypt foci

(ACF; dysplastic cells in colonic crypts that represent the earliest visible sign of potential cancer development), treatment with curcumin caused expression of BAX and caspase-8 while repressing Bcl-2. Activation of the extrinsic pathway via curcumin-induced stimulation of the FAS (also called CD95 or APO-1) receptor pathway has also been observed in a human melanoma and a non-small cell lung cancer line, resulting in transduction of death signals via caspase-8 activation[288,289].

Inflammation

The anti-inflammatory properties of curcumin are considered to be due to its ability to inhibit COX2, an inducible enzyme responsible for the metabolism of arachidonic acid to prostaglandins, which are mediators of inflammation with prostaglandin E2 (PGE2) representing the most abudant. Additionally, curcumin can down-regulate the expression of pro-inflammatory cytokines[290-293]. COX2 is over expressed in 43% of adenomas, 86% of carcinomas and further upregulated in metastasis[294,295], and its inhibition in *Apc^{Min}* mice prevents adenoma development[296,297]. In CRLM it has been shown that the enzyme activity of 15-hydroxyprostaglandin dehydrogenase (15-PGDH), an enzyme responsible for the rate limiting catabolic conversion of PGE2 in to 15-keto-$PGE_{2,}$ is responsible for controlling the levels of PGE2[298]. COX2 can be inhibited using NSAIDs, such as aspirin and celecoxib. However, these drugs are associated with side effects due to the inhibition of COX1, an isoform of COX which is constituently expressed in most tissues. In the HT-29 colorectal cancer cell line curcumin was shown to decrease only COX2 expression making it potentially more suitable for clinical use than NSAIDs[299]. COX2 is inhibited by direct interaction due to the effect of curcumin upon the NF-κB class of transcription factors, for which COX2 contains two binding sites within its promoter[291,300,301]. NF-κB cell signalling is active in colorectal cancer, and its downstream targets promote the cancer phenotype by production of anti-apoptotic proteins such as Bcl-xL, promoting growth (cyclin D1, c-Myc) and angiogenesis (MMP2 and 9, and VEGF)[301-305]. The NF-

κB family is composed of five transcription factors related by a sequence of 300 amino acids, consisting of: p50, p52, RelA (p65), c-Rel and RelB. Two of the family members, p50 and p52, are produced from larger precursors, p105 and p100, respectively, whereas the remaining are expressed in their final form ready for transcription, but are repressed by interactions with inhibitory IκB proteins[306,307]. There are two different pathways, the canonical and non-canonical pathways, which merge on the formation of a IκB Kinase (IKK) complex, consisting of catalytic kinase subunits (IKKα and/or IKKβ) and the regulatory non-enzymatic scaffold protein NEMO (NF-kappa B Essential Modulator, also known as IKKγ)[306]. The IKK complex then phosphorylates the IκB inhibitor, targeting the IκB for proteosomal degradation. This allows the previously repressed NF-κB subunits to form a transcriptional complex and bind to 9-10 base pair DNA sites, called kB sites, in the promoter and enhancer regions of genes[306]. Curcumin treatment has been demonstrated to reduce nuclear NF-κB signalling in HCT116 cells[308], and decrease NF-kappaβ/p65 at the mRNA and protein level in the colorectal cancer cell line colo 205[285].

p53 and the cell cycle

The tumour suppressor gene *p53* has proven to be an important mediator in regulating the cell cycle and apoptosis, acting as a transcription factor mediating expression of various genes involved in cell cycle control. Apoptosis regulation by p53 is not fully understood, but is mediated through caspase-9 and by some p53 target genes such as p53 up-regulated modulator of apoptosis (*PUMA*) and Fas cell surface death receptor. Curcumin has been shown to enhance expression of p53 in colorectal cancer patients, and in a recent study using the colorectal cancer cell line HCT116 curcumin caused senescence, marked by an increase in p53 and p21 in $p53^{+/+}$ mice, and p21 increase in $p53^{-/-}$ mice. Senescence was followed by autophagy with the observation of autophagosomes and increased levels of LC3-II[309].

Curcumin can also modulate cell cycle progression. Evidence shows it can cause G2/M cell cycle arrest by blocking the expression of cyclin D and B, and also causing release of cytochrome c from the mitochondria and apoptosis in a p53-dependant mechanism[310]. Other studies have also seen a decrease in cyclin D1, and cyclin E with G2/M arrest, and an increase in p53, p21 and p27[286,311]. However, in the RKO colorectal cancer cell line curcumin was found to impair p53 function by disrupting post-translational folding[312]. Overall, the results cited indicate that curcumin can modulate cell-cycle progression through causing cell cycle arrest through a variety of different mechanisms.

Angiogenesis

It is well known that angiogenesis plays a key role in tumour development and progression, the importance of which is demonstrated by the clinical use of Bevacizumab for the treatment of metastatic colorectal cancer. Curcumin has been demonstrated to exert anti-angiogenic properties by inhibiting the growth, migration, and tube forming capacity of human intestinal microvascular endothelial cells, through disrupting VEGF signalling[313]. Furthermore, curcumin reduced angiogenesis *in vivo* in mice bearing Ehrlich ascites tumour cells[314]. Another important angiogenic factor targeted by curcumin is hypoxia inducible factor 1 alpha (HIF-1α), a growth factor expressed in response to hypoxia that up-regulates expression of VEGF[315].

Tumour specificity

An advantage that curcumin has for potential use as a clinical agent is that it can exert differential effects against normal and malignant cells. For example, *in vitro* research has demonstrated that curcumin induced G2 arrest and apoptosis in breast carcinoma and hepatoma cell lines, but not in normal primary rat hepatocyte cells[316]. Human dermal fibroblasts and human epithelial colonic cells have also been reported to be less sensitive to curcumin when compared to the colorectal cancer cell line

HCT116[317,318]. Similar findings have been described when comparing immortalized normal oral mucosa cells, leukoplakia, and squamous cell carcinoma[319]. Furthermore, curcumin treatment selectively induced more apoptosis in peripheral blood mononuclear cells in patients suffering from cutaneous T-cell lymphomas compared to healthy donors[320].

The reasons for such differential effects have not been fully addressed. Some pathways affected by curcumin are simply not as active in normal cells, for example NF-κB signalling is prevalent in a large number of tumours, but is not so in many normal cells. Thus, disruption of pathways which cells are reliant upon for their survival/proliferation will have a more pronounced effect than in cells which do not rely upon these pathways. Additionally, differential uptake of curcumin between normal and malignant cells *in vitro* has been observed, which may be attributed to differences in cell membrane structure between normal and cancerous cells[321].

Stem cell pathways

Curcumin has also been shown to exhibit effects on pathways involved in stem cell regulation, such as the Notch, Wnt and hedgehog pathways. As highlighted previously, the Wnt signalling pathway plays an important role in regulating normal colonic stem cells, and is also believed to be important in regulating TICs. In HCT116 cells curcumin disrupted Wnt signalling, causing G2/M arrest, apoptosis and loss of cell-cell adhesion. Notch signalling has been shown to increase the number of CD133+ and $ALDH^{High}$ cells, thus targeting of Notch could be beneficial[322,323]. Several studies have shown that curcumin can inhibit the Notch pathway by reducing Notch-1 expression[324,325], and another study identified curcumin as targeting the γ-secretase complex proteins such as presenilin 1 and nicastrin[326]. Despite Wnt signalling playing an important role in tumour development, it has been observed that reduced Wnt signalling accompanied by concomitant increases in hedgehog signalling immediately prior to metastasis in CRC occurs specifically in the CD133+ cells, resulting in an

embryonic-stemness signature[327]. Curcumin has been shown to decrease sonic hedgehog (SHH) and GLI1 (also called glioma-associated oncogene homolog 1) expression in glioma and pancreatic cell lines, and may therefore have a role in down-regulating SHH signalling to help prevent metastasis[328,329].

1.9.4 Clinical Trials

Curcumin is under clinical investigation for the treatment and prevention of a wide range of diseases including CRC, pancreatic cancer, head and neck cancer, AML, arthritis, Alzheimer's disease and depression. There are currently 84 clinical trials listed on the clinicaltrials.gov website, 15 of which pertain directly to colorectal cancer. Presently, despite copious pre-clinical data there is little evidence of clinical efficacy for curcumin, as most clinical data comes from early phase I/II trials investigating pharmacokinetics and tolerability.

Leicester University has a strong history in the clinical evaluation of curcumin, with four phase I/II clinical trials[259,330-332], having demonstrated the safe consumption of up to 3.6 g of curcumin daily for up to 4 months (the longest time point investigated) in patients suffering with colorectal cancer refractory to treatment[258,259]. Additionally, despite pharmacokinetic analysis demonstrating poor bioavailability, potential evidence of biological activity was observed in the form of a reduced number of the DNA adduct 3-(2-deoxy-beta-di-erythro-pentafuranosyl)-pyr[1,2-alpha]-purin-10(3H)one (M_1G) in patients who had received the highest dose of 3.6 g of curcumin a day for seven days[331].

Clinical trials by other research groups have corroborated these findings regarding the safety of curcumin[257]. A recent phase IIa nonrandomized, open-label clinical trial investigating the effects of curcumin on aberrant crypt foci, found a 40% reduction in the number of ACF after one month of 4 g daily oral curcumin, when studying a cohort of 44 smokers with eight or more ACF on screening colonoscopy³³³.

Also, when 480 mg curcumin was combined with 20 mg quercetin and given orally 3 times a day for an average of 6 months to five FAP patients with prior colectomy (4 with retained rectum and 1 with an ileal anal pouch), within the remaining colon there was a significant decrease in the number and size of polyps compared to baseline by 60.4% and 50.9%, respectively[334]. A phase I/II study investigated the combination of curcumin with gemcitabine based-chemotherapy in patients suffering with pancreatic cancer, and demonstrated that 8 g of oral curcumin daily was also safe in this population as no dose limiting toxicities were observed[335].

1.9.5 Rationale for combining curcumin with FOLFOX

Extensive *in vitro* data suggest that curcumin could be an effective agent against CRC, and clinical trials have demonstrated good tolerability and the potential for beneficial biological effects in the colon, advocating further investigation of curcumin as a therapeutic agent.

Several studies have shown additive effects when combining curcumin with 5-FU *in vitro* using cell lines. For example, 5-FU induced up-regulation of NF-κB signalling in HCT116 cells, which was abrogated when used in combination with curcumin, a pathway demonstrated to be important for cell proliferation and survival[336]. In addition, the concentration required to produce 50% growth inhibition fell for both curcumin and 5-FU when cells were exposed to the combination[308]. As inhibition of TS activity is one mechanism of action of 5-FU, overexpression compensates for its inhibition, curcumin was able to prevent this as the combination of 5-FU and curcumin resulted in a lower expression of TS compared to 5-FU alone[337]. In addition, inhibition of TS using siRNA prevented the synergistic effect seen when combining curcumin and 5-FU, indicating TS is involved in the mechanism that is responsible the synergistic effects. Treatment with 5-FU also increases NF-κB signalling which was abrogated by curcumin. Interestingly, when TS was inhibited the 5-FU induced increase in NF-κB was prevented, indicating that TS is upstream in this pathway[337]. Curcumin has also

been shown to sensitise human cervical cancer cells to 5-FU. When were incubated with curcumin, p53 was up-regulated causing enhanced sensitivity to 5-FU-induced damage. This was believed to be due to the requirement for p53 mediated induction of apoptosis for cells to trigger cell death if cells acquire a large amount of DNA damage[338]. Treatments with oxaliplatin and 5-FU *in vitro* have revealed the presence of a refractory population in the colorectal cancer cell lines HCT116 and HT-29. This refractory population displayed the TIC characteristic of spheroid formation and expressed the putative TIC markers CD133, CD44 and CD166[339]. When the cells were treated with curcumin these populations decreased in size and this was mirrored by a reduction in spheroid numbers. A second study by the same group also showed that treatment of pre-treated cells with oxaliplatin and 5-FU with curcumin+oxaliplatin+5-FU also caused a significant decrease in proliferation in HCT116 and HT29 cells compared to controls, and an increase in apoptosis, which was associated with a decrease in EGFR, HER-2, AKT and COX2 expression. An increase in insulin growth factor binding protein 3 (IGFBP-3) expression (responsible for sequestering insulin growth factor receptor thus preventing stimulation), was also observed[340].

Curcumin has been shown to elicit effects against $ALDH^{High}$ cells, reducing the size of this population, and preventing *ex vivo* spheroid formation using primary normal breast epithelial cells[341]. Also, in Apc^{Min} mice, analysis of the residual tumours following curcumin treatment demonstrated a significant decrease in ALDH1A1 and CD133 expression[342]. ALDH1A1 and CD133 protein expression have also been shown to increase in FOLFOX resistant colorectal cancer cell lines, but the levels were reduced when treated with curcumin in combination with the src inhibitor dasatinib[342]. The curcumin analogue GO-Y030 has also been found to inhibit signal transducer and activator of transcription 3 phosphorylation in $ALDH^{High}$/CD133+ cells, accompanied by an increase in apoptosis in four different colorectal cancer cell lines. A decrease in spheroid formation was also observed in $ALDH^{High}$/CD133+ sorted cells following 24 hour treatment with 2.5—50 μM curcumin and subsequent analysis 10-15 days later.

Overall, curcumin appears beneficial at reducing 5-FU-induced NF-κβ signalling, and reducing TIC marker expression, advocating further investigation into its combination with FOLFOX in CRLM.

An inevitable phenomenon is the development of resistance to FOLFOX in patients. Curcumin may help abrogate resistance without increasing the amount or severity of side effects associated with many clinical agents. For example, curcumin can overcome oxaliplatin resistance both *in vitro* and *in vivo* in HCT116 oxaliplatin resistant cell lines[343]. Mice transplanted with oxaliplatin resistant cells were subject to treatment with curcumin, oxaliplatin or the combination with the latter being superior in terms of reduction in tumour volume, to either agent alone. Curcumin also abrogated the oxaliplatin-induced increase in the percentage of $ALDH^{High}$ tumour cells.

There is also evidence that curcumin may be able to reduce some common chemotherapy side effects. In rats, pre-treatment with curcumin followed by concomitant treatment with oxaliplatin, alleviated the nerve damage seen when oxaliplatin was administered alone[344]. In the Trembler-J mouse model of neuropathy curcumin alleviated the neuropathic phenotype with an increase in myelinated axons in sciatic nerves, and decreased apoptosis in Schwann cells[345].

It is common for chemotherapy regimens to cause side effects that necessitate dose de-escalation or treatment cessation. Combination treatment with curcumin may not only help improve efficacy, target TICs, reduce angiogenesis and disrupt the tumour microenvironment, but may also be able to alleviate side effects. This could potentially allow patients to finish the full course of their chemotherapy regimen without having to dose de-escalate.

1.10 **Aims**

The overall aim of this study was to assess whether adding curcumin to OX+5-FU provided a superior combination in terms of biological activity and potential efficacy in CRLM than without curcumin. For treatment of CRLM, one of the main criteria used was the effect upon spheroid growth and TIC marker expression (CD26 and CD133 expression plus ALDH activity). Markers were selected from the literature based on their reported specificity. To ensure the study remained translational and robust, only patient-derived material was used, as cell lines have been demonstrated to be less suitable for TIC research into CRC. Additionally, there are currently no commercially available cell lines derived from CRC liver metastases. Therefore, the initial objectives, which form the first results chapter of this thesis aim to characterise the patient samples collected throughout the course of the study. This included development of a method to culture patient's cells as spheroids with the hope this work would lead to the development of preclinical models that could also be used for assessing the anticancer activity of other agents in the future. The second results chapter explores which of the treatment combinations are superior, focusing on TICs and expression of TIC markers. For this analysis spheroids were used to enrich for TICs, and explant culture from patient CRLM was used as an *ex vivo* model to assess the effects of treatment on cells complete with a tumour microenvironment. Finally, the third results chapter aims to further the investigation of the combinations by assessing *in vivo* efficacy using a mouse xenograft model.

Due to sole use of patient tissue, and relevant doses, it was hoped this body of work would help aid the design of future clinical trials. Through the use and development of models which recreate the heterogeneity of the primary tumour, better than current 2D models, it was also hoped this would lay down foundations for future studies by identifying potential pharmacodynamic biomarkers that could be analysed in patient tissues to provide evidence of activity in humans.

Chapter 2: Materials and Methods

Reagents and Suppliers

Reagent	Supplier
5-FU for *in vitro* experiments	Medac, England
5-FU for NOD-SCID study	Sigma-Aldrich, Company Ltd. Dorset, UK
Aldefluor assay kit	STEMCELL Technologies Grenoble, France
Antimycotic/antibiotic	Fisher Scientific UK Ltd, Leicestershire, UK
ATPlite assay	Perkin Elmer, Cambridge, UK
B-27 supplement	Fisher Scientific UK Ltd, Leicestershire, UK
Collagaenase Type 4	Worthington Biochemical Corp. New Jersey, US
Culture plate insert, Organotypic 0.4µm pore size, 30mm diameter	Merk Millipore, Watford, UK
Curcumin	Sigma-Aldrich, Company Ltd. Dorset, UK
Diethylaminobenzaldehyde (DEAB)	Sigma-Aldrich, Company Ltd. Dorset, UK
Dimethyl sulfoxide (DMSO)	Sigma-Aldrich, Company Ltd. Dorset, UK
DMEM/F12 medium (1:1) Hyclone	Fisher Scientific UK Ltd, Leicestershire, UK
Dulbecco's modified eagle media (DMEM)	Sigma-Aldrich, Company Ltd. Dorset, UK
Epithelial Growth Factor (EGF)	Fisher Scientific UK Ltd, Leicestershire, UK
Ethanol	Fisher Scientific UK Ltd, Leicestershire, UK
Fibroblast Growth Factor (FGF)	Fisher Scientific UK Ltd, Leicestershire, UK
Foetal calf serum (FCS)	Invitrogen Ltd, Paisley, UK
Gentamycin	Sigma-Aldrich, Company Ltd. Dorset, UK
Glutamax	Invitrogen Ltd, Paisley, UK
Hanks balanced salt solution	Invitrogen Ltd, Paisley, UK
Heparin	Sigma-Aldrich, Company Ltd. Dorset, UK

HGF	Sigma-Aldrich, Company Ltd. Dorset, UK
Matrigel	BD Biosciences, Oxford, UK
McCoy's 5a modified media	Invitrogen Ltd, Paisley, UK
Media 199	Invitrogen Ltd, Paisley, UK
N-2 supplement	Fisher Scientific UK Ltd, Leicestershire, UK
Neurobasal medium	Fisher Scientific UK Ltd, Leicestershire, UK
Oxaliplatin for *in vitro* experiments	Sanofi Aventis, Surrey, UK
Oxaliplatin for NOD-SCID study	Sigma-Aldrich, Company Ltd. Dorset, UK
PBS tablets	Oxoid, Hampshire, UK
Propidium iodide	Sigma-Aldrich, Company Ltd. Dorset, UK
RNAse A	Sigma-Aldrich, Company Ltd. Dorset, UK
R-spondin	R&D Systems Europe, Oxfordshire, UK
Saline and glucose	Sigma-Aldrich, Company Ltd. Dorset, UK
Skin graft blade	Fisher Scientific UK Ltd, Leicestershire, UK
Syringes and needles	BD Biosciences, Oxford, UK
TC plasticware	Nunc/Appleton Woods
Trypan Blue	Sigma-Aldrich, Company Ltd. Dorset, UK
Trypsin/EDTA (T/E)	Invitrogen Ltd, Paisley, UK
Viewplate, 96-well,white	Perkin Elmer, Oxford, UK
WNT3a	R&D Systems Europe, Oxfordshire, UK

Table 2.1 Reagents and suppliers

2 Tissue culture

The 18Co cell line was grown under adherent conditions and maintained in 5% CO_2 at 37°C. They represent a normal colon fibroblast cell line purchased from the American Type Culture Collection. When cells reached approximately 70-80% confluency, they were passaged on to fresh plasticware.

To passage, cells were washed twice in phosphate buffered solution (PBS) and incubated in 5X trypsin/EDTA (T/E) for 5 min at 37°C. Once cells had detached, an equal volume of media containing 10% foetal calf serum (FCS) was used to inactivate the trypsin and the cells were pelleted (3 min, 240 xg). Cells were washed once in PBS, counted using a Z2 particle counter (Beckman Coulter), and re-plated at the desired cell density.

2.1 Processing of primary tumours

Tumour samples were collected from patients undergoing surgical removal of their colorectal liver metastases. Ethical approval for this fully anonymised, non-consented study was given by the Leicestershire, Northampton and Rutland Research Ethics Committee (REC reference number 09/H0402/45). Following surgical resection samples were immediately placed on ice in 10 mL of media 199 containing antibiotic/antimycotic and gentamycin.

The tumour was washed in media 199 containing antibiotic/antimycotic and gentamyacin and processed to a single cell suspension. If the tumour was large enough, it was divided up to provide small pieces of tissue (approximately 1 mm^3) to implant into each flank of a NOD-SCID mouse (2.10.1), and the remaining tissue used for explant culture (2.8.4).

To process tumours to a single cell suspension, they were first mechanically homogenised using scissors, before digestion with collagenase type IV (2000 U/mL, 40-60 min, 37ºC). A haemocytometer and trypan blue staining was used to confirm the presence of a viable single cell suspension. Subsequently, 10 mL of media 199 was

added, the suspension filtered through a 100 µm sieve and cells pelleted (5 min, 240 xg). The media was removed, the pellet re-suspended and washed again in 10 mL of media 199, and then filtered through a 40 µm sieve followed by two washes with Hanks Balanced Salt Solution. Cells were plated in 1 to 6 wells on an ultra-low attachment plate in stem cell media (see 2.3.1), and the remainder frozen in a freezing solution (90% FCS, and 10% DMSO). Cells were stored long term in liquid nitrogen until analysis.

2.2 **Stem cell media**

For the majority of spheroid cultures a defined stem cell media was used. To make 25 mL of media the following was mixed and filter sterilised into a 50 mL Falcon tube; 12.5 mL 50% neurobasal medium, 11.25 mL DMEM/F12 medium 1:1 hyclone, 0.25 mL 1% N-2 Supplement, 0.5 mL 2% B-27 Supplement, 0.5 mL 2% Antibiotic-antimycotic, 25 µL 2 ng/mL Heparin, and 10 µL of FGF and EGF to give a final concentration of 20 ng/mL of each.

2.2.1 Primary cell spheroid growth conditions and optimisation

2.2.2 Use of ultra-low attachment plates

The standard growth conditions for testing the spheroid forming potential of cells derived from patient samples was to seed cells into a 6-well ultra-low attachment plate containing 2 mL of stem cell media/well. Each well was supplemented with 500 µL of fresh stem cell media once weekly. This method has produced an approximate 50% success rate for primary colorectal cancer samples in this laboratory. However, under these conditions, only a few colorectal liver metastasis samples formed enough spheroids for experimental use, so the additional conditions below were tested to try and improve spheroid growth.

2.2.3 Assessing fibroblast-tumour direct cell co-culture for spheroid formation

18Co cells were used as a normal colonic fibroblast cell line to provide a feeder layer for tumour cell growth[78]. 18Co cells were seeded on to 6-well plates for adherent growth at 20,000/well in 2 mL of the appropriate media, and left to attach for three days (5% CO_2, 37°C). Subsequently, cells were washed with PBS, and 2 mL of stem cell media added, which contained a total of 30,000 patient-derived primary cells. Cells were then cultured in 10% CO_2 (37°C). Spheroid formation was observed by light microscopy every 7 days for 28 days using a Nikon TE 2000 U camera system combined with Eclipse software. This method was tested on five samples, and the spheroids that grew were passaged by 'blowing' the co-culture spheroids off the bottom of the plate using a Gilson p1000 pipette, and collecting spheroid-containing media. Spheroids were then centrifuged for 10 min at 150 xg, the supernatant removed and the pellet re-suspended in 1 mL of 5X T/E for 10 min at 37ºC. T/E was inactivated with an equal volume of media containing FCS, and the cells pelleted at 240 xg for 5 min. Cells were washed once in PBS and counted if required, re-pelleted, re-suspended in stem cell media and placed on pre-grown fibroblasts.

2.2.4 Assessing the potential of growth factors to promote spheroid formation

Three different patient samples that did not form spheroids under standard conditions using stem cell media in ultra-low attachment plates, were selected to see whether addition of three different growth factors would promote spheroid formation. Cells were seeded in ultra-low attachment plates in stem cell media at 50,000 cells/well. Growth factors R-spondin, Wnt-3a and Hepatocyte growth factor were added directly to each well to give a final concentration of 1 µg/mL, 100 ng/mL and 50 ng/mL, respectively[78,346]. Spheroid formation was visually assessed every 7 days for 28 days.

2.2.5 Assessing BD Matrigel as an extra-cellular matrix to promote spheroid formation

Matrigel provides a scaffold for cells to grow upon, and contains extra-cellular matrix proteins found within a tumour environment, such as laminin and collagen type IV. Matrigel was allowed to thaw overnight at 4°C, and all pipette tips and tubes used were kept at -20°C overnight, as matrigel forms a gel at room temperature. Whilst using the Matrigel it was kept on ice at all times until gelling was required. Matrigel was mixed 1:1 with cells in stem cell media and aliquoted into 2 wells of a 24 well plate. Sphere formation was assessed every seven days for 28 days.

2.2.6 Using tissue culture inserts to promote spheroid formation

Tissue culture inserts allow cells to be grown on a 6-well plate as normal, and another cell type to be grown above on a thin membrane which allows secreted factors to diffuse into the media between the two cell types (Figure 2.1).

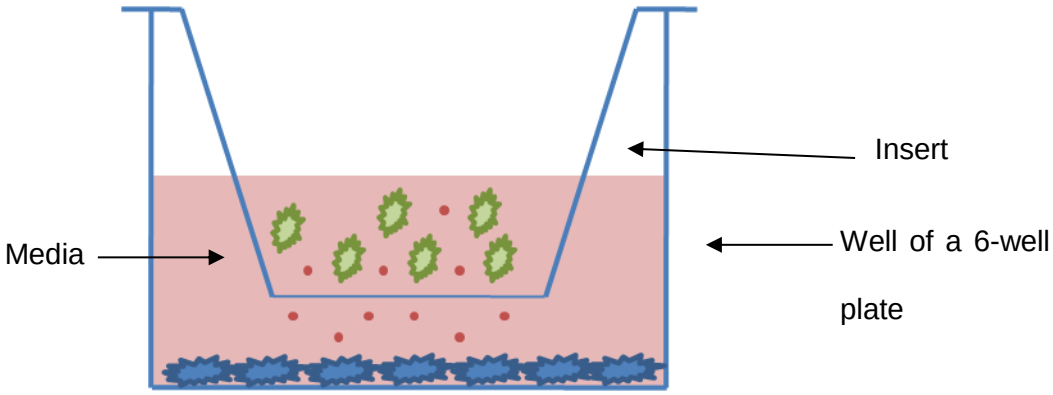

Figure 2.1 Schematic of an insert inside a 6-well plate depicting the co-culture conditions.
Blue cells represent the 18Co cells, green cells represent patient metastases cells. Red dots represent diffusible factors

18Co cells were seeded at 15,000 cells/well in 2 mL of media and left to adhere overnight. The media was then aspirated and replaced with 3 mL of stem cell media. The insert was placed into the well and a further 2 mL of stem cell media placed on top of the insert containing 30,000 cells from a patient CRLM. Sphere formation was assessed every seven days for 28 days.

2.2.7 Assessment of 18Co conditioned stem cell media on spheroid formation

The method for making conditioned stem cell media has been reported previously[78]. Stem cell media was conditioned by seeding 750,000 18Co cells into a 75cm^2 flask for 24 h. After which, cells were washed twice with 10 mL of PBS and incubated for 24 h with 10 mL of stem cell media, minus EGF and FGF. This was subsequently aspirated, cleared of any debris by centrifugation, and then mixed 1:1 with normal stem cell media. The conditioned stem cell media was used to seed 30,000 patient metastases cells in 2 mL of media/well on to an ultra-low attachment plate. Spheroid formation was assessed every seven days for 28 days.

2.3 **Passaging spheroids**

For the remaining experiments, all spheroid growth was carried out using standard conditions (stem cell media in ultra-low attachment plates). To obtain a single cell suspension to seed for an experiment or for flow cytometric analysis, spheroids were filtered through a 40 µM sieve, so that any spheroids larger than 40 µM were captured. If spheroids were being passaged to bulk up cell number then they were not filtered first. Spheroids were pelleted by centrifugation (10 min, 150 xg), the supernatant was removed, the cell pellet re-suspended in 1 mL of 5X T/E and incubated for 10 min at 37ºC. T/E was subsequently inactivated using an equal volume of media containing FCS, the cells pelleted at 240 xg for 5 min, washed in 10 mL of

PBS and counted, if required. Cells were then pelleted again and re-suspended in stem cell media and plated, or used for experiments.

2.4 **Differentiation of patient derived spheroids**

Spheroids were filtered through a 40 µM sieve, allowing single cells to pass through and spheroids larger than 40 µM to be captured. The spheroid suspension was pelleted at 240 xg and re-suspended in high glucose DMEM media, supplemented with 20% FCS. The mixture was aliquoted into normal adherent 6-well plates at 2 mL/well, which had been pre-incubated with vitronectin (approximately 1 µg/cm^2) for a minimum of 1 h. Media was replaced weekly, and cells passaged once confluency reached approximately 70%.

Cells were passaged by removing all media, washing in PBS, and incubating with 5X T/E for 5 min. T/E was inactivated using media containing FCS, and cells pelleted at 240 xg. The pellet was washed in PBS once before re-suspending and plating again under the same conditions at 200,000 cells/well. With each passage an aliquot of cells was profiled by flow cytometry for TIC marker expression. Additionally, another aliquot was also placed under low attachment conditions to assess the ability of differentiated cells to re-form spheroids, which were subsequently re-profiled for TIC marker expression once spheroids had reached an average size of approximately 50 µm.

2.5 **Flow cytometry**

All flow cytometry and fluorescence activated cell sorting (FACS) was carried out using a BD FACSAria II, with analysis undertaken using BD FACSDiva software version 7. Sterile sorts were conducted at 4°C, and the cells sorted into stem cell media. Sorts for proteome profiling were into DMEM, supplemented with 10% FCS and at 4°C.

2.5.1 Assessment of ALDH1 activity: the Aldefluor assay

Assessment of ALDH1 activity was undertaken using the Aldefluor assay kit, with all steps carried out under low light conditions. The basis of the Aldefluor assay is that the enzyme ALDH1 converts BODIPY-aminoacetaldehyde (BAAA) (which passively diffuses through the cell membrane), from a non-fluorescent molecule to BODIPY-aminoacetate (BAA) which is fluorescent, and is retained within cells in the presence of the efflux inhibitor, verapamil (Figure 2.2). BAA is excited at 488 nm and its emission detected using a 530±30 nm filter.

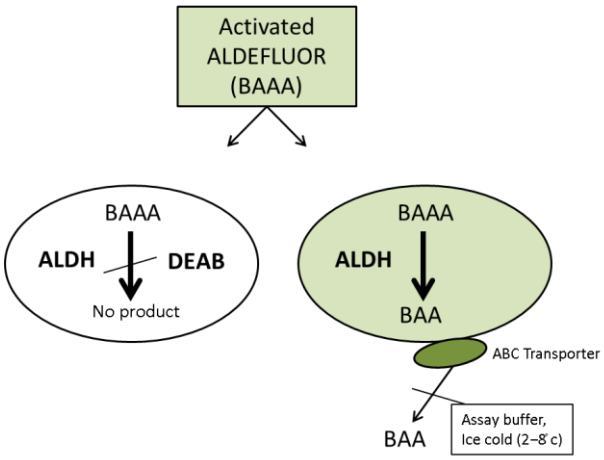

Figure 2.2 An overview of the Aldefluor assay
If the ALDH1 enzyme inhibitor (DEAB) is included in the incubation then no fluorescent product is produced from the BAAA substrate, as DEAB inhibits the ALDH enzyme activity. In the presence of a functional ALDH1 enzyme BAAA is converted to BAA which can be detected using a flow cytometer. Cells are maintained on ice until analysis (after an incubation to allow for the substrate to be metabolised) to prevent efflux of the fluorescent substrate through ABC transporters.

Up to $1x10^6$ cells were re-suspended in 1.5 mL of Aldefluor buffer, and divided into three tubes; a negative control sample to which 5 µL of DEAB was added followed by 2.5 µL of BAAA, a test sample to which 2.5 µL of Aldefluor reagent only was added, and an unstained control. The samples were incubated for 40 min at 37°C, followed by washing with 500 µL of Aldefluor buffer. After washing, cells were re-suspended in 500 µL Aldefluor buffer, and stored on ice in the dark for immediate FACS analysis.

2.5.2 Determining the activity of ALDH, and expression of EpCAM, CD133 and CD26

Cells were analysed for the combinations of ALDH activity, EpCAM and CD133, or CD26, CD133 and EpCAM expression. CD26 is conjugated to FITC and is detected using the same settings as the Aldefluor reagent BAA, so ALDH activity and CD26 expression were never both examined in the same sample together.

The Aldefluor assay protocol was followed (see 2.4.1) with the exception of washing on the final step. Following the incubation period, the samples were pelleted (3 min, 240 xg), and re-suspended in 100 µL of Aldefluor buffer. Antibodies were added to the appropriate tube at the following concentrations: CD133 1:10, EpCAM 1:10, CD26 1:5, FITC-isotype control 1:5. To assess the combinations of CD133, EpCAM and CD26 the unstained cells were used as an appropriate control, as the BAA substrate present in the Aldefluor controls resulted in considerable fluorescence in the FITC channel. Single stained controls, and combinations (standard fluorescence minus one) were used to assess whether there was any crossover between fluorescence channels.

Following incubation with the appropriate antibodies, each sample was washed with 500 µL of Aldefluor buffer, re-suspended in 500 µL Aldefluor buffer and placed on ice for immediate analysis. The unstained sample was used to gate CD133 and EpCAM, the DEAB control samples used to gate ALDH activity, with the FITC-isotype control used for CD26 gating. CD133 was conjugated to allophycocyanin (APC), excited at 635 nm and detected using the 670±14 filter. EpCAM was conjugated to R-phycoerythrin (PE), excited at 561 nm, and was detected using the 582±15 filter. Any cross-over in fluorescence between FITC, APC and PE were eliminated using the compensation feature on the BD FACSAria II software.

2.5.3 Assessment of spheroid growth capacity from cells with different expression of putative TIC markers

Spheroids were grown until they were on average approximately 50 µm in size, whereupon they were assessed for ALDH activity, CD133, CD26 and EpCAM expression. The following EpCAM+ populations were sorted by purity for growth: $ALDH^{High}$/CD133-, $ALDH^{High}$/CD133+, $ALDH^{Low}$/CD133+, $ALDH^{Low}$/CD133-, CD26+/CD133-, CD26+/CD133+, and CD26-/CD133+ and CD133-/CD26-. Cells were sorted into 250 µL of stem cell media at 4ºC and were subsequently pelleted at 240 xg for 5 min. The supernatant was removed, the cells re-suspended in 2 mL of stem cell media and put into one well of an ultra-low attachment plate. Plates were left for four weeks before counting spheroid growth and re-analysing for expression of CD133, CD26, EpCAM and ALDH activity.

2.6 **Analysis of pluripotent stem cell markers in FOLFOX treated and naïve patient samples**

To analyse differences in expression of an array of 15 pluripotent stem cell markers between FOLFOX treated and naïve patient samples, a proteome profiler array was used (R&D systems). $EpCAM^{+}$ cells were isolated from bulk tumour samples by fluorescence activated sorting and frozen until used for the array. Lysates were made by incubating sorted cells in lysis buffer (10 mL lysis buffer 16, provided in the kit, 1 phosphostop tablet, one complete protease inhibitor cocktail tablet) overnight at -80°C. For the array, 40 µg of protein was used and the manufacturer's protocol followed. In brief, each pre-printed array membrane was incubated in array buffer 1 for 1 h, the buffer removed, and the membrane incubated with array buffer 1 containing cell lysate overnight at 4°C with gentle rocking. Subsequently, each array was washed three times in wash buffer followed by incubation with the detection antibody cocktail diluted in array buffer 2/3 (2 h, with gentle rocking). Each array was washed again,

prior to incubation with streptavadin-HRP diluted in array buffer 2/3 (30 min, with gentle rocking). After washing, each array was incubated for 1 min with enhanced chemiluminescence (ECL) reagent, covered in Saran wrap, and exposed to x-ray film for 3-5 min. Densitometry was performed using the Syngene Bioimaging system, (Syngene, UK). The software package used for quantitation was Gene Tools version 3.03.03 (Syngene, UK).

2.7 **Oxaliplatin, 5-FU and curcumin treatments**

All treatments were carried out, unless otherwise stipulated, at the following concentrations: curcumin 5 µM, oxaliplatin 2 µM, 5-FU 5 µM. These concentrations are based upon previous studies and pharmacokinetic conversion of doses [347-349].

2.7.1 Treatment of spheroids derived directly from the patient or patient tissue serially passaged in NOD-SCID mice

Cells were seeded at 100,000 cells/well, with the exception of two samples, (MP4P066 and P153), where 20,000 cells were seeded/well in 2 mL of media. These two samples grew far more aggressively than previously observed for other samples, and so fewer cells were needed to produce enough spheroids for endpoint analyses. One 6-well plate was used per treatment, and P153 and MP4P066 were treated with all combinations of oxaliplatin, 5-FU and curcumin using a DMSO only control. Mouse passaged samples were treated with DMSO only, curcumin, OX+5-FU and the triple combination. DMSO concentrations were kept equal between all treatments and did not exceed 0.05%. The cells were allowed to grow for two weeks with repeat treatments of 5 µM curcumin in those incubations which contained curcumin, on days 5, 8, and 12. After 15 days, two wells per plate were used for sphere counting and size assessment.

To count the spheres, media containing spheres from one well was pelleted at 150 xg for 10 min and the supernatant discarded to leave approximately 30 µL of

media. Spheres were gently resuspended in this residual media and pipetted on to a gridded glass slide bordered by silicon grease to act as a seal. The sphere suspension was then placed onto the glass slide and a glass cover slip placed on top to form a seal. All the treatments were randomised prior to counting, and the counts undertaken blind. Flow cytometric analysis for EpCAM, CD133 and CD26 expression, and ALDH activity (see section 2.6.2) was performed on spheres from the 4 remaining wells.

2.7.2 Analysis of the expression of pluripotent stem cell markers in spheroids following FOLFOX ± curcumin treatments

Cells derived from spheroids were seeded at 100,000 cells/well with one plate/treatment. A total of four treatments only were seeded, due to the large numbers of cells required for the proteome profiler array. The treatments were: DMSO, curcumin, OX+5-FU and the triple combination. Each plate was seeded in duplicate so that cells could be analysed at 24 and 72 h. The spheroids were grown for two weeks prior to filtering through a 50 µm sieve. Spheroids were pelleted at 150 xg for 10 min, re-suspended in media containing the relevant treatments and re-plated. To harvest cells, the same procedure used for passaging cells was undertaken (2.3.7). The single cell suspension created was washed twice in 1 mL of PBS, pelleting each time at 240 xg for 5 min. After the final wash, cells were pelleted again, and the pellet frozen at -20ºC until required. For pluripotent protein expression analysis, the pluripotent stem cell marker array was used as described in 2.7

2.7.3 The effects of treatments on the proliferation of patient-derived differentiated cells

Cells were propagated for 4 passages as adherent cells before seeding at 10,000 cells/well in 100 µL of media in a 96-well plate, which had been pre-incubated with fibronectin for 1 h. Cells were left for two days to adhere before the media was

removed and replaced with media containing all combinations of curcumin, oxaliplatin and 5-FU, including a control of DMSO only. Each treatment was replicated 8 times in a 96-well Viewplate (Perkin Elmer, UK). The effects on proliferation were assessed using the ATPlite assay (Perkin Elmer, UK) seven days after cells were treated.

The ATPlite assay was performed as described in the manufacture's protocol. The ATPlite assay provides a sensitive method for detecting and quantifying adenosine triphosphate, which is a marker of cell viability, and decreases rapidly when cells undergo cell death. The method works by measuring the amount of luminescence produced when ATP reacts with D-luciferin in the presence of luciferase. The amount of light emitted directly correlates with the amount of ATP. In brief, the reagents were allowed to warm up to room temperature, and the lyophilised substrate re-constituted using 25 mL of substrate buffer solution. Fifty µL of cell lysis solution was added directly into each well containing cells in the Viewplate. The plate was then agitated at 700 rpm on a plate shaker (Shaker orbit P4, Labnet, Woodbridge, NJ) for 5 min, before addition of 50 µL of the reconstituted substrate solution The plates were again agitated for 5 min at 700 rpm, before being dark adapted for 10 min. Plates were measured using a FLUOstar Optima plate reader (BMG Labtech, Bucks, U.K.) set-up in luminescence mode.

2.7.4 The effects of treatments on air-interface organotypic explant culture

The method used was developed by Twiddy et al, Breast Cancer Research, 2010[350], and established for NSCLC by E. Karekla. Tumour tissues derived directly from resection material were cut into small (approximately 1 mm^3) pieces, and then randomly allocated onto organotypic inserts (Millipore) floating on 1.5 mL of DMEM + 1% FCS + 2% antibiotic/antimycotic. Tissues were left overnight before half of the media was removed and replaced with media containing appropriate treatments for 24 h, followed by harvesting. To harvest the tissues, inserts were gently washed in 1.5 mL

PBS to avoid disturbing the tissue orientation, and the tissue placed between sponges soaked in 70% ethanol in an immunohistochemistry cassette. The tissue was fixed for 24 h before paraffin embedding and sectioning. During this process, it was essential that the orientation of the tissues remained identifiable, in order that comparable surfaces at the air interface could be analysed following treatments.

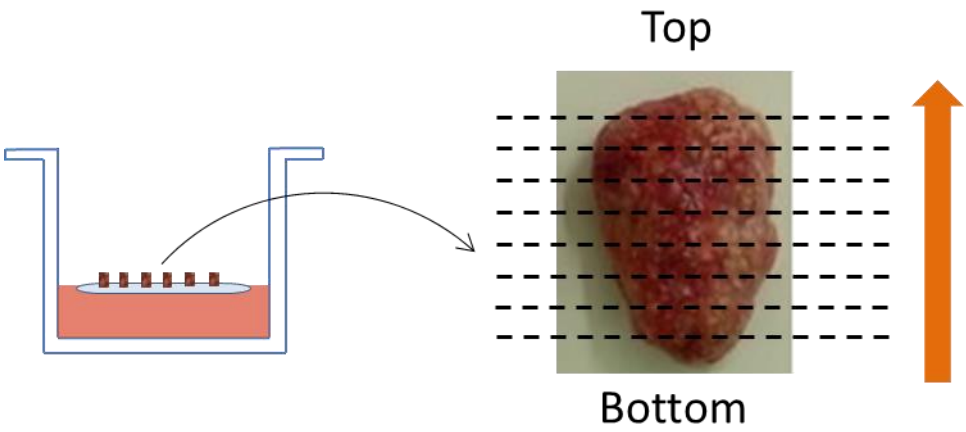

Figure 2.3 Explant culture
Depiction of tumour orientation on the organotypic inserts. Only one surface is in contact with the treated media, so maintenance of the correct orientation is essential in order to assess drug penetration throughout the explant.

2.8 **Immunohistochemistry**

2.8.1 De-paraffinization and re-hydration

Paraffin embedded tissue was cut into 4 µm sections and adhered to polysine™ coated slides (Thermo Scientific, UK). To remove the paraffin, slides were first heated to 65ºC until the paraffin melted, at which point they were immediately placed into xylene for 3 min x2 This was followed by a rehydration step consisting of immersion in 99% industrial methylated spirits (IMS), x 2 for 3 min, followed by immersion in 95% IMS x1 for 3 min, and then the slides were left under running tap water for 5 min. After de-paraffinization and re-hydration, slides were ready for antigen retrieval and subsequent staining.

2.8.2 Antigen retrieval

Two different antigen retrieval buffers were used depending upon the antibody of interest; 10 mM citrate buffer pH 6 and Tris/EDTA pH 9 (see Table 2.4). Citric acid buffer pH 6 was made by dissolving 2.1 g of citric acid monohydrate in 1 L of UP water and the pH adjusted to 6 using 2 M NaOH. Tris/EDTA buffer was made by first preparing a 100x stock solution by dissolving 0.95 g of EDTA and 3 g of Tris in 25 mL of UP water. The stock solution was then pH adjusted to 9 using HCl, and 10 mL of the stock added to 1 L of UP water to give 10 mM Tris/1.3 mM EDTA. Antigen retrieval buffer was made fresh prior to use.

For antigen retrieval, slides were placed into 1 L of antigen retrieval solution and microwaved on full power for durations of up to 20 min, depending on the antibody used.

2.8.3 Novolink polymer detection system

The Novolink polymer detection system (Novocastra Laboratories, Newcastle-upon-Tyne, United Kingdom) was used, following the manufacturer's guidelines, with variations in antibody and slide wash times. Each wash step consisted of two washes in PBS for 5 min.

After antigen retrieval, slides were cooled by immersing in PBS, and a hydrophobic barrier drawn around tissue sections. Excess PBS was removed from the slides before incubation with peroxidase block for 5 min. Slides were washed followed by incubation with protein block for 5 min. Slides were again washed before incubation with 100 µL of primary antibody diluted in PBS/3% BSA/ 0.1% triton-X-100. Negative controls were incubated with either an isotype control at the same concentration as the primary antibody, or PBS instead of the primary antibody. After primary antibody incubation, slides were washed followed by incubation with the post-primary block for 30 min, then washed again and incubated with the Novolink™ polymer for 30 min.

Afterwards, slides were washed with gentle rocking before incubating for 5 min with a working DAB solution (50 µL of DAB chromogen to 1 mL of Novolink Dab substrate buffer). Slides were then rinsed in tap water to end the reaction, and counterstained in Mayer's Haematoxylin for 2 min before leaving under running tap water for 5 min and re-hydrating though graded IMS washes (1x 95%, 2 x 99%) and twice in xylene, each for 3 min. Slides were mounted by wiping away excess xylene, placing a small amount of distyrene plasticizer xylene on a cover slip and gently placing the slide on top. A small amount of pressure was briefly placed on the cover slip using a p200 pipette tip to ensure that the distyrene plasticizer xylene spread evenly across the tissue. Slides were left overnight to dry before imaging/scoring.

Antibody	Dilution	Supplier	Incubation time	Antigen retrieval buffer
ALDH1A1	1:400	BD Biosciences	2 h at RT	Citric acid buffer pH 6
Cleaved caspase 3	1:50	New England Biolabs	2 h at RT	Tris/EDTA buffer pH 9
CD133 (AC133)	1:50	Miltenyi Biotec	2 h at RT	Citric acid buffer pH 6
CD26	1:500	Novus Bio	2 h at RT	Citric acid buffer pH 6
ERCC1	1:150	Thermo Scientific	2 h at RT	Citric acid buffer pH 6
XRCC1	1:150	Santa Cruz Biotechnology	2 h at RT	Citric acid buffer pH 6
Ki67	1:100	Dako	2 h at RT	Citric acid buffer pH 6
MLH1	1:20	BD Biosciences	2 h at RT	Citric acid buffer pH 6
MSH2	1:100	Merck	Overnight at 4ºC	Citric acid buffer pH 6
MSH6	1:100	BD Biosciences	2 h at RT	Citric acid buffer pH 6
Nanog	1:500	New England Biolabs	Overnight at 4ºC	Citric acid buffer pH 6

Table 2.2 IHC antibodies and optimised conditions of use.

2.9 **Animal Studies**

Animal studies were carried out under animal project license PPL 80/2167, granted to Leicester University by the United Kingdom Home Office. The experimental design was vetted by the Leicester University Local Ethical Committee for Animal Experimentation and met the standards required by the UKCCR for animal welfare.

All animal work was performed on male NOD.C.B-17/JHliHsd-Prkdc^{scid} (NOD-SCID) mice ordered from Harlan Laboratories aged 5-6 weeks. Mice were kept for one week to acclimatise before being used for any experimental procedures.

2.9.1 Serial passaging of colorectal liver metastasis tissue in NOD-SCID mice

Tissue for implantation was first washed three times in media containing anti biotic/antimycotic and gentamicin before cutting into small chunks of approximately 1 mm^3. NOD-SCID mice were anesthetized by exposure to isoflurane and tissue samples placed inside subcutaneous pockets made on both flanks. Mice were sutured or glutured, and the tissue left to grow for up to 6 months, after which the mouse would be culled if no tumour growth was observed. Tumours were measured once a week, and removed and passaged into a new mouse once the tumour had reached approximately 5% of the mouse's body weight (tumour diameter of approximately 17 mm), or the tumour ulcerated. Upon harvesting a tumour from a mouse, tissue not used for serial passaging was processed as described in 2.1.3.

2.9.2 Pilot Study investigating the combination of curcumin with oxaliplatin and 5-FU

A pilot study was performed to assess whether the drug concentrations and regimens used were efficacious in primary patient-derived xenografts. The combination of oxaliplatin and 5-FU has not previously been used for *in vivo* studies in our laboratory or in this mouse model, therefore this small orientation study was necessary

prior to performing more definitive large-scale experiments, if results indicated further investigations were warranted.

NOD-SCID mice were subcutaneously inoculated in their flank, with 100,000 patient spheroid derived cells in stem cell media mixed 1:1 with Matrigel. The study consisted of four groups with five mice in each:

1: Control Epikuron diet only (0.903% Epikuron)

2: Meriva® diet only (1.13% Meriva® corresponding to 0.2% curcumin and 0.903% Epikuron

3: OX+5-FU on Epikuron diet (0.903% Epikuron),

4: OX+5-FU on Meriva® diet (1.13% Meriva®)).

Mice were fed on standard irradiated pellets (5LF-2) until the first tumour became palpable. The diet was then switched to Meriva® for groups 2 and 4, and Epikuron for groups 1 and 3. Epikuron is made of phospholipids isolated from soy lecithin, which are used to encapsulate curcumin to form Meriva®^{TM}, which contains 20% curcumin by mass. After one week on Meriva®/Epikuron diet the chemotherapeutic intervention began. This consisted of *i.p.* injections of oxaliplatin (7.5 mg/kg in 5% glucose) and 5-FU (50 mg/kg in saline) once every 2 weeks. Oxaliplatin and 5-FU cannot be administered concurrently, so were given on sequential days. The mice that were not in a group receiving chemotherapy were administered ‘mock’ saline/5%-glucose injections instead.

Mice were kept on study until their tumour size reached 5% of their body weight (tumour size approximately 17 mm in diameter) or if they suffered from tumour ulceration. Mice received a maximum of 6-cycles of chemotherapy (each cycle lasts two weeks).

At the end of the study, mice were culled, and tumours harvested and divided up for the following experimental procedures: generation of a single cell suspension for flow cytometric analysis; HPLC analysis of curcuminoids; formalin fixation for

histological analysis. Additionally, the lungs, kidneys and liver were removed for pathological examination to identify any signs of treatment-related toxicity

2.9.3 Analysis of curcumin concentrations in tumours and mouse diets by high performance liquid chromatography (HPLC)

Tissue was frozen and stored at -80ºC until required. To analyse the levels of curcumin, liquid phase extraction of was performed as follows: Tissue samples were weighed, and 2 x equivalents of PBS added, prior to homogenisation. Following homogenisation, 300 µL was taken and mixed with 9:1 acetone:formic acid, vortexed, and incubated for 30 min at -20ºC. Samples were then vortexed and centrifuged at 5000 xg for 20 min. The pellet was discarded and the supernatant concentrated to dryness using a SPD1010 Speedvac® system (ThermoSavant, Holbrook, NY). The samples were reconstituted in 100 µL of 10 mM ammonium acetate in water:100% acetonitrile in a 50:50 ratio. Samples were analysed by HPLC on a Waters, UK HPLC system using a dC18 3 µm Atlantis column (Waters) kept at 25ºC. A flow rate of 1 mL/min, and injection volume was 50µL was used, with UV detection at 426 nm. Data acquisition was done using Empower software.

The above method was also used to analyse the amount of curcumin present in the Meriva® and Epikuron diets.

2.10 **Statistics**

All statistics were performed using SPSS version 18. Data were first tested for normality, and then the appropriate parametric or non-parametric paired or independent t-test was applied. P-values equal to or lower than 0.05 were considered significant. Statistical analysis of the explant culture experiments was conducted based on advice from a statistician, Dr. Maria Viskaduraki (University of Leicester Bioinformatics and Biostatistics Analysis Support Hub).

Chapter 3: Characterisation of TIC populations in CRLM

3 Introduction

The aim of this chapter was to analyse the TIC population in CRLM, and to ascertain whether there were any differences between TIC profiles in tumour tissue of patients who received chemotherapy compared to those patients who had not. An additional aim was to investigate possible associations with a number of other demographic and treatment-related factors which may affect TIC profiles. For example, it has been reported that TIC markers increase with age[351], and previous publications have described an increase in TICs after treatment with chemotherapy drugs[128].

In order to functionally assess TIC populations in CRLM, a suitable culture system was required that allowed their propagation and manipulation. Growing cells as spheroids has been reported to be a superior model of growth compared to 2D cultures, as cells maintain 3D cell-cell contact, and have gradients of nutrients and oxygen which more closely mimic *in vivo* tumours[352]. Furthermore, spheroids are enriched for TICs, maintaining cells in an undifferentiated stem-like phenotype, which has been demonstrated for several tumour types[101,353,354]. Despite the widespread use of spheroid cultures for propagating TICs, robust methodology for culturing cells directly from patients (as opposed to cell lines which grow easily), is not available in the literature, with many citations often only using small sample sets (2-5 samples)[101,355-357]. Therefore, a further aim of this chapter was to define a spheroid culture method that would allow studies to be conducted investigating how TIC populations could best be maintained long-term and also enable assessment of the effects of chemotherapy agents +/- curcumin on the TIC population of CRLM. Additionally, the expression of pluripotent stem cell markers was also determined in patient samples, some of which have previously been shown to be associated with TICs[133,135,358]. This approach may help to identify whether there are any highly expressed pluripotent stem cell markers which may lend themselves as functional TIC markers in CRLM. Overall, it is anticipated that more rigorous characterisation of the TIC markers across a

heterogeneous patient cohort, should allow for a more insightful analysis of these markers in response to therapy; this is assessed in Chapter 4.

3.1 Patient demographics

A total of 67 CRLM tissues were collected from patients undergoing resection at the Leicester General Hospital between the period of November 2009 and September 2013.

The mean patient age at time of resection was 67 ± 9 (SEM) years (N=43 with known age), with 24 females and 42 males (the gender of one patient remained unascribed). Information regarding whether a patient had received chemotherapy was only obtainable for 50 people, and revealed that 36 patients had previously been treated, whilst the remaining 14 were chemotherapy naïve. A summary of the chemotherapy information for the 36 patients who received it is presented in table 3.1.

Patient treatment information	Patient numbers
Patients in receipt of chemotherapy	36
Neo-adjuvant hemotherapy for primary tumours	4
Adjuvant chemotherapy for primary tumours	29
Neo-adjuvant chemotherapy for liver metastases	10
Treatment modality (%):	
FOLFOX	38
Capecitabine	35
Folfox+Cetuximab/Bevacizumab	21
FOLFIRI	3
CAPOX	3

Table 3.1 A summary of the chemotherapy information for the patients in receipt of chemotherapy within the cohort of patients used

3.2 **Expression of TIC markers**

Tumours were profiled for the following TIC markers; EpCAM, CD133 and CD26 expression, and ALDH activity. The flow cytometry profiles for five patients were omitted due to no viable cells. Inclusion of EpCAM in this context was two-fold; not only was it used to identify epithelial cells, thereby preventing interference by contaminating surrounding stromal cells, but it is also thought that high EpCAM expression is associated with TIC traits[359]. Analysis of CD26 expression began half way through the study following publication of an article demonstrating it may be a specific marker for metastatic TICs[136], and therefore a smaller number of samples were analysed (43/62) compared to the other three markers (62/62). All possible marker combinations were assessed, with the exception of the ALDH/CD26 combination, due to similar fluorescence emission spectra for ALDEFLUOR (520-540 nm), and FITC-conjugated CD26 (525 nm). However, this was not considered to be problematic, as the $ALDH^{High}$ population was very small, or was absent, in the majority of CRLM samples. An example of the gating used is demonstrated in figure 3.1, and this was used throughout this thesis. The same gating method was also used when CD133 was combined with CD26.

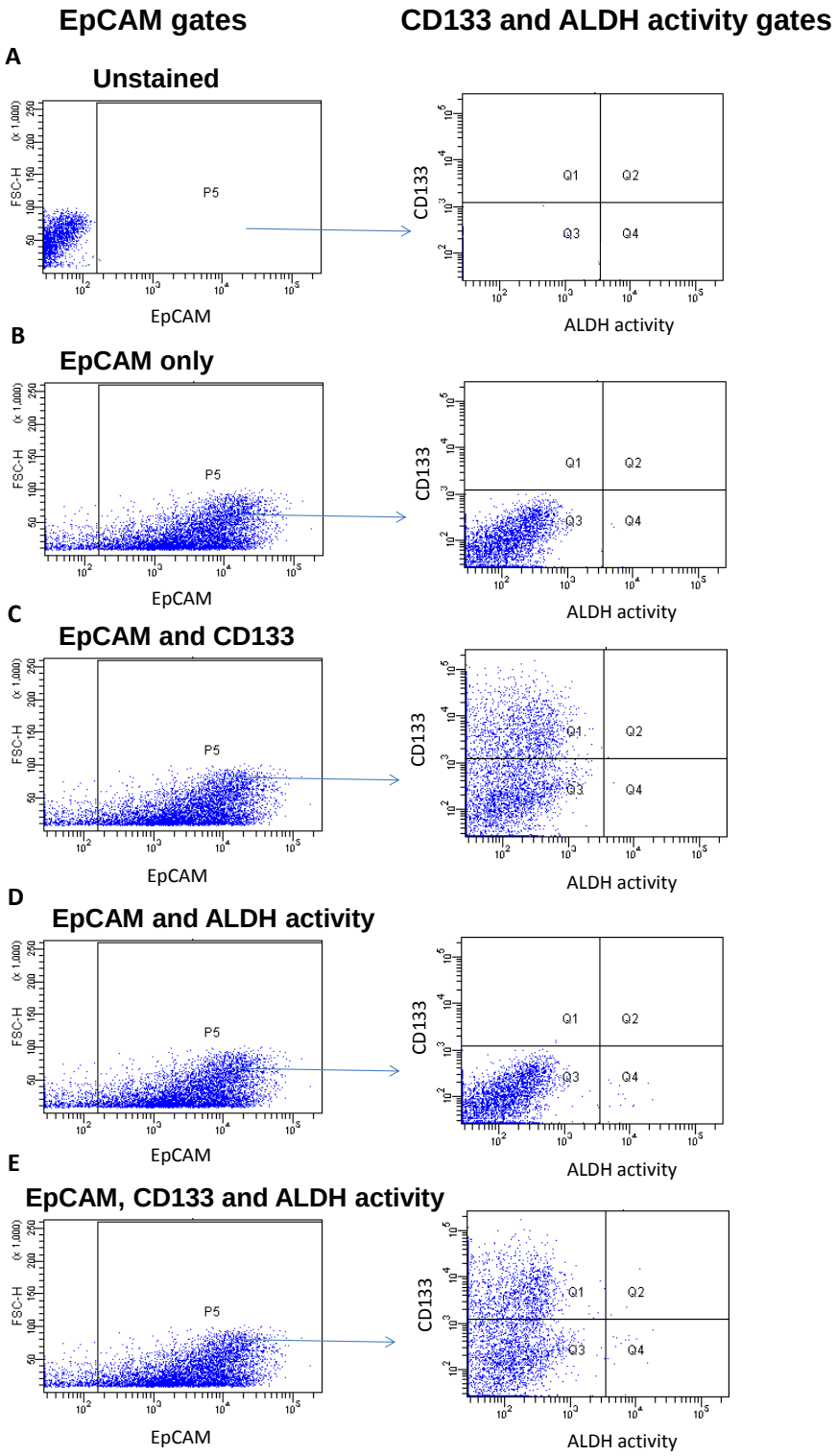

Figure 3.1 An example of the gating used for flow cytometric analysis of EpCAM, CD133 and ALDH activity

The left dot plots represent EpCAM staining and the right correspond to the expression for CD133 with ALDH activity (within the EpCAM positive population). (A) Unstained cells, used to set the EpCAM gate. (B) EpCAM antibody only, to set the gating for CD133 with ALDH activity. (C) EpCAM with the CD133 antibody. (D) EpCAM antibody and the aldefluor reagent (note the very small positive population). (E) EpCAM and the CD133 antibodies, and the aldefluor reagent.

To assess whether differences between expression patterns of TIC markers were associated with patient demographics, their expression was correlated with gender, age and chemotherapy status (Figure 3.2). Significant increases were seen between males and females for expression of TIC marker combinations incorporating CD133 within the EpCAM+ population of 6-11%, with females having a higher expression than males. No significant differences were seen between the percentage of EpCAM+ cells with gender. Age was not correlated with the activity/expression of each TIC marker within the EpCAM+ population, or the overall EpCAM levels, exhibiting an R correlation value of 0.01, 0.009, 0.00001 and 0.0002 for ALDH, CD133, CD26 and EpCAM alone, respectively (Figure 3.2D).

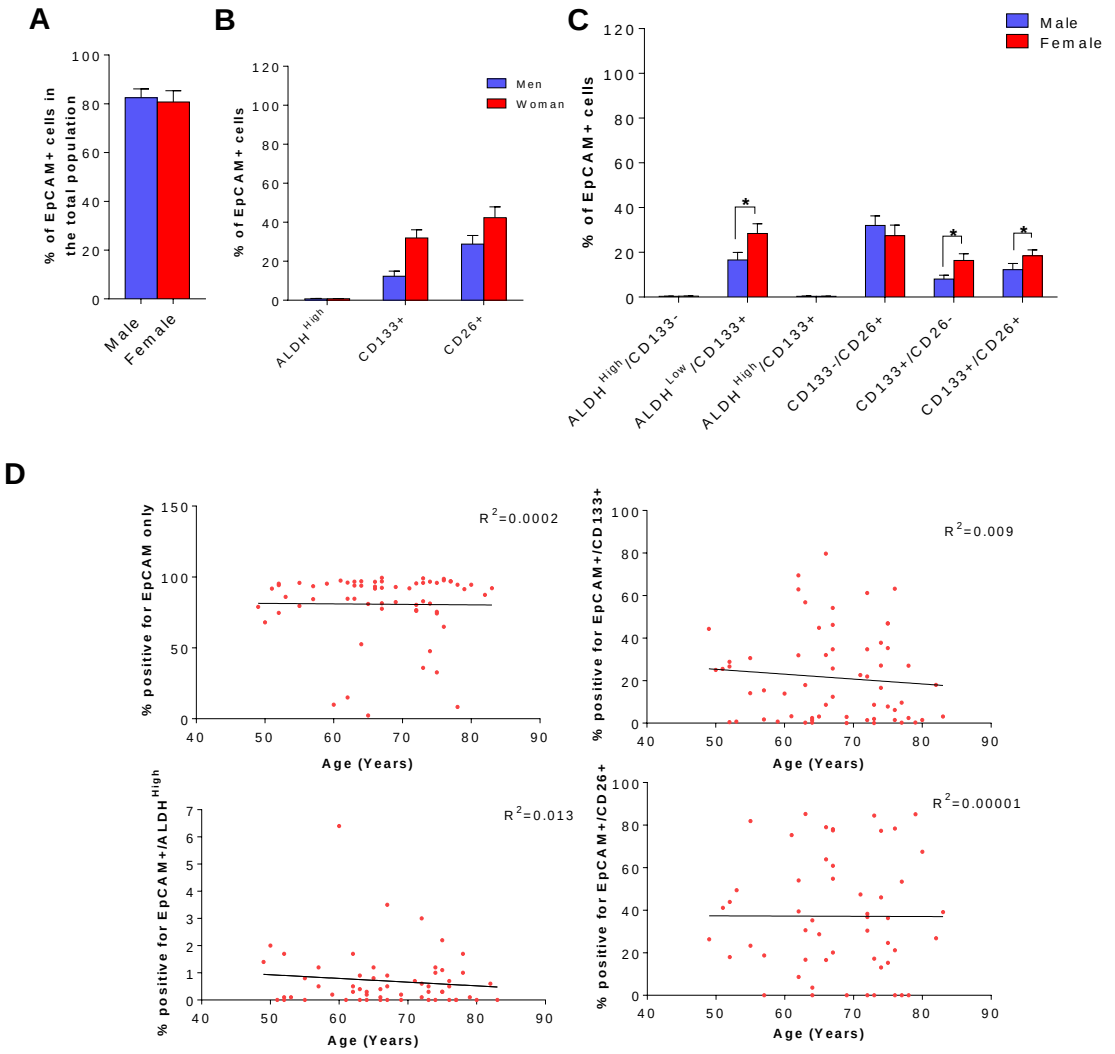

Figure 3.2 Analysis of the effects of age and gender on TIC marker expression
(A) The effects of gender on EpCAM expression analysed by flow cytometry in samples taken from patients undergoing resection for colorectal liver metastasis, male N=39, female N=22. (B) The same patients in (A) but analysing the average TIC marker expression/activity as a percentage of the EpCAM population. In (C) the same data presented in (B) is represented but with combinations of the markers. Error bars represent the SEM. * indicates significant differences where =P≤0.05. (D) To assess whether age is associated with TIC marker expression, a scatter plot of age vs expression/activity was performed with a line of best fit and the R^2 value indicating correlation: EpCAM N=62, CD133 N=62, ALDH N=62, CD26 N=44.

Significant differences were also observed when patients were stratified based on their chemotherapy status (Figure 3.3A). Patients who had not received chemotherapy at any point prior to surgery (chemo-naïve) had significantly higher levels of $ALDH^{Low}$/CD133+ cells compared to patients who had received therapy (chemo-treated), 25.8% vs 14.8% respectively, P=0.009. The CD26-/CD133+ and CD26+/CD133+ populations also decreased by 7% and 2%, respectively, in the naïve vs treated cohort but these changes were not significant. Additionally, patients who had received chemotherapy exhibited increased CD26+/CD133- expression (25% naïve vs 33% treated, example of a patient shown in figure 3.3B); this difference did not reach significance due to one chemo-naïve patient having very high CD26+/CD133 expression compared to the rest of the chemo-naïve group. The proportion of $ALDH^{High}$ cells was so low that is was hard to detect any differences between populations. Chemo-naïve and -treated populations of $ALDH^{High}$/CD133- and $ALDH^{High}$CD133+ cells were 0.43% vs 0.39% and 0.45% vs 0.24%, respectively. However, these results mask data that was only revealed when patients were further stratified by gender (Figure 3.3C). These results demonstrate that it is the male patients that account for the decrease in the $ALDH^{Low}$/CD133+ population, with no significant differences seen between male and female TIC marker expression when comparing only naïve patients. Yet males who had received therapy had a significant decrease in $ALDH^{Low}$/CD133+ cells compared to women who had received therapy (P=0.025, 23 vs 5% in women and men respectively). A significant decrease was also seen in the CD133+/CD26+ population in males who received therapy compared to women (P=0.024, 18 vs 2% in women and men respectively).

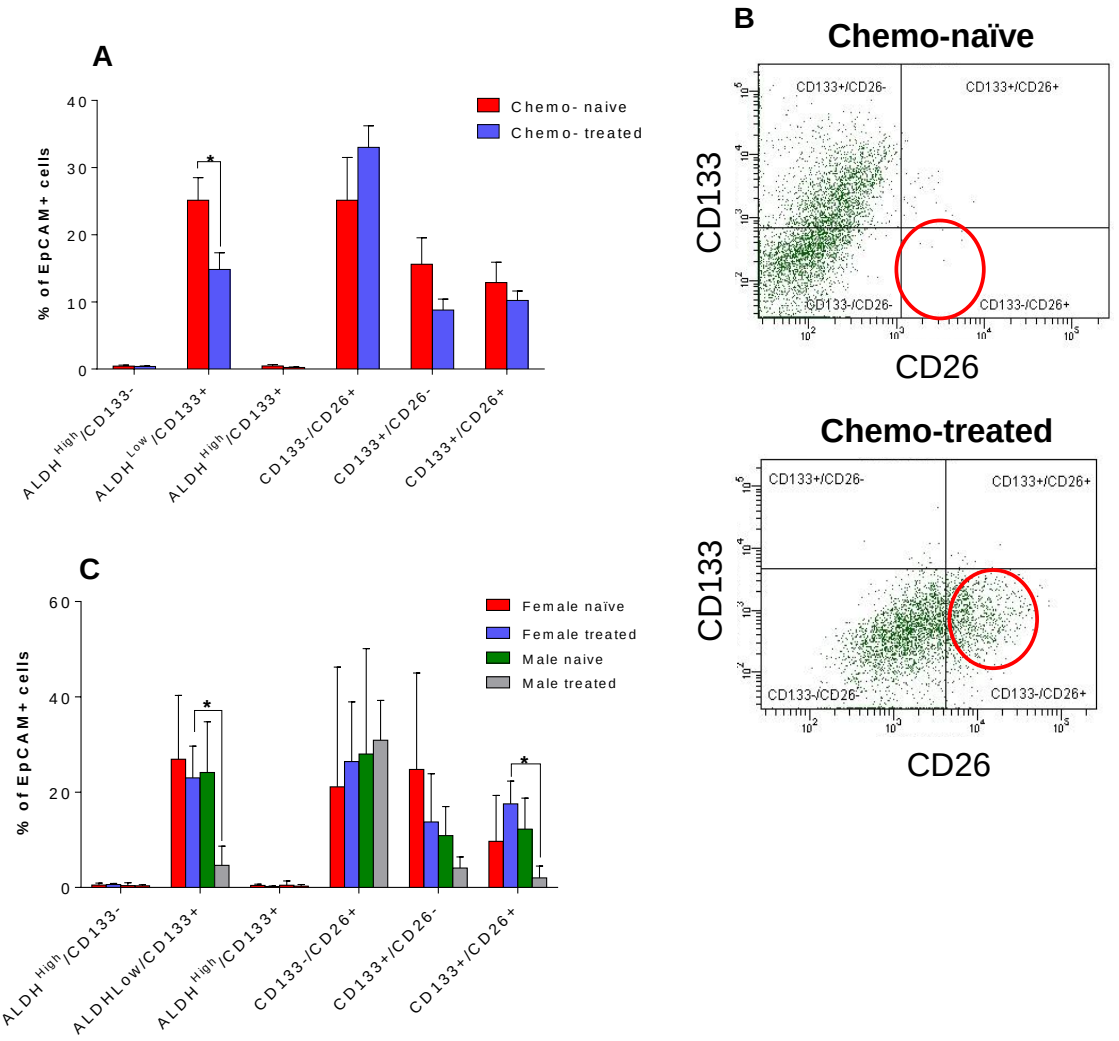

Figure 3.3 Assessment of TIC marker expression in patients who had received no chemotherapy (chemo-naïve) against patients who received chemotherapy (chemo-treated.)

(A) Chart displaying the average TIC marker expression in EpCAM+ cells, stratified by patient chemotherapy status. Chemo-naïve N=11, chemo-treated N=27. (B) An example of CD133 and CD26 staining in one chemo-naïve patient (top) and one chemo-treated (bottom), with red circle indicating the increase in the CD26+/CD133- population in the treated patient. (C) Expression of TIC markers stratified by gender and whether the patient had received chemotherapy. N=4, 12, 7 and 15 for female chemo-naïve and treated, and male chemo-naïve and treated, respectively. For both (A) and (C), error bars represent the SEM, and * indicates significant differences, where $P<0.05$.

3.3 **Expression of pluripotent stem cell markers in CRLM EpCAM+ tumour cells**

To assess whether the different TIC populations were associated with expression of proteins involved in pluripotency, as has previously been described in TICs[133-135,360,361], a pluripotent stem cell array kit was used (Figure 3.4). This kit contained a membrane on which 15 primary antibodies specific to pluripotent proteins were immobilised. Single cells generated from processing patient tumours were sorted to obtain an EpCAM+ (pure epithelial) population, and were subsequently used for the pluripotent stem cell array data. The data generated from the array was correlated with the FACS data regarding each samples TIC expression profile.

If the cell surface markers used identify TIC populations, they may also be associated with pluripotent stem cell proteins. This would be easier to see if the extreme values were used, so therefore the expression of TIC markers, analysed by flow cytometry, was used to stratify patients into ‘low’ and ‘high’ expressing samples.

The pluripotent expression profiles between each group were then averaged and compared. To define the ‘high’ and ‘low’ populations, out of the 23 patients analysed the top three highest and lowest expressing samples were selected. For ALDH activity, 6 patient samples were used for the ‘low’ group as they all possessed the same level of ALDH activity. The expression of pluripotent stem cell markers between chemo-naïve and chemo-treated patients was also interrogated across all of the samples analysed. The results showed there were no significant differences between any of the proteins in any of the groups investigated.

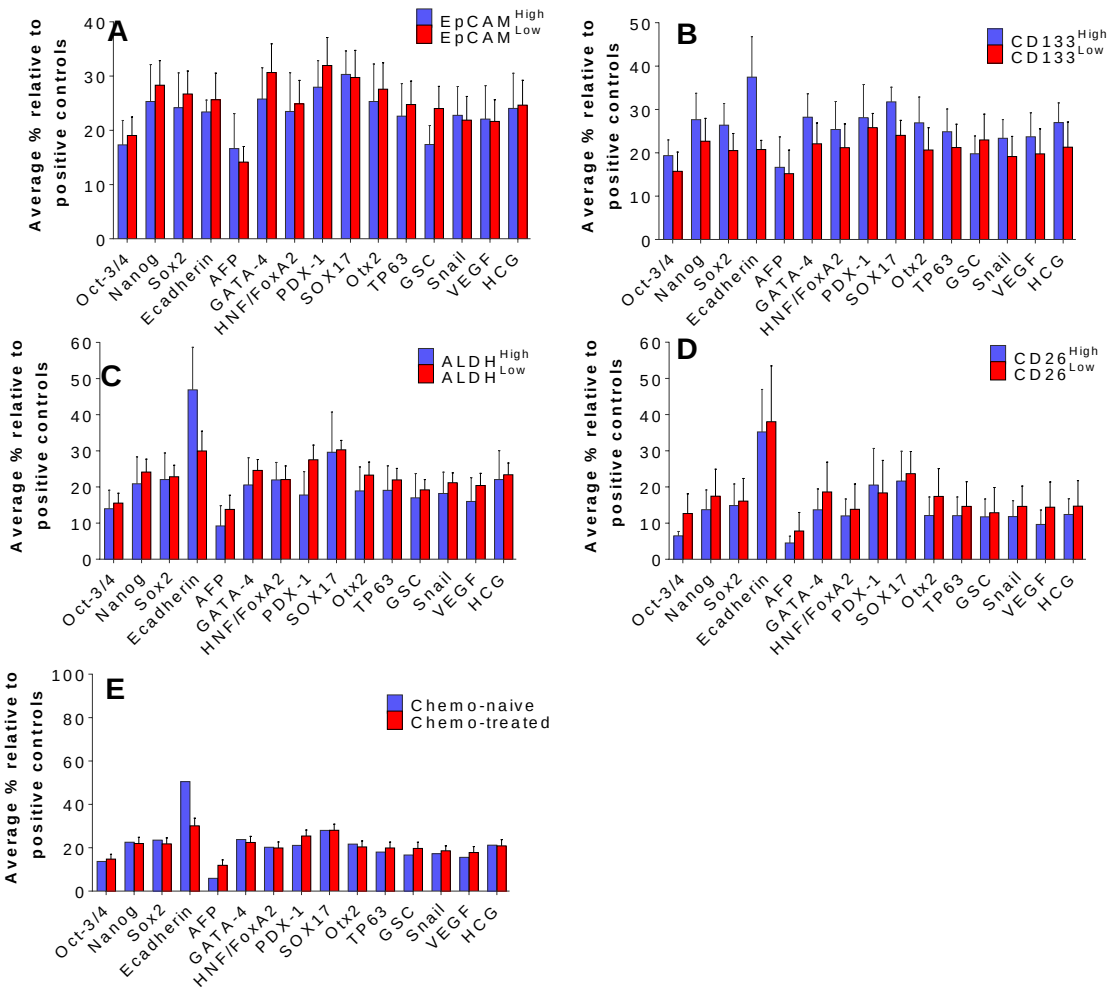

Figure 3.4 Expression of a panel of pluripotent stem cell markers in CRLM EpCAM+ cells stratified by TIC marker expression

The proteome profiler array was performed and a correlative analysis carried out with the patients corresponding FACS data. A total of 23 patients were profiled using the array, with the top three and lowest three expressing samples for each TIC marker, as determined by flow cytometry, being averaged and compared (except for $ALDH^{Low}$ activity as six patients had no activity and so were averaged together). (A) EpCAM, (B) CD133, (C) ALDH and (D) CD26. Additionally, the proteome profiler data for chemo-naïve (N=2) and chemo-treated (N=13) patients was averaged and compared (E). Error bars represent the SEM. For the chemo-naïve group only the average is shown due to a low numbers of patients. Expression was determined relative to positive control spots on the array, which were used to normalise data.

3.4 **Spheroid growth - method development**

Spheroid growth was undertaken using single cells derived from tissue obtained directly from patients. Spheroid growth has been examined in many different cancers with varying success rates. In our laboratory, an approximate initial spheroid formation rate of 62% was observed in CRLM, but this value overstates the true efficiency as only a few spheroid-forming samples were capable of being passaged and propagated. The remaining samples produced a few small spheroids. The inability to passage the cells using the original methods meant the samples could not be propagated to give sufficient cells for experimental use. To address this, a number of different methods were tested to see whether spheroid propagation could be enhanced.

To try and facilitate spheroid growth, a direct co-culture method using normal colonic fibroblasts (18Co cells) was attempted (Figure 3.5). 18Co cells have been used previously in co-culture methods in order to provide a more favourable environment for tumour cell growth, through production of ligands such as HGF[78]. The 18Co cells were used as a feeder layer on which single cells derived directly from patient primary colorectal, and colorectal liver metastases samples were seeded. Using the direct co-culture method a spheroid formation rate of 100% was observed across 5 samples, suggesting this method could have potential as a reliable system for use in subsequent spheroid culture experiments.

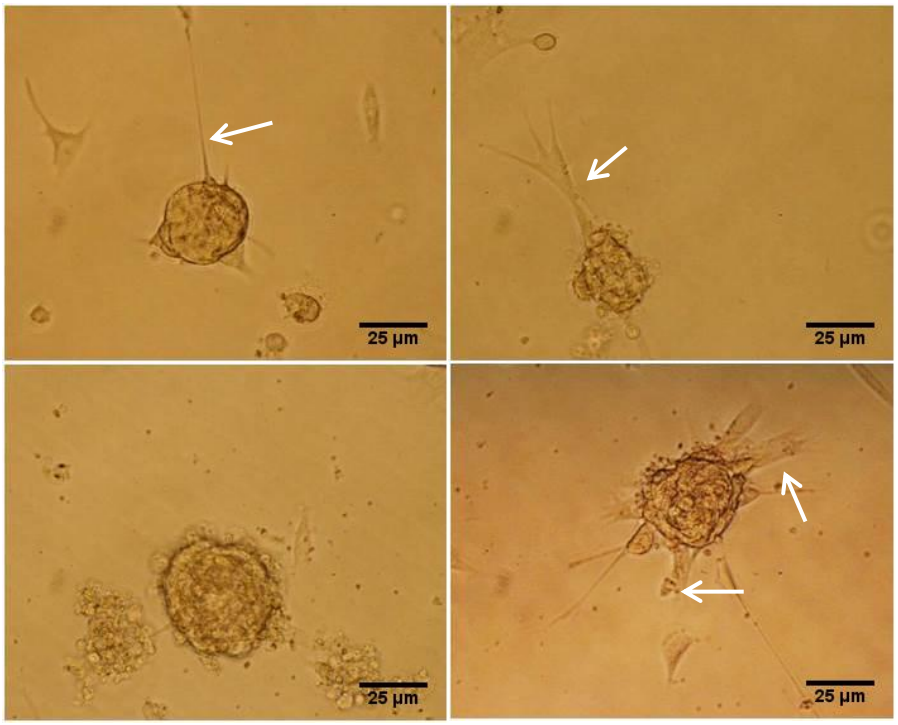

Figure 3.5 Light microscopy pictures showing an example of the spheroids produced by co-culture of primary patient tumour cells on 18Co cells.
The top row shows typical spheroids grown from a colorectal cancer sample, and the bottom row shows spheroids grown from a colorectal liver metastasis sample. Arrows depict the fibroblast extensions produced by the 18Co cells. Imaged using a X20 objective.

To distinguish between which cells were derived from the patient tumours, and which were 18Co cells, the epithelial marker EpCAM was used which is over-expressed in epithelial cancer. It is also not expressed by the 18Co fibroblast cells. This is demonstrated in the top row of figure 3.6, 18Co cells do not express any of the TIC markers in the top row because the results are represented as a proportion of the EpCAM+ population, and the 18Co cell line does not contain an EpCAM+ population (Figure 3.6). Flow cytometric analysis of the spheroids revealed an EpCAM+ population of 9-15%, indicating that tumour cells were incorporated within the spheroids (Figure 3.6). However, EpCAM expression was much lower in the co-culture spheroids than in patient tissue (Figure 3.6 bottom left vs bottom middle), which is reduced by 60% ± 17 (SEM); this reduction is likely to be due to dilution with the 18Co cells.

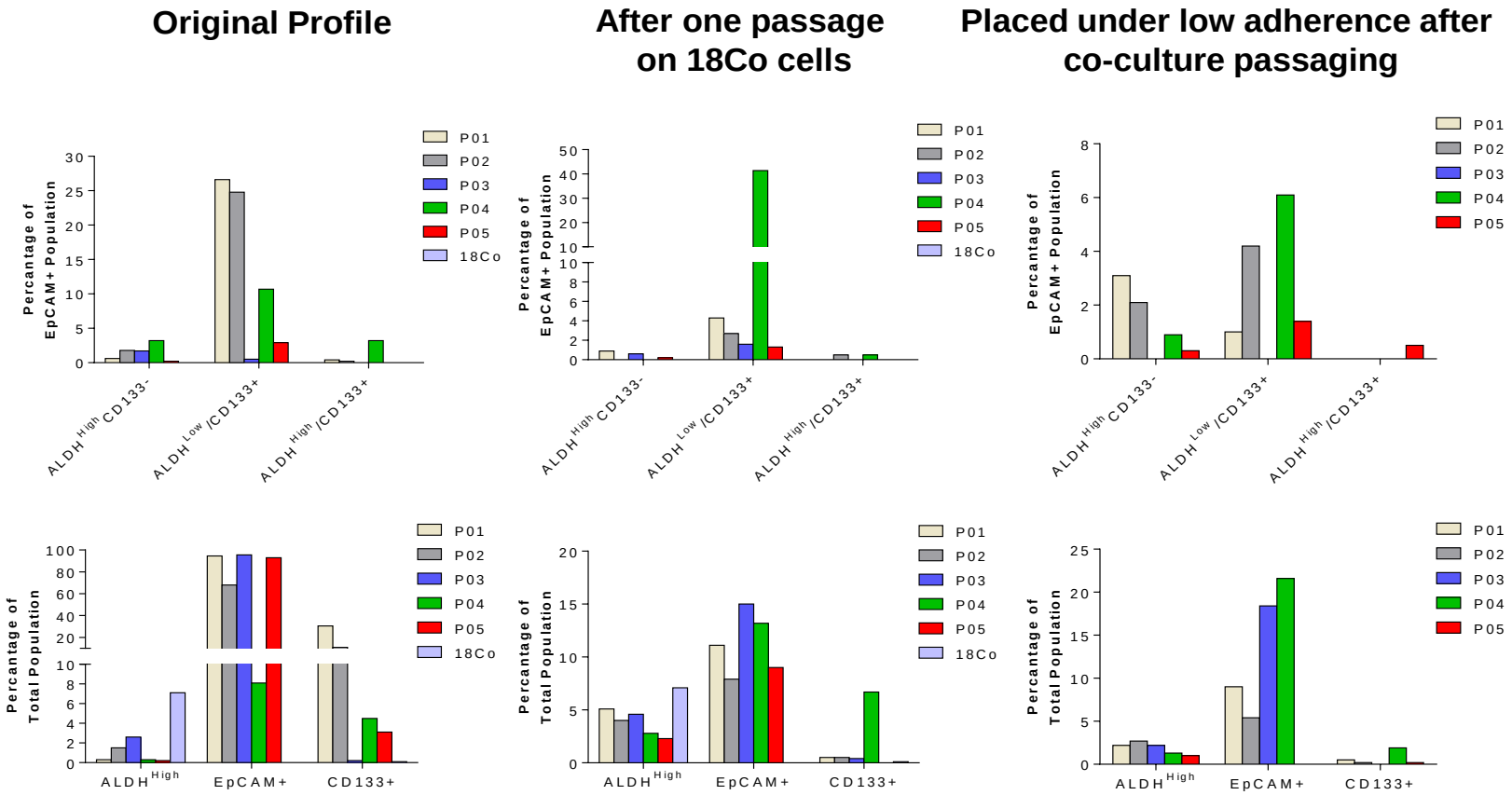

Figure 3.6 Flow cytometric profiling of spheroids, grown by co-culturing patient tumour cells with 18Co fibroblasts, for ALDH activity and expression of EpCAM and CD133.

The top row depicts the data described as a percentage of the EpCAM+ cell population. The bottom row describes the same data as a percentage of the whole population. The analysis was carried out on CRLM samples from 5 different patients (P01-05) and the 18Co cell line N=1. The original flow cytometric profiles derived from analysing tissue straight from the patient are displayed on the far left. The profiles generated from passaging cells once on 18Co cells are displayed in the middle. Some spheroids for the analysis of the middle graphs were saved and placed in low attachment conditions, and were then reprofiled with the results displayed on the right.

When analysing the whole population (not EpCAM+ cells only) the average percentage of $ALDH^{High}$ cells increased following co-culture from 0.98% to 3.76%, whereas the CD133 population decreased on average from 9.84% to 1.62%, giving the initial impression that co-culture seemed to selectively support the $ALDH^{High}$ population. The 18Co cells have a large fraction of cells with an average high ALDH activity of 6%, which is higher than any of the primary tumours, when expressed as a percentage of the total cell population. When analysing the same data for the spheroids passaged on 18Co cells, but in combination with EpCAM expression, the EpCAM+/$ALDH^{High}$ population was on average 0.34% (Figure 3.6, bottom row). These results are likely due to the 18Co cell line representing the majority of the $ALDH^{High}$ population when analysing the whole population, and since the 18Co line doesn't express EpCAM, when analysing the EpCAM+ population the $ALDH^{High}$ population decreases. This also highlights the need for robust markers such as EpCAM, to distinguish between the different cell types.

In an attempt to try and enhance the EpCAM+ population and further decrease 18Co incorporation into the spheroids, spheroids grown from the 18Co-tumour cell co-cultures were transferred to ultra-low attachment plates in the absence of fibroblasts. Results from this were ambiguous, as a decrease in the percentage of EpCAM+ cells was observed in 3/5 of the samples on average by 4.5%, and there was an average increase in 2/5 samples of 5.9% (Figure 3.6).

To see if the samples grew at different rates, the number and size of spheroids were measured, and 18Co cells alone were included as a control (Figure 3.7). Both the size and number of spheroids formed from 18Co-tumour cell co-cultures were smaller than 18Co cells alone, giving further evidence to suggest that spheroid growth in this system was being driven purely by the 18Co cells, independently from any spheroid forming capacity of the tumour cells.

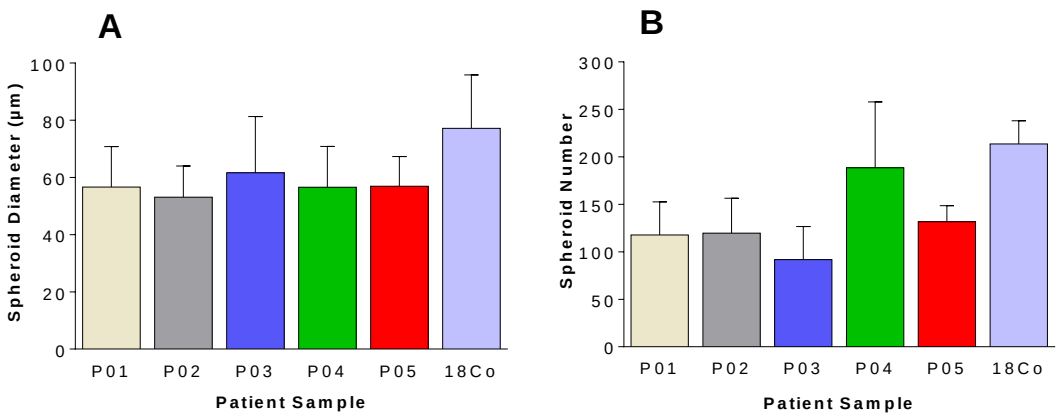

Figure 3.7 The size and number of co-culture derived spheroids
(A) The average spheroid diameter, and (B), average spheroid number, for colorectal liver metastasis samples from 5 different patients (P01-05) grown as co-cultures with 18Co cells. 18Co cells grown alone were also included. The average (± SEM) number/diameter of spheroids from three wells on a six-well plate was determined, on a single occasion for each sample.

When two samples, a primary colorectal tumour and a colorectal liver metastases were serially passaged and maintained in the 18Co co-culture conditions, by passage four there was no detectable EpCAM+ population, but a rise in ALDH1^{High} cells was observed (Figure 3.8). This was likely to be due to the 18Co cells taking over the co-culture.

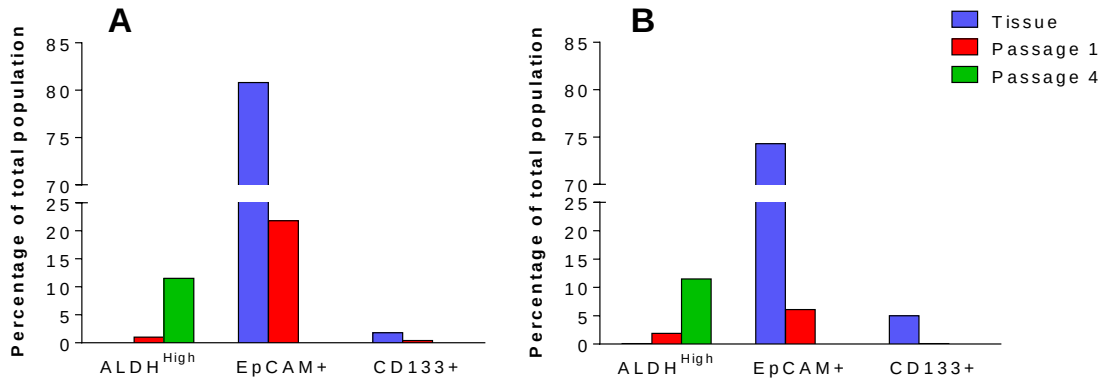

Figure 3.8 The effects of serially passaging CRLM cells in co-culture with 18Co cells
(A-B) The effect of passaging tumour cells for 4 passages with 18Co cells on the expression of EpCAM, CD133 and ALDH^{High} activity. (A): Colorectal cancer (B): colorectal liver metastasis, N=1 for each tissue type. Tissue refers to the original sample analysed straight from the patient.

As an alternative approach to the co-culture, three growth factors (R-spondin, Wnt-3a and HGF) were added to stem cell media and patient metastases cells were cultured in this enriched medium under standard conditions on ultra-low attachment plates. All combinations of the growth factors were tried, but none resulted in spheroid formation in any of the three samples tested (Figure 3.9). Additionally, matrigel was used to provide a scaffold for cells to grow upon, but this also failed to promote spheroid formation in the samples tested (Figure 3.9). Two further methods were attempted: using inserts to culture two cell types separately while allowing growth factors to diffuse between the two, and using 18Co-conditioned stem cell media; neither of these methods enhanced spheroid formation from CRLM cells.

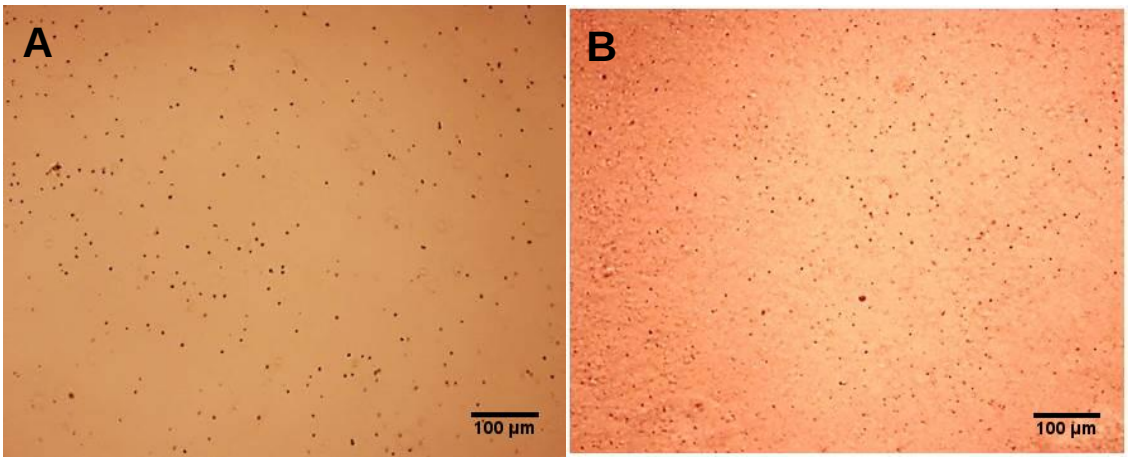

Figure 3.9 The effects of growing single cells in media supplemented with growth factors, or in matrigel.
(A) Demonstrates the lack of growth promotion provided by culturing CRLM cells in media supplemented with R-spondin, WNT3A and HGF. The same results were seen when cells were embedded in matrigel (B), using the standard spheroid culturing media.

3.5 **Characterisation of spheroids**

3.5.1 Correlation of spheroid growth with TIC marker expression

To examine whether the expression of TIC markers was associated with the extent of spheroid growth, spheroid formation was correlated with expression levels using a designated score devised to take into account the number and size of spheroids. The scoring system was: 0 = no spheroids, 1 = less than 5 spheroids, 2 = small and 5-10 spheroids, 3 = large and 5-10 spheroids, 4 = large and over 10 spheroids which were able to be passaged (Figure 3.10). Assessment was carried out using 3-wells on a 6-well plates seeding 30,000 cells/well.

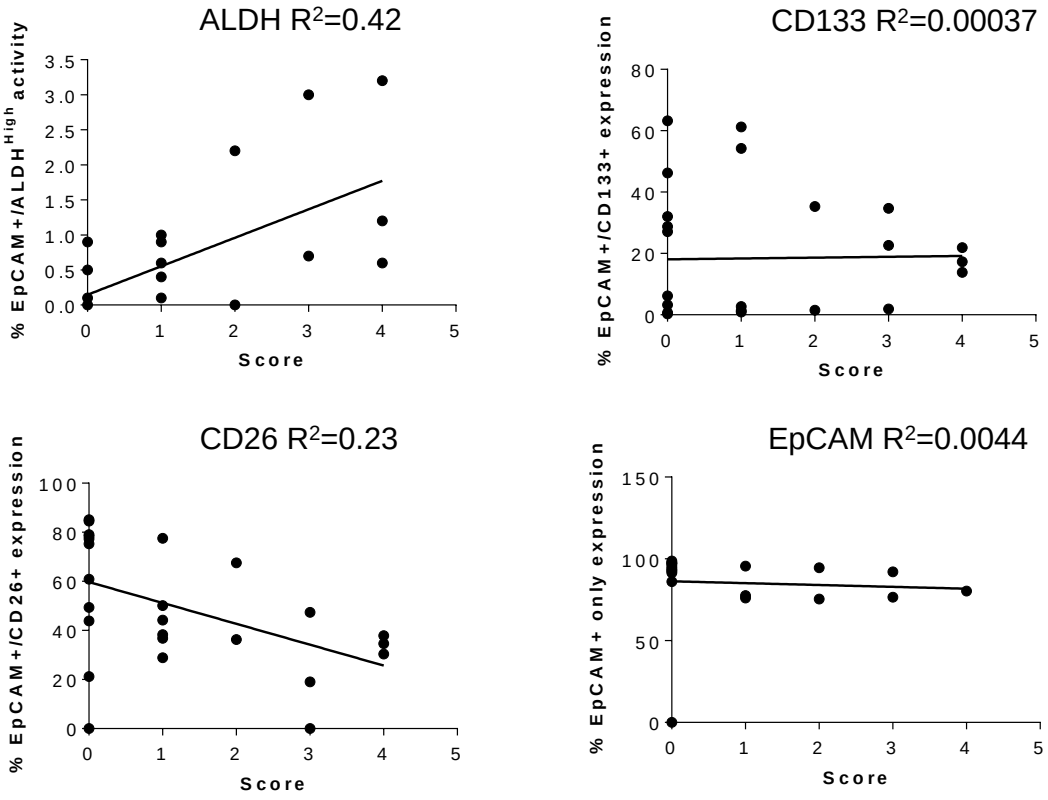

Figure 3.10 Correlation of TIC markers with spheroid growth capacity in patient samples.
Spheroids that grew from patient and mouse-passaged samples were scored (0-4) based on the number and size of spheroids (N=20 and 6 for samples derived directly from patient of xenograft tumour tissue respectively). The expression of TIC marker levels in the corresponding tissue was then correlated with spheroid score. The R^2 value represents the correlation, with 1 representing a perfect correlation.

The results show ALDH activity has a positive association with spheroid growth R^2=0.42 P=0.0003, whilst CD26 is negatively correlated with spheroid growth R^2=0.23 P=0.0134. The expression of CD133 and EpCAM does not appear to show any correlation, with R^2 values of 0.00037 and 0.0044 (P=0.9259 and 0.7815), respectively.

3.5.2 Assessing the ability of sorted TIC populations to form spheroids

To further characterise which populations were most likely to represent CRLM TICs, spheroids were grown, and sorted to isolate each candidate TIC population (Figure 3.11). Following the sort, cells were plated under spheroid forming conditions to assess which EpCAM+ populations harbour cells with the self-renewal capacity required to generate a spheroid. It was found that each sorted population was able to form spheroids but to varying extents (Figure 3.11).

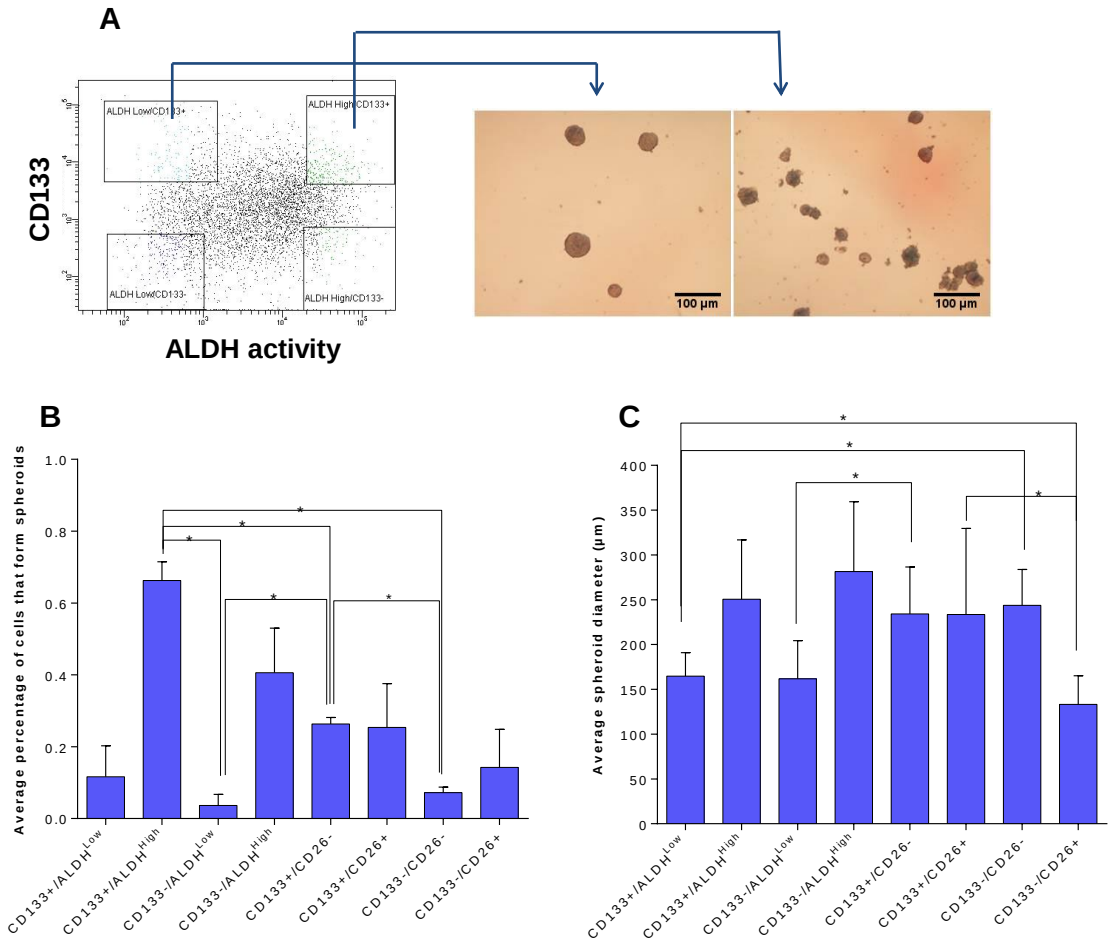

Figure 3.11 Sorting spheroids based on EpCAM+ TIC marker expression and re-analysing spheroid growth

(A) An example of the sorting gates used to isolate different spheroid populations, choosing the ~5% of cells exhibiting the highest or lowest fluorescence for each combination of marker (either CD133 and ALDH activity, or CD133 and CD26). Only the EpCAM positive population was used for analysis. To the right is an example of the spheroids grown from two different populations. (B) The average number of spheroids grown from each sorted population, counted manually using light microscopy. (C) The average size of spheroids grown from each sorted population, measured manually using light microscopy. For (B) and (C) the data is from a single patient performed in triplicate, error bars represent SEM. Significant differences between populations are indicated by *, where P≤0.05.

$ALDH^{High}$ combinations formed the most spheroids with the $ALDH^{High}$/CD133+ and $ALDH^{High}$/CD133- populations possessing a spheroid formation capacity of 0.6 and 0.9% respectively (Figure 3.11). The $ALDH^{High}$/CD133+ double positive population formed significantly more spheroids than the $ALDH^{Low}$/CD133-, CD133+/CD26- and CD133-/CD26- populations. The CD133+/CD26- population grew significantly more spheroids than the CD133-/CD26- (P=0.041) and $ALDH^{Low}$/CD133- (0.005) populations. The spheroid formation rate was generally low, which is probably due to mechanical injury and loss of cell viability caused during the sorting process. Significant differences in spheroid diameter was also seen (Figure 3.11).

A small number of spheroids were found to arise from the $ALDH^{Low}$/CD133-, and CD26-/CD133- populations. This may be explained by a decreased purity in the cell sort over prolonged sort times due to the fluorescence intensity decreasing over the duration of the sort. This would result in $ALDH^{High}$ cells falling to $ALDH^{Low}$ on the FACS dot plot, so that cells may no longer be confidently ascribed to their respective TIC classifications.

All sorted populations were then re-analysed following spheroid growth (Figure 3.12). It was found that all populations were able to recapitulate similar TIC expression profiles, irrespective of which TIC marker was used to isolate them, and showing a similar profile to the original, unsorted, spheroids which were used for the experiment.

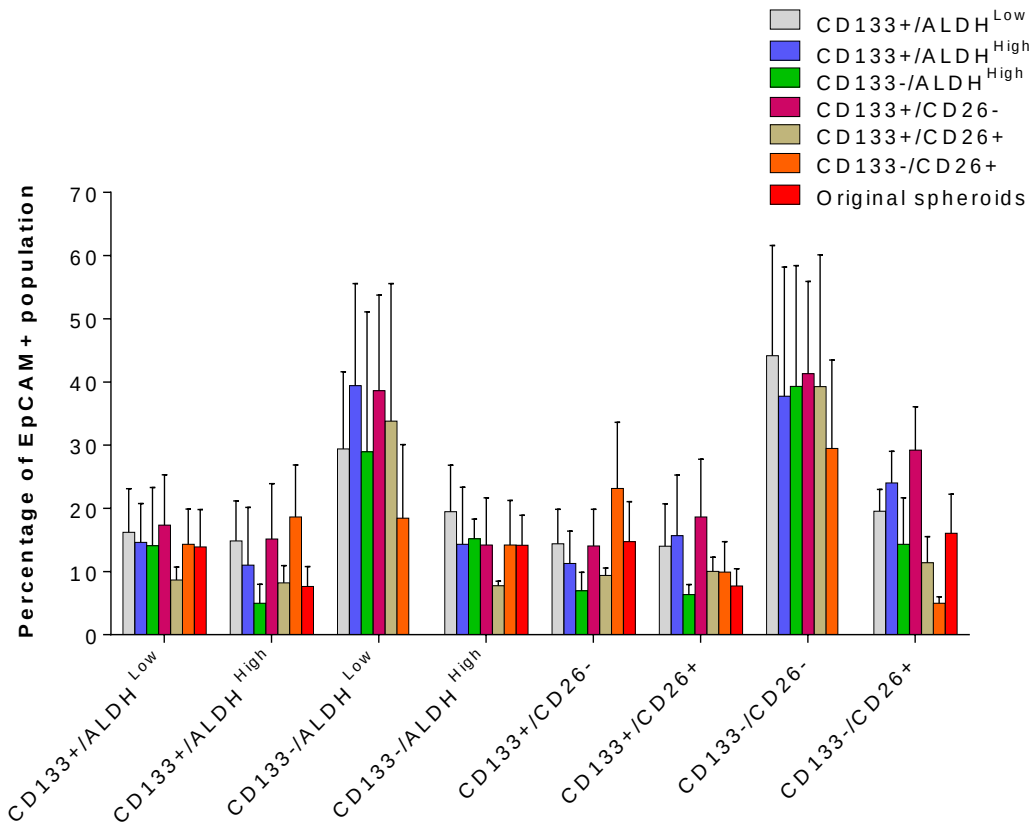

Figure 3.12 Expression of TIC markers in spheroids generated from the sorting of cells based on TIC levels as in figure 11
Cells sorted from spheroids, derived from a patient sample, were left to grow before assessing for TIC marker expression, analysing only the EpCAM+ population. The original spheroid flow cytometry profile produced from the cells used for sorting are also included for comparison. Data is from a single patient performed in triplicate, error bars represent SEM.

3.5.3 TIC marker expression following differentiation of cells

The rationale for using spheroid culture is the reported enrichment in, and preservation of, TIC cells observed within this culture system. Therefore, expression of TIC markers were analysed in patient tissue and compared to expression observed when culturing cells either as spheroids, or as differentiated cells derived from spheroids (Figures 3.13 and 3.14). Before differentiating spheroids, they were first cultured as spheroids for 14 passages, in an attempt to remove any contaminating fibroblasts. Spheroids were then cultured under adherent conditions using vitronectin-coated plasticware, and DMEM media containing 20% FCS. Previously the addition of

serum and putting spheroids under adherent conditions has been shown to promote differentiation demonstrated by a decrease in CD133 expression, and an increase in villin expression indicating enterocyte differentiation, and alcian blue and periodic acid–Schiff staining indicating goblet-like cell differentiation[362].

Spheroids attached over 48 hours, with outgrowth observed by day 5 (Figure 3.13). By day 10, spheroid outgrowth was extensive although the original spheroid was still visible. By day 30, all spheroids had either flattened out or had detached. At this point cells were passaged.

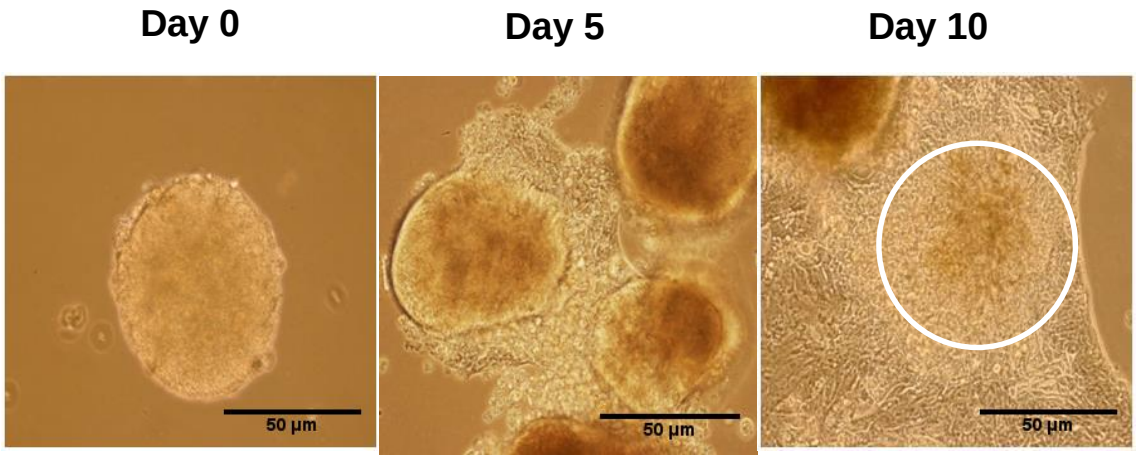

Figure 3.13 Light microscopy images of spheroid differentiation
Spheroid differentiation over 10 days. Clear spheroid boundaries are observable at day 0, which disappear with time. By day 10 some spheroids can be seen to have flattened out and to have lost all spheroid boundaries and shape (white circle). Images were taken using a X20 objective.

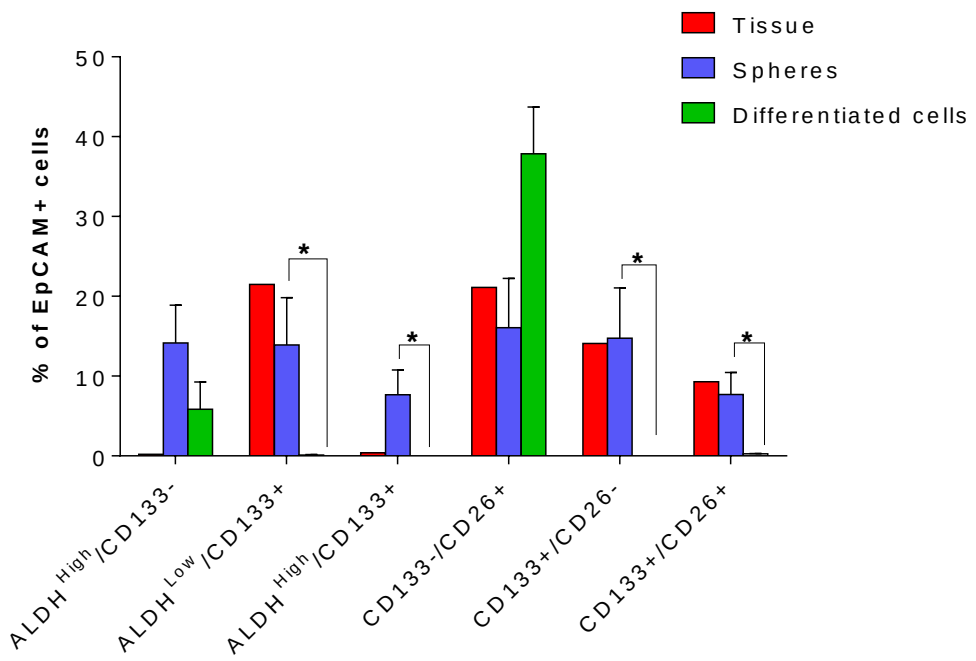

Figure 3.14 Comparison of TIC marker expression between the original tissue, spheroids and differentiated cells
Comparison of the expression of TIC marker expression for sample P153 when it was taken directly from the patient tissue, spheres (N=4), and when spheroids were differentiated, the same sample was analysed on three separate occasions, *=P≤0.05. Error bars represent SEM.

Figure 3.14 indicates that culturing cells as spheroids causes an increase in the proportion of $ALDH^{High}$/CD133- and $ALDH^{High}$/CD133+ cells by 14% and 7%, respectively, compared to the patient tumour tissue. Whilst the expression of CD133 in spheroids generally matches the tissue population, it appears CD133+ cells are not supported by differentiating culture conditions, as its expression is only detected in the $ALDH^{Low}$/CD133+ and CD133+/CD26+ populations at trace amounts (0.1 and 0.26% respectively). Spheroids have significantly higher ALDH activity and CD133 expression compared to differentiated cells (Figure 3.14).

3.6 The effects of serially passaging tumour tissue in NOD-SCID mice on spheroid growth and TIC marker expression

To provide a source of cells for *in vivo* studies, and also as a means of increasing spheroid growth for *ex vivo* treatment assays, patient samples were subcutaneously implanted into NOD-SCID mice and left to form tumours. If no tumours were observed after 6 months then the mouse was sacrificed. In total, 26 samples were implanted into mice, however only 15 grew (58%) on the first passage. Subsequently, 10/13 grew on passage 2 (77%), and then 100% of all subsequent samples grew (Table 3.2). Out of the 11 samples analysed for their spheroid formation capability, and comparing growth before and after passaging cells once in NOD-SCID mice, 8 samples (73%) showed an increased spheroid formation than before.

Passage	Number of Samples that grew in mice
1	15/26
2	10/13
3	7/7
4	5/5
5	2/2

Table 3.2 The number of CRLM samples that grew in each mouse passage

In this study, H+E staining was assessed by a pathologist who reported the tumours to be only moderately differentiated, and to have maintained the characteristics of the original tumours (Figure 3.15). However, an increase in the amount of fibrosis and fibrotic reaction was observed in the original tissue compared to passaged tissue. A summary provided by the pathologist, describing the tumour H+E staining through each passage can be found in the appendix (Table 8.2).

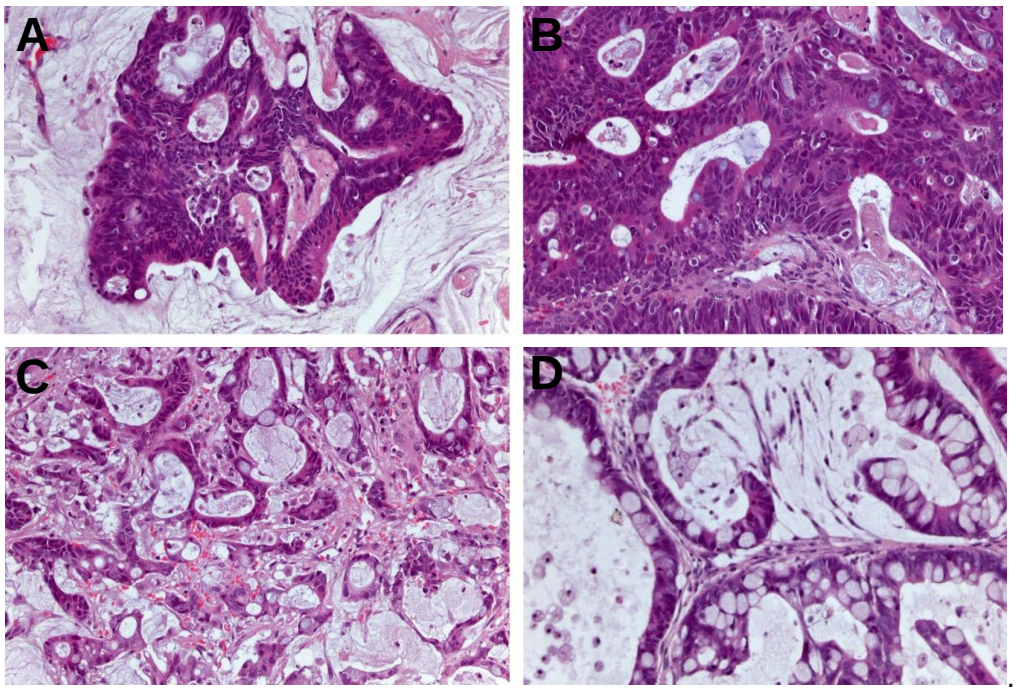

Figure 3.15 Assessment of histological characteristics after repeated subcutaneous passaging of tumour tissue in NOD-SCID mice.
(A) Shows a mucinous adenocarcinoma metastasis. (B) The same sample after two mouse passages shows cells of a similar type although the mucinous/stromal element is less in (B). (C) Represents another mucin-secreting carcinoma which retains its histological characteristics after one mouse passage (D).

After each passage, the bulk of the tumour that was not re-implanted into another mouse, or used for formalin fixation, was processed into a single cell suspension. This allowed seeding of the cells for growth, whilst the remainder were frozen for subsequent profiling by flow cytometry. Serial passaging resulted in a significant increase in the CD26+/CD133- population at passage 1 compared with the original tissues (P=0.005), and a further enrichment at passage 2 compared with tissue from passage 1 (P=0.045) (Figure 3.16A). There was also a significant decrease in the CD133+/CD26- population when comparing tissue from passage 1 with patient tissue (P=0.048). There was an observable inter-patient difference in growth rates between implanted samples during the first passage (Figure 3.16B), therefore, the expression of TIC markers was compared between the fast and slow growing samples (Figure

3.16C+D). Samples that reached a volume of 300 mm^3 by week 6 were classified as fast growing (N=6) and samples that grew slower than this were classified as slow growing (N=9).

Expression of CD26+/CD133- in the original tumour directly from the patient, and after one passage, was higher in samples that grew faster when xenotransplantated, although the differences failed to reach significance (Figure 3.16 C+D). In contrast, the opposite trend was observed for all populations containing CD133+ cells (except $ALDH^{High}$/CD133+ due to such a small $ALDH^{High}$ population), with the CD133+/CD26- population being significantly increased in the slow growing tumour samples (P=0.0330029. These results indicate that CD26+/CD133- cells may potentially be associated with a tumour's rate of grow, and ability to be propagated in mice.

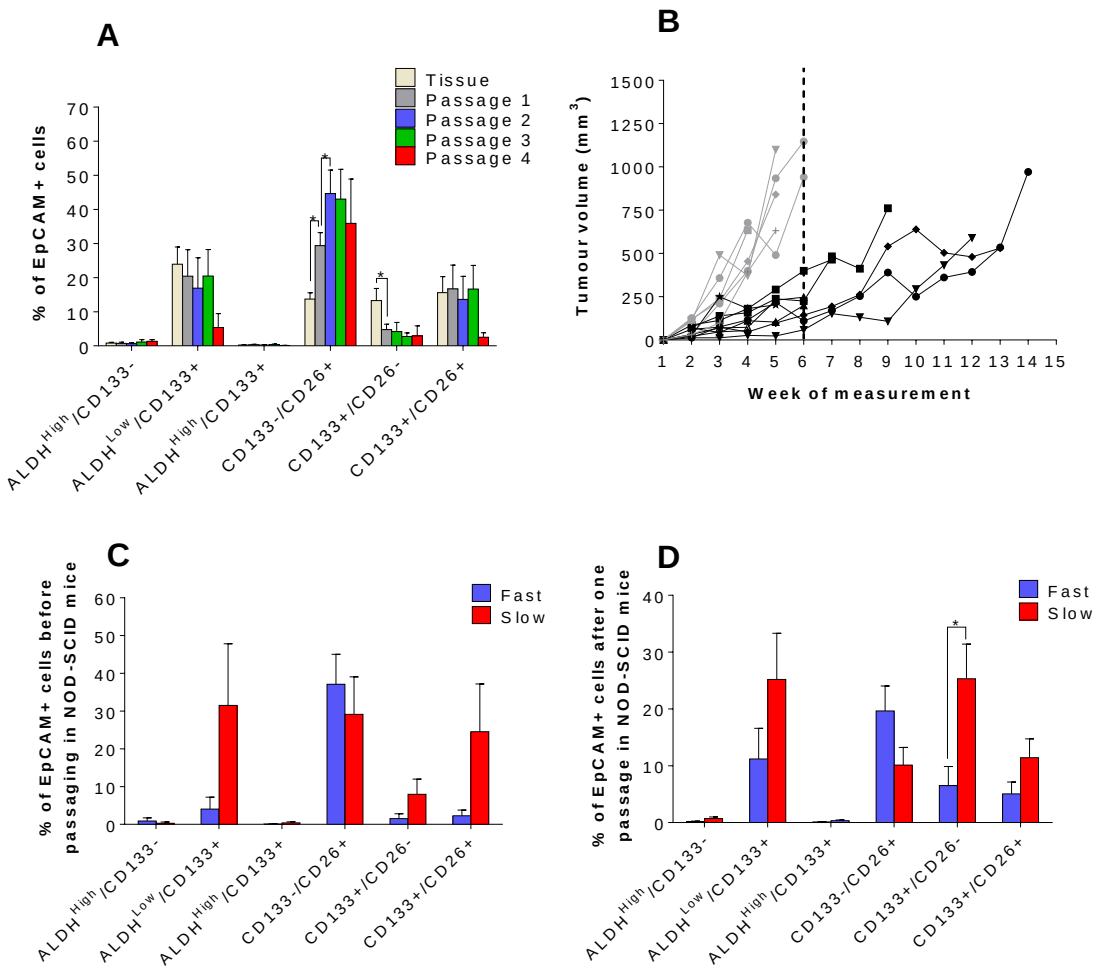

Figure 3.16 Assessment of tumour tissue serially passaged through NOD-SCID mice.

(A) Flow cytometry analysis of TIC markers after each passage in mice and the original patient tissue. Tissue N=12, Passage 1 N=11, Passage 2 N=7, Passage 3 N=6 and passage 4 N=2. Error bars represent SEM and significant differences are designated by *, where P≤0.05. (B) Tumour growth rates following first implantation into NOD-SCID mice, tumour volume is plotted against the number of weeks grown, N=15. Growth rate differences could be seen between samples with some growing slowly (black lines) and some fast (grey lines). Samples with a tumour volume of 300 cm^3 by week 6 were considered fast growing (dotted line highlights week 6). (C) Comparison of TIC marker profiles in the fast and slow growing samples before passaging (directly from patient). (D) Comparison of TIC marker profiles in fast vs slow growing samples after one passage in NOD-SCID mice. Data represent the average and SEM of 5 fast and 5 slow growing tumours.

3.7 **Discussion**

The large amount of literature in favour of the view that tumour formation, and growth, is fuelled by TICs, highlights this population as an important factor in determining a patient's response to therapeutics. Indeed, this population in various cancer types has been described as being resistant to therapy. However, investigations into TICs have mainly focused on the primary cancer site, and it has been assumed that the same markers can be readily extrapolated to the metastatic site. This chapter began by investigating two markers commonly used to identify colorectal cancer TICs: ALDH activity and CD133 expression[96,118,130,362,363], due to the lack of specific validated TIC markers for metastasis. These markers have previously been functionally established to mark cells in colorectal cancer that have the capability to be a TIC. CD133 has additionally been shown to be associated with metastasis, with increasing levels reported prior to metastasis[364]. However, research into CD133 has also been controversial with both positive and negative cells metastasising in a mouse model of colorectal cancer[117]. Despite these controversies, the role of CD133 in CRLM was investigated in this project as it was one of the original markers used to describe CRC TICs. CD26 expression was additionally investigated after it was identified as a specific metastatic marker in a publication by Pang *et al*., who reported CD26+ cells as increasing prior to metastasis and also that CD26 positivity designates cells with TIC capabilities that exhibit resistance to oxaliplatin and 5-FU[136]. However, there are few studies alluding to the role of CD26 as a TIC marker. Authors of the original publication recently published a follow-up study, reporting the use of CD26 as an immunohistochemical prognostic marker. High levels of CD26 expression were indicative of metastasis and a worse overall survival. However, unlike ALDH and CD133, which have been demonstrated to demarcate normal stem cells in addition to TICs, within the normal colon CD26 expression appears to increase with increasing differentiation. Despite the lack of information regarding the specificity of CD26 as a

TIC marker, as no other marker has yet been described solely as a metastatic TIC marker, CD26 was investigated in conjunction with EpCAM and CD133.

TIC marker expression in patient CRLM

TIC markers were analysed in CRLM tissues to assess expression levels within the tumour. The limited demographic data obtained from patients included age, gender and history of prior chemotherapy. The findings show there is a higher number of CD26+/CD133- cells in patients who had previously received therapy, tentatively implicating these markers as defining a more chemo-resistant population. This observation is in line with a previous publication that demonstrated increased CD26 expression after treatment of patient-derived xenografts with 5-FU or oxaliplatin[136]. However, CD133 expression in the study described here was shown to be significantly decreased in patients who had received therapy, which is in contrast to data using cell lines[365] and patient-derived colorectal cancer spheroids, in which CD133+ cells are resistant to chemo- and chemoradiotherapy therapy[154,366]. The results from further stratification of patients by gender and chemotherapy status revealed that the significant decrease in CD133 was restricted to the male cohort, which has not been previously reported, and provides evidence for the need to assess TICs and chemotherapy resistance within the context of gender. Since gender was not reported in the studies that found CD133+ cells to be chemoresistant, there may be some discrepancy due to the gender of patients from which cells were originally derived. Limited availability of demographic data meant that the time frames for therapeutic intervention could not be fully assessed for each patient, i.e. patients that had recent chemotherapy to down-size their metastasis may have been grouped with patients who received chemotherapy a long time before liver resection or as part of adjuvant therapy for their primary tumour. There were only a few patients whose chemotherapy was confirmed to be specifically for down-staging their metastasis, but an average 12% increase in CD26+/CD133- cells was still observed when these patients were

considered separately despite the very limited sample size, suggesting this to be a genuine finding irrespective of the time elapsed since therapy (Figure 7.4, appendix). Contrary to the majority of published data alluding to CD133+ cells being a chemoresistant population, one study found CD133- cells from the human colorectal cancer cell line LoVo to be more chemoresistant than CD133+ cells, with a lower caspase activity following treatment with 5-FU[367]. It appears the CD133- chemo-resistant cells defined in the study are likely to be CD26+, as they were shown to adhere more to collagen, a known substrate for the CD26 protein. This indirectly adds credence to CD26 identifying a resistant population. These studies support the finding and view that CD26+ cells are resistant while CD133+ cells may be sensitive to treatment, at least in some cases/males[367].

It is important to note that most of the data analysing CD133 chemosensitivity is generated from primary CRC, and not CRLM. It is very likely that in the established metastasis CD133+ cells act differently, or demarcates an alternative population, when compared with their primary cancer-derived counterparts. Heterogeneity between similar cellular subsets may arise, for example, due to the changes in extra-cellular matrix proteins observed between primary and metastatic tumour sites[368], especially since CD133+ cells have been shown to be more interactive with the microenvironment than the CD133- cell population[369]. In addition, only a very small fraction of cells survive the metastatic process. CD133 marks a broad population, and it is likely that many of these cells will not be imbued with the characteristics necessary to metastasise and colonise the metastatic niche, meaning that there will be a likely heterogeneity within the CD133 population at the primary cancer site. These reasons may explain some of the discrepancies between the findings in this report and previous research.

Immunohistochemical analysis of colorectal adenocarcinoma tissue has previously identified that age and gender can affect stem cell marker expression, with an increase in CD133 expression reported in males[370]. The study presented here has identified CD133 expression as being higher in females (when analysing the total

population), but once genders have been stratified according to whether or not they have previously received chemotherapy, chemotherapy naïve patients exhibit similar levels overall between genders. Discrepancies between studies regarding CD133 levels may also have arisen as a consequence of the choice of CD133 antibody, with only the AC133 epitope (used within this thesis) believed to specifically mark the TIC population[119]. Contrary to the publication stating CD133+ cells are increased in men[370], other studies have reported similar levels between genders as seen in this thesis, once genders are stratified using their chemotherapy status[371]. The reason for decreased sensitivity to therapy of $ALDH^{High}$/CD133+ cells within the female cohort remains unknown, and represents a novel finding.

The attempt at correlating a patient's expression of TIC markers (as determined by FACS) with expression of embryonic proteins within the EpCAM population, did not identify any differences between markers. This method is not very powerful at detecting differences, and a better option would be to sort the actual different combinations of markers directly for the arrays. However, this remains technically difficult as it would require many cells to be sorted for each combination to yield enough protein for the array.

Spheroids and TIC marker expression

In order to further study TIC markers, an *in vitro* culture model was required. Spheroids have been reported to enrich for TICs, and represent a better model than 2D monolayer cultures, as cells in spheroid structures retain cell-cell adherence properties similar to those observed *in vivo*[372]. This cannot be recapitulated using standard adherent culture conditions. A spheroid culture method using low attachment plates and a defined serum free medium containing the growth factors EGF and FGF, was already established in our laboratory. This method provided a success rate of approximately 50% for primary colorectal cancer samples, but proved less effective for culturing CRLM, possibly due to the cells derived from metastasis being adapted to a

different niche and therefore requiring different conditions for their propagation. Previous studies on colorectal cancer have used various methods to try and improve spheroid formation, such as mild digestion of tumours to retain cell contacts, passage in xenografts prior to culture, the addition of specific growth factors, and the use of matrigel[357]. Through the addition of other factors to the media that were not tested in this thesis, such as using a Rho kinase inhibitor to prevent anoikis, in combination with matrigel, would likely improve the ability to initiate spheroids from new samples as this method for growing organoids has now proven to be robust, and widely used. The only methods undertaken within this thesis that resulted in increased spheroid formation were the direct co-culture method and xenograft passaging. Despite the co-culture method producing spheroids, growth was driven by the fibroblast cells, and thus it did not test the self-renewal capacity of the tumour cells, which is one of the reasons for using spheroids. This co-culture method may be useful for studying other aspects of biology, such as fibroblasts-epithelial cell interactions to assess the effect of the tumour stroma on biological phenomena such as EMT or cytokine production[373], but for this study the model did not fulfil the requirements for further use as an *ex vivo* model for testing drug efficacy. Therefore, the standard culture conditions were employed throughout the study. Using these standard conditions to culture cells from xenograft samples increased spheroid formation rates but the spheroids generally could not be serially passaged and so were used directly for the experimental treatment in chapter 4. It was noted that samples which formed passageable spheroids prior to xenografting also produced passageable spheroids post-xenograft. However, samples that were initially unable to form spheroids, formed non- passageable spheroids post-xenograft. This latter phenomenon could be explained if the transit-amplifying population were selected for *in vivo*, which are devoid of long-term self-renewal capacity, but are able to produce short-lived spheroids when placed into culture. Of note, the number of $ALDH^{High}$ and CD133+ cells were increased in spheroids derived from xenografts compared to cells derived directly from patient tissue. The finding that xenografting

increases spheroid formation has been reported previously, with a notable publication about characterising TICs through culturing organoids[374] (a similar model to spheroids) also requiring a xenograft passage to promote organoid formation. The reason for the xenograft-driven increase in spheroid formation is unknown, but may be due to the foreign mouse microenvironment providing a selective pressure, resulting in enrichment of cells with self-renewal capacity.

While most samples formed only low numbers of spheroids which could not be propagated, it was possible to demonstrate that $ALDH^{High}$ cells have the greatest spheroid forming capacity and CD26 expression is negatively correlated with spheroid formation. However, one patient sample grew well under standard conditions, and spheroids were characterised to help underpin the functional properties of the TIC populations under investigation. The results from this sample confirmed the correlations between ALDH activity and spheroid growth, and also demonstrated that CD26 enriches for a spheroid forming population relative to the unstained population, but to a lesser degree than the $ALDH^{High}$ population. When analysing the spheroid growth based on a scoring system and correlating it with the original patient expression of each TIC marker, CD26 expression negatively correlated with spheroid growth. However, when sorted cells from one patient were tested for spheroid growth, the CD26+ population grew more spheroids relative to the unstained cells. These conflicting results may be due to only a small proportion of the CD26+ population containing spheroid forming cells, and so when there is a large CD26+ population it masks the spheroid forming population. This may also explain the observation that the CD133+ and $ALDH^{High}$ populations form more spheroids than the CD26+ population, as they identify a more pure TIC population. The CD26+/CD133- population, which was identified to be increased in patients who had received therapy, was also the slowest growing and generated the smallest spheroids. This decreased proliferation rate may explain the observed increase in CD26+/CD133- cells following chemotherapy, as oxaliplatin and 5-FU target rapidly dividing cells through disrupting DNA and RNA

structure and function. There is likely to be to heterogeneity within the populations marked by each TIC marker. The fact that the CD26+/CD133- population only contains a small spheroid forming component, demonstrating there is heterogeneity between cells, may also explain why the population is only modestly increased in patients, as the non-TICs marked by this combination mask changes in the true TICs. The view that TIC cells are slow-dividing, resistant to therapy and form spheroids would indicate that CD26 expression may demarcate a population of TICs. However, cells with $ALDH^{High}$ activity formed the most spheroids overall, and significantly more than the negative population. The finding that all three markers stain cells capable of forming spheroids, and that only a small number of spheroids are formed by the negative population indicates that there are multiple populations with the self-renewal capacity to function as a TIC, and that these 3 markers encompass the majority of cells with the self-renewal capacity required for spheroid growth. Furthermore, their proliferation and self-renewal rates may determine their ability to survive in the face of a cytotoxic insult such as chemotherapy. This is highlighted in an article from John Dick's laboratory. In this publication by Kreso *et al.,* the authors assessed the clonal expansion and reduction of primary colorectal cancer clones in serial xenografts, produced from lentivirally marked single cells. By assessing clone size, heterogeneity was seen between the marked cells, with some clones being persistent in all passages, some disappearing after one passage, some emerging in late passages and others appearing in early passages and reappearing in later passages. After challenging the mice bearing xenografts with oxaliplatin and then re-seeding cells into untreated mice and assessing growth, it was found that clones that were undetected in earlier passages were increased, whereas persistent clones, candidates for tumour maintenance, were decreased. These findings demonstrate in an un-biased manner that cells which are proliferating less and are more quiescent, are more likely to survive chemotherapy and then contribute later to tumour growth, whereas tumour maintenance is maintained by an alternative proliferating TIC clone[375]. This supports

the finding in this thesis that multiple TIC populations exist, with varying degrees of resistance to therapy, and this is likely to be related to proliferation.

Since the ALDH^{High} population is very low or undetectable in samples derived from patients and xenografts, it may be that this population is repressed or exhibits greater quiescence *in vivo.* Alternatively, these cells could divide asymmetrically so their number does not expand. It cannot be ruled out that cells marked by ALDH^{High} activity do not have a significant role *in vivo* and are, in fact, an artefact of culturing. However, due to the large amount of research identifying the ALDH^{High} population as an important factor in primary CRC, this seems unlikely. It appears that high ALDH activity/CD133 and CD26 expression mark two independent TIC populations; one that is rapidly cycling (marked by high ALDH activity and/or CD133+) and one that is relatively more quiescent/differentiated (marked by high CD26+/CD133- expression). In breast cancer, a recent publication has revealed two populations of TICs, one marked by ALDH^{High} cells which are epithelial and rapidly dividing, while an alternative migratory-like cell is found on the tumour periphery, marked by CD24-/CD44+ expression[376]. This finding is in agreement with the observation here that ALDH^{High} activity marks a rapidly dividing cell in spheroid populations. In the publication by Pang *et al.,*[136] that identified CD26+ as a metastatic TIC, with CD26 expression preceding metastasis, it is possible that CD26 was marking a less proliferative migratory cell responsible for metastasis. This notion stems from the fact the authors further identified that the CD26+/CD133+ population contained a higher expression of EMT related proteins such as TWIST, SLUG, and N-cadherin, whilst E-cadherin was down-regulated. Additionally, cells that are going through EMT divide at a slower frequency than fully epithelial cells.

If CD26, CD133 and ALDH^{High} markers all define a subset of TIC cells, it may explain the observed plasticity that all three can reform spheroids that contain a similar expression pattern. Not only do the sorted cells re-form all populations, but they appear to produce similar levels to the profile observed in the original spheroids from which the

sorted cells were obtained. The plasticity seen here has also been observed in other studies, but has been explained by contrasting mechanisms. One explanation by Gupta *et al.,*[377] is that cells stochastically transition between TIC and non-TIC states; whereas Takeda *et al.,* demonstrated an interconversion between two stem cell populations, each with different properties. Crypt base columnar cells, which are more actively cycling than the +4 HOPX (HOP Homeobox) population, were found to interconvert between each other in the normal mouse small intestine[378]. More differentiated cells have also been shown to gain TIC markers via TGF-β signalling through surrounding stroma, demonstrating that local signalling through the microenvironment can also contribute to heterogeneity[111]. It may be that the culture system used in the present study causes the sorted cell fractions to gain spheroid forming ability and re-form spheroids, but negative cells are too differentiated and do not have the ability to be recalled to a spheroid forming state. Therefore, the growth conditions may allow cells to re-enter a TIC state and reform a certain population, which may explain why similar TIC levels were observed in spheroids used pre-sorting compared to spheroids produced post-sorting.

The experiments analysing TIC marker expression profiles of cells cultured under spheroid and differentiating conditions highlight CD133+ and $ALDH^{High}$ activity to mark a more stem-like population as they are both enriched under spheroid forming conditions, with CD133 expression undetectable under differentiating conditions. This is in agreement with literature describing high ALDH activity and CD133 expression to identify normal colon stem cells, and colorectal cancer TICs. CD26 expression is increased under differentiating conditions, with CD26 expression also previously reported to be upregulated in response to confluency in the HCT-116 and HCT-15 colorectal cancer cell lines while c-Myc was down-regulated[379]. The expression of c-Myc was shown to be a negative regulator of CD26, and since c-Myc is a driver of proliferation this points to CD26 being a less proliferative population, at least *in vitro*. The majority of reports about CD26 in the normal colon suggest it marks differentiated

cells with only a few accounts of CD26 marking TICs, but not normal stem cells. However, additional markers should be tested to confirm that the spheroids placed under adherent conditions do differentiate, through assessing up-regulation of genes such as MUC2, CK20, EMP1 along with staining for mucins such as a PAS stain. Irrespective of this, these culture conditions have previously been demonstrated to induce up-regulation of CK20 and villin[362].

The majority of evidence supports CD26 as marking a more differentiated cell and $ALDH^{High}$ and CD133 demarcating a more undifferentiated cell. The contrary results that CD26 may also mark some cells with a more undifferentiated, spheroid forming phenotype may be the result of differentiated cells being recalled into a TIC state. This has been described in colorectal cancer with Notch signalling in $ALDH^{Medium}$ and CD133 medium cell populations (which the authors presumed to represent an intermediate between an undifferentiated TIC, and a differentiated cell) inducing an increase in spheroid formation[380]. Dedifferentiation has also been described through induction of OCT4 and SOX2 signalling in malignant melanoma and prostate cancer, respectively[358,381].

TIC markers in CRLM xenografts

The mouse passage data demonstrate that CD26 expression was associated with faster growth for the first passage in mice. Over consecutive passages, the xenograft success rate increased, concurrent with an increase in CD26+ expression. Since the sorted spheroid experiment highlighted the CD26 population as possessing the least spheroid-forming capacity, and that this population was enriched under adherent conditions, it may be that the CD26 population represents a transit-amplifying population. Previous xenografts using malignant mesothelioma and renal clear cell carcinoma have shown that treatment with an antibody against CD26 caused a decrease in tumour burden and increased survival, demonstrating the importance of the CD26+ population in tumour maintenance and growth[382,383]. Since CD26 has been

described as a metastatic TIC marker, its enrichment is fitting with a previous study describing an enrichment of metastatic cells through serial passaging of primary CRC cells in nude mice[384].

Conclusion

In summary, this chapter has identified that *in vitro,* $ALDH^{High}$ activity identifies a population which more readily forms spheres than CD133, and CD26 positive cells. However, when sorted into respective populations, each population has sufficient plasticity to form all of the other populations. Furthermore, all populations are capable of forming spheroids, which suggests a TIC hierarchy in the order of $ALDH^{High}$ >CD133>CD26. Within the patient tumour itself, $ALDH^{High}$ cells represent the rarest population, making it difficult to define whether this population represents the best target for interventional strategies. Hence, the approach undertaken in the following chapter is to assess effects of intervention on each population. Furthermore, it has been established that the best method to improve spheroid formation for use in *ex vivo* models is through the use of xenografts.

Chapter 4: Anticancer activity of curcumin in combination with oxaliplatin and 5-FU on primary cultures

4 Introduction

As discussed in the previous chapter, the use of spheroids enables an enrichment of TICs, allowing investigation of their response to treatment with chemotherapeutics and dietary derived agents, such as curcumin. To this end, both spheroids and organotypic models were treated with the two main drugs used in frontline chemotherapy for treatment of both primary and metastatic colorectal cancer, namely oxaliplatin and 5-FU. Oxaliplatin and 5-FU were tested in combination with curcumin, with the rationale that the addition of curcumin might provide a superior treatment. This hypothesis stems from reports that demonstrated combining oxaliplatin with curcumin produces superior in *vitro*[385,386] and *in vivo*[343] efficacy compared to either agent alone. Clinically, patients frequently relapse after chemotherapy, an observation that can be explained by the hierarchical model of cancer. The nature of these drugs is that they target cells that are rapidly dividing. Several publications have demonstrated that curcumin can induce cell death *in vitro,* in cells identified by TIC markers[340,343,387]. Furthermore, curcumin has been demonstrated to target pathways that are thought to be essential for TIC maintenance such as the Wnt pathway, and the cell cycle. Therefore, it is hoped that the combination of these compounds should effectively eradicate cells that are rapidly cycling, in addition to targeting cells that are more dependent on TIC pathways, and not necessarily rapidly proliferating. While other studies have investigated curcumin in combination with Ox+5-FU in colorectal cancer cell lines, this is the first study to investigate CRLM and also solely use patient derived tissue.

4.1 **Spheroid treatments**

4.1.1 Spheroids derived directly from patient tissue

Only one sample grew aggressively enough directly from the patient to provide the required number of cells for treatment with all combinations of oxaliplatin, 5-FU and curcumin. However, some experiments were conducted on cells derived from xenograft tissue of CRLM samples, and one experiment conducted on a primary CRC sample. Therefore to clarify the material used for each experiment the information is presented in table 4.1.

Single cells derived from spheroids were seeded into media that contained the various treatments. In an attempt to recapitulate the clinical scenario where patients receive rounds of chemotherapy every 14 days, spheroids were left for 14 days before analysis on day 15, thus imitating one cycle of chemotherapy. However, incubations that contained curcumin received repeated doses of curcumin on days 5, 8 and 12 (Figure 4.1). Repeated doses were used as patients would receive curcumin daily, however culture conditions would not permit a complete daily change of the media as cells are in suspension, so curcumin had to be added directly into the media and only every couple days otherwise the DMSO concentration would become too high and have toxic effects. Additionally, curcumin is rapidly degraded in serum free media[388] (media for culturing spheroids contains no serum) and so additional treatments are required to increase spheroid exposure to curcumin. Spheroids were counted and measured after treatment, using spheroid size and number as a readout of efficacy, with analysis of TIC marker expression undertaken via flow cytometry.

Following treatment, the number of spheroids was significantly reduced by 70% or more in all incubations when compared to DMSO, but no significant difference was seen between treatments (Figure 4.1). However, the curcumin combinations (curc+OX, curc+5-FU and the triple combination) show an extremely low number of spheroids (2.6-1.2% of the DMSO). Surprisingly, curcumin alone was more effective at reducing spheroid number than oxaliplatin or 5-FU alone, which was also true for spheroid size.

Spheroid size was also significantly reduced by 42-76% after all treatments compared to DMSO control, but again there were no significant difference between treatments. Curcumin significantly down regulated the $ALDH^{High}$/CD133- population to a larger extent than the OX+5-FU combination when compared to DMSO, $ALDH^{High}$/CD133- was 12% in the DMSO treatment compared to 3% and 1.1% after OX+5-FU (P=0.001) and curcumin (P=0.033) respectively. No other significant changes were seen. However, none of the combinations containing curcumin could be profiled due to such low cell numbers, giving a further indication that combinations containing curcumin had a more pronounced effect on spheroid number than combinations without.

Figure	Sample	Chemotherapy	Gender	Age (years)
4.1, 4.2, 4.5, 4.6, 4.7	CRLM P153	Yes, for downstaging of CRLM.	Female	72
4.3	Xenograft CRLM P088	Oxaliplatin, cap	Male	63
4.3	Xenograft CRLM P093	Adju	Male	76
4.3	Xenograft CRLM P103	No therapy.	Male	52
4.4	Stage II CRC P066	Unkown	Male	

Table 4.1 A summary of the samples used for each experiment.
Colorectal liver metastasis (CRLM), colorectal cancer (CRC)

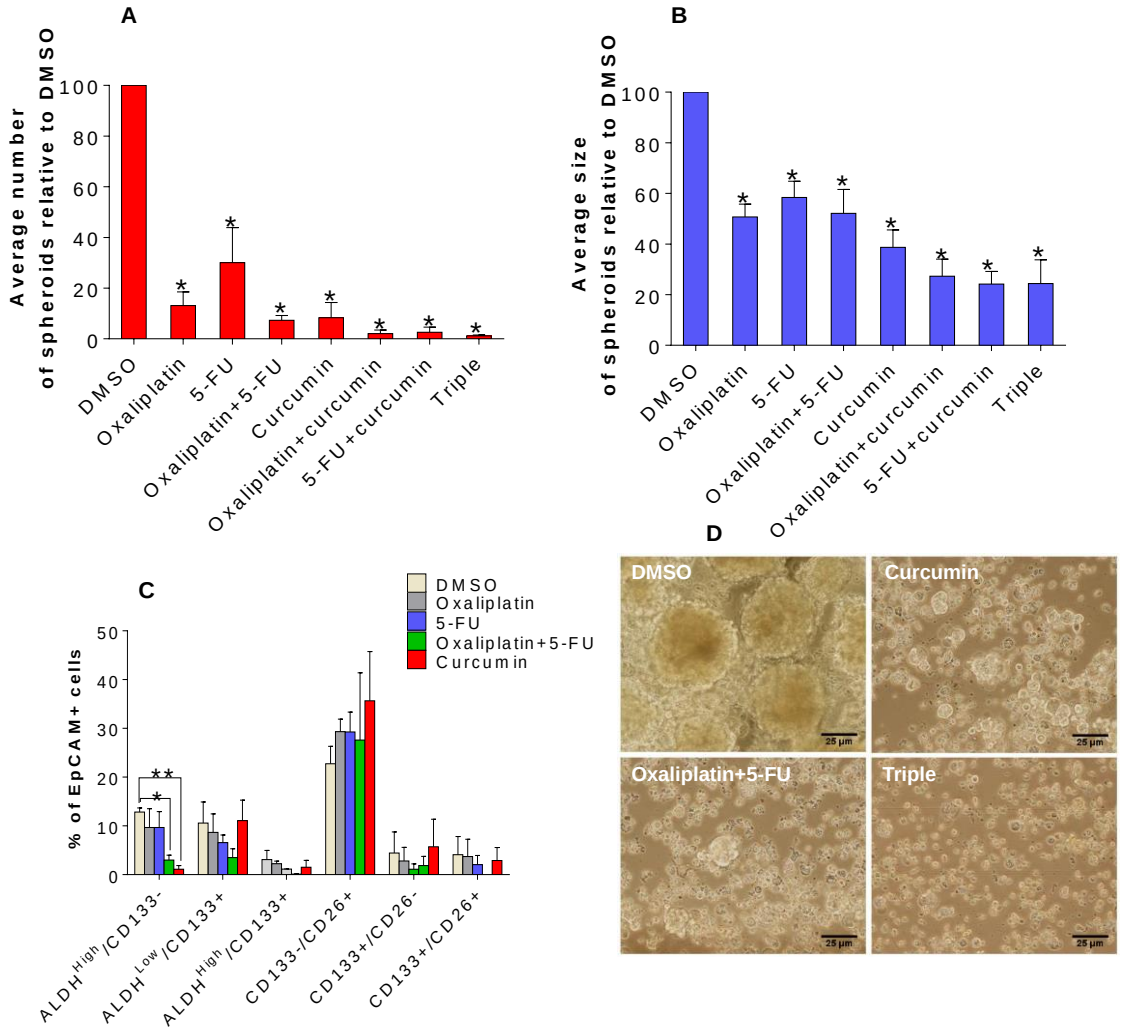

Figure 4.1 The effects of combinations of curcumin, oxaliplatin and 5-FU on spheroid growth from single cells derived directly from a CRLM patient sample. (A) Spheroid number and (B) size (µm) after treatment, represented as a percentage of the DMSO control. (C) Profile of TIC markers expression in spheroids after treatment, represented as a percentage of the EpCAM+ population. Combination treatments with curcumin were not analysed as there was not enough cells available. The triple treatment represents the combination of curcumin+OX+5-FU. No significant differences between treatments were seen. (D) Representative light microscopy (x20 objective) photos of spheroids after treatment. For all analyses, experiments were performed on three separate occasions using the same sample, and the error bars represent SEM. Significant differences compared to the DMSO control are indicated by * and **, where P≤0.05, and **P≤0.001 respectively.

Spheroids were also left to grow until the average spheroid diameter was 50 µm, prior to commencing treating (Figure 4.2). This experiment is different to the previous as it tests the ability of the combinations to kill cells in established spheroids rather than preventing cells from forming spheroids. Similar to seeding single cells into treated media, as in Figure 4.1, treatments caused a significant decrease when compared to DMSO, and there were no significant differences between the individual treatments. However, the magnitude of effect on spheroid number was smaller, with an average 60% reduction relative to DMSO control incubations, compared to 91% when cells were seeded into treated media. In contrast to the considerable effects on spheroid size seen with all treatments, there were no significant differences observed in spheroid diameter or TIC markers with any of the seven types of treatment. These differences also reflect the ability of the treatments to either prevent spheroid formation (seeding cells into treated media) or kill cells in established spheroids (treating fully formed spheroids).

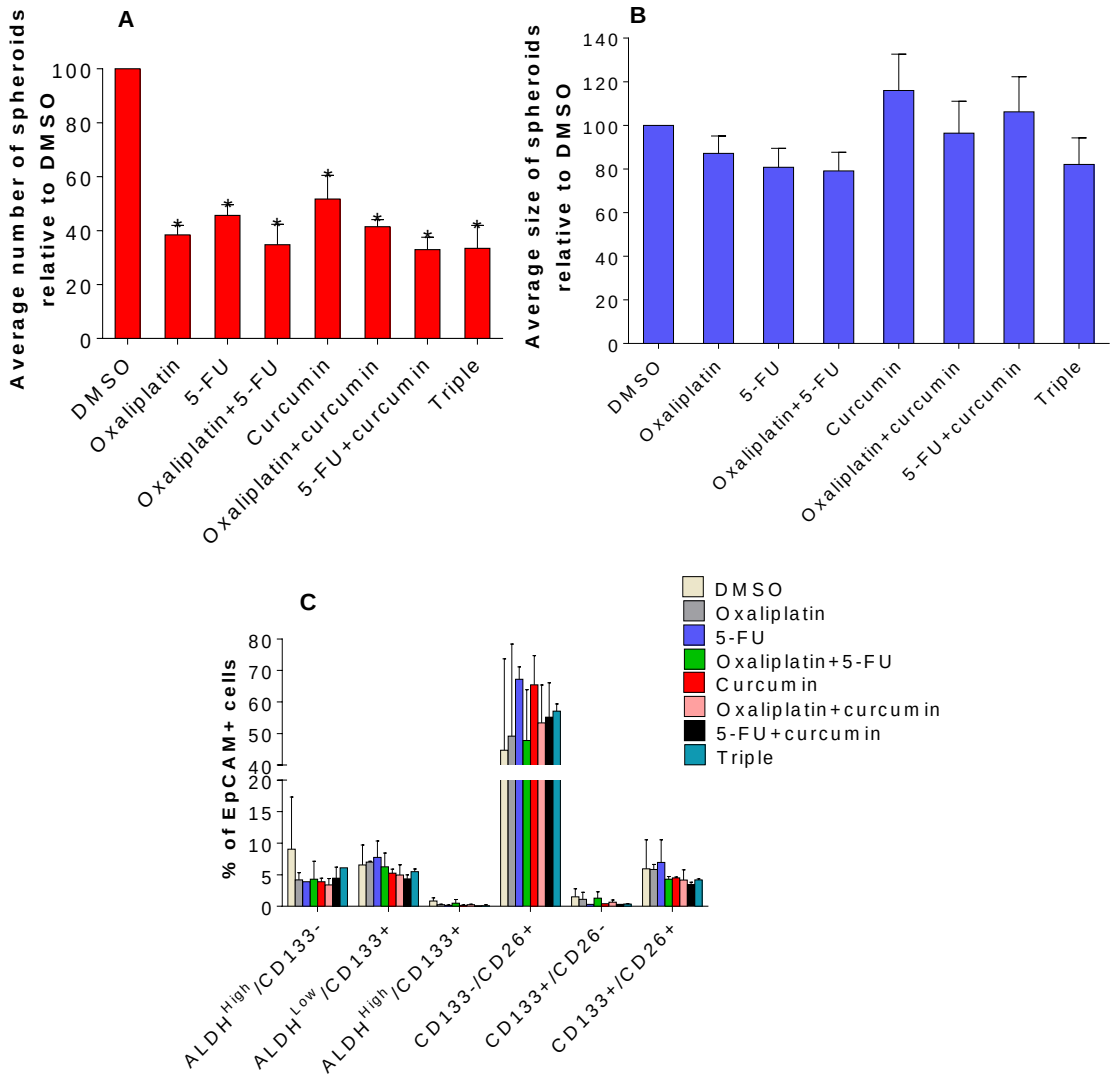

Figure 4.2 The effects of combinations of curcumin, oxaliplatin and 5-FU on established spheroids derived directly from a CRLM patient sample.
(A) Spheroid number, and (B) spheroid size (µm) after treatment, represented as a percentage of the DMSO treatment. (C) Expression of TIC markers in spheroids after treatment, represented as a percentage of the EpCAM+ population. N=3, error represents SEM. For all analyses, experiments were performed on three separate occasions using the same sample, and the error bars represent SEM. Significant differences compared to the DMSO control are indicated by *, where P≤0.05.

4.1.2 Activity of curcumin in spheroids derived from serially passaging CRLM tissue in NOD-SCID mice

In order to increase the spheroid forming capacity of CRLM cells, they were passaged through mice, as described in section 3.7. Cells underwent the same treatment as the samples described in section 4.2.1.

Because the percentage of spheroid forming cells was not known *a priori* for samples passaged first in NOD-SCID mice, a larger number of cells were seeded compared to the sample taken directly from the patient (5X the number) as that sample was known to grow well. Due to the small number of cells obtained from the mouse xenografts, and the large number of cells required for a single experiment, the treatments analysed were: DMSO only, curcumin, OX+5-FU, and curcumin+OX+5-FU (triple combination). However, there was one exception to this as a sample that was derived from a primary colorectal cancer readily grew spheroids, and was also propagated through mice as a means to provide a continuous source of cells. This sample was able to be tested with all combinations of treatments. For this reason, and the fact it was a colon derived sample, the data generated from this sample is grouped and presented on its own.

Five of the xenograft samples passaged in NOD-SCID mice that grew spheroids were treated, two of these were from the same patient so a total of three different patients (two in duplicate) were treated. The data from the replicates were averaged and then the data from the three samples combined. The results show there is no effect on spheroid size, but that the triple combination significantly decreases spheroid numbers in comparison to DMSO ($P=0.028$) and curcumin alone, ($P=0.047$) (Figure 4.3). Treatment with curcumin or OX+5-FU caused non-significant decreases in spheroid number when compared to DMSO, with the order of decreasing efficacy being DMSO>curcumin>OX+5-FU>triple combination. The TIC expression in treated spheroids shows no significant effects, but there was a trend towards an increase in CD133 expression with the triple combination.

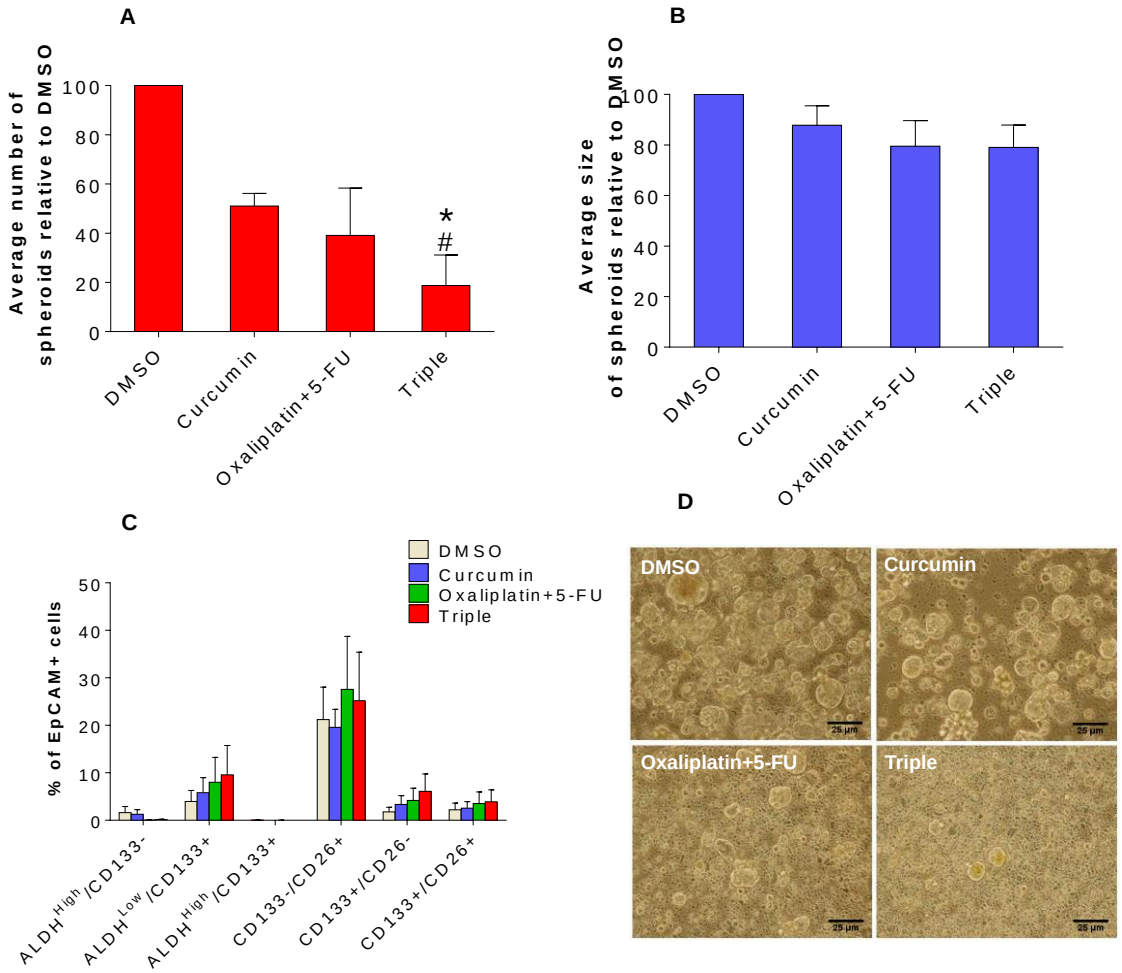

Figure 4.3 The effects of combinations of curcumin, oxaliplatin and 5-FU on spheroids grown from single cells derived from serial passage of CLRM tissue in NOD-SCID mice.

(A) Spheroid number and (B) spheroid size (µm) after treatment, represented as a percentage of the DMSO treatment sample. The experiment was repeated once on 5 samples derived from 3 patients, two samples were duplicates of the same sample but were averaged to produce one data point. (C) Flow cytometric TIC expression data on spheroids after treatment, represented as a percentage of the EpCAM+ population, analysed in four of the samples. All error bars represent SEM, *=P≤0.05. (D) Representative x20 light microscopy photos of spheroids after treatment.

Similar to the aggressive CLRM sample in figure 4.1, the primary colorectal sample analysed in figure 4.4 demonstrated dramatic significant reductions in spheroid numbers across all treatments compared to the DMSO solvent control. A decrease of 72% or more, in the number of spheroids, after all treatments was seen relative to the DMSO. However, no significant differences were seen between individual treatments with respect to spheroid number, although any combination including curcumin contained so few spheroids (less than 1.5% the number of spheroids produced with DMSO treatment) that they could not be profiled by flow cytometry. The size of spheroids was significantly reduced in samples that were exposed to 5-FU alone (P=0.008), or OX+5-FU (P=0.01), when compared to DMSO, or compared to oxaliplatin, P=0.004 and 0.002 respectively. There was a notable but non-significant decrease in the $ALDH^{High}$/CD133- population with OX+5-FU treatment, with curcumin also being able to reduce this population (Figure 4.4C). OX+5-FU also increased the CD26+/CD133- population, which was not observed for curcumin alone.

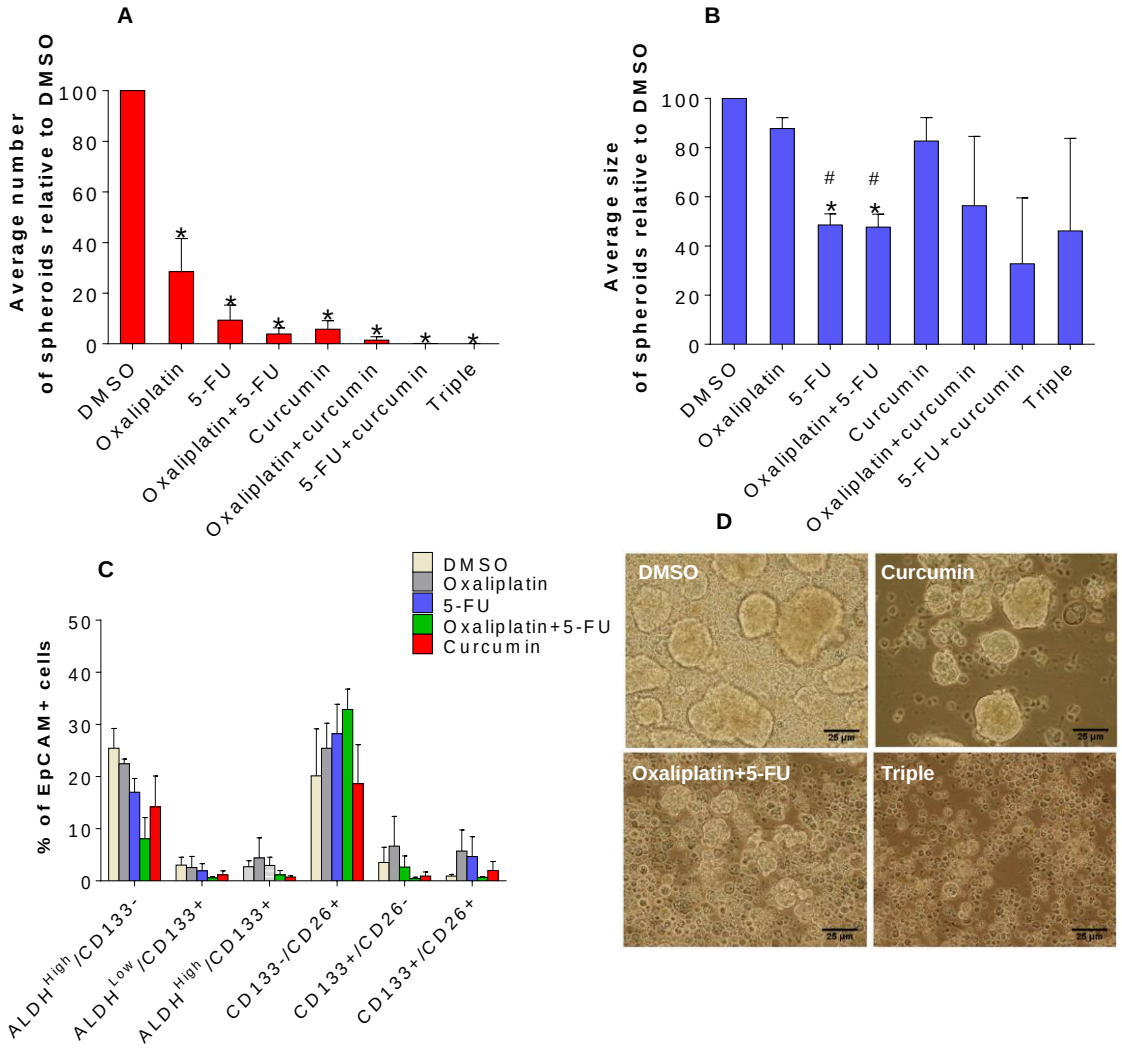

Figure 4.4 The effects of combinations of curcumin, oxaliplatin and 5-FU on spheroid growth from single cells derived from an aggressive colorectal cancer sample propagated by passaging in NOD-SCID mice.
(A) Spheroid number and (B) spheroid size (µm) after treatment, represented as a percentage of the DMSO treatment. (C) TIC marker expression in spheroids after treatment, represented as a percentage of the EpCAM+ population. The experiment was carried out on three separate occasions using the same sample. All error bars represent SEM, *=P≤0.05, #=P≤0.05 compared to DMSO and oxaliplatin respectively. (D) Representative x20 light microscopy photographs of spheroids after treatment.

4.2 **The effects of treatments on pluripotent stem cell markers**

In order to deduce what may be causing the observed decreases in spheroid number following treatment, spheroids that had already grown to an average of 50 µm in size underwent a single treatment with either DMSO, curcumin, OX+5-FU or the triple combination and were analysed at two time points, 24 and 72 hours (Figure 4.5). At the specified time points, spheroids were harvested and lysates generated for analysis using the proteome profiler array. These time points were selected so that changes in early or late response proteins could be identified. Thus far during the investigations, spheroid treatment data had only been to demonstrate anti-proliferative/cytotoxic effects of the treatments under investigation. The proteome profiler array was used to determine whether a shorter treatment time would be sufficient to show an overall response in the spheroid population as a whole, whilst the later time points may be indicative of responses in resistant populations.

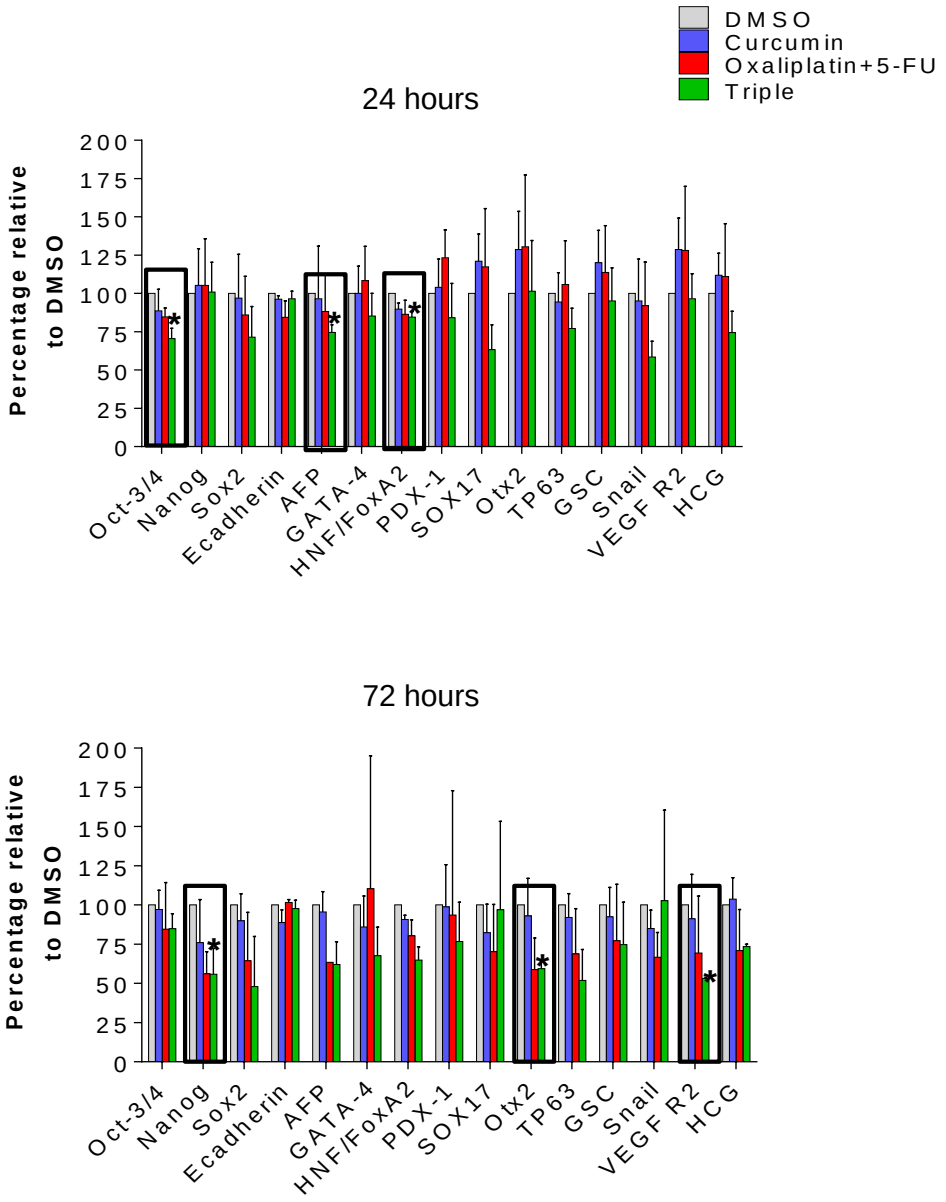

Figure 4.5 Expression of pluripotent stem cell markers in spheroids following 24 and 72 hours of treatment

Spheroids were grown until they were approximately 50 µm in size and were treated with DMSO, curcumin, OX+5-FU or the triple combination for 24 or 72 h, before being harvested and lysates produced for use with the pluripotent stem cell array. Expression is represented as a percentage of the DMSO control. Values for expression were determined by densitometry. The experiment was carried out on three separate occasions using the same sample. Significant differences compared to DMSO are indicated by *, where P≤0.05. Black boxes highlight the proteins that are significantly down-regulated. α-Fetoprotein (AFP), GATA-4 (GATA Binding Protein 4), HNF-3β/FoxA2 (Hepatocyte nuclear factor 3 beta/Forkhead box A2), PDX-1/IPF1 (Pancreatic and duodenal homeobox 1/Insulin promoter factor 1), SOX17 (sex determining region Y-box 17), Otx2 (Orthodenticle homeobox 2), TP63/TP73L (Tumour protein P63/ Tumour protein p73-Like), Goosecoid (GSC), HCG (Human chorionic gonadotropin).

Significant differences in the expression of oct3/4 (P=0.048), AFP (P=0.036) and HNF/FoxA2 (P=0.05) were seen after 24 hours of treatment in the triple combination, when compared to the DMSO control treatment. After 72 hours of exposure there was a significant down-regulation in the expression of nanog (P=0.049), Otx2 (P=0.049) and VEGFR2 proteins (P=0.05) when the triple combination was compared to the DMSO control.

4.3 **The effect of FOLFOX±curcumin on patient derived differentiated cells**

The previous work using spheroids focused on affects that addition of curcumin with OX+5-FU had on spheroid growth and expression of TIC markers. To study the effects on differentiated cells, spheroids from a single patient were allowed to attach to vitronectin-coated plasticware and left to spread out and form a monolayer of cells. These culture methnods (the addition of serum and putting spheroids under adherent conditions) have been shown to promote differentiation demonstrated by a decrease in CD133 expression, and an increase in villin expression indicating enterocyte differentiation, and alcian blue and periodic acid–Schiff staining indicating goblet-like cell differentiation[362]. These were then harvested and seeded on a 96-well plate and treated for six days (Figure 4.6). On the seventh day, cells were analysed using the ATPlite assay, which measures the amount of cellular ATP as a direct indicator of cell number. These results demonstrated a significant 28-50% decrease in the number of cells after treatment with all singlular and combinations of drugs compared to DMSO ($P \leq 0.05$ for all), except oxaliplatin in combination with curcumin which showed no significant affects, and curcumin alone, which induced a small but significant increase in cell number (P=0.019).

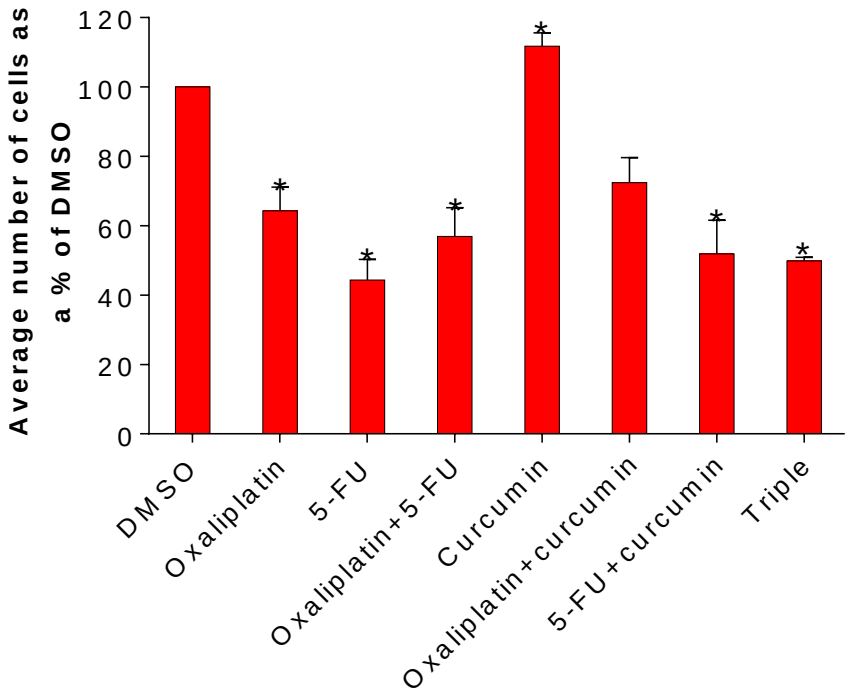

Figure 4.6 The effect on cell number after treating differentiated spheroid cells for 7 days
The ATPLite assay was used to assess viable cell numbers after 10,000 cells/well were seeded into a 96-well plate and left to attach for two days before treating for seven days. Cells were analysed on the seventh day. Each treatment was replicated eight times on the plate, and the experiment repeated in triplicate with cells from a single patient. Significant differences are indicated by *, where P≤0.05 compared to DMSO control.

The same patient sample was then further propagated to enable analysis of the TIC marker expression levels, and the same treatment schedule used for the spheroids. Differentiated CRLM cells were very slow to grow, meaning that propagation of large cell numbers was not practical. This limited the number of treatments that could be undertaken for flow cytometric analysis. Treatments were therefore restricted to DMSO, curcumin, OX+5-FU and the triple combination (Figure 4.7).

The results demonstrated a significant >86% decrease in cell numbers after treatment with OX+5-FU, and the triple combination, when compared to the DMSO control, P=0.008 and 0.009, respectively. Curcumin alone did not affect overall cell number, and did not augment the cytotoxic effects of OX+5-FU. This is also true for the effects on the expression of TIC markers, where the OX+5-FU and triple combination significantly increase the CD26+/CD133- population compared to DMSO, P=0.027 and 0.008 respectively, with curcumin having no effect on its own or additional effect when used in combination. The OX+5-FU combination also significantly decreased the $ALDH^{High}$/CD133- population compared to curcumin (P=0.039), whereas the triple combination causes a similar, but non-significant decrease. Combinations containing CD133 were extremely low (maximum 0.1%) or undetectable.

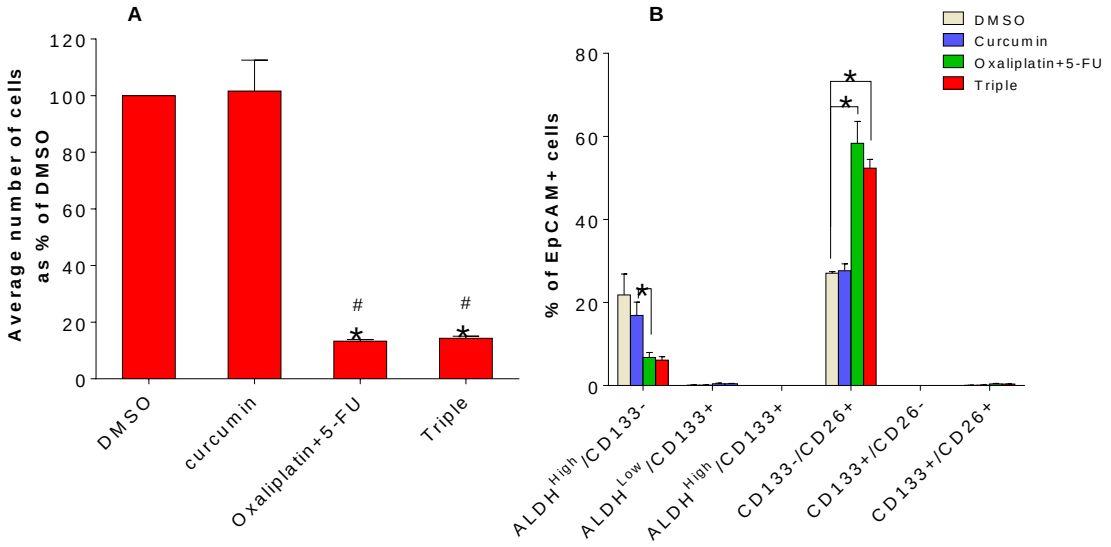

Figure 4.7 The effect on cell number and TIC marker expression after treating differentiated spheroid cells for 4 days
Differentiated cells were treated using the same treatment regimen that was used for treating spheroids (see section 4.2.1). (A) Effect of treatments on cell number, relative to the DMSO solvent control. Viable cells were counted using trypan blue staining. (B) Comparison of the expression profiles of EpCAM+ TIC markers in treated cells. Experiments were performed on three separate occasions, using one patient-derived sample. Significant differences relative to the DMSO control are indicated by *, where P≤0.05, and # represents significant differences compared to curcumin, P≤0.05.

4.4 Air-interface organotypic explant culture

In parallel to treating spheroids, an alternative method termed air organotypic explant culture (abbreviated to explant culture), was also used to further investigate the effects of curcumin in combination with OX+5-FU. The method used was developed by Twiddy et al, Breast Cancer Research, 2010[350], and established for NSCLC by E. Karekla. Through culturing small pieces of tissue directly from the patient, the microenvironmental complexity of the patient's tumour is retained; this model can therefore provide complementary information to the spheroid cultures. This would enable investigation into whether the treatment combinations have differential effects

on the tumour cells in the context of a microenvironment, which has an important role in tumour regulation.

The explant culture method is called an air-interface organotypic explant culture because part of the tumour surface is exposed to the air while another side is in contact with an organotypic membrane floating on top of culture medium. This is reported to help reduce anoxia[389]. However, as one side of the tumour is in contact with the media, (and therefore in closer proximity to any drug treatment in solution), it is possible that cytotoxic effects would not be uniform across the tissue. In order to assess whether drug gradients could be observed across the tissues, ten serial sections were cut across the tissues, which were kept in their original orientation. The first section corresponded to the tissue closest to the media, and each subsequent slide corresponded to one 'step up', with slide ten being the tissue furthest away from the media. Slides one (or bottom) and ten (or top) were stained for ki67 to assess whether equivocal treatment effects were observed. Furthermore, slides two and eight were stained for caspase-3. This approach aimed to validate the use of all of the sections in-between.

Indeed equal effects were seen, and no statistical differences were seen between the front and the back in each patient analysed using a paired t-test, validating the explant model for a maximum of ten slides from the tissue that was in contact with the media (Figure 4.8).

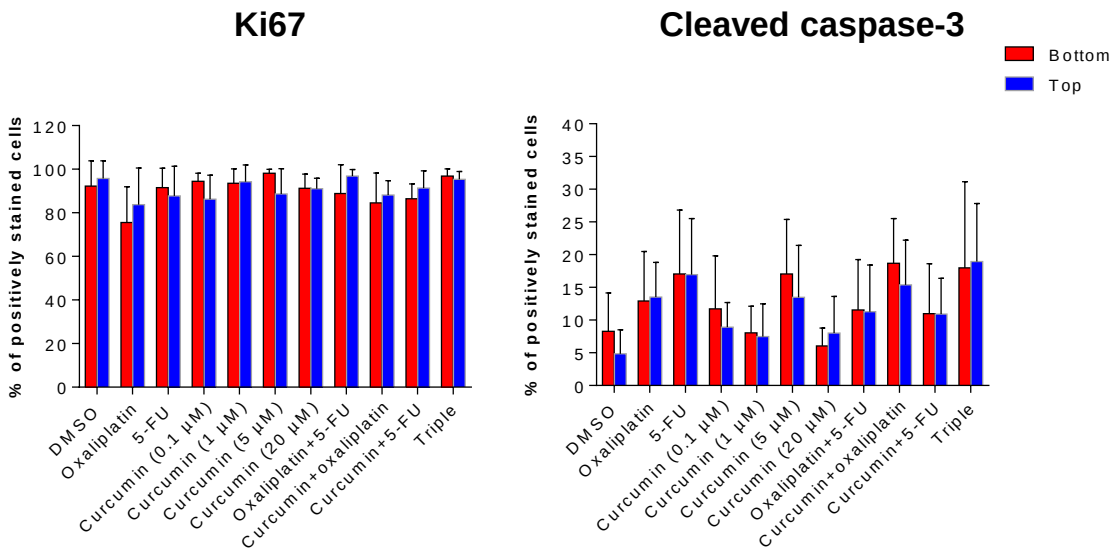

Figure 4.8 Comparison of the antiproliferative and pro-apoptotic effects of various treatments in sections from the bottom and top of the CRLM tissue explants.
Proliferation and apoptosis was assessed by scoring the number of cells stained positive for ki67 and caspase-3, respectively. Slides were scored blind by two investigators, counting up to ten fields of view per piece of explant tissue (nine pieces were used for each treatment). Only tumour cells were scored. Results for each image were averaged between investigators and then the average score of all the images for each treatment averaged. Equal effects were seen between the part of the tissue in contact with the media (the bottom), and tissue corresponding to approximately 40 µm above (the top). Representative results are shown for one patient sample; this analysis was performed on all ten samples used for explant analysis. No significant differences were seen in any patient between the bottom and top.

4.4.1 Effects of FOLFOX±curcumin on proliferation and apoptosis

Each sample was analysed for expression of ki67 as an indicator of proliferation, and cleaved caspase-3 as a marker of apoptosis. After immunostaining, slides were imaged using a x40 objective and then randomised. The pictures were blind-scored by two investigators, only counting the tumour cells, with each image producing a number which represented the percentage of positive tumour cells in that image, for either ki67 or cleaved caspase-3. On each slide there were nine pieces of tissue, with each tissue having a maximum of ten images taken. The results were averaged across the two investigators for each image, and then the score for each

image plotted on a dot plot (Figure 4.9). For the statistics, paired sample t-tests were carried out on each patient, but all of the data from each patient were first tested for normality prior to analysis. If there was mixed data, i.e. some treatment groups were normally distributed and some not, then a parametric t-test (used for normally distributed data) and a non-parametric t-test (used for non-normally distributed data) were both carried when comparing groups of differing normality. All analysis was performed in accordance with guidance provided by the Bioinformatics and Biostatistics Support Hub bio-statistician (Dr Maria Viskaduraki).

All the single and combinations of curcumin, oxaliplatin, and 5-FU were tested, and in some later explants, higher and lower concentrations of curcumin were also examined as single treatments (0.1, 1 and 20 μM). However, this produces a large amount of statistical data. To simplify the analyses, only the most relevant treatments were compared. The single combinations were omitted as in a clinical setting oxaliplatin is not used as a single agent, and 5-FU is rarely used alone. The remaining treatments were analysed to determine whether they were significantly more efficacious than vehicle (DMSO) treatment or significantly efficacious than OX+5-FU treatment. Treatments termed ‘significantly better’ refer to either a significant decrease in ki67, or increase in cleaved caspase-3 staining, compared to the reference treatment (DMSO, or OX+5-FU). These comparators were chosen as comparisons to DMSO will demonstrate whether treatment combinations have any effect, and will also show whether a tumour exhibits resistance to OX+5-FU. The comparisons to OX+5-FU were chosen as they are the basis of the FOLFOX treatment used in the clinic and thus provided a benchmark for treatments to improve upon.

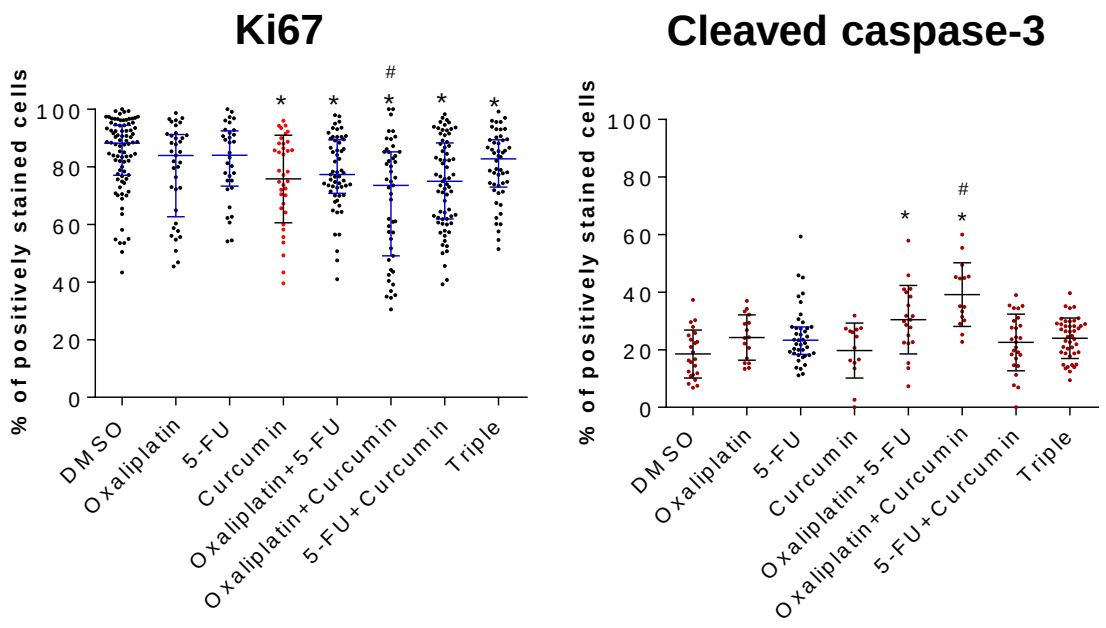

Figure 4.9 Examples of ki67 and cleaved caspase-3 results produced from scoring of explant immunostaining
Normally distributed data are displayed as red dots, black error bars, the average and the standard deviation. Non-normally distributed data are displayed as black dots with blue error bars. Significant differences are indicated where *represents P≤0.05 compared to DMSO, # corresponds to P≤0.05 compared to OX+5-FU. Analysis was undertaken as described in the text above. Each data point represents an average score from one field of view. CRLM tissue was used with results from one patient shown, with the same analysis carried out on a total of ten patients.

In total, 17 samples were explanted however only 10 of these contained enough epithelial cells to proceeded and stain for analysis of treatments. A summary of results from ten different patient explant cultures is presented in Table 4.2, with examples of typical staining patterns presented in Figure 4.10; all the individual analyses are available in the appendix. The data demonstrate that curcumin alone was able to significantly decrease proliferation, and increases apoptosis in 3/10 and 5/10 patients, respectively, when compared to DMSO. This is similar to OX+5-FU, which caused a significant decrease in proliferation and increase in apoptosis in 2/10 and 6/10 patients, respectively, when compared to DMSO. Curcumin also caused significantly more apoptosis in 2/10 patients compared to OX+5-FU. The curc+OX combination is significantly better than the DMSO control in 8/10 patients for both apoptosis and 6/10

for proliferation, which is an improvement on the OX+5-FU combination. The triple combination was only better than curcumin alone and OX+5-FU at reducing proliferation, with 4/10 patients showing a significant reduction in proliferation. The superior treatment based on this data, when comparing whether the treatments perform significantly better than OX+5-FU, is the curc+OX combination, when using these specific endpoint markers of efficacy.

To determine the number of patients that would be needed to find a robust significance difference between patients, power statistics were applied to the data from the ten patients. The number of patients in the study is low (N=10) and so the chances of detecting a significant difference is low. To detect a difference in the mean values for ki67 staining between the triple and DMSO treatments, 45 patients per group would be needed in order to achieve 80% power at the 0.05 significance level, or 250 patients per group to detect a significant difference between OX+5-FU and the triple combination. To achieve 80% power at the 0.05 significance level for differences in the DMSO and triple treatment for cleaved-caspase 3 staining, 64 patients would be needed, and 6300 patients needed to see a difference between OX+5-FU and the triple treatment.

Treatment observations	Marker	Curcumin	Oxaliplatin+ Curcumin	5-FU+ Curcumin	Oxaliplatin+ 5-FU	Triple
Significantly better than DMSO	*Ki67*	3/10	6/10	5/10	2/10	4/10
	Cleaved caspase-3	5/10	8/10	5/10	6/10	4/10
Significantly better than OX+5-FU	*Ki67*	1/10	3/10	1/10	N/A	0/10
	Cleaved caspase-3	2/10	2/10	1/10	N/A	2/10

Table 4.2 A summary of the effects of various treatment combinations on explant proliferation and apoptosis

The blue row shows the results from analysis of ki67 immunostaining, and the white rows display data generated from analysing cleaved caspase-3 staining. N/A=not applicable. CRLM tissue was divided up and up to nine pieces of tissue were used per treatment. This was performed on a total of 10 patients. Tissue sections from each treatment were used to stain immunhistochemically for ki67 and cleaved-caspase 3. The slides were scored blind by two investigators and the results averaged. This was done for each patient, with statistical analysis using paired t-tests also performed on each patient explant. The number of patients that had a significant decrease in staining for ki67, or significant increase in staining for cleaved-caspase 3, is represented over the total number of patients.

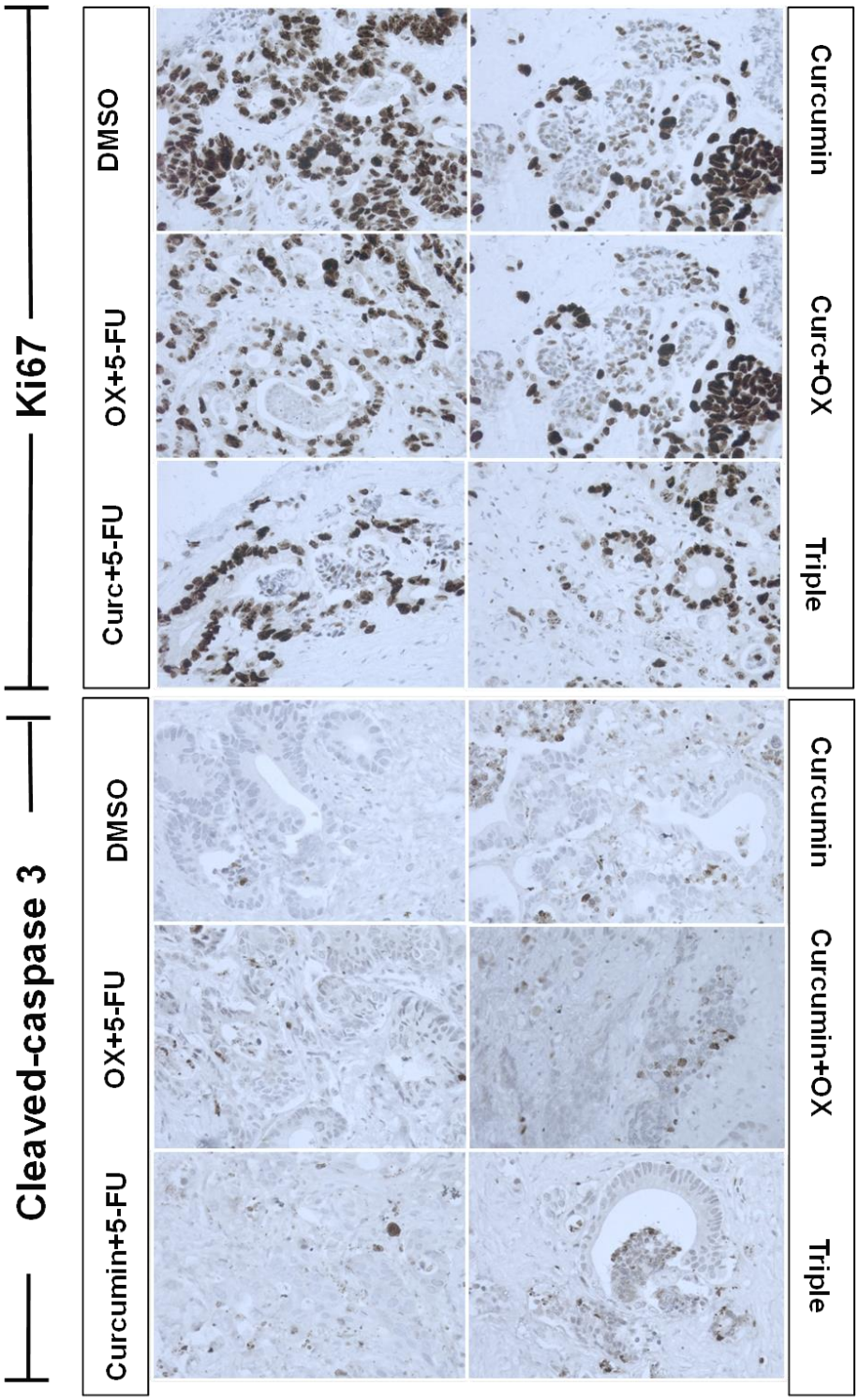

Figure 4.10 Examples of ki67 and cleaved-caspase 3 staining of CRLM tissue sections from explant cultures after treatment with drug combinations for 24 hours.

CRLM tissue from ten patients was used for explant culture and treated for 24 hours with curcumin, 5-FU and oxaliplatin, and combinations, with the triple combination representing all three drugs. Treated tissue was used for IHC to assess ki67 and cleaved-caspase expression. Examples of staining for each treatment are shown

4.4.2 The effects of FOLFOX±curcumin on TIC markers in CRLM explant cultures

To assess whether curcumin alone, or chemotherapy combinations containing curcumin can target the TIC population in treated CRLM explant cultures, immunostaining was carried out for the three main markers used in this study; CD133, CD26, and ALDH1A1. Flow cytometric data relies on determining the activity of ALDH enzymes, rather than the specific ALDH1A1 protein levels, but there is ambiguity in the literature as to whether ALDH1A1 protein levels provide accurate discrimination for TIC populations, although one study has shown them both (activity and expression) to be linked in colorectal cancer[128]. Additionally, nanog was chosen for further investigation, as it was identified by the proteome profiler array as one of the proteins that was down-regulated after treatments. Furthermore, in our laboratory it has been shown to be overexpressed in the $ALDH^{High}$ population in colorectal cancer cell lines compared to the $ALDH^{Low}$ fraction, and its down-regulation by curcumin correlates with reduced spheroid growth (A. Karmokar unpublished data).

One slide from each of the treated explants was used to stain for the TIC markers. Scoring was performed blind by a single pathologist. The scoring results generated a single score for each TIC marker, and was in the form of: no expression (-), low expression (+), medium expression (++) and high expression (+++). Due to the data being ordinal it is unamenable to statistical analysis and so the data is only presented in a fraction with the patients that had a decreased expression after treatment over the total number of patients. An example of this analysis is shown in table 4.3. The results from scoring each of the ten individual patient samples for each treatment are presented in the appendix; examples of the different staining for treatments is shown in figure 11, and a summary of the results is presented in table 4.4.

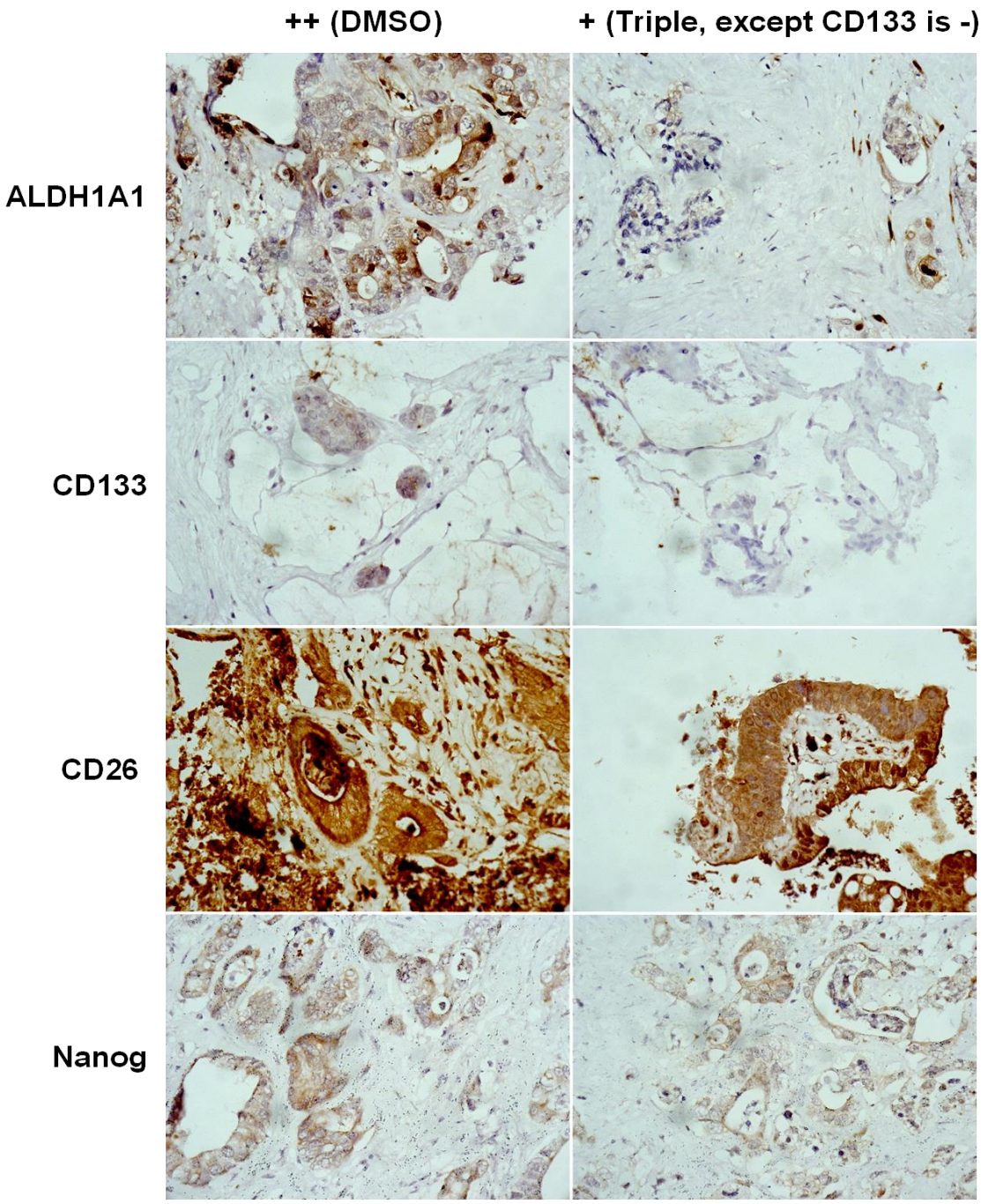

Figure 4.11 Examples of ALDH1A1, CD133, CD26 and nanog staining of CRLM tissue sections from explant cultures after treatment with DMSO or the triple combination for 24 hours

CRLM tissue from ten patients was used for explant culture and treated for 24 hours with curcumin, 5-FU and oxaliplatin, and combinations, with the triple combination representing all three drugs. Treated tissue was used for IHC to assess expression of TIC markers. All slides were scored by a trained pathologist using the score system; (+) minimal, (++) moderated and (+++) strong staining, staining of mucosubstances and stromal cells was not included in the overall score and only clearly viable cells were included. Examples of staining from DMSO treatments that gave a score of (++) are presented on the left, and examples of staining that a gave "+" score (except for CD133 which displays a (–) score) is presented on the right.

Treatment	P093	P102	P103	P104	P115	P122	P141	P155	P184	P188
DMSO	-	+++	-	++	+	++	+++	+	+++	-
Curcumin+ oxaliplatin	-	++	-	+	+	-	+++	-	+++	+
Changes in staining	ND	Less	ND	Less	ND	Less	ND	Less	ND	More

Table 4.3 An example of how staining differences between explant samples for TIC markers was assessed, and summarised.
In this example there are a total of ten patient samples, with four that show a decreased in staining compared to DMSO treatment. This is determined as the staining intensity assessed by no expression (-), low expression (+), medium expression (++) and high expression (+++) is lower in 4/10 patients. This is highlighted in the bottom row indicated by 'Less', no difference in staining ('ND') in this example is seen in 5/10 samples, and one sample shows an increase, indicated by 'more'.

Treatment observations	TIC Marker	Curcumin	Oxaliplatin+ Curcumin	5-FU+ Curcumin	Oxaliplatin+ 5-FU	Triple
Better than DMSO	*ALDH1A1*	4/10 (40%)	4/10 (40%)	2/10 (20%)	2/10 (20%)	3/10 (30%)
	CD133	3/9 (33%)	5/9 (56%)	4/8 (50%)	3/9 (33%)	2/7 (29%)
	CD26	1/9 (11%)	1/9 (11%)	1/10 (10%)	1/10 (10%)	2/10 (20%)
	Nanog	2/8 (25%)	1/9 (11%)	2/10 (20%)	2/10 (20%)	1/8 (12.5%)
Better than OX+5-FU	*ALDH1A1*	3/10 (30%)	3/10 (30%)	1/10 (10%)	N/A	2/10 (20%)
	CD133	3/9 (33%)	4/9 (44%)	3/8 (37.5%)	N/A	1/7 (14%)
	CD26	0/9 (0%)	0/9 (0%)	0/10 (0%)	N/A	1/10 (10%)
	Nanog	2/8 (25%)	2/9 (22%)	2/10 (20%)	N/A	1/8 (12.5%)

Table 4.4 Immunohistological assessment of CRLM explant cultures for TIC markers
Ten CRLM samples from different patients were used for explant culture, and CD133, ALDH1A1, CD26 and nanog expression assessed following treatment with combinations of curcumin, oxaliplatin and 5-FU. The changes in expression of these markers were used to assess the ability of the treatments to reduce the number of TICs *ex vivo*. A trained pathologist who was blinded to the treatment groups assessed expression of the TIC markers. Samples were scored using a (-), (+), (++) and (+++) grading system based on staining intensity and number of stained cells. A treatment was counted as more efficacious (better) in a particular patient if it had a lower score than the corresponding DMSO or OX+5-FU incubations. The denominator represents the total number of patients, some are less than ten as the sections were deemed to contain insufficient tumour tissue to accurately assess. The numerator represents the number of samples deemed more efficacious than the DMSO or OX+5-FU groups.

The results from assessing the TIC markers, and using these markers as end points to assess the efficacy of treatments, revealed the combination of curc+OX to be the most superior, with 4/10 and 5/9 samples having a decrease in ALDH1A1 and CD133 staining, respectively, compared to DMSO (Table 4.4). Also, when compared to OX+5-FU, the curc+OX combination was again the best at causing a significant decrease in 3/10 and 4/9 samples for ALDH1A1 and CD133, respectively. Curcumin alone also showed a better response in terms of reduced ALDH1A1 staining in 4/10 samples compared to 2/10 in the OX+5-FU group, when comparing to DMSO. No difference in the number of responders was observed with CD133 expression between curcumin and OX+5-FU vs DMSO. The triple combination had a similar overall effect to OX+5-FU when compared to the DMSO control, but also down-regulated a proportion of responders to a greater degree than OX+5-FU as some patients show a decreased amount of expression relative to OX+5-FU.

For CD26, only one patient in each group showed a better response compared to DMSO, except for the triple combination, with CD26 expression decreased in two patients. Compared to OX+5-FU, only one patient showed a superior CD26 decrease, which was following treatment with the triple combination. When analysing nanog expression, 2 patients in all groups showed a better response when compared to the OX+5-FU group, with the exception of the triple group in which only one patient responded better than the OX+5-FU group.

4.5 **IHC expression analysis of proteins involved in chemoresistance in CRLM**

It has been suggested that MMR/MSI can predict a lack of response to 5-FU, which is supported by data from both *in vitro* and clinical studies[227-229], and mutations in ERCC1[237-239] and XRCC1[243,244] can predict response to oxaliplatin treatment. Expression of MLH1, MSH2 and MSH6 have been demonstrated to be silenced by methylation or mutations which directly links to lack of protein expression, while

polymorphisms in ERCC1 and XRCC1 have been shown to reduce their protein expression. Therefore by assessing the expression at the protein level it is possible to deduce whether patents may have a mutation or methylation of the corresponding gene.

The expression of the DNA repair proteins was analysed in patient CRLM tissue by IHC and subsequently assessed by a qualified pathologist (Figure 4.12 and Table 4.5). This was to determine if a correlation between treatment responses from the explant culture data could be due to differences in the expression of proteins involved in DNA repair. Additionally, this analysis was also to try and identify whether any of these proteins could also act as a predictor of curcumin response. Differences in staining intensity could be seen between patients (Figure 4.12 and Table 4.5), however no truly negative samples were detected.

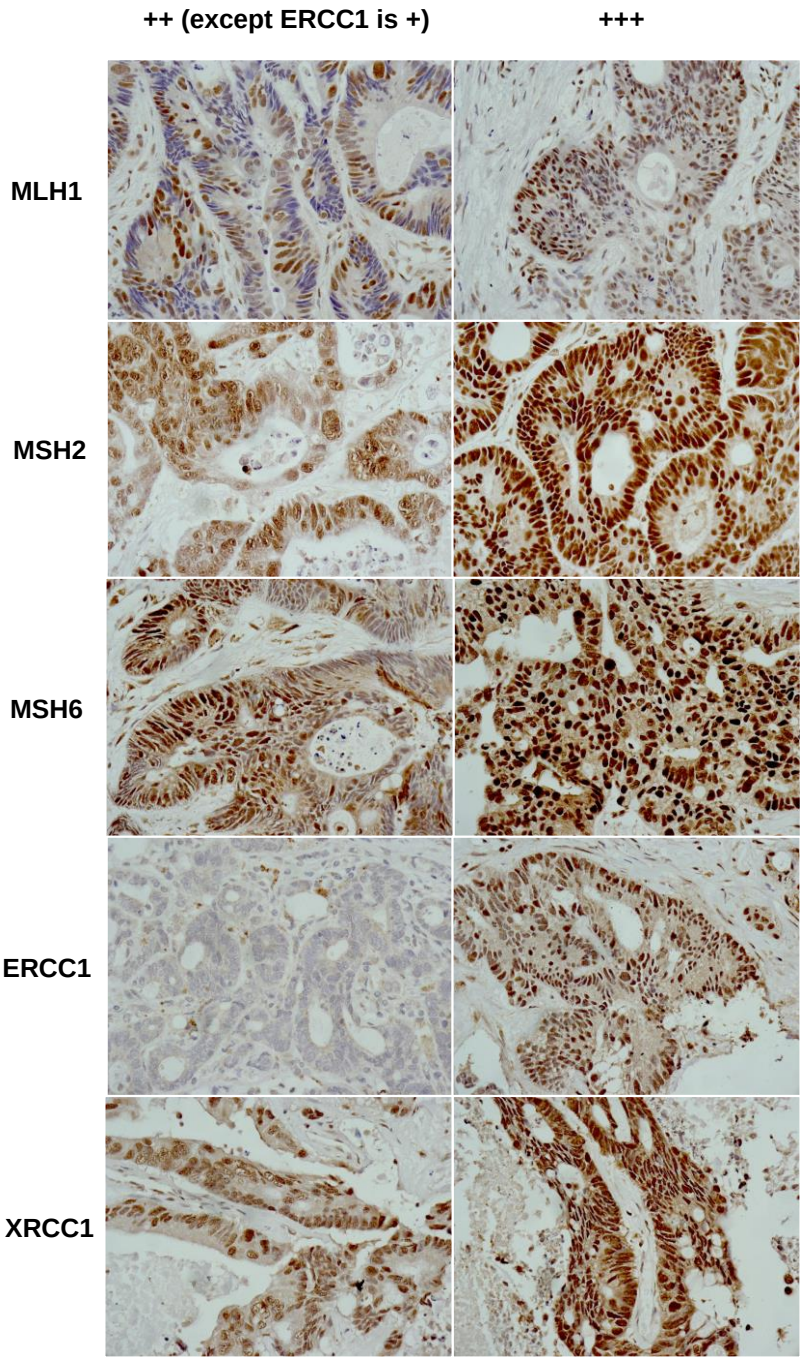

Figure 4.12 An example of the immunostaining produced when analysing proteins involved in chemoresistance in CRLM by IHC (objective lens X40).
The same patients used for the explant treatment were also stained for DNA repair enzymes using CRLM tissue taken directly from the patient (not explanted tissue). The staining was scored by a trained pathologist. Sections were scored on a three point scale; minimal (+), moderate (++) and marked (+++). The ubiquitous staining of smooth muscle and fibroblast nuclei in most sections was used as an internal positive control. Above, examples of (++) staining on the left (except for ERCC1 which shows a (+) staining) compared to (+++) staining on the right.

Patient	MLH1	MSH2	MSH6	ERCC1	XRCC1
P093	++	+++	+++	++	+++
P102	++	+++	+++	++	++
P103	+++	+++	+++	+++	+++
P104	++	+++	+++	+++	+++
P115	++	++	++	+	++
P122	+++	+++	+++	+	+++
P141	++	+++	+++	+	+++
P155	+++	+++	+++	++	+++
P184	+++	+++	++	++	+++
P188	++	++	++	++	+++

Table 4.5 Analysis of the basal expression of DNA mismatch repair proteins by IHC in the 10 CRLM patient samples used for explant culture.
A trained pathologist assessed the staining and assigned a score of either (+), (++) or (+++) with more plus symbols representing a greater amount of expression.

Despite not finding any truly negative patients, it may be that there are still differences in response between patients who have higher or lower expression for the markers investigated. Therefore, the different level of expression of the DNA repair proteins were used to stratify the ki76 and cleaved-caspase 3 explant culture data. For this analysis, patients with the same scoring were grouped together (i.e. all patients with ++ staining for MLH were grouped together) and only groups that contained a minimum of three patients (n=3) were included for comparison. These groups with different staining intensity were then compared for proliferation and apoptosis using the previous explant data, this left only MLH1 and MSH6 as these were the only groups which contained 3 patients. Patients that had a lower scoring intensity for MLH1 responded significantly better to oxaliplatin and curc+OX, with a decrease in ki67 staining of 89 vs 71%, and 89 vs 62% compared to DMSO, respectively, P=0.015 for both. However, it is important to note that the basal level of proliferation slightly differed for each group (87 vs 82%). There was a trend for increased apoptosis in the lower intensity staining group for MLH1. MLH6 didn't show any significant effects, however the opposite trend for cleaved-caspase staining was seen.

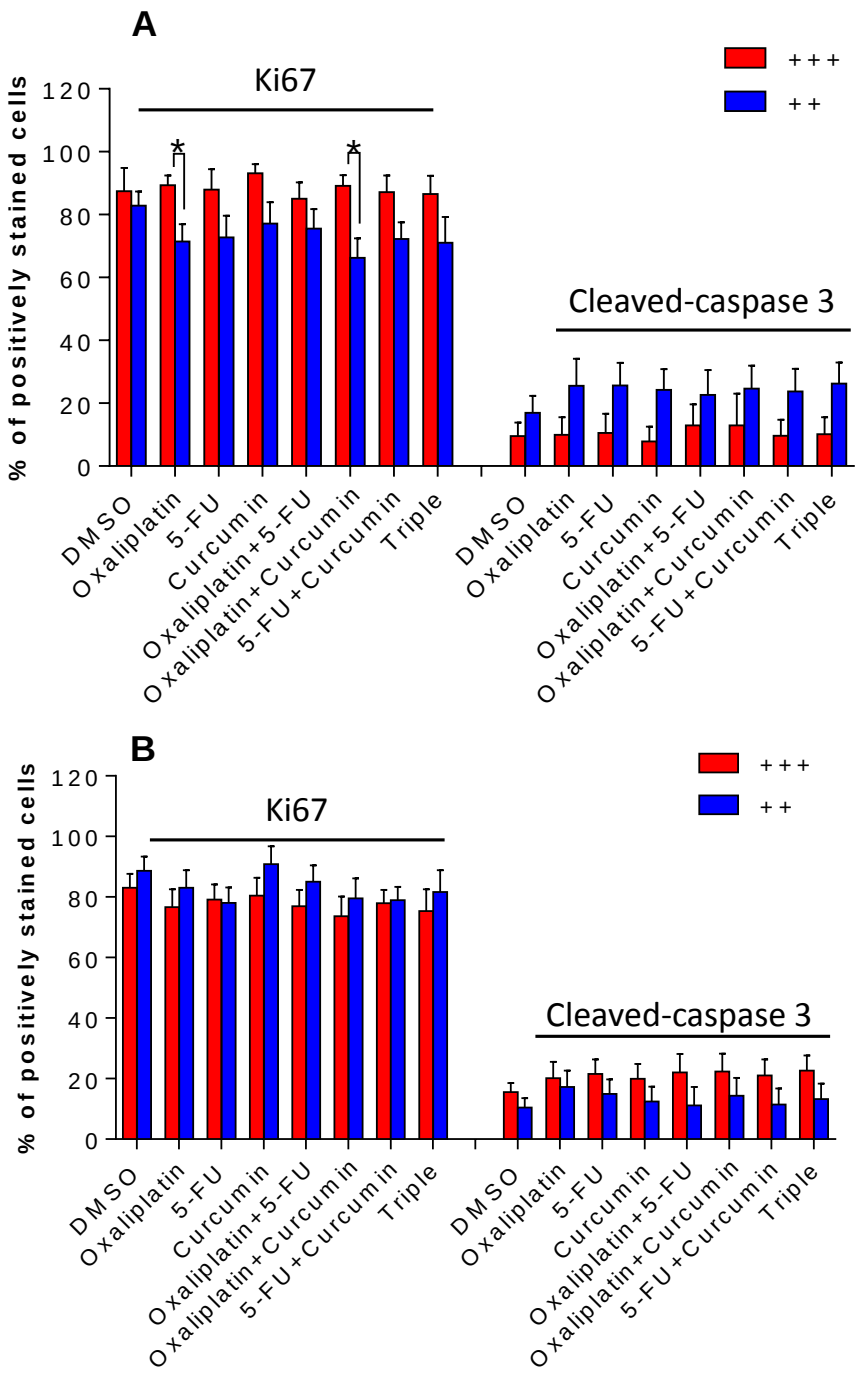

Figure 4.13 The average cleaved caspase-3 and ki67 staining scores for each treatment stratified based upon expression levels of MLH1 (A) and MSH6 (B). Mismatch repair protein expression was assessed immunohistochemically and graded by a trained pathologist. The more '+' symbols indicates a greater amount and intensity of staining. Patients with the same scoring vale for a given marker were grouped together and only groups that contained three or more patients were included (N=3). This data was then combined with the explant ki67 and cleaved-caspase 3 staining data to see if responses differed with MMR protein expression. An independent sample t-test was applied, *=P<0.05. N=6 and 4 for MLH1 (++) and (+++) groups respectively, and N=3 and 7 for (++) and (+++) respectively.

4.6 **Discussion**

Previous research suggests that TICs may be a chemotherapy resistant population[128]. Targeting the TIC population could therefore result in a much greater efficacy in the long term than non-specifically targeting cells. However, in the short term the effects may be less noticeable using conventional measures of efficacy as the TIC population is likely to represent only a small proportion of a tumour, and so the tumour mass and volume may initially be unaffected. Therefore, when investigating a potential new therapeutic it is pertinent to investigate its effects on the TIC population.

Spheroid growth is sensitive to treatment with OX, 5-FU and curcumin

In order to initially ascertain how TICs derived from CRLM were affected by oxaliplatin and 5-FU, and whether curcumin could potentiate any observed effects, spheroids were treated and assessed for size, number and TIC marker expression. Spheroids have been shown to represent a useful model for analysis of putative anti-cancer drugs, due to being more representative of a tumour[352]. For such reasons they are being exploited for the development of high-throughput drug screening[390,391]. Most literature cites TICs and spheroids as being resistant to conventional treatment[154], however the single fast growing CRLM sample analysed direct from the patient formed significantly less spheroids in response to all treatments examined. This was also seen in a second sample derived from a primary colorectal cancer tissue. These samples had a very high proliferative capacity compared to all other samples, and it may have been that this sensitivity was reflected in the fact that oxaliplatin and 5-FU both act via mechanisms related to cellular proliferation. It is also likely to be a reflection of the methods used. Here, cells were seeded in media containing treatment, whereas most studies treat fully formed spheroids[154]. Exposing single cells may have enhanced the drug toxicity effects, as the cells may be more proliferative while forming the spheroid than when fully formed. Also, when they are fully formed spheroids it is possible that,

due to the larger number of potentially metabolically active cells and three dimensional structures, the concentration each cell is exposed to is reduced.

Studies have revealed large spheroids have gradients of oxygen and nutrients, causing differences in proliferation throughout the spheroid with only the outer ring containing proliferating cells, followed by an inner ring of less-proliferative cells surrounding a central necrotic core[352]. Therefore, treatments on large spheroids that use drugs targeting proliferative cells are likely to only see small decreases in size, as only the outer ring of cells would be affected. Additionally, cell-cell contact has also been demonstrated to increase drug resistance[392]. This may explain the reduced response seen when fully formed spheroids were treated. Surprisingly, curcumin appeared to have a similar efficacy to oxaliplatin and 5-FU. Despite there not being any significant differences between treated samples with respect to spheroid number, there was a trend towards a lower number of spheroids in combinations containing curcumin. The results demonstrating spheroid sensitivity to curcumin are in line with published data from colorectal cancer cell lines, which also showed that curcumin enhanced OX+5-FU-mediated spheroid disintegration[339]. However, spheroid sensitivity to oxaliplatin and 5-FU is contradictory to the hypothesis that TICs are resistant to cytotoxic chemotherapy. Todaro *et al*., describe an established spheroid system that also demonstrated a small decrease in established spheroid viability after a 24 hour exposure to oxaliplatin and 5-FU[154]. It may be that a small proportion of the cells have resistant characteristics, whilst others retain their drug sensitivity as small numbers of spheroids were observed growing in treated media. It could also be possible that the resistant spheroids did not contain cells expressing the stem cell markers that have been used in this study, this would explain why no marker is enriched after therapy.

Treatments effects on TIC markers

Flow cytometry was used to directly assess the effects on TIC markers, however combination treatments containing curcumin on primary CRLM and CRC spheroids resulted in such low numbers of cells it was not possible to profile them, which demonstrates that addition of curcumin to oxaliplain+5-FU is beneficial in targeting TICs.

Previous research has established that the markers used here can be modulated by OX+5-FU and curcumin. For example, CD133 expression has been reported to be higher in FOLFOX resistant cells[342]. Additionally, treatment with curcumin decreases ALDH1A1 and CD133 expression in *Apc^{Min}* mice given oral curcumin for 5 consecutive days, for 4-weeks[342].

For CRLM and CRC samples, the main effect on TIC markers induced by curcumin was a significant decrease in the ALDH^{High}/CD133- population. Recent research into CRC and head and neck cancer cell lines has also shown that curcumin decreases ALDH expression and activity in spheroids and xenografts, accompanied by decreased growth[386,393,394]. OX+5-FU caused a decrease in CD133 expression in these studies, reflecting the results found in chapter 3 when analysing patient samples and stratifying by chemotherapy. As the reports of CD133+ cell resistance to therapy stems from primary CRC, it may be that in CRLM the CD133+ cells are sensitive to therapy. A previous trial studying metastatic CRC found that high CD133 expression in tumour tissue before post-operative FOLFOX and Bevacizumab was associated with a better response rate[395]. It may be interpreted that this was due to the CD133+ population being sensitive to therapy, because if there are high levels and this population of cells is killed then it would lead to greater tumour shrinkage, explaining why a better response was seen. Unfortunately, the study did not present any data on patients who were treated prior to surgery and so CD133 comparisons between treated and chemo-naïve patients could not be made. The CD26+/CD133- population, identified as being more chemo-resistant in the previous chapter, did not show a decrease after curcumin

treatment, except in the primary CRC derived spheroids. The differences in sensitivity between the CD133+ populations and the CD26+/CD133- population may be a result of proliferation rates, as oxaliplatin+5-FU targets rapidly dividing cells, however this would need to experimentally proven.

As no single population appears to increase after treatment but spheroid number and size decreases, the treatments may be non-specifically inhibiting all populations, with the $ALDH^{High}$ population showing an increased sensitivity. It is possible that treatments cause disaggregation of spheroids without causing apoptosis, (reflecting decreases in spheroid counts), although curcumin has been demonstrated to promote apoptosis in spheroids that have disintegrated[393]. These results were also reflected in experiments with the xenograft-derived spheroids.

It is also possible that no enrichment in a TIC marker was seen due to the cellular components of the spheroids possessing the ability to recapitulate all of the cell types within the original spheroid. It may be that this also occurs following treatment-induced cell death, and so the long time points are too late to see an enrichment. Therefore, analysis of both earlier and much longer time points is needed to determine whether there is an enrichment in these markers immediately after treatment, and if the remaining spheres would grow unhindered if re-challenged with OX+5-FU. A recent study has demonstrated that when spheroids grown from colorectal cancer cell lines are treated with curcumin, and then passaged, the cells do not grow for up to 28 days after which they started to form small spheroids. This highlights that spheroids are sensitive to curcumin treatment but that there is a resistant population that remains quiescent after treatment. However, they did not re-challenge with curcumin to see if the cells could still respond to treatment[393]. Overall, the data accumulated on spheroid treatments points to curcumin possessing an anti-proliferative effect, which demonstrates agreement between published cell line data and patient derived samples.

Importantly, curcumin does not negatively affect the cytotoxicity of either oxaliplatin or 5-FU alone, or in combination. The triple combination of curcumin with

OX+5-FU appears superior, due to the enhanced effect against spheroid growth. The dosing regimen used in this study was only every 3-4 days due to practical constraints with curcumin having a reported half-life of 8 hours in media containing 10% FCS, and reduced stability in media with less FCS[388]. The media used for treating spheroids contained no FCS and so curcumin was likely to have an even shorter half-life, with no accumulation in the media. In the clinical setting, patients would be able to take oral curcumin daily which may result in more regular, daily, exposure to curcumin and therefore curcumin may have greater activity.

Curcumin does not target adherent CRLM cells

In order to try and establish whether the enhanced effect observed on spheroid growth with curcumin in combination with OX+5-FU was due to effects on the more differentiated population, cells were cultured under adherent conditions to differentiate them prior to treatment. Curcumin caused a small, but significant increase in cell number and no difference on TIC marker expression, demonstrating that it does not inhibit the growth of differentiated CRLM cells at the concentrations used in this experimental condition. It has not previously been demonstrated that curcumin may promote proliferation in CRC, but it has been shown to promote differentiation and in breast models it decreases self-renewal in mammary spheroids, but does not affect differentiated cell numbers[341]. While this study by Ginestier,C *et al*., used cells derived from normal breast tissue, similar mechanisms may apply to cancer cells, as the authors also found a decrease in ALDH1A1 expression following curcumin treatment[130]. OX+5-FU caused a significant decrease in cell number, and increase in CD26+CD133- expressing cells, which was not affected by curcumin. The increase in CD26+/CD133- cells after oxaliplatin and 5-FU treatment reinforces this population as a chemo-resistant population, but it was not targeted by curcumin. CD26 has been described to be associated with adhesion to fibronectin and collagen[136]. To adhere to plasticware and differentiate the spheroids, fibronectin coated plates were used, which

may reflect why CD26+ cells were increased under these culture conditions. OX+5-FU, alone and when combined with curcumin, also caused a significant decrease in $ALDH^{High}$ activity, further demonstrating the sensitivity of this to OX+5-FU, and curcumin.

Curcumin enhances the ability of OX+5-FU to target embryonic stem cell markers in spheroids

To try and identify novel targets related to spheroid growth that treatments may be affecting, and to identify additional TIC markers, a proteome profiler array was used to analyse the expression of pluripotent stem cell markers in response to treatment. The early time point used (24 hours) was to identify embryonic proteins whose expression is inititally altered in response to the treatments, whereas a later time point (72 hours) would reveal proteins expressed in surviving cells and therefore identify embryonic proteins that are involved in resistance. Previous research has highlighted a role for pluripotent stem cell markers in cancer, and key embryonic proteins such as nanog have been demonstrated to be expressed in spheroids. The transcriptional network that maintains the embryonic stem cell is co-ordinated through nanog, Oct4 and Sox2/3 which co-regulate a large number of genes[396]. Whereas nanog has been described as a promoter of self-renewal in cancer, Oct4 has been shown to be overexpressed, but it is not well characterised in cancer[397]. Nanog functions to promote a progenitor phenotype, and prevent differentiation in embryonic, mesenchymal and induced pluripotent stem cells by positively regulating the expression of genes important in maintaining a stem cell state, and repressing lineage specification[396,398]. However, recently it has been shown that nanog is dispensable for induced pluripotency under optimal conditions and through the addition of ascorbic acid[399]. Ectopic over-expression of Oct4 has been proven to block differentiation and maintain a progenitor phenotype, generating tumours in the skin and adenocarcinoma *in situ*–like dysplasia in the intestine, using an Oct4 inducible mouse model[400]. When the

expression of Oct4 is forced in malignant melanoma cell lines, it promotes de-differentiation of cells and is required for tumour maintanence[358].

The array identified six proteins that were down-regulated, all of which were by the triple combination, when compared to DMSO treatments. The affected proteins included Oct4 at the 24 hour time point and nanog at the 72 hour time point. Forced nanog expression has been shown to increase clonogenicity and tumourigenicity in xenografts, and high expression is linked to poor survival[133]. Furthermore, nanog expression has been shown to increase 8-122-fold during colon spheroid formation and drive proliferation, with a nanog knock-down model resulting in decreased spheroid formation[361]. The functional role for nanog in spheroid formation appears to correlate with the curcumin-mediated decrease in nanog and associated decrease in spheroid number. Other proteins identified as significantly down-regulated by the triple combination include AFP and HNF/FoxA2 after 24 hours compared to DMSO control, and Otx2 and VEGFR2 at the 72 hour time point compared to DMSO. These results both establish that genes involved in embryogenesis are expressed in spheroids, and that they can be further down-regulated by adding curcumin to OX+5-FU. The decrease in VEGF has been described before in a colorectal cancer cell line xenograft model after treatment with curcumin[387]. It is possible to speculate that the down-regulation of these proteins may play a role in spheroid growth, and may mark the clonogenic population more precisely than cell surface markers. Proteins such as nanog have a known functional role in self-renewal, whereas the functional role of cell surface markers in TICs, such as CD133, are less well understood. Previous reports have described cancer cells using an embryonic program[401] and disruption of this program, may be one potential mechanism through which curcumin selectively affects tumours. For example, Oct4, which was down-regulated after 24 hours following curcumin treatment, is expressed in tumour cells but not in normal somatic tissue[397]. Furthermore, Oct4 has been found to be overexpressed in oxaliplatin-resistant colorectal cancer cell lines, with knockdown reducing tumourigenicity, and higher

expression predicting distant recurrence in patients after chemoradiotherapy[402,403]. In our laboratory, nanog has been demonstrated to be down regulated in colorectal cancer spheroids following curcumin treatments, corroborating findings in the colorectal metastasis model, that curcumin may interfere with proteins typically associated with embryonic stem cell programming. Additionally, nanog binds the promoter of BMI1, a regulator of self-renewal whose inhibition has been recently described to significantly impair tumourigenicity. BMI1 has also been shown to be expressed in ALDH1 cells, therefore, it is possible to speculate that curcumin is causing the observed decrease in $ALDH^{High}$ cells by decreasing nanog and subsequent self-renewal, driven by BMI1. If this was proven true it would provide substantial support for the use of curcumin as a TIC-targeting agent, as self-renewal is a hallmark of TICs. Further research is needed to elucidate the role of nanog in spheroid growth and therapy resistane. Through tranducing the cells with a label to track expression of the proteins of interest identified by the array, such as nanog with EGFP, the cells expressing this marker could then be tracked during treatment. Additionally, this would allow sorting of live cells into nanog positive and negative cells to see whether the populations differ in their ability to function as a TIC e.g. form spheroids, or grow tumours in mice. The other significantly down-regulated markers AFP, HNF/FoxA2 and Otx2 represent novel target genes of curcumin that have not been described before in the literature, however, further research is required to establish the relevance of these markers and that they are necessary for cells to exhibit tumour initiating capacity. Of note, other markers were also seen to decrease (although not significantly due to the large variation) following addition of curcumin, such as SNAIL, which is a master regulator of EMT and has been previously described to be highly expressed in colon spheroids, together with VEGF[404].

Curcumin enhances treatment efficacy in explant culture

Since the efficiency of spheroid formation from patient samples was limited, explant cultures were employed as an alternative model to assess the effects of

treatment combinations in a larger patient cohort. This technique additionally provided the stromal component of the tumours, which is increasingly recognised as playing a critical role in tumour response to therapy and regulation of TICs[78,380,405], and should therefore more rigorously test whether curcumin has clinical potential. Fibroblasts for example, have been shown to interact with metastatic cells through paracrine signalling releasing IL11, which promotes organ colonisation. Macrophages are also an additional source of cytokines (including IL1β), which are thought to contribute to the promotion of Wnt signalling. Without modelling these extra-cellular interactions it is not possible to accurately assess tumour response to a drug, which may be a contributing factor in the attrition rates for drugs that enter clinical trials following pre-clinical evaluation. Recent findings have alluded to the micro-environment affecting drug action, resulting in secretion of cytokines, which ultimately led to promotion of TIC growth. This is exemplified in a study that found treatment of CAFs resulted in secretion of cytokines such as IL17A that increased TIC self-renewal[405], suggesting the microenvironment plays a role in regulating TIC survival/growth after therapy.

Explant culture methods similar to those described within this thesis, have demonstrated that normal colon and colorectal cancer tissue can be cultured for up to two days and retain metabolic activity and a normal morphology[406]. In breast cancer explants, the dietary agent resveratrol was tested as an adjuvant with cyclophosphamide[407], and various antiviral drugs and xenobiotics have been assessed for safety and cytokine production in intestinal inflammation and ulcerative colitis[408-410]. The use of explant tissue may not only provide a model that more accurately mimics an *in vivo* environment, but also helps adhere to principles of the three R's for animal welfare; reduction, refinement and replacement.

The use of curcumin in explant culture for cancer research has not been described before, but previous research has used curcumin in explant culture to assess effects on cartilage inflammation and osteoarthritis[411]. Reduced IL-8 signalling has also been observed following curcumin treatment of porcine vaginal explants with

Staphylococcus aureus, resulting in protection from Staphylococcal Toxic Shock Syndrome Toxin-1[412].

Explants were treated for a short period of time (24 hours), after an adaption period of up to 12 hours. This approach was adopted based on experiments using lung cancer tissue which demonstrated a decrease in viability with time, with 24 hours representing the best time point for viability (Unpublished data, E. Karekla). Significant differences were observed between treatments despite such short exposure times.

Overall, the treatment results point to the curc+OX combination as being the most efficacious, causing a significant effect in most patients for both apoptosis and proliferation. The same trend was observed for the effects on CD133 and ALDH1A1 expression, with the combination of oxaliplatin and curcumin showing either the greatest down-regulation (ALDH) or equal greatest (CD133 and nanog) when compared to OX+5-FU. Generally, few effects were seen on nanog, which conflicts with the data generated from the proteome profiler. This may be due to the finding that nanog was down-regulated in the proteome profiler data at the 72 hour time point, with no down-regulation after 24 hours. The explant data was analysed after 24 hours of treatment, and thus may not have yet down-regulated nanog.

The potential anti-tumour benefit of adding curcumin to oxaliplatin has been described in a study by Howells *et al*.,[343]. The authors assessed the effect of combining Meriva® (a liposomal curcumin formulation) with oxaliplatin in a colorectal cancer (HCT116) nude xenograft model. Oxaliplatin in combination with Meriva® significantly decreased tumour volume when compared to oxaliplatin alone. Additionally, in HCT116 sensitive and resistant cells oxaliplatin induced an up-regulation of ALDH activity, which was abrogated when combined with curcumin.

Chemoresistance markers and their relation to explant results

The staining for the mismatch repair protein MLH1 demonstrated that patients who have a lower expression respond significantly better to *ex vivo* challenge with

curc+OX, than high expressers. A MMR proficient cell line has previously been demonstrated to be less sensitive to curcumin than an isogenic MMR repair deficient cell line[413]. Curcumin was found to induce double strand breaks in MMR proficient cells, but not in MMR deficient cells, which also had increased levels of apoptosis. This was due to less double strand break formation and subsequent cell cycle arrest, with the cells progressing through the cell cycle and dying by mitotic catastrophe. A follow-up study revealed that knock-down of MLH1 or MLH2 also caused the cells to be sensitised to curcumin[413]. MMR deficiency is reported to indicate a lack of benefit from 5-FU, however with oxaliplatin the MMR status cannot predict for response, therefore, it was surprising that patients with reduced staining for MLH1 had a greater decrease in proliferation. While these studies investigated the loss of expression, the small patient cohort used in this thesis was unable to identify a truly negative sample. However, decreased staining was seen, and it might be expected that lower expression would also result in less DNA damage repair. However, despite the finding that curcumin+OX was superior in patients with lower MLH1 staining, it is in a very small cohort; but the previous MLH1 and curcumin link makes this marker interesting to investigate in a larger powered study. Identification of a mechanistically important biomarker that predicts efficacy would be helpful for identifying patients who could receive a benefit from curcumin. This would also allow better discrimination in humans regarding the potential effects of curcumin, and stratification of patients based on this marker may reveal a large benefit with curcumin, as unstratified patients would include responsive and non-responsive patients which would mask the potential curcumin benefit.

Conclusion

The results across all of the treatment data suggest that the addition of curcumin to the FOLFOX regimen is beneficial. Curcumin alone appears to have significant effects on spheroid growth, possibly mediated by promoting a decrease in ALDH activity. Curcumin also shows a positive effect on TIC markers *ex vivo* in tumour

explants, but not however, on the differentiated cells *in vitro*. The effects of 5-FU and oxaliplatin were both enhanced when combined with curcumin. Crucially, curcumin did not show any deleterious effects when combined with either oxaliplatin or 5-FU. Surprisingly, the combination of curcumin and oxaliplatin appears to be the most superior combination for which low MLH1 expression may be a predictive biomarker of potential efficacy.

Chapter 5: The effects of curcumin±oxaliplatin and 5-FU *in vivo*

4.7 **Introduction**

The aim of this chapter was to assess the combination of curcumin with oxaliplatin and 5-FU *in vivo*, as *in vivo* studies have been shown to more accurately reflect the true response to drug regimens, especially when using rationally chosen drug doses[414]. An additional secondary objective was to assess the feasibility of using changes in animal health and histological assessment of the liver, lung and kidneys to assess curcumin's ability to reduce the side effects of oxaliplatin+5FU. These tissues were chosen as changes in these tissue such as sinusoidal obstruction have been reported following FOLFOX, which can be detected through histological assessment[415]. Lung tissue has also been described to undergo fibrosis in response to oxaliplatin in some rare cases, however when it does occur it can have fatal effects in patients[416]. A typical side effect seen in response to oxaliplatin is neurotoxicity, however due to animal licence constraints this was not investigated. The combination of oxaliplatin and 5-FU have not previously been used in mouse models in our laboratory, and so an initial experiment was required to test whether the doses used were suitable for use in NOD-SCID mice. A pilot study was first undertaken in order to determine appropriate dosing regimens (Figure 5.1).

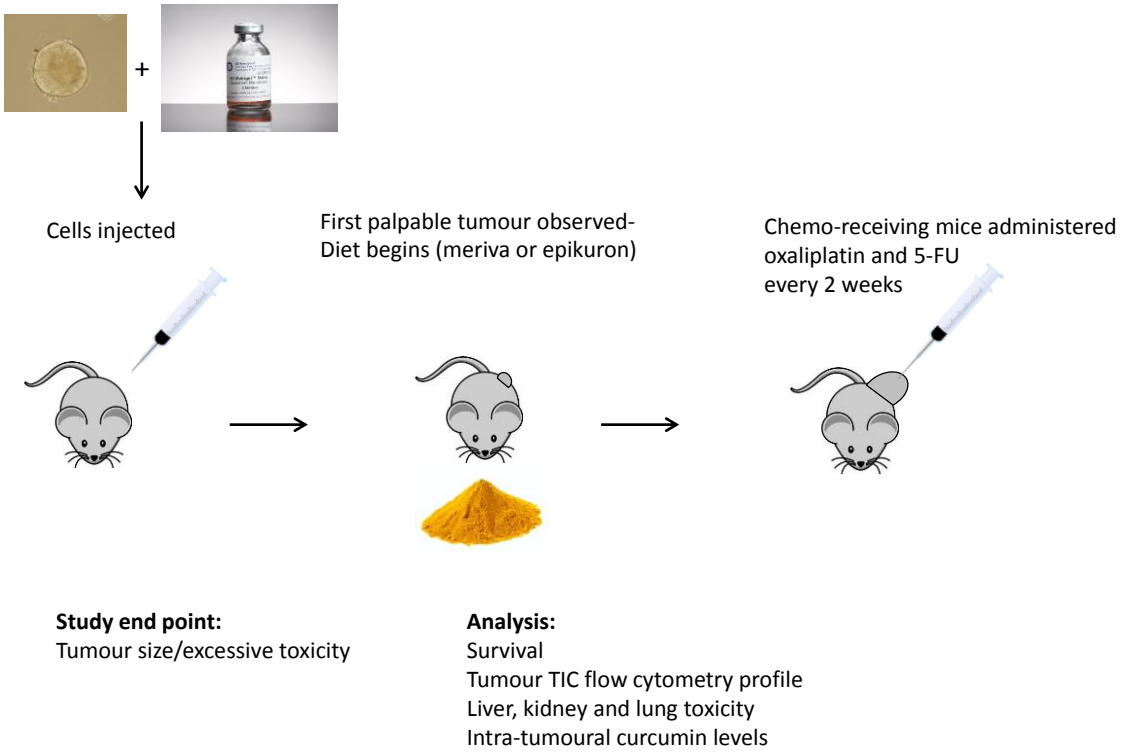

Figure 5.1 An overview of the experimental plan for the investigation of Meriva®±oxaliplatin and 5-FU in NOD-SCID mouse xenografts.
To begin the experiment, 100,000 cells from patient-derived spheroids were injected subcutaneously into mice. After the first palpable tumour was detected in any mouse the study was started, animals were placed on diet (Meriva® or Epikuron) for one week. Following this, oxaliplatin, 5-FU or mock saline injections commenced and were repeated every 2 weeks. Tumours were measured twice weekly using digital callipers. Mice were taken off study when they had either shown signs of poor health, tumour ulceration, or lost 5% of their body weight (tumour size approximately 17 mm in diameter).

4.8 Analysing the ability of curcumin to reduce oxaliplatin and 5-FU toxicities

To assess whether curcumin could help reduce 5-FU and oxaliplatin associated side effects, the liver, lungs and kidneys were harvested when mice were sacrificed and fixed in formalin. Previous research has shown histological observable effects such as sinusoidal obstruction, or lung fibrosis, which are both sometimes seen in humans in response to FOLFOX[416,417], and necrosis and a distorted liver architecture as previously reported in mice in response to 5-FU[418]. There have also been rare cases of nephrotoxicity after oxaliplatin reported in humans[419]. The H+E stained sections were assessed by a trained pathologist, who concluded that there were a few mild histological abnormalities in 2/5 mice treated with the triple combination and 1/5 control mice (no Meriva®, and no OX+5-FU), as summarised in Table 5.1. This observation indicates the abnormalities may not be related to treatment, as they were also observed in a control mouse.

Treatment	Findings
Epikuron (control)	1/5: Kidney - moderate focal tubular degeneration with pigment
Meriva®	Nothing
OX+5-FU	Nothing
Triple combination	2/5: Kidney - marked focal tubular degeneration (both mice), and fibrosis (in one mouse), and arterial necrosis (in another)

Table 5.1 Summary of toxicity findings based on H+E staining of mouse lung, kidney and liver tissue. Histological observations were undertaken by a trained pathologist.

.

Changes in animal weight can serve as an indicator of health status (Figure 5.2). No significant difference was observed between treatment groups, with a steady increase in weight seen over the duration of the study, except at the last two time points for mice on the Meriva® only diet. However, by this time point there was only one animal still on study, with the decrease in weight likely to be symptomatic of tumour burden.

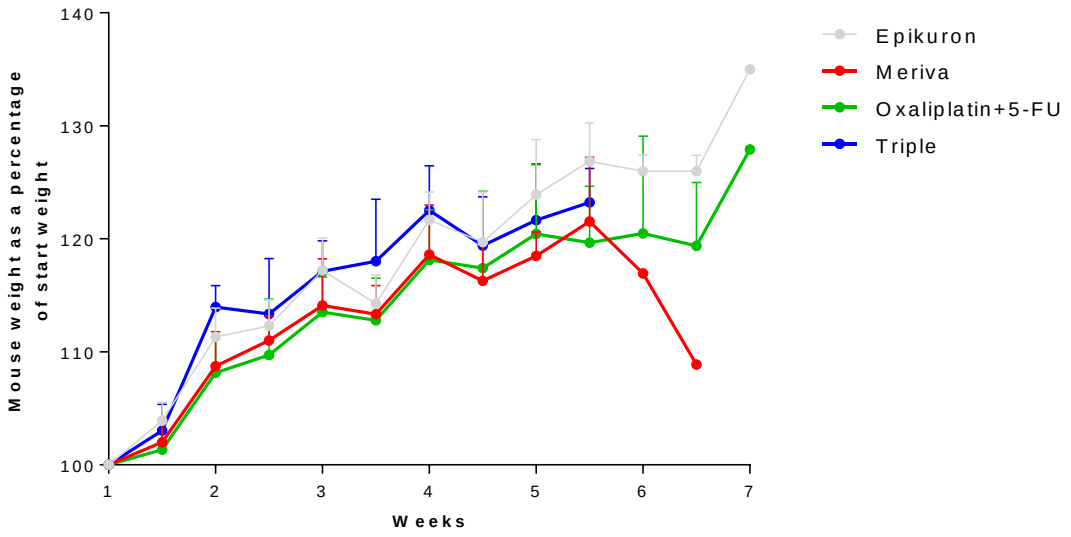

Figure 5.2 Mouse weight changes over the duration of the pilot study.
The weight of NOD-SCID mice was recorded once a week, and then averaged for the number of surviving mice. Some of the later time points do not have error bars due to there being less than three mice. N=5 until week 5, and then N=2, 1, 4 for Epikuron, Meriva, oxaliplatin+5-FU in week 6 respectively, and N=1 for Epikuron and oxaliplatin+5-FU in week 7. Error bars represent the standard deviation.

4.9 **Treatment effects on tumour volume and survival**

To assess efficacy of the treatments, the effects on tumour volume, and mouse survival were analysed. According to the experimental plan, mice were to be culled when the tumour reached a maximum size of 17 mm in diameter, or had lost 5% body weight. However, in this study all mice were culled prior to this endpoint (as advised by animal technicians), due to observable deterioration in health or problems associated with tumour size causing ulceration.

There were no significant differences between groups for average tumour volume or survival (Log-rank (Mantel-Cox) test P=0.1, Gehan-Breslow-Wilcoxon test, P=0.1, Figure 5.3). Mice in all groups survived until week 5 when they started presenting with large tumours, or complications requiring them to be culled, and by week 8 all mice were culled. The order of survival, based on when the last mouse in a group was sacrificed was oxalplatin+5-FU/epikuron>triple combination>Meriva®, however this was not significant.

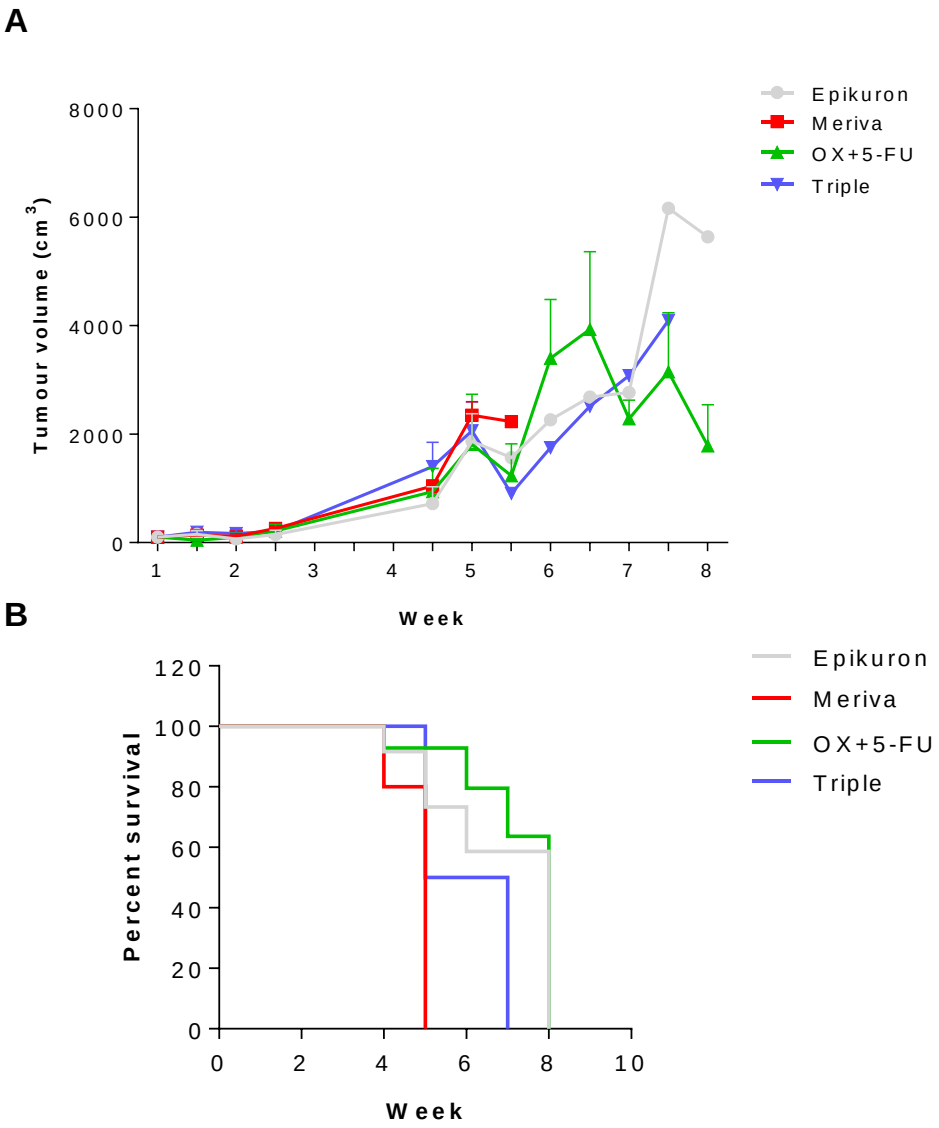

Figure 5.3 The effects of treatment on tumour volume and survival of NOD-SCID mice.

(A) Average tumour volume. Tumours were measured twice a week (Monday and Friday) using calibrated digital callipers. Tumour volume was calculated using tumour width and length with the following formula; tumour volume=0.5 x(lengthxwidth^2). Error bars represent the SEM. At week 5 N= 2, 1, 4 and 1 for Epikuron, Meriva, OX+5-FU and triple respectively. At week 6 N=1, 3 and 1 and week 7 N=1, 3 and 1 for Epikuron, oxaliplatin+5-FU and triple respectively. At week 8 N= 1 and 2 for Epikuron and OX+5-FU. The last measurement was taken before sacrificing mice. (B) Mouse survival analysis. The number of mice for each group at the start of the study was 5, except for the Meriva® group N=4, as one mouse was culled early for non-study related health effects. At week 4 N=4, 3, 4 and 5 for Epikuron, Meriva, OX+5-FU and triple respectively. At week 5 N= 2, 4 and 1 for Epikuron, OX+5-FU and triple and at week 6 N=1, 3 and 1 for Epikuron, OX+5-FU and triple. At week 7 N=1 and 2 for Epikuron and OX+5-FU.

4.10 Effects of Meriva®±oxaliplatin and 5-FU on TIC markers in NOD-SCID xenografts

As the TIC population has been postulated to drive tumour progression, and responses in tumour growth may not immediately translate into differences in tumour volume, the effect of treatments was assessed by flow cytometry analysis of CD133 and CD26 expression, plus ALDH activity within the EpCAM+ population.

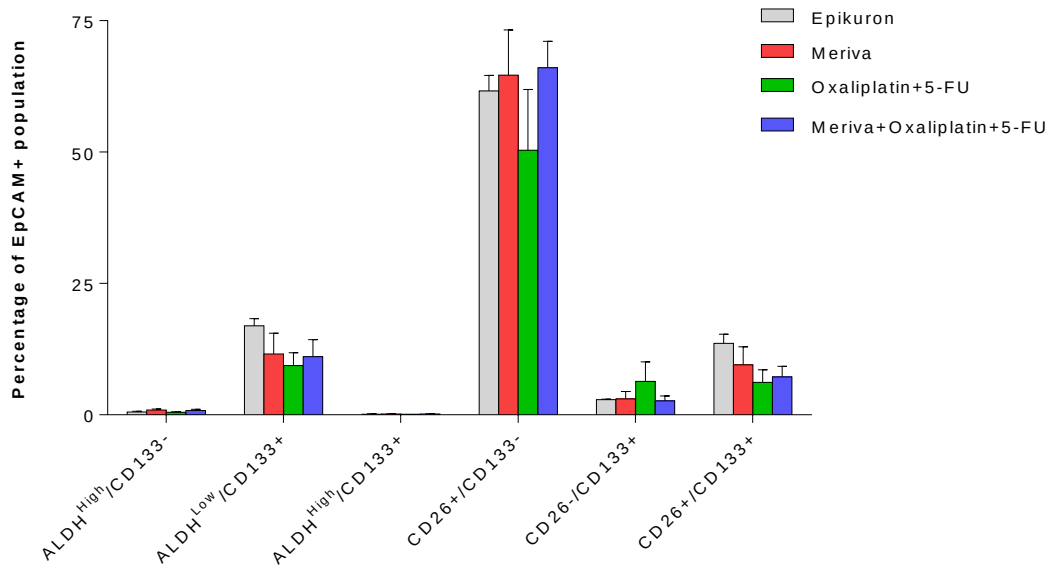

Figure 5.4 Expression of TIC markers in human tumour cells from treated NOD-SCID mice
The expression of TIC markers was analysed in tumours from the pilot study by flow cytometry. No significant differences were detected between treatment groups. N=5, except for the Meriva® group, where N=4, error bars represent the SEM.

No significant differences were seen between any of the groups for expression of the TIC markers analysed, with high expression of CD26+/CD133- (50-66%), and generally low levels of CD133 ($ALDH^{Low}$/CD133+ 9.4-17%, CD26-/CD133+ 2.6-6.4%

and CD26+/CD133+ 6.2-13.6%), and almost undetectable levels of ALDH activity ($ALDH^{High}$/CD133- 0.5-0.9% and $ALDH^{High}$/CD133+ 0.-0.2%).

4.11 **Intra-tumour and dietary curcumin levels**

Due to the lack of efficacy of Meriva®, which is in contrast to previous findings from our laboratory in CRC models[343], curcumin levels in the Meriva® diet were analysed to confirm that curcumin was present and that there were no problems with the batch of Meriva® used. Additionally, the curcumin concentration in tumours from the four mice receiving Meriva® (as one was culled early due to poor health) and the five control mice were compared by HPLC-UV analysis. The results indicate that curcuminoids were present in the Meriva® diet, but not in the epikuron diet, as expected (Figure 5.5 and 5.6). Curcuminoids could not be detected in the tumours from epikuron or Meriva® receiving mice (Figure 5.5 and 5.6). To see whether the lack of detection of curcumin was due to rapid metabolism, but detectable metabolites were present, xenografts were analysed for their presence but they were not detected.

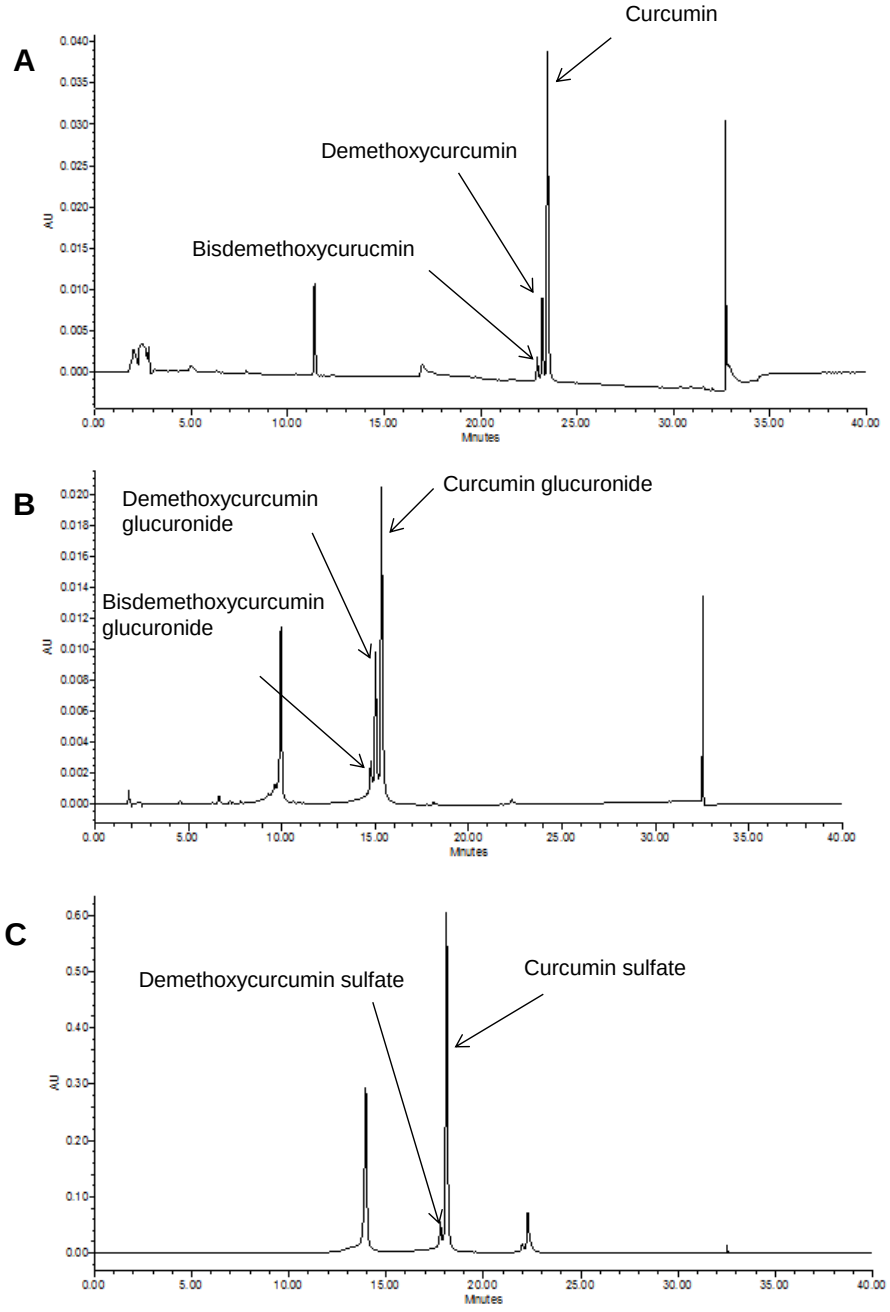

Figure 5.5 Representative HPLC-UV chromatograms from the analysis of curcumin, and its sulfate and glucuronide metabolite standards.
Chromatograms show the analysis of (A) curcuminoids from sigma (B) curcumin glucuronide and (C) curcumin sulfate standards synthesized in house.

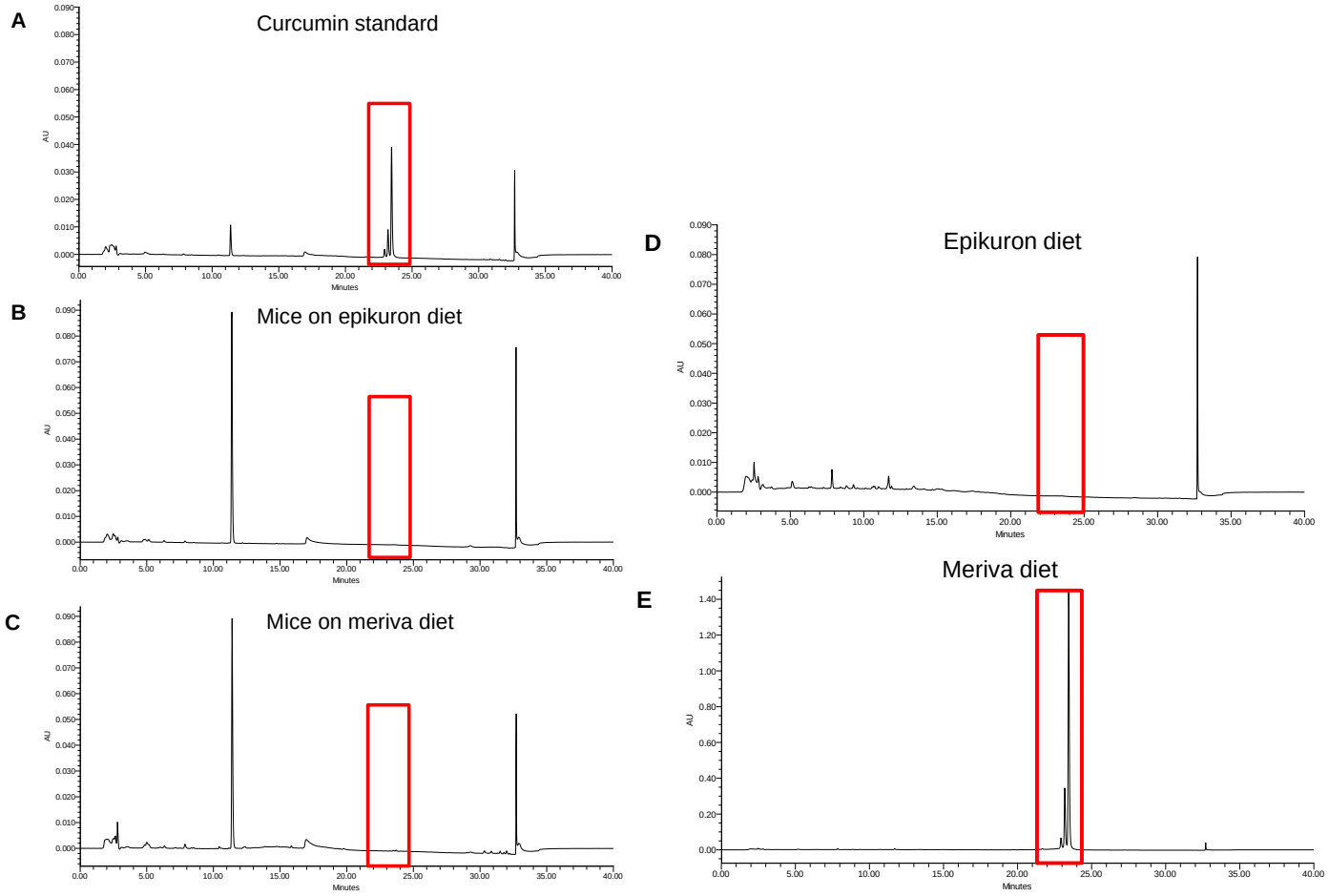

Figure 5.6 Representative HPLC-UV analysis of curcuminoids in tumour extracts from mice on the pilot study, and in the diets.
To assess whether curcumin could be detected in xenograft tumours and in the Meriva® diet, HPLC was used. The chromatogram in (A) shows curcuminoid standards within the red box. Curcumin was not detected in the tumour tissue regardless of the diet mice were fed (B) and (C).As expected, curcumin was not present in the control Epikuron (D) diet but was detected in the Meriva® diet (E).

4.12 **Discussion**

Typically, cancer drug development pathways from laboratory to clinic follow a route of *in vitro* screening followed by the use of cell line xenografts. In the UK, the MHRA regulates clinical trials and in order to apply to test an investigational drug in a clinical trial data from an *in vivo* study is necessary, due to the International Helsinki declaration and a European Directive. This affords insight into the effectiveness of a treatment and provides information on any possible side effects, and it may aid in deciding a starting dose for humans[420]. The use of patient-derived xenografts allows maintenance of the original tumour with greater fidelity than observed for cell line-derived xenografts, particularly for gene expression and mutation signatures[421]. The use of animal models also offers the opportunity to test for any toxicity effects that could not be observed *in vitro*.

In the study presented here, mice were fed a patented formulation of curcumin called Meriva®[422]. This formulation consists of curcumin and soy lecithin in a 1:2 weight ratio, and then two parts microcrystalline cellulose, producing an overall final curcumin content of 20%. Meriva® has been shown to improve curcumin bioavailability in rats and humans[276,423]. Poor bioavailability of curcumin is not a major issue for *in vitro* studies, but has hindered the clinical development of curcumin, particularly for indications that require systemic delivery to target organs. Since the development of Meriva®, studies have demonstrated that combining Meriva® with oxaliplatin gives superior efficacy than oxaliplatin alone in terms of reducing tumour volume in mice, whilst a separate study revealed that Meriva® significantly improved osteoarthritis in humans[343,424].

Animal Health and response to treatments

Animal weights can be used to assess health, with large decreases in weight indicating poor health. Over the duration of the study, mouse weights were recorded once a week for this purpose with no significant differences seen between groups. Neuropathy is

one major limiting toxicity caused by oxaliplatin[425], but the animal licence under which this study was performed did not allow investigations into this. Neurotoxicity has been studied before in mice given oxaliplatin and curcumin, with curcumin reducing the amount of oxaliplatin in the sciatic nerve[344], curcumin has also been shown to reduce neuropathic pain in mice[426]. Curcumin may therefore have a dual role at promoting therapeutic efficacy whilst reducing side-effects. At the end of the study the lungs, kidneys and liver were taken to assess toxicity, as 5-FU and especially oxaliplatin have been shown to cause liver damage in CRLM patients, causing sinusoidal congestion which can persist for up to 6 months after therapy, but which has no effect on clinical outcome[417,427]. Oxaliplatin has been shown to also cause renal damage, but only in rare cases[419,428]. In the treated mice very few effects were noticed, but two mice in the triple-treated group had marked tubular degeneration, and also fibrosis (in one of the two mice), and arterial necrosis (in the other mouse), both observed in the kidney. However, one mouse in the control group had moderate tubular degeneration in the kidney, and no effects were seen in the Meriva® or OX+5-FU group. Due to the control also demonstrating some mild toxicity, it appears the abnormalities may not be related to treatment. It may be that in future studies to investigate toxicity, it would be more appropriate to amend the project licence used to allow investigation into neurotoxicity, as it has both been detected in mice and represents one of the major side effects to oxaliplatin. The toxicity data together with the mouse weight data results indicate that the treatments were well-tolerated. The lack of therapy induced toxicity is likely due to the low doses used. This may also explain the subsequent observations that there were no differences between the control group and OX+5-FU when assessing tumour volume, mouse survival, and the flow cytometry data. The amount of oxaliplatin in a previous study by our group used the same dose of oxaliplatin as used in this thesis (7.5 mg/kg) but twice a week vs once every two weeks. However, this thesis used oxaliplatin in combination with 5-FU and therefore the less frequent dosing was considered to have the potential be active against tumour growth. It is important to note

that the regimen used in this thesis was different to most studies, as treatments were less frequent in order to recapitulate the clinical regimen, however it appears that dosing this infrequently is ineffective in mice xenografts. The length of the study in this thesis is also slightly longer than other reported studies. All mice were culled in this thesis by week 8, other reported studies have ended at 3-4 weeks[136,343].

Previous mouse studies have demonstrated that treatment with either oxaliplatin or 5-FU three times weekly for 28 days at 10, 20, or 30 mg/kg or oxaliplatin twice weekly for 28 days at 10 or 20 mg/kg all caused a significant decrease in tumour volume and enrichment of CD133+/CD26+ cells compared to saline[136]. However, another study has demonstrated that in nude mice bearing HT29 xenografts, a single treatment with oxaliplatin or 5-FU at half the maximum tolerated dose (10 mg/kg and 50 mg/kg for oxaliplatin and 5-FU respectively) had no significant effect compared to the control, whereas the combination did[429]. These studies demonstrate efficacy when dosing is conducted at more regular intervals or in a combination, but treating regularly does not reflect the clinical regimen. Previous research has demonstrated that by treating at a clinically relevant dose (including 5-FU) and following a similar regimen to the clinical counterpart, the results are more accurate at representing patient response[430,431]. Due to the nature of the ethics used for the collection of patient samples, little information was obtained on the sample used for these xenograft studies, regarding the original response to chemotherapeutic intervention. It may have been that this tumour was inherently resistant to FOLFOX, but this would contradict the results obtained for the spheroid treatments, which showed the sample to be sensitive to all treatments. It may be that the addition of the microenvironment presented a confounding factor, altering the effects seen *in vitro*. In breast cancer a tumour stromal derived gene signature could predict resistance to pre-operative chemotherapy, demonstrating that the stroma must play a role in tumour resistance[432]. Microenvironmental mediated chemo-resistance is multimodal, resistance can be promoted through providing certain secreted factors such as IL17A. The

microenvironment can also act as a physical barrier which drugs need to penetrate to reach the tumour population, also oxygen gradients due to poor vasculature cause hypoxic regions which promote resistance through re-pressing cell proliferation. These reasons both highlight the need for *in vivo* studies and the reasons why many drugs are unsuccessful despite appearing promising in *in vitro* screens. Unfortunately, it was not possible to obtain details on whether the patient from which the tumour used for the xenograft studies came from responded to chemotherapy; such information would help determine whether the results can be explained though a higher resistance *in vivo* due to microenvironmental reasons.

The number of patients tested in the mice posed a problem (n=1), which should be addressed for future studies. As a source of cells for the *in vivo* study, patient cells were cultured as spheroids. However, as only one CRLM grew well enough for this, the sample size for the study was severely restricted. Some patients will be more resistant to the treatment than other patients, stressing the need for a larger cohort of patients that ideally capture a spectrum of the mutations found in CRLM. This problem could be prevented in future studies if the xenograft study was initiated using patient tumour tissue as opposed to *in vitro* cultured cells. As demonstrated in chapter 3, xenografts could be successfully established from patient tumour tissue meaning this approach is feasible.

Previous *in vivo* xenograft studies

The dose of Meriva® used in the current study is the same as that used in a previous investigation that demonstrated a significant decrease in tumour volume[343]. Despite differences in the mouse strain (nude mice Vs NOD-SCID) and the cells used (HCT116 vs patient spheroid derived cells) it was surprising that no effect was observed, especially considering the *ex vivo* results obtained with this same sample, as outlined in the previous chapter. Therefore, another possibility other than the presence of a microenvironment causing this discrepancy is that spheroids have a poor

predictive value for *in vivo* response. To investigate the reason why a lack of response was observed with curcumin, HPLC analysis was conducted on the Meriva® diet to ensure that curcumin was present. The results demonstrated that curcumin was present, and absent from the carrier phospholipid, as expected. Upon analysis of the tumours from mice in the control and Meriva® groups, no curcumin or its metabolite levels could be detected. Following oral administration of curcumin, previous rodent studies have demonstrated curcuminoids to be present near the limits of detection in the plasma and at very low levels in the liver; furthermore, they are eliminated completely from the liver and gastrointestinal tract[269] between 3-6 hours. Since the tumours were engrafted subcutaneously, the route for curcumin to reach the tumour would be through the systemic circulation in the blood. The tumours grew well, and thus must have been well-vascularised. These data, in combination with the lack of effect, point to three possibilities; 1) curcumin is not being sufficiently well absorbed by the tumour cells; 2) curcumin is rapidly metabolised and rapidly cleared from the tumour or plasma and thus is not detected; 3) curcumin is present, but below the limits of detection. Any of these possibilities means that cells would have been exposed to curcumin for either a short time or at very low concentration and therefore curcumin may have had little effect. Alternative ways to design the *in vivo* study would include administering the curcumin through oral gavage or through IP or IV injections; this would ensure that the mice receive a regular known dose of curcumin. It is possible that the taste of curcumin in the food alters the eating behaviour of the mice so that they eat less and therefore receive less curcumin. Future research would benefit from taking blood samples, as this would enable measurement of the curcumin levels to confirm it is present in the system and to ensure that an effective dose was administered, and so if no effects were seen it would be known that the lack of effect is not due to curcumin being absent.

In the experimental design adopted in this study, mice received Meriva® in their diet for one week before commencing chemotherapeutic injections (oxaliplatin and 5-

FU), as this reflected a complementary on-going clinical trial being run at the University of Leicester in patients with metastatic colorectal cancer. This approach may be beneficial for sensitising tumours to chemotherapeutics, which has been described previously with curcumin and 5-FU[337]. The regimen of oxaliplatin and 5-FU injections was selected to try and reflect the clinical scenario where patients receive oxaliplatin and 5-FU infusions over a two day period, every two weeks. Low doses have been used before in mouse models but there are no pre-clinical reports that reflect clinically relevant doses and regimens of OX+5-FU. This may be due to the lack of efficacy, as observed in this study, with negative/ineffective treatments less likely to be published. Using an equation that allows conversion of mouse doses to human does (shown below)[433], normalised through body surface area, the doses used are ¼ of the human dose. However, calculation of the dose required if you convert the human dose back to mouse is above the maximum tolerated dose for oxaliplatin, and around the MTD for 5-FU in mice[429]. The results here indicate that higher doses are required for effect if using a 2 weekly dosing regimen, but an equivalent human dose is not feasible.

$$\text{HED, mg/kg} = \text{Animal dose, mg/kg X} \left(\frac{\text{Animal } k_m \text{ value}}{\text{Human } k_m \text{ value}}\right)$$

HED=Humanised dose. The k_m factor is generated by dividing body weight (kg) by BSA (m^2). Assuming an average body weight of 60 and 0.02 mg/kg, and body surface area of 1.6 and 0.007 m^2 for humans and mice respectively, a k_m factor of 37 and 3 are generated. Conversion of mg/kg to mg/m^2 can be achieved by multiplying by the k_m factor[433].

Conclusions

One problem associated with this study, was the small number of mice in each group (N=5) in combination with presentation of tumour related side-effects, which meant mice had to be culled early due to ethical and licence requirements. No tumours reached 17 mm in diameter (tumour size end-point). A common problem was the ulceration or blood filling of tumours, which is specific to subcutaneous engraftments in

mice, and does not present in patients. Additionally, one mouse in the group receiving Meriva® only was excluded from analysis, as it was culled due to poor health un-related to treatment. Evidence suggests that tumour ulceration, a problem in this study, may relate to the sample used as previously certain cell lines have been shown to be prone to tumour ulceration. Therefore the use of other samples may circumvent this problem. Also, the choice of mouse strain may also influence the study, as NOD-SCID mice are not as resilient as other strains. The previous study with oxaliplatin and Meriva® was carried out using nude mice and a cell line, but these are less suitable for growth of patient-derived xenografts. Further issues that present with use of the NOD-SCID mice include their reported propensity to develop thymus lymphomas at approximately 7 months of age, which could preclude longer term studies investigating relapse following treatment. Whilst this pilot xenograft study did not demonstrate efficacy for any of the treatments, there were many confounding factors that can be addressed and optimised in future studies.

Chapter 6: Final Discussion

Metastatic colorectal cancer represents a difficult tumour group to study, which is reflected in the lack of research in this area. The vast majority of publications on TICs in CRC focus on the primary cancer site, or use genetically modified mouse (GEM) models, meaning that data focusing on mCRC are scarce. Since 15-25% of patients present at the clinic already with a metastatic lesion, and 50-60% develop mCRC during the course of their disease, it is essential to further investigate late stage disease so that the potential for enhancing resectability or improving palliation can be explored. Within the research field for primary CRC, there are several landmark studies on TICs that use GEM, which often don't draw attention to the major caveats of these models. These include the inability of these models to develop an invading tumour and metastasis, the inability to be serially transplanted (cited by many as one of the functional definitions of TICs), and the fact that the tumours typically appear in the small intestine and not the colon. In humans, tumours rarely appear in the small intestine. Despite reconciliations which have managed to successfully apply findings from these mouse models to human colorectal cancer, this still represents a hurdle for research to overcome. The development of models that bear greater relevance to mCRC is therefore a priority.

To study TICs present in metastatic tissue models have been developed that includes spheroid culture. Despite observing consistent and reproducible growth of spheroids from tissue derived from primary colorectal cancers (Karmokar, personal communication, unpublished), spheroids do not readily form from CRLM. This may be caused by a large proportion of patients having received pre-operative chemotherapy and therefore tumours can consist largely of necrotic material, which, when combined with culture conditions that are likely to sub-optimal, present challenges for TIC investigations. During the course of this thesis there have been major developments in organoid technology, a method developed to grow normal stem cells *in vitro* from a number of different tissues, which has been successfully adapted for growth of

colorectal tumours[357,434]. These organoids have been demonstrated to successfully recapitulate the patients tumours from which they are derived. Future work would benefit from using these methods of culturing patient cells, allowing a greater number of patients to be assessed. Whilst the spheroid model proved problematic, this led to further investigations into the explant culture model as an alternate method for exploring this pathology, and response to therapeutic intervention.

Explant culture provided a useful system for assessing treatment efficacy, and represents an under used model, providing lots of information regarding cellular interactions whilst retaining tumour architecture, which is a major factor in supporting the stem cell niche. Further research utilising this model would best be focussed on the interaction of curcumin with microenvironmental factors including tumour regulatory cytokines. An important factor involved in a tumours response to therapy is the microenvironment. This is lost *in vitro* and in xenografts it is normally reduced compared to the patients, as it is composed of a mixture of mouse and human cells. Additionally, for xenografts immunocompromised mice are used, therefore depending on the strain of mouse various components of the microenvironment derived from the immune system will be missing. The use of explant cultures, although not ideal for long term culture, maintains the microenvironment complexity seen in the patient as it is literally a small piece of the tumour. This is a major benefit as the interplay between the microenvironment has been shown to be involved with response to therapy, and to regulate TIC properties. For example, matched patient samples from before and after treatment demonstrated an increased IL17A after therapy in CAFs[405]. The authors then went on to demonstrate that IL17A could promote growth of TICs and increase NF-κβ signalling. Recent research has also highlighted the role of the immune system in driving tumour formation[435,436], which may also be modelled in the explant system if there are infiltrating immune cells. This could provide novel data for the mechanisms of action for curcumin as this has not been previously investigated in CRC, but reports show that in breast cancer curcumin can affect the microenvironment by promoting

senescence of CAFs, and also by preventing an exosomal mediated suppression of natural killer cell tumour toxicity[437,438]. Additionally, using the technique on tumours from genetically engineered mice would allow investigation of specific genes/cells while reducing the required number of mice as one mouse tumour could provide lots of tissue for explant culture. However, the short time points that can be used hinder the versatility of this model, which could possibly be improved through better culturing conditions or by using thinner sections (produced using a vibratome) that may remain viable for longer. However, if validated they could help reduce the dependency on mice for clinical drug screening.

Curcumin appears to be a promising treatment due the observed anti-tumour effects *ex vivo*, and its lack of side-effects when administered as a single agent or in conjunction with chemotherapy (i.e. it does not reduce the effect of OX or 5-FU, or have a pro-tumour effect when administered alone). These findings are underscored by the explant data, which involves little disruption of the tumour and its microenvironment. This data set demonstrates that *ex vivo,* curcumin can improve the efficacy of 5-FU and notably oxaliplatin. Currently there are no front-line therapies that consist of oxaliplatin without 5-FU, and it is unlikely that curcumin would be approved for use solely with oxaliplatin. If curcumin was to be translated into a clinical setting it is unlikely to replace any of the standard drugs, but as curcumin does not have a detrimental effect on the combination treatment of oxaliplatin and 5-FU, it could be easily added in as an adjunct. In this role patients could benefit from possible increased responses and a decrease in side-effects. Additionally, as curcumin alone does not have any severe side effects patients could also continue on taking curcumin during palliative care in a bid to hopefully improve the patient's outlook.

Curcumin appears to be able to target the $ALDH^{High}$ populations, which is in line with previous reports. However, $ALDH^{High}$ activity was extremely low in a proportion of patients and not detectable in the remaining patients. It would be interesting to see if the patients who had no detectable ALDH activity benefitted less from curcumin than

patients who had detectable high ALDH activity. If the belief the TIC population is small is true, then even though it represents a small population of the tumour, targeting this fraction could result in efficacy. This would also raise the question of why ALDH activity is missing in some samples, and whether there is an alternative TIC marker that should be investigated in patients with no activity. The Swanton group has demonstrated significant intratumoural heterogeneity in non–small cell lung cancer and clear cell renal carcinomas[112-114]. This research has highlighted that within a tumour there are many subclones that contain different mutation spectrums. This may reconcile both the stochastic theory with the hierarchical theory, as subclones will indepdendantly evolve in a stochastic manner driving tumour evolution, and would also respond differently to therapy. It is possible that different sublcones within CRLM are marked by different TIC markers, each with different properties such as the CD26 and ALDH high populations.

In the future, it would be interesting to further assess CD26 as a resistant population. Drugs have been developed to target CD26 for diabetes[439], which are safe and approved for use, and so it remains an intriguing possibility that there could be a role for these drugs in targeting the CD26+ population in mCRC. Due to the small number of patients that were treated and assessed for expression of markers of chemoresistance, it was not possible to ascertain whether a specific sub-set of patients can benefit from curcumin. Ideally, this study should be expanded to a far larger patient cohort, with an expanded panel of markers to investigate.

Improvements in this study could be made by assessing whether the sorted spheroids could be passaged; an end point regularly used to test self-renewal capacity. This would be best used following treatment, to assess the ability to affect self-renewal. Particular interest lies in the potential for curcumin to disrupt nanog and BMI1 expression, as BMI1 knockdown was recently proposed as a method to treat TICs and cancer. However, in the triple treatment group there were so few spheroids this would require a very large scale-up to obtain enough viable cells after treatment to passage and analyse.

The method for culturing TICs used within this thesis proved inefficient at establishing cultures from new patient samples and therefore posed a significant problem. During the preparation of this thesis a novel method for culturing colorectal cancer TICs was reported by the Clevers group[434]. This new approach, which is a modified version of the method required for culturing normal colon stem cells, gives a better success rate than the spheroid model used throughout the present work. Use of the organoid method mentioned above would allow more samples to be investigated for their responses to curcumin and OX+5-FU. This would mean that the generated data would be more representative of the patient cohort. Additionally, research would proceed at a quicker pace as fewer samples would have to be collected in order to generate cultures to study. Also, as more samples would be established *in vitro*, a larger number of samples would be available to study *in vivo*. An alternative to injecting cultured cells (as used in this thesis) would have been to subcutaneously implant small pieces of a dissected tumour into mice. Assessing chemotherapy using this method has previously been shown to produce similar response rates to anticancer drugs between patients and their corresponding xenografts[440]. Since xenografts were successfully established during this thesis this would have been easily feasible. A drawback of this study was that it did not manage to reach the stage where a mechanism could be properly addressed. Through the improvements mentioned above, it may have been possible to investigate this at an earlier stage and perform the protein profiler array (after treatments) on more patients, making the results more robust. The proteome profiler array data for nanog needs to be validated using western blots, and additional research addressing its role in TICs should be performed. This could be undertaken using an inducible knock-down system such as the tet-off system. This would allow gene expression to be knocked-down at different stages of spheroid and xenograft growth to see whether it is needed for tumour growth, or only for tumour initiation. Comparisons between the treatment response of spheroids where nanog is either on or off would also identify whether it plays a role in chemosensitivity. Finally, if

it was found that nanog was indeed related to resistance then performing microarrays on spheroids that are proficient, or have nanog knocked-down, may identify expression signatures involved in resistance and genes related to TIC properties.

In addition to validating a role for nanog in TICs and therapy resistance, future research directed towards gaining an insight into the roles of the other TIC markers used (CD26, CD133 and ALDH activity) in chemotherapy resistance is needed. One approach would be to knock-down the genes using siRNA to identify whether the genes play any functional roles in resistance. Alternatively, a recent breakthrough in genome editing in the Zang laboratory[441], the crispr-cas9 system, allows insertion of DNA through homologous recombination. Through serial rounds of crispr editing it is feasible to introduce a reporter gene flanked by lox-p sites, and creERT2 (the cre enzyme modified so it is bound to the estrogen receptor, and re-locates to the nucleus upon tamoxifen treatment) expressed from your gene of interest (i.e. CD26, CD133 or ALDH1A1) thus allowing lineage tracing upon addition of tamoxifen. This has been proven in mice to be an effective way of identifying a stem cell population, and would give an insight into the contribution of each population to tumour growth. If this was done for each gene of interest, but with a different colour reporter, the cells could then be mixed and implanted into mice. If the reporter gene is induced early during growth, after waiting several weeks for tumours to grow, the contribution of each stem cell population to the tumour could be viewed. Alternatively, an inducible caspase could be placed under the expression of the TIC gene of interest, but preceded by a stop codon but flanked by lox-p sites. With constitutive expression of creERT2 at another locus, once the cells are treated with tamoxifen the creERT2 would move into the nucleus and remove the stop codons, allowing expression of the caspase cassette which would result in death of any cells that express that gene. This would identify whether the cells expressing the TIC gene of interest are necessary for tumour growth, as tumours should fail to initiate or propagate once the death cassette is expressed, if the gene does truly identify a TIC.

Despite many obstacles, this study has provided an insight into the growth characteristics and treatment response of CRLM-derived TICs *in vitro*. Based on these data several conclusions can be drawn: 1. Cells are highly plastic, and can readily re-express markers, 2. Spheroid formation cannot be defined as a population delineated by a single TIC marker, but can be initiated by at least three populations, each with varying degrees of proliferative capacity. The existence of multiple TIC populations has important implications for therapy, as it will be necessary to target all of them for a complete remission. The idea of multiple populations has recently been demonstrated in breast cancer, with an alternative TIC first proposed by Brapletz, T *et al.,* in 2005[193]. Also, lentivirally tracking cells has demonstrated multiple populations in CRC with self-renewal capacity[375], and these findings appear to be extendable to CRLM.

The overall results from the treatment data corroborates the CD26+/CD133- population as a resistant population when analysing the patient TIC marker expressions stratified by chemotherapy status and treatment of differentiated spheroids, but did not identify a resistant population within spheroids. This may be due to the spheroids that grew all forming a balanced population by the two week time point used. These results did show a trend for an increased effect on spheroid number with curcumin. The benefit of curcumin was also demonstrated in the explant data where it affected proliferation and apoptosis, and appeared best when combined with oxaliplatin. However, surprisingly little effect was seen on spheroids that had differentiated. Therefore, the lack of effect on differentiated spheroids may contrast with the explant data, as the effects in explants includes additional cell types, a large proportion of which will represent more differentiated cancer cells, especially with the TIC population postulated to be relatively small. Therefore, the significant differences seen probably represent, at least partially, the response of the differentiated cells, which contrasts with the lack of effect in differentiated spheroids. The differences may be explained through the differences in the models i.e. 2D culture of only epithelial tumour cells vs 3D culture with multiple cell types present. This would suggest that *in*

vivo curcumin mediates its effects on differentiated cells though regulation of the microenvironment. Additionally, curcumin appears to affect the growth and expression of ESC genes in CRLM TICs, advocating further investigation on the use of curcumin in this malignancy.

This study contributes to the knowledge about the effects of curcumin in combination with OX and 5-FU on CRLM derived from patient samples, which has not been previously described. Furthermore, the use of explant culture has provided insight into patient response *ex vivo*, which has also not been reported before in CRC. With growing interest in using curcumin as an adjuvant to chemotherapy this knowledge should prove useful for guiding future pre-clinical investigations into curcumin, and in paving the way for larger studies, with pertinent methods having been developed in this thesis. Overall, the combined data advocate translating curcumin to the clinic.

References

1. Shark CG. The economic burden of cancer in europe. *European Journal of Hospital Pharmacy: Science and Practice*. 2006;12:53.

2. Siegel R, Naishadham D, Jemal A. Cancer statistics, 2012. *CA Cancer J Clin*. 2012;62(1):10-29.

3. Spano D, Heck C, De Antonellis P, Christofori G, Zollo M. Molecular networks that regulate cancer metastasis. *Semin Cancer Biol*. 2012;22(3):234-249.

4. Kanas GP, Taylor A, Primrose JN, et al. Survival after liver resection in metastatic colorectal cancer: Review and meta-analysis of prognostic factors. *Clin Epidemiol*. 2012;4:283-301.

5. Dy GK, Hobday TJ, Nelson G, et al. Long-term survivors of metastatic colorectal cancer treated with systemic chemotherapy alone: A north central cancer treatment group review of 3811 patients, N0144. *Clin Colorectal Cancer*. 2009;8(2):88-93.

6. Adam R, Delvart V, Pascal G, et al. Rescue surgery for unresectable colorectal liver metastases downstaged by chemotherapy: A model to predict long-term survival. *Ann Surg*. 2004;240(4):644-57; discussion 657-8.

7. Ardito F, Vellone M, Cassano A, et al. Chance of cure following liver resection for initially unresectable colorectal metastases: Analysis of actual 5-year survival. *Journal of Gastrointestinal Surgery*. 2013;17(2):352-359.

8. Nuzzo G, Giuliante F, Ardito F, et al. Liver resection for primarily unresectable colorectal metastases downsized by chemotherapy. *J Gastrointest Surg*. 2007;11(3):318-324.

9. Jemal A, Center MM, DeSantis C, Ward EM. Global patterns of cancer incidence and mortality rates and trends. *Cancer Epidemiol Biomarkers Prev*. 2010;19(8):1893-1907.

10. Center MM, Jemal A, Ward E. International trends in colorectal cancer incidence rates. *Cancer Epidemiol Biomarkers Prev*. 2009;18(6):1688-1694.

11. Kanavos P. The rising burden of cancer in the developing world. *Annals of Oncology*. 2006;17(suppl 8):viii15-viii23.

12. Sasco AJ, Secretan MB, Straif K. Tobacco smoking and cancer: A brief review of recent epidemiological evidence. *Lung Cancer*. 2004;45 Suppl 2:S3-9.

13. Haggar FA, Boushey RP. Colorectal cancer epidemiology: Incidence, mortality, survival, and risk factors. *Clin Colon Rectal Surg*. 2009;22(4):191-197.

14. Flood DM, Weiss NS, Cook LS, Emerson JC, Schwartz SM, Potter JD. Colorectal cancer incidence in asian migrants to the united states and their descendants. *Cancer Causes Control*. 2000;11(5):403-411.

15. Lichtenstein P, Holm NV, Verkasalo PK, et al. Environmental and heritable factors in the causation of cancer--analyses of cohorts of twins from sweden, denmark, and finland. *N Engl J Med*. 2000;343(2):78-85.

16. Cunningham D, Atkin W, Lenz HJ, et al. Colorectal cancer. *Lancet*. 2010;375(9719):1030-1047.

17. Hursting SD, Thornquist M, Henderson MM. Types of dietary fat and the incidence of cancer at five sites. *Prev Med*. 1990;19(3):242-253.

18. Miller AB, Howe GR, Jain M, Craib KJ, Harrison L. Food items and food groups as risk factors in a case-control study of diet and colo-rectal cancer. *Int J Cancer*. 1983;32(2):155-161.

19. Giovannucci E, Stampfer MJ, Colditz G, Rimm EB, Willett WC. Relationship of diet to risk of colorectal adenoma in men. *J Natl Cancer Inst*. 1992;84(2):91-98.

20. Rao CV, Hirose Y, Indranie C, Reddy BS. Modulation of experimental colon tumorigenesis by types and amounts of dietary fatty acids. *Cancer Res*. 2001;61(5):1927-1933.

21. Steck SE, Butler LM, Keku T, et al. Nucleotide excision repair gene polymorphisms, meat intake and colon cancer risk. *Mutat Res Fundam Mol Mech Mutagen*. 2014;762:24-31.

22. Chao A, Thun MJ, Connell CJ,et al. MEat consumption and risk of colorectal cancer. *JAMA*. 2005;293(2):172-182.

23. Butler LM, Sinha R, Millikan RC, et al. Heterocyclic amines, meat intake, and association with colon cancer in a population-based study. *Am J Epidemiol*. 2003;157(5):434-445.

24. Howe GR, Benito E, Castelleto R, et al. Dietary intake of fiber and decreased risk of cancers of the colon and rectum: Evidence from the combined analysis of 13 case-control studies. *J Natl Cancer Inst*. 1992;84(24):1887-1896.

25. Satia-Abouta J, Galanko JA, Martin CF, Ammerman A, Sandler RS. Food groups and colon cancer risk in african-americans and caucasians. *Int J Cancer*. 2004;109(5):728-736.

26. Nothlings U, Yamamoto JF, Wilkens LR, et al. Meat and heterocyclic amine intake, smoking, NAT1 and NAT2 polymorphisms, and colorectal cancer risk in the multiethnic cohort study. *Cancer Epidemiol Biomarkers Prev*. 2009;18(7):2098-2106.

27. Friedenreich CM, Orenstein MR. Physical activity and cancer prevention: Etiologic evidence and biological mechanisms. *J Nutr*. 2002;132(11 Suppl):3456S-3464S.

28. Almendingen K, Hofstad B, Vatn MH. Does high body fatness increase the risk of presence and growth of colorectal adenomas followed up in situ for 3 years? *Am J Gastroenterol*. 2001;96(7):2238-2246.

29. Tiemersma EW, Wark PA, Ocké MC, et al. Alcohol consumption, alcohol dehydrogenase 3 polymorphism, and colorectal adenomas. *Cancer Epidemiology Biomarkers & Prevention*. 2003;12(5):419-425.

30. Giovannucci E, Stampfer MJ, Colditz GA, et al. Folate, methionine, and alcohol intake and risk of colorectal adenoma. *J Natl Cancer Inst*. 1993;85(11):875-883.

31. Potten CS, Kellett M, Roberts SA, Rew DA, Wilson GD. Measurement of in vivo proliferation in human colorectal mucosa using bromodeoxyuridine. *Gut*. 1992;33(1):71-78.

32. Bach SP, Renehan AG, Potten CS. Stem cells: The intestinal stem cell as a paradigm. *Carcinogenesis*. 2000;21(3):469-476.

33. Medema JP, Vermeulen L. Microenvironmental regulation of stem cells in intestinal homeostasis and cancer. *Nature*. 2011;474(7351):318-326.

34. D. W. Powell, R. C. Mifflin, J. D. Valentich, S. E. Crowe, J. I. Saada, A. B. West. Myofibroblasts. II. intestinal subepithelial myofibroblasts. *American Journal of Physiology - Cell Physiolog*. 1999;277(2):C183-C201.

35. Kosinski C, Li VS, Chan AS, et al. Gene expression patterns of human colon tops and basal crypts and BMP antagonists as intestinal stem cell niche factors. *Proc Natl Acad Sci U S A*. 2007;104(39):15418-15423.

36. Patrick A. Adegboyega M, Randy C. Mifflin P, John F. DiMari P, Jamal I. Saada M, Don W. Powell M. - Immunohistochemical study of myofibroblasts in normal colonic mucosa, hyperplastic polyps, and adenomatous colorectal polyps. - *Archives of Pathology & Laboratory Medicine*. 2002(- 7):- 829.

37. Kuhnert F, Davis CR, Wang HT, et al. Essential requirement for wnt signaling in proliferation of adult small intestine and colon revealed by adenoviral expression of dickkopf-1. *Proc Natl Acad Sci U S A*. 2004;101(1):266-271.

38. Gregorieff A, Pinto D, Begthel H, Destree O, Kielman M, Clevers H. Expression pattern of wnt signaling components in the adult intestine. *Gastroenterology*. 2005;129(2):626-638.

39. Cavallo RA, Cox RT, Moline MM, et al. Drosophila tcf and groucho interact to repress wingless signalling activity. *Nature*. 1998;395(6702):604-608.

40. Behrens J, von Kries JP, Kuhl M, et al. Functional interaction of beta-catenin with the transcription factor LEF-1. *Nature*. 1996;382(6592):638-642.

41. Fevr T, Robine S, Louvard D, Huelsken J. Wnt/beta-catenin is essential for intestinal homeostasis and maintenance of intestinal stem cells. *Mol Cell Biol*. 2007;27(21):7551-7559.

42. van de Wetering M, Sancho E, Verweij C, et al. The beta-catenin/TCF-4 complex imposes a crypt progenitor phenotype on colorectal cancer cells. *Cell*. 2002;111(2):241-250.

43. Bhanot P, Brink M, Samos CH, et al. A new member of the frizzled family from drosophila functions as a wingless receptor. *Nature*. 1996;382(6588):225-230.

44. Pinson KI, Brennan J, Monkley S, Avery BJ, Skarnes WC. An LDL-receptor-related protein mediates wnt signalling in mice. *Nature*. 2000;407(6803):535-538.

45. Tamai K, Semenov M, Kato Y, et al. LDL-receptor-related proteins in wnt signal transduction. *Nature*. 2000;407(6803):530-535.

46. Aberle H, Bauer A, Stappert J, Kispert A, Kemler R. Beta-catenin is a target for the ubiquitin-proteasome pathway. *EMBO J*. 1997;16(13):3797-3804.

47. van Es JH, Haegebarth A, Kujala P, et al. A critical role for the wnt effector Tcf4 in adult intestinal homeostatic self-renewal. *Mol Cell Biol*. 2012;32(10):1918-1927.

48. Van der Flier LG, Sabates-Bellver J, Oving I, et al. The intestinal wnt/TCF signature. *Gastroenterology*. 2007;132(2):628-632.

49. Barker N, van Es JH, Kuipers J, et al. Identification of stem cells in small intestine and colon by marker gene Lgr5. *Nature*. 2007;449(7165):1003-1007.

50. Batlle E, Henderson JT, Beghtel H, et al. Beta-catenin and TCF mediate cell positioning in the intestinal epithelium by controlling the expression of EphB/ephrinB. *Cell*. 2002;111(2):251-263.

51. van der Flier LG, van Gijn ME, Hatzis P, et al. Transcription factor achaete scute-like 2 controls intestinal stem cell fate. *Cell*. 2009;136(5):903-912.

52. Mikels AJ, Nusse R. Wnts as ligands: Processing, secretion and reception. *Oncogene*. 2006;25(57):7461-7468.

53. Derynck R, Zhang YE. Smad-dependent and smad-independent pathways in TGF-beta family signalling. *Nature*. 2003;425(6958):577-584.

54. Hardwick JC, Kodach LL, Offerhaus GJ, van den Brink GR. Bone morphogenetic protein signalling in colorectal cancer. *Nat Rev Cancer*. 2008;8(10):806-812.

55. Shi Y, Massagué J. Mechanisms of TGF-β signaling from cell membrane to the nucleus. *Cell*. 2003;113(6):685-700.

56. Whissell G, Montagni E, Martinelli P, et al. The transcription factor GATA6 enables self-renewal of colon adenoma stem cells by repressing BMP gene expression. *Nat Cell Biol*. 2014;16(7):695-707.

57. He XC, Zhang J, Tong WG, et al. BMP signaling inhibits intestinal stem cell self-renewal through suppression of wnt-beta-catenin signaling. *Nat Genet*. 2004;36(10):1117-1121.

58. Haramis AG, Begthel H, van den Born M, et al. De novo crypt formation and juvenile polyposis on BMP inhibition in mouse intestine. *Science*. 2004;303(5664):1684-1686.

59. Qiao L, Wong BCY. Role of notch signaling in colorectal cancer. *Carcinogenesis*. 2009;30(12):1979-1986.

60. van Es JH, van Gijn ME, Riccio O, et al. Notch/gamma-secretase inhibition turns proliferative cells in intestinal crypts and adenomas into goblet cells. *Nature*. 2005;435(7044):959-963.

61. van Es JH, de Geest N, van de Born M, Clevers H, Hassan BA. Intestinal stem cells lacking the Math1 tumour suppressor are refractory to notch inhibitors. *Nat Commun*. 2010;1:18.

62. Fre S, Huyghe M, Mourikis P, Robine S, Louvard D, Artavanis-Tsakonas S. Notch signals control the fate of immature progenitor cells in the intestine. *Nature*. 2005;435(7044):964-968.

63. Riccio O, van Gijn ME, Bezdek AC, et al. Loss of intestinal crypt progenitor cells owing to inactivation of both Notch1 and Notch2 is accompanied by derepression of CDK inhibitors p27Kip1 and p57Kip2. *EMBO Rep*. 2008;9(4):377-383.

64. Fearon ER, Vogelstein B. A genetic model for colorectal tumorigenesis. *Cell*. 1990;61(5):759-767.

65. Andreyev HJN, Norman AR, Clarke PA, Cunningham D, Oates JR. Kirsten ras mutations in patients with colorectal cancer: The multicenter “RASCAL” study. *Journal of the National Cancer Institute*. 1998;90(9):675-684.

66. Smith G, Carey FA, Beattie J, et al. Mutations in APC, kirsten-ras, and p53—alternative genetic pathways to colorectal cancer. *Proceedings of the National Academy of Sciences*. 2002;99(14):9433-9438.

67. Cawkwell L, Lewis FA, Quirke P. Frequency of allele loss of DCC, p53, RBI, WT1, NF1, NM23 and APC/MCC in colorectal cancer assayed by fluorescent multiplex polymerase chain reaction. *Br J Cancer*. 1994;70(5):813-818.

68. Xing Y, Clements WK, Kimelman D, Xu W. Crystal structure of a ß-catenin/axin complex suggests a mechanism for the ß-catenin destruction complex. *Genes & Development*. 2003;17(22):2753-2764.

69. Henderson BR. Nuclear-cytoplasmic shuttling of APC regulates beta-catenin subcellular localization and turnover. *Nat Cell Biol*. 2000;2(9):653-660.

70. He TC, Sparks AB, Rago C, et al. Identification of c-MYC as a target of the APC pathway. *Science*. 1998;281(5382):1509-1512.

71. Tetsu O, McCormick F. Beta-catenin regulates expression of cyclin D1 in colon carcinoma cells. *Nature*. 1999;398(6726):422-426.

72. Ichii S, Horii A, Nakatsuru S, Furuyama J, Utsunomiya J, Nakamura Y. Inactivation of both APC alleles in an early stage of colon adenomas in a patient with familial adenomatous polyposis (FAP). *Hum Mol Genet*. 1992;1(6):387-390.

73. Nishisho I, Nakamura Y, Miyoshi Y, et al. Mutations of chromosome 5q21 genes in FAP and colorectal cancer patients. *Science*. 1991;253(5020):665-669.

74. Groden J, Thliveris A, Samowitz W, et al. Identification and characterization of the familial adenomatous polyposis coli gene. *Cell*. 1991;66(3):589-600.

75. Sansom OJ, Reed KR, Hayes AJ, et al. Loss of apc in vivo immediately perturbs wnt signaling, differentiation, and migration. *Genes Dev*. 2004;18(12):1385-1390.

76. Horst D, Chen J, Morikawa T, Ogino S, Kirchner T, Shivdasani RA. Differential WNT activity in colorectal cancer confers limited tumorigenic potential and is regulated by MAPK signaling. *Cancer Research*. 2012.

77. Rad R, Cadinanos J, Rad L, et al. A genetic progression model of braf(V600E)-induced intestinal tumorigenesis reveals targets for therapeutic intervention. *Cancer Cell*. 2013;24(1):15-29.

78. Vermeulen L, De Sousa E Melo F, van der Heijden M, et al. Wnt activity defines colon cancer stem cells and is regulated by the microenvironment. *Nat Cell Biol*. 2010;12(5):468-476.

79. Voloshanenko O, Erdmann G, Dubash TD, et al. Wnt secretion is required to maintain high levels of wnt activity in colon cancer cells. *Nat Commun*. 2013;4:2610.

80. Hemminki A, Peltomaki P, Mecklin JP, et al. Loss of the wild type MLH1 gene is a feature of hereditary nonpolyposis colorectal cancer. *Nat Genet*. 1994;8(4):405-410.

81. Kane MF, Loda M, Gaida GM, et al. Methylation of the hMLH1 promoter correlates with lack of expression of hMLH1 in sporadic colon tumors and mismatch repair-defective human tumor cell lines. *Cancer Res*. 1997;57(5):808-811.

82. Cunningham JM, Christensen ER, Tester DJ, et al. Hypermethylation of the hMLH1 promoter in colon cancer with microsatellite instability. *Cancer Res*. 1998;58(15):3455-3460.

83. Li G. Mechanisms and functions of DNA mismatch repair. *Cell Res*. 2008;18(1):85-98.

84. Markowitz S, Wang J, Myeroff L, et al. Inactivation of the type II TGF-beta receptor in colon cancer cells with microsatellite instability. *Science*. 1995;268(5215):1336-1338.

85. Iacopetta B, Grieu F, Amanuel B. Microsatellite instability in colorectal cancer. *Asia Pac J Clin Oncol*. 2010;6(4):260-269.

86. Ahuja N, Mohan AL, Li Q, et al. Association between CpG island methylation and microsatellite instability in colorectal cancer. *Cancer Res*. 1997;57(16):3370-3374.

87. De Sousa E Melo F, Wang X, Jansen M, et al. Poor-prognosis colon cancer is defined by a molecularly distinct subtype and develops from serrated precursor lesions. *Nat Med*. 2013;19(5):614-618.

88. Shen L, Toyota M, Kondo Y, et al. Integrated genetic and epigenetic analysis identifies three different subclasses of colon cancer. *Proceedings of the National Academy of Sciences*. 2007;104(47):18654-18659.

89. ARMITAGE P, DOLL R. The age distribution of cancer and a multi-stage theory of carcinogenesis. *Br J Cancer*. 1954;8(1):1-12.

90. Nakamura S, Kino I. Morphogenesis of minute adenomas in familial polyposis coli. *J Natl Cancer Inst*. 1984;73(1):41-49.

91. Preston SL, Wong WM, Chan AO, et al. Bottom-up histogenesis of colorectal adenomas: Origin in the monocryptal adenoma and initial expansion by crypt fission. *Cancer Res*. 2003;63(13):3819-3825.

92. Shih IM, Wang TL, Traverso G, et al. Top-down morphogenesis of colorectal tumors. *Proc Natl Acad Sci U S A*. 2001;98(5):2640-2645.

93. Schwitalla S, Fingerle AA, Cammareri P, et al. Intestinal tumorigenesis initiated by dedifferentiation and acquisition of stem-cell-like properties. *Cell*. 2013;152(1-2):25-38.

94. Bonnet D, Dick JE. Human acute myeloid leukemia is organized as a hierarchy that originates from a primitive hematopoietic cell. *Nat Med*. 1997;3(7):730-737.

95. Al-Hajj M, Wicha MS, Benito-Hernandez A, Morrison SJ, Clarke MF. Prospective identification of tumorigenic breast cancer cells. *Proceedings of the National Academy of Sciences of the United States of America*. ;100(7):3983-3988.

96. O'Brien CA, Pollett A, Gallinger S, Dick JE. A human colon cancer cell capable of initiating tumour growth in immunodeficient mice. *Nature*. 2007;445(7123):106-110.

97. Curley MD, Therrien VA, Cummings CL, et al. CD133 expression defines a tumor initiating cell population in primary human ovarian cancer. *Stem Cells*. 2009;27(12):2875-2883.

98. Singh SK, Clarke ID, Terasaki M, et al. Identification of a cancer stem cell in human brain tumors. *Cancer Res*. 2003;63(18):5821-5828.

99. Singh SK, Hawkins C, Clarke ID, et al. Identification of human brain tumour initiating cells. *Nature*. 2004;432(7015):396-401.

100. Yang ZF, Ho DW, Ng MN, et al. Significance of CD90+ cancer stem cells in human liver cancer. *Cancer Cell*. 2008;13(2):153-166.

101. Ricci-Vitiani L, Lombardi DG, Pilozzi E, et al. Identification and expansion of human colon-cancer-initiating cells. *Nature*. 2007;445(7123):111-115.

102. Prince ME, Sivanandan R, Kaczorowski A, et al. Identification of a subpopulation of cells with cancer stem cell properties in head and neck squamous cell carcinoma. *Proc Natl Acad Sci U S A*. 2007;104(3):973-978.

103. Li C, Heidt DG, Dalerba P, et al. Identification of pancreatic cancer stem cells. *Cancer Res*. 2007;67(3):1030-1037.

104. Eramo A, Lotti F, Sette G, et al. Identification and expansion of the tumorigenic lung cancer stem cell population. *Cell Death Differ*. 2008;15(3):504-514.

105. Dalerba P, Dylla SJ, Park IK, et al. Phenotypic characterization of human colorectal cancer stem cells. *Proc Natl Acad Sci U S A*. 2007;104(24):10158-10163.

106. Barker N, Ridgway RA, van Es JH, et al. Crypt stem cells as the cells-of-origin of intestinal cancer. *Nature*. 2009;457(7229):608-611.

107. Schepers AG, Snippert HJ, Stange DE, et al. Lineage tracing reveals Lgr5+ stem cell activity in mouse intestinal adenomas. *Science*. 2012;337(6095):730-735.

108. Chen J, Li Y, Yu TS, et al. A restricted cell population propagates glioblastoma growth after chemotherapy. *Nature*. 2012;488(7412):522-526.

109. Rath P, Lal B, Ajala O, et al. In vivo c-met pathway inhibition depletes human glioma xenografts of tumor-propagating stem-like cells. *Transl Oncol*. 2013;6(2):104-111.

110. van Leenders, Geert J. L. H., Sookhlall R, Teubel WJ, et al. Activation of c-MET induces a stem-like phenotype in human prostate cancer. *PLoS ONE*. 2011;6(11):e26753.

111. Chaffer CL, Marjanovic ND, Lee T, et al. Poised chromatin at the ZEB1 promoter enables breast cancer cell plasticity and enhances tumorigenicity. *Cell*. 2013;154(1):61-74.

112. de Bruin EC, McGranahan N, Mitter R, et al. Spatial and temporal diversity in genomic instability processes defines lung cancer evolution. *Science*. 2014;346(6206):251-256.

113. Gerlinger M, Horswell S, Larkin J, et al. Genomic architecture and evolution of clear cell renal cell carcinomas defined by multiregion sequencing. *Nat Genet*. 2014;46(3):225-233.

114. Gerlinger M, Rowan AJ, Horswell S, et al. Intratumor heterogeneity and branched evolution revealed by multiregion sequencing. *N Engl J Med*. 2012;366(10):883-892.

115. Yin S, Li J, Hu C, et al. CD133 positive hepatocellular carcinoma cells possess high capacity for tumorigenicity. *Int J Cancer*. 2007;120(7):1444-1450.

116. Collins AT, Berry PA, Hyde C, Stower MJ, Maitland NJ. Prospective identification of tumorigenic prostate cancer stem cells. *Cancer Res*. 2005;65(23):10946-10951.

117. Shmelkov SV, Butler JM, Hooper AT, et al. CD133 expression is not restricted to stem cells, and both CD133+ and CD133- metastatic colon cancer cells initiate tumors. *J Clin Invest*. 2008;118(6):2111-2120.

118. Huang EH, Hynes MJ, Zhang T, et al. Aldehyde dehydrogenase 1 is a marker for normal and malignant human colonic stem cells (SC) and tracks SC overpopulation during colon tumorigenesis. *Cancer Res*. 2009;69(8):3382-3389.

119. Kemper K, Sprick MR, de Bree M, et al. The AC133 epitope, but not the CD133 protein, is lost upon cancer stem cell differentiation. *Cancer Res*. 2010;70(2):719-729.

120. Bellizzi A, Sebastian S, Ceglia P, et al. Co-expression of CD133(+)/CD44(+) in human colon cancer and liver metastasis. *J Cell Physiol*. 2013;228(2):408-415.

121. Nadal R, Ortega FG, Salido M, et al. CD133 expression in circulating tumor cells from breast cancer patients: Potential role in resistance to chemotherapy. *Int J Cancer*. 2013.

122. Sartelet H, Imbriglio T, Nyalendo C, et al. CD133 expression is associated with poor outcome in neuroblastoma via chemoresistance mediated by the AKT pathway. *Histopathology*. 2012;60(7):1144-1155.

123. Iida H, Suzuki M, Goitsuka R, Ueno H. Hypoxia induces CD133 expression in human lung cancer cells by up-regulation of OCT3/4 and SOX2. *Int J Oncol*. 2012;40(1):71-79.

124. Chen H, Luo Z, Dong L, et al. CD133/prominin-1-mediated autophagy and glucose uptake beneficial for hepatoma cell survival. *PLoS One*. 2013;8(2):e56878.

125. Song Y, Zhang S, Guo X, et al. Autophagy contributes to the survival of CD133+ liver cancer stem cells in the hypoxic and nutrient-deprived tumor microenvironment. *Cancer Lett*. ;339(1):70-81.

126. Chute JP, Muramoto GG, Whitesides J, et al. Inhibition of aldehyde dehydrogenase and retinoid signaling induces the expansion of human hematopoietic stem cells. *Proc Natl Acad Sci U S A*. 2006;103(31):11707-11712.

127. Bunting KD, Townsend AJ. De novo expression of transfected human class 1 aldehyde dehydrogenase (ALDH) causes resistance to oxazaphosphorine anti-cancer alkylating agents in hamster V79 cell lines. elevated class 1 ALDH activity is closely correlated with reduction in DNA interstrand cross-linking and lethality. *J Biol Chem*. 1996;271(20):11884-11890.

128. Dylla SJ, Beviglia L, Park IK, et al. Colorectal cancer stem cells are enriched in xenogeneic tumors following chemotherapy. *PLoS One*. 2008;3(6):e2428.

129. Gerber JM, Smith BD, Ngwang B, et al. A clinically relevant population of leukemic CD34(+)CD38(-) cells in acute myeloid leukemia. *Blood*. 2012;119(15):3571-3577.

130. Ginestier C, Hur MH, Charafe-Jauffret E, et al. ALDH1 is a marker of normal and malignant human mammary stem cells and a predictor of poor clinical outcome. *Cell Stem Cell*. 2007;1(5):555-567.

131. Jiang F, Qiu Q, Khanna A, et al. Aldehyde dehydrogenase 1 is a tumor stem cell-associated marker in lung cancer. *Mol Cancer Res*. 2009;7(3):330-338.

132. Kim MP, Fleming JB, Wang H, et al. ALDH activity selectively defines an enhanced tumor-initiating cell population relative to CD133 expression in human pancreatic adenocarcinoma. *PLoS ONE*. 2011;6(6):e20636.

133. Zhang J, Espinoza LA, Kinders RJ, et al. NANOG modulates stemness in human colorectal cancer. *Oncogene*. 2012.

134. Xu F, Dai C, Zhang R, Zhao Y, Peng S, Jia C. Nanog: A potential biomarker for liver metastasis of colorectal cancer. *Dig Dis Sci*. 2012;57(9):2340-2346.

135. Jeter CR, Liu B, Liu X, et al. NANOG promotes cancer stem cell characteristics and prostate cancer resistance to androgen deprivation. *Oncogene*. 2011;30(36):3833-3845.

136. Pang R, Law WL, Chu AC, et al. A subpopulation of CD26+ cancer stem cells with metastatic capacity in human colorectal cancer. *Cell Stem Cell*. 2010;6(6):603-615.

137. Tanaka T, Camerini D, Seed B, et al. Cloning and functional expression of the T cell activation antigen CD26. *J Immunol*. 1992;149(2):481-486.

138. Dang NH, Torimoto Y, Schlossman SF, Morimoto C. Human CD4 helper T cell activation: Functional involvement of two distinct collagen receptors, 1F7 and VLA integrin family. *J Exp Med*. 1990;172(2):649-652.

139. Dong RP, Tachibana K, Hegen M, et al. Determination of adenosine deaminase binding domain on CD26 and its immunoregulatory effect on T cell activation. *J Immunol*. 1997;159(12):6070-6076.

140. Antonioli L, Blandizzi C, Pacher P, Hasko G. Immunity, inflammation and cancer: A leading role for adenosine. *Nat Rev Cancer*. 2013;13(12):842-857.

141. Ma DF, Kondo T, Nakazawa T, et al. Hypoxia-inducible adenosine A2B receptor modulates proliferation of colon carcinoma cells. *Hum Pathol*. 2010;41(11):1550-1557.

142. Karagiannis T, Paschos P, Paletas K, Matthews DR, Tsapas A. Dipeptidyl peptidase-4 inhibitors for treatment of type 2 diabetes mellitus in the clinical setting: Systematic review and meta-analysis. *BMJ*. 2012;344:e1369.

143. Fishman P, Bar-Yehuda S, Ohana G, et al. An agonist to the A3 adenosine receptor inhibits colon carcinoma growth in mice via modulation of GSK-3 beta and NF-kappa B. *Oncogene*. 2004;23(14):2465-2471.

144. Morrison ME, Vijayasaradhi S, Engelstein D, Albino AP, Houghton AN. A marker for neoplastic progression of human melanocytes is a cell surface ectopeptidase. *J Exp Med*. 1993;177(4):1135-1143.

145. Pethiyagoda CL, Welch DR, Fleming TP. Dipeptidyl peptidase IV (DPPIV) inhibits cellular invasion of melanoma cells. *Clin Exp Metastasis*. 2000;18(5):391-400.

146. Yamazaki H, Naito M, Ghani FI, Dang NH, Iwata S, Morimoto C. Characterization of cancer stem cell properties of CD24 and CD26-positive human malignant mesothelioma cells. *Biochem Biophys Res Commun*. 2012;419(3):529-536.

147. Dourado M, Sarmento AB, Pereira SV, et al. CD26/DPPIV expression and 8-azaguanine response in T-acute lymphoblastic leukaemia cell lines in culture. *Pathophysiology*. 2007;14(1):3-10.

148. Herrmann H, Sadovnik I, Cerny-Reiterer S, et al. Dipeptidylpeptidase IV (CD26) defines leukemic stem cells (LSC) in chronic myeloid leukemia. *Blood*. 2014;123(25):3951-3962.

149. King JB, von Furstenberg RJ, Smith BJ, McNaughton KK, Galanko JA, Henning SJ. CD24 can be used to isolate Lgr5+ putative colonic epithelial stem cells in mice. *Am J Physiol Gastrointest Liver Physiol*. 2012;303(4):G443-52.

150. Proctor E, Waghray M, Lee CJ, et al. Bmi1 enhances tumorigenicity and cancer stem cell function in pancreatic adenocarcinoma. *PLoS ONE*. 2013;8(2):e55820.

151. Du L, Wang H, He L, et al. CD44 is of functional importance for colorectal cancer stem cells. *Clinical Cancer Research*. 2008;14(21):6751-6760.

152. Levin TG, Powell AE, Davies PS, et al. Characterization of the intestinal cancer stem cell marker CD166 in the human and mouse gastrointestinal tract. *Gastroenterology*. 2010;139(6):2072-2082.e5.

153. Hwang-Verslues WW, Kuo WH, Chang PH, et al. Multiple lineages of human breast cancer stem/progenitor cells identified by profiling with stem cell markers. *PLoS One*. 2009;4(12):e8377.

154. Todaro M, Alea MP, Di Stefano AB, et al. Colon cancer stem cells dictate tumor growth and resist cell death by production of interleukin-4. *Cell Stem Cell*. 2007;1(4):389-402.

155. Hostettler L, Zlobec I, Terracciano L, Lugli A. ABCG5-positivity in tumor buds is an indicator of poor prognosis in node-negative colorectal cancer patients. *World J Gastroenterol*. 2010;16(6):732-739.

156. Monzani E, Facchetti F, Galmozzi E, et al. Melanoma contains CD133 and ABCG2 positive cells with enhanced tumourigenic potential. *Eur J Cancer*. 2007;43(5):935-946.

157. Zen Y, Fujii T, Yoshikawa S, et al. Histological and culture studies with respect to ABCG2 expression support the existence of a cancer cell hierarchy in human hepatocellular carcinoma. *Am J Pathol*. 2007;170(5):1750-1762.

158. Moore N, Lyle S. Quiescent, slow-cycling stem cell populations in cancer: A review of the evidence and discussion of significance. *J Oncol*. 2011;2011:396076. Epub 2010 Sep 29.

159. Butler TP, Gullino PM. Quantitation of cell shedding into efferent blood of mammary adenocarcinoma. *Cancer Res*. 1975;35(3):512-516.

160. Yan C, Grimm WA, Garner WL, et al. Epithelial to mesenchymal transition in human skin wound healing is induced by tumor necrosis factor-alpha through bone morphogenic protein-2. *Am J Pathol*. 2010;176(5):2247-2258.

161. Kalluri R, Weinberg RA. The basics of epithelial-mesenchymal transition. *J Clin Invest*. 2009;119(6):1420-1428.

162. Yang J, Mani SA, Donaher JL, et al. Twist, a master regulator of morphogenesis, plays an essential role in tumor metastasis. *Cell*. 2004;117(7):927-939.

163. Cano A, Perez-Moreno MA, Rodrigo I, et al. The transcription factor snail controls epithelial-mesenchymal transitions by repressing E-cadherin expression. *Nat Cell Biol*. 2000;2(2):76-83.

164. De Craene B, Gilbert B, Stove C, Bruyneel E, van Roy F, Berx G. The transcription factor snail induces tumor cell invasion through modulation of the epithelial cell differentiation program. *Cancer Res*. 2005;65(14):6237-6244.

165. Wheeler JM, Kim HC, Efstathiou JA, Ilyas M, Mortensen NJ, Bodmer WF. Hypermethylation of the promoter region of the E-cadherin gene (CDH1) in sporadic and ulcerative colitis associated colorectal cancer. *Gut*. 2001;48(3):367-371.

166. Pelaez IM, Kalogeropoulou M, Ferraro A, et al. Oncogenic RAS alters the global and gene-specific histone modification pattern during epithelial-mesenchymal transition in colorectal carcinoma cells. *Int J Biochem Cell Biol*. 2010;42(6):911-920.

167. Hennig G, Behrens J, Truss M, Frisch S, Reichmann E, Birchmeier W. Progression of carcinoma cells is associated with alterations in chromatin structure and factor binding at the E-cadherin promoter in vivo. *Oncogene*. 1995;11(3):475-484.

168. Hazan RB, Phillips GR, Qiao RF, Norton L, Aaronson SA. Exogenous expression of N-cadherin in breast cancer cells induces cell migration, invasion, and metastasis. *J Cell Biol*. 2000;148(4):779-790.

169. Leupold JH, Asangani I, Maurer GD, Lengyel E, Post S, Allgayer H. Src induces urokinase receptor gene expression and invasion/intravasation via activator protein-1/p-c-jun in colorectal cancer. *Mol Cancer Res*. 2007;5(5):485-496.

170. Dano K, Behrendt N, Hoyer-Hansen G, et al. Plasminogen activation and cancer. *Thromb Haemost*. 2005;93(4):676-681.

171. Almholt K, Lund LR, Rygaard J, et al. Reduced metastasis of transgenic mammary cancer in urokinase-deficient mice. *Int J Cancer*. 2005;113(4):525-532.

172. Kim TS, Kim YB. Correlation between expression of matrix metalloproteinase-2 (MMP-2), and matrix metalloproteinase-9 (MMP-9) and angiogenesis in colorectal adenocarcinoma. *J Korean Med Sci*. 1999;14(3):263-270.

173. Chu D, Zhao Z, Zhou Y, et al. Matrix metalloproteinase-9 is associated with relapse and prognosis of patients with colorectal cancer. *Ann Surg Oncol*. 2011.

174. Owens LV, Xu L, Craven RJ, et al. Overexpression of the focal adhesion kinase (p125FAK) in invasive human tumors. *Cancer Res*. 1995;55(13):2752-2755.

175. Zeng Q, Chen S, You Z, et al. Hepatocyte growth factor inhibits anoikis in head and neck squamous cell carcinoma cells by activation of ERK and akt signaling independent of NFkappa B. *J Biol Chem*. 2002;277(28):25203-25208.

176. McLean GW, Komiyama NH, Serrels B, et al. Specific deletion of focal adhesion kinase suppresses tumor formation and blocks malignant progression. *Genes Dev*. 2004;18(24):2998-3003.

177. Weiss L. Biomechanical destruction of cancer cells in skeletal muscle: A rate-regulator for hematogenous metastasis. *Clin Exp Metastasis*. 1989;7(5):483-491.

178. Weiss L. Biomechanical destruction of cancer cells in the heart: A rate regulator for hematogenous metastasis. *Invasion Metastasis*. 1988;8(4):228-237.

179. Weiss L, Nannmark U, Johansson BR, Bagge U. Lethal deformation of cancer cells in the microcirculation: A potential rate regulator of hematogenous metastasis. *Int J Cancer*. 1992;50(1):103-107.

180. Kluger HM, Chelouche Lev D, Kluger Y, et al. Using a xenograft model of human breast cancer metastasis to find genes associated with clinically aggressive disease. *Cancer Res*. 2005;65(13):5578-5587.

181. Ziegler T, Silacci P, Harrison VJ, Hayoz D. Nitric oxide synthase expression in endothelial cells exposed to mechanical forces. *Hypertension*. 1998;32(2):351-355.

182. Honn KV, Tang DG, Grossi IM, et al. Enhanced endothelial cell retraction mediated by 12(S)-HETE: A proposed mechanism for the role of platelets in tumor cell metastasis. *Exp Cell Res*. 1994;210(1):1-9.

183. Karnezis T, Shayan R, Caesar C, et al. VEGF-D promotes tumor metastasis by regulating prostaglandins produced by the collecting lymphatic endothelium. *Cancer Cell*. 2012;21(2):181-195.

184. Schumacher D, Strilic B, Sivaraj KK, Wettschureck N, Offermanns S. Platelet-derived nucleotides promote tumor-cell transendothelial migration and metastasis via P2Y2 receptor. *Cancer Cell*. 2013;24(1):130-137.

185. Brown DM, Ruoslahti E. Metadherin, a cell surface protein in breast tumors that mediates lung metastasis. *Cancer Cell*. 2004;5(4):365-374.

186. Minn AJ, Kang Y, Serganova I, et al. Distinct organ-specific metastatic potential of individual breast cancer cells and primary tumors. *J Clin Invest*. 2005;115(1):44-55.

187. Dieter SM, Ball CR, Hoffmann CM, et al. Distinct types of tumor-initiating cells form human colon cancer tumors and metastases. *Cell Stem Cell*. 2011;9(4):357-365.

188. Schmidt-Kittler O, Ragg T, Daskalakis A, et al. From latent disseminated cells to overt metastasis: Genetic analysis of systemic breast cancer progression. *Proc Natl Acad Sci U S A*. 2003;100(13):7737-7742.

189. Braun S, Pantel K, Muller P, et al. Cytokeratin-positive cells in the bone marrow and survival of patients with stage I, II, or III breast cancer. *N Engl J Med*. 2000;342(8):525-533.

190. Husemann Y, Geigl JB, Schubert F, et al. Systemic spread is an early step in breast cancer. *Cancer Cell*. 2008;13(1):58-68.

191. Hess KR, Varadhachary GR, Taylor SH, et al. Metastatic patterns in adenocarcinoma. *Cancer*. 2006;106(7):1624-1633.

192. Lalor PF, Lai WK, Curbishley SM, Shetty S, Adams DH. Human hepatic sinusoidal endothelial cells can be distinguished by expression of phenotypic markers related to their specialised functions in vivo. *World J Gastroenterol*. 2006;12(34):5429-5439.

193. Brabletz T, Jung A, Spaderna S, Hlubek F, Kirchner T. Opinion: Migrating cancer stem cells - an integrated concept of malignant tumour progression. *Nat Rev Cancer*. 2005;5(9):744-749.

194. Biddle A, Liang X, Gammon L, et al. Cancer stem cells in squamous cell carcinoma switch between two distinct phenotypes that are preferentially migratory or proliferative. *Cancer Res*. 2011.

195. Mani SA, Guo W, Liao MJ, et al. The epithelial-mesenchymal transition generates cells with properties of stem cells. *Cell*. 2008;133(4):704-715.

196. Obrocea F, Sajin M, Marinescu EC, Stoica D. Colorectal cancer and the 7th revision of the TNM staging system: Review of changes and suggestions for uniform pathologic reporting. *Rom J Morphol Embryol*. 2011;52(2):537-544.

197. Labianca R, Nordlinger B, Beretta GD, Brouquet A, Cervantes A, ESMO Guidelines Working Group. Primary colon cancer: ESMO clinical practice guidelines for diagnosis, adjuvant treatment and follow-up. *Ann Oncol*. 2010;21 Suppl 5:v70-7.

198. Jover R, Nguyen TP, Perez-Carbonell L, et al. 5-fluorouracil adjuvant chemotherapy does not increase survival in patients with CpG island methylator phenotype colorectal cancer. *Gastroenterology*. 2011;140(4):1174-1181.

199. Allen P, Kemeny N, Jarnagin W, DeMatteo R, Blumgart L, Fong Y. Importance of response to neoadjuvant chemotherapy in patients undergoing resection of synchronous colorectal liver metastases. *Journal of Gastrointestinal Surgery*. 2003;7(1):109-117.

200. Benoist S, Brouquet A, Penna C, et al. Complete response of colorectal liver metastases after chemotherapy: Does it mean cure? *J Clin Oncol*. 2006;24(24):3939-3945.

201. Benoist S, Nordlinger B. The role of preoperative chemotherapy in patients with resectable colorectal liver metastases. *Ann Surg Oncol*. 2009;16(9):2385-2390.

202. Fong Y, Fortner J, Sun RL, Brennan MF, Blumgart LH. Clinical score for predicting recurrence after hepatic resection for metastatic colorectal cancer: Analysis of 1001 consecutive cases. *Ann Surg*. 1999;230(3):309-18; discussion 318-21.

203. Longley DB, Harkin DP, Johnston PG. 5-fluorouracil: Mechanisms of action and clinical strategies. *Nat Rev Cancer*. 2003;3(5):330-338.

204. Alvarez P, Marchal JA, Boulaiz H, et al. 5-fluorouracil derivatives: A patent review. *Expert Opin Ther Pat*. 2012;22(2):107-123.

205. Park JG, Collins JM, Gazdar AF, et al. Enhancement of fluorinated pyrimidine-induced cytotoxicity by leucovorin in human colorectal carcinoma cell lines. *J Natl Cancer Inst*. 1988;80(19):1560-1564.

206. Noordhuis P, Holwerda U, Van der Wilt CL, et al. 5-fluorouracil incorporation into RNA and DNA in relation to thymidylate synthase inhibition of human colorectal cancers. *Annals of Oncology*. 2004;15(7):1025-1032.

207. Miwa M, Ura M, Nishida M, et al. Design of a novel oral fluoropyrimidine carbamate, capecitabine, which generates 5-fluorouracil selectively in tumours by enzymes concentrated in human liver and cancer tissue. *Eur J Cancer*. 1998;34(8):1274-1281.

208. Budman DR, Meropol NJ, Reigner B, et al. Preliminary studies of a novel oral fluoropyrimidine carbamate: Capecitabine. *J Clin Oncol*. 1998;16(5):1795-1802.

209. Dranitsaris G, Shah A, Spirovski B, Vincent M. Severe diarrhea in patients with advanced-stage colorectal cancer receiving FOLFOX or FOLFIRI chemotherapy: The development of a risk prediction tool. *Clin Colorectal Cancer*. 2007;6(5):367-373.

210. Ocvirk J, Brodowicz T, Wrba F, et al. Cetuximab plus FOLFOX6 or FOLFIRI in metastatic colorectal cancer: CECOG trial. *World J Gastroenterol*. 2010;16(25):3133-3143.

211. WEHLER TC, CAO Y, GALLE PR, THEOBALD M, MOEHLER M, SCHIMANSKI CC. Combination therapies with oxaliplatin and oral capecitabine or intravenous 5-FU show similar toxicity profiles in gastrointestinal carcinoma patients if hand-food syndrome prophylaxis is performed continuously. *Oncol Lett*. 2012;3(6):1191-1194.

212. Todd RC, Lippard SJ. Inhibition of transcription by platinum antitumor compounds. *Metallomics*. 2009;1(4):280-291.

213. de Gramont A, Tournigand C, Louvet C, et al. Oxaliplatin, folinic acid and 5-fluorouracil (folfox) in pretreated patients with metastatic advanced cancer. the GERCOD. *Rev Med Interne*. 1997;18(10):769-775.

214. de Gramont A, Figer A, Seymour M, et al. Leucovorin and fluorouracil with or without oxaliplatin as first-line treatment in advanced colorectal cancer. *J Clin Oncol*. 2000;18(16):2938-2947.

215. Giacchetti S, Perpoint B, Zidani R, et al. Phase III multicenter randomized trial of oxaliplatin added to chronomodulated fluorouracil-leucovorin as first-line treatment of metastatic colorectal cancer. *J Clin Oncol*. 2000;18(1):136-147.

216. Cassidy J, Tabernero J, Twelves C, et al. XELOX (capecitabine plus oxaliplatin): Active first-line therapy for patients with metastatic colorectal cancer. *J Clin Oncol*. 2004;22(11):2084-2091.

217. Cassidy J, Clarke S, Diaz-Rubio E, et al. XELOX vs FOLFOX-4 as first-line therapy for metastatic colorectal cancer: NO16966 updated results. *Br J Cancer*. 2011;105(1):58-64.

218. Douillard JY, Cunningham D, Roth AD, et al. Irinotecan combined with fluorouracil compared with fluorouracil alone as first-line treatment for metastatic colorectal cancer: A multicentre randomised trial. *Lancet*. 2000;355(9209):1041-1047.

219. Saltz LB, Cox JV, Blanke C, et al. Irinotecan plus fluorouracil and leucovorin for metastatic colorectal cancer. irinotecan study group. *N Engl J Med*. 2000;343(13):905-914.

220. Kabbinavar FF, Schulz J, McCleod M, et al. Addition of bevacizumab to bolus fluorouracil and leucovorin in first-line metastatic colorectal cancer: Results of a randomized phase II trial. *J Clin Oncol*. 2005;23(16):3697-3705.

221. Goldstein NI, Prewett M, Zuklys K, Rockwell P, Mendelsohn J. Biological efficacy of a chimeric antibody to the epidermal growth factor receptor in a human tumor xenograft model. *Clin Cancer Res*. 1995;1(11):1311-1318.

222. Prewett MC, Hooper AT, Bassi R, Ellis LM, Waksal HW, Hicklin DJ. Enhanced antitumor activity of anti-epidermal growth factor receptor monoclonal antibody IMC-C225 in combination with irinotecan (CPT-11) against human colorectal tumor xenografts. *Clin Cancer Res*. 2002;8(5):994-1003.

223. Karapetis CS, Khambata-Ford S, Jonker DJ, et al. K-ras mutations and benefit from cetuximab in advanced colorectal cancer. *N Engl J Med*. 2008;359(17):1757-1765.

224. Yang XD, Jia XC, Corvalan JR, Wang P, Davis CG, Jakobovits A. Eradication of established tumors by a fully human monoclonal antibody to the epidermal growth factor receptor without concomitant chemotherapy. *Cancer Res*. 1999;59(6):1236-1243.

225. Van Cutsem E, Peeters M, Siena S, et al. Open-label phase III trial of panitumumab plus best supportive care compared with best supportive care alone in patients with chemotherapy-refractory metastatic colorectal cancer. *J Clin Oncol*. 2007;25(13):1658-1664.

226. Gibson TB, Ranganathan A, Grothey A. Randomized phase III trial results of panitumumab, a fully human anti-epidermal growth factor receptor monoclonal antibody, in metastatic colorectal cancer. *Clin Colorectal Cancer*. 2006;6(1):29-31.

227. Bracht K, Nicholls AM, Liu Y, Bodmer WF. 5-fluorouracil response in a large panel of colorectal cancer cell lines is associated with mismatch repair deficiency. *Br J Cancer*. 2010;103(3):340-346.

228. Jover R, Zapater P, Castells A, et al. Mismatch repair status in the prediction of benefit from adjuvant fluorouracil chemotherapy in colorectal cancer. *Gut*. 2006;55(6):848-855.

229. Ribic CM, Sargent DJ, Moore MJ, et al. Tumor microsatellite-instability status as a predictor of benefit from fluorouracil-based adjuvant chemotherapy for colon cancer. *N Engl J Med*. 2003;349(3):247-257.

230. Sinicrope FA, Foster NR, Thibodeau SN, et al. DNA mismatch repair status and colon cancer recurrence and survival in clinical trials of 5-fluorouracil-based adjuvant therapy. *Journal of the National Cancer Institute*. 2011;103(11):863-875.

231. Cohen V, Panet-Raymond V, Sabbaghian N, Morin I, Batist G, Rozen R. Methylenetetrahydrofolate reductase polymorphism in advanced colorectal cancer: A

novel genomic predictor of clinical response to fluoropyrimidine-based chemotherapy. *Clinical Cancer Research*. 2003;9(5):1611-1615.

232. Jakobsen A, Nielsen JN, Gyldenkerne N, Lindeberg J. Thymidylate synthase and methylenetetrahydrofolate reductase gene polymorphism in normal tissue as predictors of fluorouracil sensitivity. *Journal of Clinical Oncology*. 2005;23(7):1365-1369.

233. Marcuello E, Altes A, Menoyo A, Rio ED, Baiget M. Methylenetetrahydrofolate reductase gene polymorphisms: Genomic predictors of clinical response to fluoropyrimidine-based chemotherapy? *Cancer Chemother Pharmacol*. 2006;57(6):835-840.

234. Wisotzkey JD, Toman J, Bell T, Monk JS, Jones D. MTHFR (C677T) polymorphisms and stage III colon cancer: Response to therapy. *Mol Diagn*. 1999;4(2):95-99.

235. Van Kuilenburg AB, Meinsma R, Zoetekouw L, Van Gennip AH. High prevalence of the IVS14 + 1G>A mutation in the dihydropyrimidine dehydrogenase gene of patients with severe 5-fluorouracil-associated toxicity. *Pharmacogenetics*. 2002;12(7):555-558.

236. Offer SM, Wegner NJ, Fossum C, Wang K, Diasio RB. Phenotypic profiling of DPYD variations relevant to 5-fluorouracil sensitivity using real-time cellular analysis and in vitro measurement of enzyme activity. *Cancer Res*. 2013;73(6):1958-1968.

237. Li P, Fang YJ, Li F, Ou QJ, Chen G, Ma G. ERCC1, defective mismatch repair status as predictive biomarkers of survival for stage III colon cancer patients receiving oxaliplatin-based adjuvant chemotherapy. *Br J Cancer*. 2013;108(6):1238-1244.

238. Stoehlmacher J, Park DJ, Zhang W, et al. A multivariate analysis of genomic polymorphisms: Prediction of clinical outcome to 5-FU/oxaliplatin combination chemotherapy in refractory colorectal cancer. *Br J Cancer*. 2004;91(2):344-354.

239. Pare L, Marcuello E, Altes A, et al. Pharmacogenetic prediction of clinical outcome in advanced colorectal cancer patients receiving oxaliplatin/5-fluorouracil as first-line chemotherapy. *Br J Cancer*. 2008;99(7):1050-1055.

240. Kim SH, Kwon HC, Oh SY, et al. Prognostic value of ERCC1, thymidylate synthase, and glutathione S-transferase pi for 5-FU/oxaliplatin chemotherapy in advanced colorectal cancer. *Am J Clin Oncol*. 2009;32(1):38-43.

241. Shirota Y, Stoehlmacher J, Brabender J, et al. ERCC1 and thymidylate synthase mRNA levels predict survival for colorectal cancer patients receiving combination oxaliplatin and fluorouracil chemotherapy. *J Clin Oncol*. 2001;19(23):4298-4304.

242. Friboulet L, Postel-Vinay S, Sourisseau T, et al. ERCC1 function in nuclear excision and interstrand crosslink repair pathways is mediated exclusively by the ERCC1-202 isoform. *Cell Cycle*. 2013;12(20):3298-3306.

243. Lv H, Li Q, Qiu W, et al. Genetic polymorphism of XRCC1 correlated with response to oxaliplatin-based chemotherapy in advanced colorectal cancer. *Pathol Oncol Res*. 2012;18(4):1009-1014.

244. Cheng XD, Lu WG, Ye F, Wan XY, Xie X. The association of XRCC1 gene single nucleotide polymorphisms with response to neoadjuvant chemotherapy in locally advanced cervical carcinoma. *J Exp Clin Cancer Res*. 2009;28(1):91-9966-28-91.

245. Liang J, Jiang T, Yao RY, Liu ZM, Lv HY, Qi WW. The combination of ERCC1 and XRCC1 gene polymorphisms better predicts clinical outcome to oxaliplatin-based chemotherapy in metastatic colorectal cancer. *Cancer Chemother Pharmacol*. 2010;66(3):493-500.

246. Bardelli A, Janne PA. The road to resistance: EGFR mutation and cetuximab. *Nat Med*. 2012;18(2):199-200.

247. De Roock W, Claes B, Bernasconi D, et al. Effects of KRAS, BRAF, NRAS, and PIK3CA mutations on the efficacy of cetuximab plus chemotherapy in chemotherapy-refractory metastatic colorectal cancer: A retrospective consortium analysis. *Lancet Oncol*. 2010;11(8):753-762.

248. Amado RG, Wolf M, Peeters M, et al. Wild-type KRAS is required for panitumumab efficacy in patients with metastatic colorectal cancer. *J Clin Oncol*. 2008;26(10):1626-1634.

249. Diaz LA,Jr, Williams RT, Wu J, et al. The molecular evolution of acquired resistance to targeted EGFR blockade in colorectal cancers. *Nature*. 2012;486(7404):537-540.

250. Bokemeyer C, Bondarenko I, Hartmann JT, et al. Efficacy according to biomarker status of cetuximab plus FOLFOX-4 as first-line treatment for metastatic colorectal cancer: The OPUS study. *Ann Oncol*. 2011;22(7):1535-1546.

251. Van Cutsem E, Kohne CH, Lang I, et al. Cetuximab plus irinotecan, fluorouracil, and leucovorin as first-line treatment for metastatic colorectal cancer: Updated analysis of overall survival according to tumor KRAS and BRAF mutation status. *J Clin Oncol*. 2011;29(15):2011-2019.

252. Di Nicolantonio F, Martini M, Molinari F, et al. Wild-type BRAF is required for response to panitumumab or cetuximab in metastatic colorectal cancer. *J Clin Oncol*. 2008;26(35):5705-5712.

253. Mao C, Yang ZY, Hu XF, Chen Q, Tang JL. PIK3CA exon 20 mutations as a potential biomarker for resistance to anti-EGFR monoclonal antibodies in KRAS wild-type metastatic colorectal cancer: A systematic review and meta-analysis. *Annals of Oncology*. 2012;23(6):1518-1525.

254. Sartore-Bianchi A, Martini M, Molinari F, et al. PIK3CA mutations in colorectal cancer are associated with clinical resistance to EGFR-targeted monoclonal antibodies. *Cancer Res*. 2009;69(5):1851-1857.

255. Rastogi T, Devesa S, Mangtani P, et al. Cancer incidence rates among south asians in four geographic regions: India, singapore, UK and US. *International Journal of Epidemiology*. 2008;37(1):147-160.

256. Smith LK, Botha JL, Benghiat A, Steward WP. Latest trends in cancer incidence among UK south asians in leicester. *Br J Cancer*. 2003;89(1):70-73.

257. Cheng AL, Hsu CH, Lin JK, et al. Phase I clinical trial of curcumin, a chemopreventive agent, in patients with high-risk or pre-malignant lesions. *Anticancer Res*. 2001;21(4B):2895-2900.

258. Sharma RA, McLelland HR, Hill KA, et al. Pharmacodynamic and pharmacokinetic study of oral curcuma extract in patients with colorectal cancer. *Clin Cancer Res*. 2001;7(7):1894-1900.

259. Sharma RA, Euden SA, Platton SL, et al. Phase I clinical trial of oral curcumin: Biomarkers of systemic activity and compliance. *Clin Cancer Res*. 2004;10(20):6847-6854.

260. Ravindranath V, Chandrasekhara N. Metabolism of curcumin--studies with [3H]curcumin. *Toxicology*. 1981;22(4):337-344.

261. Holder GM, Plummer JL, Ryan AJ. The metabolism and excretion of curcumin (1,7-bis-(4-hydroxy-3-methoxyphenyl)-1,6-heptadiene-3,5-dione) in the rat. *Xenobiotica*. 1978;8(12):761-768.

262. Asai A, Miyazawa T. Occurrence of orally administered curcuminoid as glucuronide and glucuronide/sulfate conjugates in rat plasma. *Life Sci*. 2000;67(23):2785-2793.

263. Mukhopadhyay A, Basu N, Ghatak N, Gujral PK. Anti-inflammatory and irritant activities of curcumin analogues in rats. *Agents Actions*. 1982;12(4):508-515.

264. Osawa T, Sugiyama Y, Inayoshi M, Kawakishi S. Antioxidative activity of tetrahydrocurcuminoids. *Biosci Biotechnol Biochem*. 1995;59(9):1609-1612.

265. Sugiyama Y, Kawakishi S, Osawa T. Involvement of the beta-diketone moiety in the antioxidative mechanism of tetrahydrocurcumin. *Biochem Pharmacol*. 1996;52(4):519-525.

266. Ireson C, Orr S, Jones DJ, et al. Characterization of metabolites of the chemopreventive agent curcumin in human and rat hepatocytes and in the rat in vivo, and evaluation of their ability to inhibit phorbol ester-induced prostaglandin E2 production. *Cancer Res*. 2001;61(3):1058-1064.

267. Zhang H, Sun XF. Overexpression of cyclooxygenase-2 correlates with advanced stages of colorectal cancer. *Am J Gastroenterol*. 2002;97(4):1037-1041.

268. Kunnumakkara AB, Guha S, Krishnan S, Diagaradjane P, Gelovani J, Aggarwal BB. Curcumin potentiates antitumor activity of gemcitabine in an orthotopic model of pancreatic cancer through suppression of proliferation, angiogenesis, and inhibition of nuclear factor-κB–Regulated gene products. *Cancer Research*. 2007;67(8):3853-3861.

269. Perkins S, Verschoyle RD, Hill K, et al. Chemopreventive efficacy and pharmacokinetics of curcumin in the min/+ mouse, a model of familial adenomatous polyposis. *Cancer Epidemiol Biomarkers Prev*. 2002;11(6):535-540.

270. Huang AC, Lin SY, Su CC, et al. Effects of curcumin on N-bis(2-hydroxypropyl) nitrosamine (DHPN)-induced lung and liver tumorigenesis in BALB/c mice in vivo. *In Vivo*. 2008;22(6):781-785.

271. Azuine MA, Bhide SV. Chemopreventive effect of turmeric against stomach and skin tumors induced by chemical carcinogens in swiss mice. *Nutr Cancer*. 1992;17(1):77-83.

272. Ushida J, Sugie S, Kawabata K, et al. Chemopreventive effect of curcumin on N-nitrosomethylbenzylamine-induced esophageal carcinogenesis in rats. *Jpn J Cancer Res*. 2000;91(9):893-898.

273. Li N, Chen X, Liao J, et al. Inhibition of 7,12-dimethylbenz[a]anthracene (DMBA)-induced oral carcinogenesis in hamsters by tea and curcumin. *Carcinogenesis*. 2002;23(8):1307-1313.

274. Shoba G, Joy D, Joseph T, Majeed M, Rajendran R, Srinivas PS. Influence of piperine on the pharmacokinetics of curcumin in animals and human volunteers. *Planta Med*. 1998;64(4):353-356.

275. Li L, Ahmed B, Mehta K, Kurzrock R. Liposomal curcumin with and without oxaliplatin: Effects on cell growth, apoptosis, and angiogenesis in colorectal cancer. *Mol Cancer Ther*. 2007;6(4):1276-1282.

276. Marczylo TH, Verschoyle RD, Cooke DN, Morazzoni P, Steward WP, Gescher AJ. Comparison of systemic availability of curcumin with that of curcumin formulated with phosphatidylcholine. *Cancer Chemother Pharmacol*. 2007;60(2):171-177.

277. Subramaniam D, May R, Sureban SM, et al. Diphenyl difluoroketone: A curcumin derivative with potent in vivo anticancer activity. *Cancer Res*. 2008;68(6):1962-1969.

278. Tamvakopoulos C, Dimas K, Sofianos ZD, et al. Metabolism and anticancer activity of the curcumin analogue, dimethoxycurcumin. *Clin Cancer Res*. 2007;13(4):1269-1277.

279. Khopde SM, Priyadarsini KI, Guha SN, Satav JG, Venkatesan P, Rao MN. Inhibition of radiation-induced lipid peroxidation by tetrahydrocurcumin: Possible mechanisms by pulse radiolysis. *Biosci Biotechnol Biochem*. 2000;64(3):503-509.

280. Sreejayan, Rao MN. Curcuminoids as potent inhibitors of lipid peroxidation. *J Pharm Pharmacol*. 1994;46(12):1013-1016.

281. Sandur SK, Ichikawa H, Pandey MK, et al. Role of pro-oxidants and antioxidants in the anti-inflammatory and apoptotic effects of curcumin (diferuloylmethane). *Free Radic Biol Med*. 2007;43(4):568-580.

282. Banerjee A, Kunwar A, Mishra B, Priyadarsini KI. Concentration dependent antioxidant/pro-oxidant activity of curcumin studies from AAPH induced hemolysis of RBCs. *Chem Biol Interact*. 2008;174(2):134-139.

283. Ramachandran C, Rodriguez S, Ramachandran R, et al. Expression profiles of apoptotic genes induced by curcumin in human breast cancer and mammary epithelial cell lines. *Anticancer Res*. 2005;25(5):3293-3302.

284. Elmore S. Apoptosis: A review of programmed cell death. *Toxicol Pathol*. 2007;35(4):495-516.

285. Su CC, Chen GW, Lin JG, Wu LT, Chung JG. Curcumin inhibits cell migration of human colon cancer colo 205 cells through the inhibition of nuclear factor kappa B /p65 and down-regulates cyclooxygenase-2 and matrix metalloproteinase-2 expressions. *Anticancer Res*. 2006;26(2A):1281-1288.

286. Choudhuri T, Pal S, Das T, Sa G. Curcumin selectively induces apoptosis in deregulated cyclin D1-expressed cells at G2 phase of cell cycle in a p53-dependent manner. *J Biol Chem*. 2005;280(20):20059-20068.

287. Gogada R, Amadori M, Zhang H, et al. Curcumin induces apaf-1-dependent, p21-mediated caspase activation and apoptosis. *Cell Cycle*. 2011;10(23):4128-4137.

288. Bush JA, Cheung KJ,Jr, Li G. Curcumin induces apoptosis in human melanoma cells through a fas receptor/caspase-8 pathway independent of p53. *Exp Cell Res*. 2001;271(2):305-314.

289. Wu SH, Hang LW, Yang JS, et al. Curcumin induces apoptosis in human non-small cell lung cancer NCI-H460 cells through ER stress and caspase cascade- and mitochondria-dependent pathways. *Anticancer Res*. 2010;30(6):2125-2133.

290. Camacho-Barquero L, Villegas I, Sanchez-Calvo JM, et al. Curcumin, a curcuma longa constituent, acts on MAPK p38 pathway modulating COX-2 and iNOS expression in chronic experimental colitis. *Int Immunopharmacol*. 2007;7(3):333-342.

291. Plummer SM, Holloway KA, Manson MM, et al. Inhibition of cyclo-oxygenase 2 expression in colon cells by the chemopreventive agent curcumin involves inhibition of NF-kappaB activation via the NIK/IKK signalling complex. *Oncogene*. 1999;18(44):6013-6020.

292. Bachmeier BE, Mohrenz IV, Mirisola V, et al. Curcumin downregulates the inflammatory cytokines CXCL1 and -2 in breast cancer cells via NFkappaB. *Carcinogenesis*. 2008;29(4):779-789.

293. Ukil A, Maity S, Karmakar S, Datta N, Vedasiromoni JR, Das PK. Curcumin, the major component of food flavour turmeric, reduces mucosal injury in trinitrobenzene sulphonic acid-induced colitis. *Br J Pharmacol*. 2003;139(2):209-218.

294. Xiong B, Sun TJ, Hu WD, Cheng FL, Mao M, Zhou YF. Expression of cyclooxygenase-2 in colorectal cancer and its clinical significance. *World J Gastroenterol*. 2005;11(8):1105-1108.

295. Chen W, Wei S, Liu JM, Hsiao M, Kou-Lin J, Yang WK. Tumor invasiveness and liver metastasis of colon cancer cells correlated with cyclooxygenase-2 (COX-2) expression and inhibited by a COX-2?selective inhibitor, etodolac. *International Journal of Cancer*. 2001;91(6):894-899.

296. Eberhart CE, Coffey RJ, Radhika A, Giardiello FM, Ferrenbach S, DuBois RN. Up-regulation of cyclooxygenase 2 gene expression in human colorectal adenomas and adenocarcinomas. *Gastroenterology*. 1994;107(4):1183-1188.

297. Oshima M, Dinchuk JE, Kargman SL, et al. Suppression of intestinal polyposis in apc delta716 knockout mice by inhibition of cyclooxygenase 2 (COX-2). *Cell*. 1996;87(5):803-809.

298. Young AL, Chalmers CR, Hawcroft G, et al. Regional differences in prostaglandin E2 metabolism in human colorectal cancer liver metastases. *BMC Cancer*. 2013;13:92-2407-13-92.

299. Goel A, Boland CR, Chauhan DP. Specific inhibition of cyclooxygenase-2 (COX-2) expression by dietary curcumin in HT-29 human colon cancer cells. *Cancer Lett*. 2001;172(2):111-118.

300. Crofford LJ, Tan B, McCarthy CJ, Hla T. Involvement of nuclear factor kappa B in the regulation of cyclooxygenase-2 expression by interleukin-1 in rheumatoid synoviocytes. *Arthritis Rheum*. 1997;40(2):226-236.

301. Guttridge DC, Albanese C, Reuther JY, Pestell RG, Baldwin AS,Jr. NF-kappaB controls cell growth and differentiation through transcriptional regulation of cyclin D1. *Mol Cell Biol*. 1999;19(8):5785-5799.

302. Chen C, Edelstein LC, Gelinas C. The rel/NF-kappaB family directly activates expression of the apoptosis inhibitor bcl-x(L). *Mol Cell Biol*. 2000;20(8):2687-2695.

303. Albanese C, Wu K, D'Amico M, et al. IKKalpha regulates mitogenic signaling through transcriptional induction of cyclin D1 via tcf. *Mol Biol Cell*. 2003;14(2):585-599.

304. Duyao MP, Buckler AJ, Sonenshein GE. Interaction of an NF-kappa B-like factor with a site upstream of the c-myc promoter. *Proc Natl Acad Sci U S A*. 1990;87(12):4727-4731.

305. Lin ML, Lu YC, Chung JG, et al. Down-regulation of MMP-2 through the p38 MAPK-NF-kappaB-dependent pathway by aloe-emodin leads to inhibition of nasopharyngeal carcinoma cell invasion. *Mol Carcinog*. 2010;49(9):783-797.

306. Perkins ND. The diverse and complex roles of NF-kappaB subunits in cancer. *Nat Rev Cancer*. 2012;12(2):121-132.

307. Dixit V, Mak TW. NF-κB signaling: Many roads lead to madrid. *Cell*. 2002;111(5):615-619.

308. - Shakibaei M, - Mobasheri A, - Lueders C, - Busch F, - Shayan P, - Goel A. - Curcumin enhances the effect of chemotherapy against colorectal cancer cells by inhibition of NF-κB and src protein kinase signaling pathways. - *PLoS ONE*. (- 2):- e57218.

309. Mosieniak G, Adamowicz M, Alster O, et al. Curcumin induces permanent growth arrest of human colon cancer cells: Link between senescence and autophagy. *Mech Ageing Dev*. 2012;133(6):444-455.

310. Moragoda L, Jaszewski R, Majumdar AP. Curcumin induced modulation of cell cycle and apoptosis in gastric and colon cancer cells. *Anticancer Res*. 2001;21(2A):873-878.

311. Song G, Mao YB, Cai QF, Yao LM, Ouyang GL, Bao SD. Curcumin induces human HT-29 colon adenocarcinoma cell apoptosis by activating p53 and regulating apoptosis-related protein expression. *Braz J Med Biol Res*. 2005;38(12):1791-1798.

312. Moos PJ, Edes K, Mullally JE, Fitzpatrick FA. Curcumin impairs tumor suppressor p53 function in colon cancer cells. *Carcinogenesis*. 2004;25(9):1611-1617.

313. Binion DG, Otterson MF, Rafiee P. Curcumin inhibits VEGF-mediated angiogenesis in human intestinal microvascular endothelial cells through COX-2 and MAPK inhibition. *Gut*. 2008;57(11):1509-1517.

314. Belakavadi M, Salimath BP. Mechanism of inhibition of ascites tumor growth in mice by curcumin is mediated by NF-kB and caspase activated DNase. *Mol Cell Biochem*. 2005;273(1-2):57-67.

315. Bae MK, Kim SH, Jeong JW, et al. Curcumin inhibits hypoxia-induced angiogenesis via down-regulation of HIF-1. *Oncol Rep*. 2006;15(6):1557-1562.

316. Syng-Ai C, Kumari AL, Khar A. Effect of curcumin on normal and tumor cells: Role of glutathione and bcl-2. *Mol Cancer Ther*. 2004;3(9):1101-1108.

317. Watson JL, Hill R, Lee PW, Giacomantonio CA, Hoskin DW. Curcumin induces apoptosis in HCT-116 human colon cancer cells in a p21-independent manner. *Exp Mol Pathol*. 2008;84(3):230-233.

318. Howells LM, Mitra A, Manson MM. Comparison of oxaliplatin- and curcumin-mediated antiproliferative effects in colorectal cell lines. *Int J Cancer*. 2007;121(1):175-183.

319. Chakravarti N, Kadara H, Yoon DJ, et al. Differential inhibition of protein translation machinery by curcumin in normal, immortalized, and malignant oral epithelial cells. *Cancer Prev Res (Phila)*. 2010;3(3):331-338.

320. Zhang C, Li B, Zhang X, Hazarika P, Aggarwal BB, Duvic M. Curcumin selectively induces apoptosis in cutaneous T-cell lymphoma cell lines and patients' PBMCs: Potential role for STAT-3 and NF-kappaB signaling. *J Invest Dermatol*. 2010;130(8):2110-2119.

321. Kunwar A, Barik A, Mishra B, Rathinasamy K, Pandey R, Priyadarsini KI. Quantitative cellular uptake, localization and cytotoxicity of curcumin in normal and tumor cells. *Biochim Biophys Acta*. 2008;1780(4):673-679.

322. Sullivan JP, Spinola M, Dodge M, et al. Aldehyde dehydrogenase activity selects for lung adenocarcinoma stem cells dependent on notch signaling. *Cancer Res*. 2010;70(23):9937-9948.

323. Mu X, Isaac C, Greco N, Huard J, Weiss K. Notch signaling is associated with ALDH activity and an aggressive metastatic phenotype in murine osteosarcoma cells. *Front Oncol*. 2013;3:143.

324. Wang Z, Zhang Y, Banerjee S, Li Y, Sarkar FH. Notch-1 down-regulation by curcumin is associated with the inhibition of cell growth and the induction of apoptosis in pancreatic cancer cells. *Cancer*. 2006;106(11):2503-2513.

325. Li Y, Zhang J, Ma D, et al. Curcumin inhibits proliferation and invasion of osteosarcoma cells through inactivation of notch-1 signaling. *FEBS Journal*. 2012;279(12):2247-2259.

326. - Subramaniam D, - Ponnurangam S, - Ramamoorthy P, et al. - Curcumin induces cell death in esophageal cancer cells through modulating notch signaling. - *PLoS ONE*. (- 2):- e30590.

327. Varnat F, Siegl-Cachedenier I, Malerba M, Gervaz P, Ruiz i Altaba A. Loss of WNT-TCF addiction and enhancement of HH-GLI1 signalling define the metastatic transition of human colon carcinomas. *EMBO Mol Med*. 2010;2(11):440-457.

328. Du W, Feng Y, Wang X, et al. Curcumin suppresses malignant glioma cells growth and induces apoptosis by inhibition of SHH/GLI1 signaling pathway in vitro and vivo. *CNS Neuroscience & Therapeutics*. 2013:n/a-n/a.

329. Sun XD, Liu XE, Huang DS. Curcumin reverses the epithelial-mesenchymal transition of pancreatic cancer cells by inhibiting the hedgehog signaling pathway. *Oncol Rep*. 2013;29(6):2401-2407.

330. Garcea G, Jones DJ, Singh R, et al. Detection of curcumin and its metabolites in hepatic tissue and portal blood of patients following oral administration. *Br J Cancer*. 2004;90(5):1011-1015.

331. Garcea G, Berry DP, Jones DJ, et al. Consumption of the putative chemopreventive agent curcumin by cancer patients: Assessment of curcumin levels in the colorectum and their pharmacodynamic consequences. *Cancer Epidemiol Biomarkers Prev*. 2005;14(1):120-125.

332. Irving GR, Howells LM, Sale S, et al. Prolonged biologically active colonic tissue levels of curcumin achieved after oral administration--a clinical pilot study including assessment of patient acceptability. *Cancer Prev Res (Phila)*. 2013;6(2):119-128.

333. Carroll RE, Benya RV, Turgeon DK, et al. Phase IIa clinical trial of curcumin for the prevention of colorectal neoplasia. *Cancer Prev Res (Phila)*. 2011;4(3):354-364.

334. Cruz-Correa M, Shoskes DA, Sanchez P, et al. Combination treatment with curcumin and quercetin of adenomas in familial adenomatous polyposis. *Clin Gastroenterol Hepatol*. 2006;4(8):1035-1038.

335. Kanai M, Yoshimura K, Asada M, et al. A phase I/II study of gemcitabine-based chemotherapy plus curcumin for patients with gemcitabine-resistant pancreatic cancer. *Cancer Chemother Pharmacol*. 2011;68(1):157-164.

336. Bharti AC, Aggarwal BB. Chemopreventive agents induce suppression of nuclear factor-kappaB leading to chemosensitization. *Ann N Y Acad Sci*. 2002;973:392-395.

337. Vinod BS, Antony J, Nair HH, et al. Mechanistic evaluation of the signaling events regulating curcumin-mediated chemosensitization of breast cancer cells to 5-fluorouracil. *Cell Death Dis*. 2013;4:e505.

338. Seong-Ho A, Dong-Heui K, Jung-Hoon K, Myeong-Seon L. Synergistic effects of 5-fluorouracil (FU) and curcumin on human cervical cancer cells . . 2010;40(4):229-235.

339. Yu Y, Kanwar SS, Patel BB, Nautiyal J, Sarkar FH, Majumdar AP. Elimination of colon cancer stem-like cells by the combination of curcumin and FOLFOX. *Transl Oncol*. 2009;2(4):321-328.

340. Patel BB, Gupta D, Elliott AA, Sengupta V, Yu Y, Majumdar AP. Curcumin targets FOLFOX-surviving colon cancer cells via inhibition of EGFRs and IGF-1R. *Anticancer Res*. 2010;30(2):319-325.

341. Kakarala M, Brenner DE, Korkaya H, et al. Targeting breast stem cells with the cancer preventive compounds curcumin and piperine. *Breast Cancer Res Treat*. 2010;122(3):777-785.

342. Nautiyal J, Kanwar SS, Yu Y, Majumdar AP. Combination of dasatinib and curcumin eliminates chemo-resistant colon cancer cells. *J Mol Signal*. 2011;6:7-2187-6-7.

343. Howells LM, Sale S, Sriramareddy SN, et al. Curcumin ameliorates oxaliplatin-induced chemo-resistance in HCT116 colorectal cancer cells in vitro and in vivo. *Int J Cancer*. 2010.

344. Al Moundhri MS, Al-Salam S, Al Mahrouqee A, Beegam S, Ali BH. The effect of curcumin on oxaliplatin and cisplatin neurotoxicity in rats: Some behavioral, biochemical, and histopathological studies. *J Med Toxicol*. 2013;9(1):25-33.

345. Khajavi M, Shiga K, Wiszniewski W, et al. Oral curcumin mitigates the clinical and neuropathologic phenotype of the trembler-J mouse: A potential therapy for inherited neuropathy. *Am J Hum Genet*. 2007;81(3):438-453.

346. Sato T, van Es JH, Snippert HJ, et al. Paneth cells constitute the niche for Lgr5 stem cells in intestinal crypts. *Nature*. 2011;469(7330):415-418.

347. Takimoto CH, Graham MA, Lockwood G, et al. Oxaliplatin pharmacokinetics and pharmacodynamics in adult cancer patients with impaired renal function. *Clinical Cancer Research*. 2007;13(16):4832-4839.

348. Peters GJ, Lankelma J, Kok RM, et al. Prolonged retention of high concentrations of 5-fluorouracil in human and murine tumors as compared with plasma. *Cancer Chemother Pharmacol*. 1993;31(4):269-276.

349. Burz C, Berindan-Neagoe IB, Balacescu O, et al. Clinical and pharmacokinetics study of oxaliplatin in colon cancer patients. *J Gastrointestin Liver Dis*. 2009;18(1):39-43.

350. Twiddy D, Naik S, Mistry R, et al. - A TRAIL-R1-specific ligand in combination with doxorubicin selectively targets primary breast tumour cells for apoptosis. - *Breast Cancer Research : BCR*. 2010(- Suppl 1):- P58.

351. Patel BB, Yu Y, Du J, Levi E, Phillip PA, Majumdar AP. Age-related increase in colorectal cancer stem cells in macroscopically normal mucosa of patients with adenomas: A risk factor for colon cancer. *Biochem Biophys Res Commun*. 2009;378(3):344-347.

352. Hirschhaeuser F, Menne H, Dittfeld C, West J, Mueller-Klieser W, Kunz-Schughart LA. Multicellular tumor spheroids: An underestimated tool is catching up again. *J Biotechnol*. 2010;148(1):3-15.

353. Lee J, Kotliarova S, Kotliarov Y, et al. Tumor stem cells derived from glioblastomas cultured in bFGF and EGF more closely mirror the phenotype and genotype of primary tumors than do serum-cultured cell lines. *Cancer Cell*. 2006;9(5):391-403.

354. Zhang S, Balch C, Chan MW, et al. Identification and characterization of ovarian cancer-initiating cells from primary human tumors. *Cancer Research*. 2008;68(11):4311-4320.

355. Ray S, Langan RC, Mullinax JE, et al. Establishment of human ultra-low passage colorectal cancer cell lines using spheroids from fresh surgical specimens suitable for in vitro and in vivo studies. *J Cancer*. 2012;3:196-206.

356. Van Houdt W, Emmink B, Pham T, et al. Comparative proteomics of colon cancer stem cells and differentiated tumor cells identifies BIRC6 as a potential therapeutic target. *Molecular & Cellular Proteomics*. 2011;10(12).

357. Jung P, Sato T, Merlos-Suarez A, et al. Isolation and in vitro expansion of human colonic stem cells. *Nat Med*. 2011;17(10):1225-1227.

358. Kumar SM, Liu S, Lu H, et al. Acquired cancer stem cell phenotypes through Oct4-mediated dedifferentiation. *Oncogene*. 2012;31(47):4898-4911.

359. Munz M, Baeuerle PA, Gires O. The emerging role of EpCAM in cancer and stem cell signaling. *Cancer Res*. 2009;69(14):5627-5629.

360. Chiou S, Wang M, Chou Y, et al. Coexpression of Oct4 and nanog enhances malignancy in lung adenocarcinoma by inducing cancer stem Cell–Like properties and Epithelial–Mesenchymal transdifferentiation. *Cancer Research*. 2010;70(24):10433-10444.

361. Ibrahim EE, Babaei-Jadidi R, Saadeddin A, et al. Embryonic NANOG activity defines colorectal cancer stem cells and modulates through AP1- and TCF-dependent mechanisms. *Stem Cells*. 2012;30(10):2076-2087.

362. Vermeulen L, Todaro M, de Sousa Mello F, et al. Single-cell cloning of colon cancer stem cells reveals a multi-lineage differentiation capacity. *Proc Natl Acad Sci U S A*. 2008;105(36):13427-13432.

363. Carpentino JE, Hynes MJ, Appelman HD, et al. Aldehyde dehydrogenase-expressing colon stem cells contribute to tumorigenesis in the transition from colitis to cancer. *Cancer Res*. 2009;69(20):8208-8215.

364. Ren F, Sheng WQ, Du X. CD133: A cancer stem cells marker, is used in colorectal cancers. *World J Gastroenterol*. 2013;19(17):2603-2611.

365. Dallas NA, Xia L, Fan F, et al. Chemoresistant colorectal cancer cells, the cancer stem cell phenotype, and increased sensitivity to insulin-like growth factor-I receptor inhibition. *Cancer Res*. 2009;69(5):1951-1957.

366. Yasuda H, Tanaka K, Saigusa S, et al. Elevated CD133, but not VEGF or EGFR, as a predictive marker of distant recurrence after preoperative chemoradiotherapy in rectal cancer. *Oncol Rep*. 2009;22(4):709-717.

367. Hongo K, Tanaka J, Tsuno NH, et al. CD133(-) cells, derived from a single human colon cancer cell line, are more resistant to 5-fluorouracil (FU) than CD133(+) cells, dependent on the beta1-integrin signaling. *J Surg Res*. 2012;175(2):278-288.

368. Malanchi I, Santamaria-Martinez A, Susanto E, et al. Interactions between cancer stem cells and their niche govern metastatic colonization. *Nature*. 2011;481(7379):85-89.

369. Chao C, Carmical JR, Ives KL, et al. CD133+ colon cancer cells are more interactive with the tumor microenvironment than CD133- cells. *Lab Invest*. 2012;92(3):420-436.

370. Choi D, Lee HW, Hur KY, et al. Cancer stem cell markers CD133 and CD24 correlate with invasiveness and differentiation in colorectal adenocarcinoma. *World J Gastroenterol*. 2009;15(18):2258-2264.

371. Horst D, Kriegl L, Engel J, Kirchner T, Jung A. CD133 expression is an independent prognostic marker for low survival in colorectal cancer. *Br J Cancer*. 2008;99(8):1285-1289.

372. Hamilton G. Multicellular spheroids as an in vitro tumor model. *Cancer Lett*. 1998;131(1):29-34.

373. Koshida Y, Kuranami M, Watanabe M. Interaction between stromal fibroblasts and colorectal cancer cells in the expression of vascular endothelial growth factor. *J Surg Res*. 2006;134(2):270-277.

374. Merlos-Suarez A, Barriga FM, Jung P, et al. The intestinal stem cell signature identifies colorectal cancer stem cells and predicts disease relapse. *Cell Stem Cell*. 2011;8(5):511-524.

375. Kreso A, O'Brien CA, van Galen P, et al. Variable clonal repopulation dynamics influence chemotherapy response in colorectal cancer. *Science*. 2013;339(6119):543-548.

376. Liu S, Cong Y, Wang D, et al. Breast cancer stem cells transition between epithelial and mesenchymal states reflective of their normal counterparts. *Stem Cell Reports*. 2013;2(1):78-91.

377. Gupta PB, Fillmore CM, Jiang G, et al. Stochastic state transitions give rise to phenotypic equilibrium in populations of cancer cells. *Cell*. 2011;146(4):633-644.

378. Takeda N, Jain R, LeBoeuf MR, Wang Q, Lu MM, Epstein JA. Interconversion between intestinal stem cell populations in distinct niches. *Science*. 2011;334(6061):1420-1424.

379. Abe M, Havre PA, Urasaki Y, et al. Mechanisms of confluence-dependent expression of CD26 in colon cancer cell lines. *BMC Cancer*. 2011;11:51-2407-11-51.

380. Lu J, Ye X, Fan F, et al. Endothelial cells promote the colorectal cancer stem cell phenotype through a soluble form of jagged-1. *Cancer Cell*. 2013;23(2):171-185.

381. Herreros-Villanueva M, Zhang JS, Koenig A, et al. SOX2 promotes dedifferentiation and imparts stem cell-like features to pancreatic cancer cells. *Oncogenesis*. 2013;2:e61.

382. Inamoto T, Yamochi T, Ohnuma K, et al. Anti-CD26 monoclonal antibody-mediated G1-S arrest of human renal clear cell carcinoma caki-2 is associated with retinoblastoma substrate dephosphorylation, cyclin-dependent kinase 2 reduction, p27(kip1) enhancement, and disruption of binding to the extracellular matrix. *Clin Cancer Res*. 2006;12(11 Pt 1):3470-3477.

383. Inamoto T, Yamada T, Ohnuma K, et al. Humanized anti-CD26 monoclonal antibody as a treatment for malignant mesothelioma tumors. *Clin Cancer Res*. 2007;13(14):4191-4200.

384. Morikawa K, Walker SM, Jessup JM, Fidler IJ. In vivo selection of highly metastatic cells from surgical specimens of different primary human colon carcinomas implanted into nude mice. *Cancer Research*. 1988;48(7):1943-1948.

385. Patel BB, Sengupta R, Qazi S, et al. Curcumin enhances the effects of 5-fluorouracil and oxaliplatin in mediating growth inhibition of colon cancer cells by modulating EGFR and IGF-1R. *Int J Cancer*. 2008;122(2):267-273.

386. Shakibaei M, Buhrmann C, Kraehe P, Shayan P, Lueders C, Goel A. Curcumin chemosensitizes 5-fluorouracil resistant MMR-deficient human colon cancer cells in high density cultures. *PLoS ONE*. 2014;9(1):e85397.

387. Kunnumakkara AB, Diagaradjane P, Guha S, et al. Curcumin sensitizes human colorectal cancer xenografts in nude mice to gamma-radiation by targeting nuclear factor-kappaB-regulated gene products. *Clin Cancer Res*. 2008;14(7):2128-2136.

388. Wang YJ, Pan MH, Cheng AL, et al. Stability of curcumin in buffer solutions and characterization of its degradation products. *J Pharm Biomed Anal*. 1997;15(12):1867-1876.

389. Randall KJ, Turton J, Foster JR. Explant culture of gastrointestinal tissue: A review of methods and applications. *Cell Biol Toxicol*. 2011;27(4):267-284.

390. Reid BG, Jerjian T, Patel P, et al. Live multicellular tumor spheroid models for high-content imaging and screening in cancer drug discovery. *Curr Chem Genomics Transl Med*. 2014;8(Suppl-1):27-35.

391. Friedrich J, Seidel C, Ebner R, Kunz-Schughart LA. Spheroid-based drug screen: Considerations and practical approach. *Nat Protoc*. 2009;4(3):309-324.

392. St Croix B, Kerbel RS. Cell adhesion and drug resistance in cancer. *Curr Opin Oncol*. 1997;9(6):549-556.

393. Kantara C, O'Connell M, Sarkar S, Moya S, Ullrich R, Singh P. Curcumin promotes autophagic survival of a subset of colon cancer stem cells, which are ablated by DCLK1-siRNA. *Cancer Research*. 2014.

394. Yu CC, Tsai LL, Wang ML, et al. miR145 targets the SOX9/ADAM17 axis to inhibit tumor-initiating cells and IL-6-mediated paracrine effects in head and neck cancer. *Cancer Res*. 2013;73(11):3425-3440.

395. Pohl A, El-Khoueiry A, Yang D, et al. Pharmacogenetic profiling of CD133 is associated with response rate (RR) and progression-free survival (PFS) in patients with metastatic colorectal cancer (mCRC), treated with bevacizumab-based chemotherapy. *Pharmacogenomics J*. 2013;13(2):173-180.

396. Wang Z, Oron E, Nelson B, Razis S, Ivanova N. Distinct lineage specification roles for NANOG, OCT4, and SOX2 in human embryonic stem cells. *Cell Stem Cell*. 2012;10(4):440-454.

397. Monk M, Holding C. Human embryonic genes re-expressed in cancer cells. *Oncogene*. 2001;20(56):8085-8091.

398. Tsai CC, Su PF, Huang YF, Yew TL, Hung SC. Oct4 and nanog directly regulate Dnmt1 to maintain self-renewal and undifferentiated state in mesenchymal stem cells. *Mol Cell*. 2012;47(2):169-182.

399. Schwarz BA, Bar-Nur O, Silva JC, Hochedlinger K. Nanog is dispensable for the generation of induced pluripotent stem cells. *Curr Biol*. 2014;24(3):347-350.

400. Hochedlinger K, Yamada Y, Beard C, Jaenisch R. Ectopic expression of oct-4 blocks progenitor-cell differentiation and causes dysplasia in epithelial tissues. *Cell*. 2005;121(3):465-477.

401. Kaiser S, Park YK, Franklin JL, et al. Transcriptional recapitulation and subversion of embryonic colon development by mouse colon tumor models and human colon cancer. *Genome Biol*. 2007;8(7):R131.

402. Wen K, Fu Z, Wu X, Feng J, Chen W, Qian J. Oct-4 is required for an antiapoptotic behavior of chemoresistant colorectal cancer cells enriched for cancer stem cells: Effects associated with STAT3/survivin. *Cancer Lett*. 2013;333(1):56-65.

403. Saigusa S, Tanaka K, Toiyama Y, et al. Correlation of CD133, OCT4, and SOX2 in rectal cancer and their association with distant recurrence after chemoradiotherapy. *Ann Surg Oncol*. 2009;16(12):3488-3498.

404. Hwang W, Yang M, Tsai M, et al. SNAIL regulates interleukin-8 expression, stem Cellâ€“Like activity, and tumorigenicity of human colorectal carcinoma cells. *Gastroenterology*. ;141(1):279-291.e5.

405. Lotti F, Jarrar AM, Pai RK, et al. Chemotherapy activates cancer-associated fibroblasts to maintain colorectal cancer-initiating cells by IL-17A. *The Journal of Experimental Medicine*. 2013;210(13):2851-2872.

406. Dame MK, Bhagavathula N, Mankey C, et al. Human colon tissue in organ culture: Preservation of normal and neoplastic characteristics. *In Vitro Cell Dev Biol Anim*. 2010;46(2):114-122.

407. Singh N, Nigam M, Ranjan V, et al. Resveratrol as an adjunct therapy in cyclophosphamide-treated MCF-7 cells and breast tumor explants. *Cancer Science*. 2011;102(5):1059-1067.

408. Garrett WS, Lord GM, Punit S, et al. Communicable ulcerative colitis induced by T-bet deficiency in the innate immune system. *Cell*. 2007;131(1):33-45.

409. Siegmund B, Lehr H, Fantuzzi G, Dinarello CA. IL-1β-converting enzyme (caspase-1) in intestinal inflammation. *Proceedings of the National Academy of Sciences*. 2001;98(23):13249-13254.

410. Rakoff-Nahoum S, Paglino J, Eslami-Varzaneh F, Edberg S, Medzhitov R. Recognition of commensal microflora by toll-like receptors is required for intestinal homeostasis. *Cell*. 2004;118(2):229-241.

411. Clutterbuck AL, Mobasheri A, Shakibaei M, Allaway D, Harris P. Interleukin-1??induced extracellular matrix degradation and glycosaminoglycan release is inhibited by curcumin in an explant model of cartilage inflammation. *Ann N Y Acad Sci*. 2009;1171(1):428-435.

412. - Schaefers MM, - Breshears LM, - Anderson MJ, et al. - Epithelial proinflammatory response and curcumin-mediated protection from staphylococcal toxic shock syndrome toxin-1. - *PLoS ONE*. (- 3):- e32813.

413. Jiang Z, Jin S, Yalowich JC, Brown KD, Rajasekaran B. The mismatch repair system modulates curcumin sensitivity through induction of DNA strand breaks and activation of G2-M checkpoint. *Mol Cancer Ther*. 2010;9(3):558-568.

414. Kerbel RS. Human tumor xenografts as predictive preclinical models for anticancer drug activity in humans: Better than commonly perceived-but they can be improved. *Cancer Biol Ther*. 2003;2(4 Suppl 1):S134-9.

415. Lehmann K, Rickenbacher A, Weber A, Pestalozzi BC, Clavien PA. Chemotherapy before liver resection of colorectal metastases: Friend or foe? *Ann Surg*. 2012;255(2):237-247.

416. Ryu CG, Jung EJ, Kim G, Kim SR, Hwang DY. Oxaliplatin-induced pulmonary fibrosis: Two case reports. *J Korean Soc Coloproctol*. 2011;27(5):266-269.

417. Rubbia-Brandt L, Audard V, Sartoretti P, et al. Severe hepatic sinusoidal obstruction associated with oxaliplatin-based chemotherapy in patients with metastatic colorectal cancer. *Annals of Oncology*. 2004;15(3):460-466.

418. Abou-Zeid N. Ameliorative effect of vitamin C against 5-fuorouracil-induced hepatotoxicity in mice: A light and electron microscope study. *The Journal of Basic & Applied Zoology*. (0).

419. Kawazoe H, Kawazoe H, Sugishita H, et al. Nephrotoxicity induced by repeated cycles of oxaliplatin in a japanese colorectal cancer patient with moderate renal impairment. *Gan To Kagaku Ryoho*. 2010;37(6):1153-1157.

420. MHRA. Http://Www.mhra.gov.uk/safetyinformation/generalsafetyinformationandadvice/adviceandinformationforconsumers/MymedicineFromlaboratorytopharmacyshelf/pre-clinicalresearch/.

421. Julien S, Merino-Trigo A, Lacroix L, et al. Characterization of a large panel of patient-derived tumor xenografts representing the clinical heterogeneity of human colorectal cancer. *Clin Cancer Res*. 2012;18(19):5314-5328.

422. http://www.phytosomes.info/public/meriva.asp. .

423. Cuomo,John, Appendino,Giovanni, Dern A,S., et al. .

424. Belcaro G, Cesarone MR, Dugall M, et al. Product-evaluation registry of meriva(R), a curcumin-phosphatidylcholine complex, for the complementary management of osteoarthritis. *Panminerva Med*. 2010;52(2 Suppl 1):55-62.

425. Saif MW, Reardon J. Management of oxaliplatin-induced peripheral neuropathy. *Ther Clin Risk Manag*. 2005;1(4):249-258.

426. Zhu X, Li Q, Chang R, et al. Curcumin alleviates neuropathic pain by inhibiting p300/CBP histone acetyltransferase activity-regulated expression of BDNF and cox-2 in a rat model. *PLoS ONE*. 2014;9(3):e91303.

427. Hubert C, Fervaille C, Sempoux C, et al. Prevalence and clinical relevance of pathological hepatic changes occurring after neoadjuvant chemotherapy for colorectal liver metastases. *Surgery*. 2010;147(2):185-194.

428. Joybari AY, Sarbaz S, Azadeh P, et al. Oxaliplatin-induced renal tubular vacuolization. *Ann Pharmacother*. 2014;48(6):796-800.

429. Raymond E, Buquet-Fagot C, Djelloul S, et al. Antitumor activity of oxaliplatin in combination with 5-fluorouracil and the thymidylate synthase inhibitor AG337 in human colon, breast and ovarian cancers. *Anticancer Drugs*. 1997;8(9):876-885.

430. Inaba M, Tashiro T, Kkobayashi T, et al. Responsiveness of human gastric tumors implanted in nude mice to clinically equivalent doses of various antitumor agents. *Cancer Science*. 1988;79(4):517-522.

431. Tashiro T, Inaba M, Kobayashi T, et al. Responsiveness of human lung cancer/nude mouse to antitumor agents in a model using clinically equivalent doses. *Cancer Chemother Pharmacol*. 1989;24(3):187-192.

432. Farmer P, Bonnefoi H, Anderle P, et al. A stroma-related gene signature predicts resistance to neoadjuvant chemotherapy in breast cancer. *Nat Med*. 2009;15(1):68-74.

433. Reagan-Shaw S, Nihal M, Ahmad N. Dose translation from animal to human studies revisited. *The FASEB Journal*. 2008;22(3):659-661.

434. Sato T, Stange DE, Ferrante M, et al. Long-term expansion of epithelial organoids from human colon, adenoma, adenocarcinoma, and barrett's epithelium. *Gastroenterology*. 2011;141(5):1762-1772.

435. De Simone V, Franze E, Ronchetti G, et al. Th17-type cytokines, IL-6 and TNF-alpha synergistically activate STAT3 and NF-kB to promote colorectal cancer cell growth. *Oncogene*. 2014.

436. Di Caro G, Marchesi F, Laghi L, Grizzi F. Immune cells: Plastic players along colorectal cancer progression. *J Cell Mol Med*. 2013;17(9):1088-1095.

437. Hendrayani SF, Al-Khalaf HH, Aboussekhra A. Curcumin triggers p16-dependent senescence in active breast cancer-associated fibroblasts and suppresses their paracrine procarcinogenic Effects1,2. *Neoplasia*. 2013;15(6):631-640.

438. Zhang HG, Kim H, Liu C, et al. Curcumin reverses breast tumor exosomes mediated immune suppression of NK cell tumor cytotoxicity. *Biochim Biophys Acta*. 2007;1773(7):1116-1123.

439. Deacon CF. Dipeptidyl peptidase-4 inhibitors in the treatment of type 2 diabetes: A comparative review. *Diabetes, Obesity and Metabolism*. 2011;13(1):7-18.

440. Fichtner I, Slisow W, Gill J, et al. Anticancer drug response and expression of molecular markers in early-passage xenotransplanted colon carcinomas. *Eur J Cancer*. 2004;40(2):298-307.

441. Cong L, Ran FA, Cox D, et al. Multiplex genome engineering using CRISPR/cas systems. *Science*. 2013;339(6121):819-823.

Appendix

	Group	First week of study	First palpable tumour (any group) observed	1 week on Meriva®/epikuron diet		2 weeks later		2 weeks later		2 weeks later		2 weeks later		2 weeks later		End of study
Chemotherapy round			*Diet starts*	*Round 1 of chemotherapy*		*Round 2 of chemotherapy*		*Round 3 of chemotherapy*		*Round 4 of chemotherapy*		*Round 5 of chemotherapy*		*Round 6 (last round) of chemotherapy*		*End of study*
Treatment group	Group 1 (Control)	Inject 100,000 cells subcutaneously into flank	Epikuron diet starts	Saline/5% glucose injections begin instead of chemotherapeutics		Saline/5% glucose injections		Saline/5% glucose injections		Saline/5% glucose injections		Saline/5% glucose injections		Saline/5% glucose injections		Mice will be left until they are culled due to tumour volume, or a difference in survival between groups is observed. During this period mice will receive no more IP injections but the Meriva®/epikuron diet will continue. When mice are culled any tumours and appropriate organs will be harvested. If no differences between groups is seen after 4 weeks then all remaining mice will be culled.
	Group 2 (Meriva® diet)	Inject 100,000 cells subcutaneously into flank	Meriva® diet starts	Saline/5% glucose injections begin instead of chemotherapeutics		Saline/5% glucose injections		Saline/5% glucose injections		Saline/5% glucose injections		Saline/5% glucose injections		Saline/5% glucose injections		
	Group 3 (OX+5-FU)	Inject 100,000 cells subcutaneously into flank	Epikuron diet starts	First Chemotherapeutic injections begin		Second round of chemotherapeutics		Third round of chemotherapeutics.		Fourth round of chemotherapeutics.		Fifth round of chemotherapeutics.		Sixth round of chemotherapeutics.		
	Group 4 (OX+5-FU+Meriva® diet	Inject 100,000 cells subcutaneously into flank	Meriva® diet starts	First chemotherapeutic injections begin		Second round of chemotherapeutics		Third round of chemotherapeutics.		Fourth round of chemotherapeutics.		Fifth round of chemotherapeutics.		Sixth round of chemotherapeutics.		
IP schedule			Palpable tumour observed, on the following Monday diet starts	Monday-5% glucose mock/Oxaliplatin IP injection	Tuesday-Saline mock/5-FU IP injection	Monday-5% glucose mock/Oxaliplatin IP injection	Tuesday-Saline mock/5-FU IP injection	Monday-5% glucose mock/Oxaliplatin IP injection	Tuesday-Saline mock/5-FU IP injection	Monday-5% glucose mock/Oxaliplatin IP injection	Tuesday-Saline mock/5-FU IP injection	Monday-5% glucose mock/Oxaliplatin IP injection	Tuesday-Saline mock/5-FU IP injection	Monday-5% glucose mock/Oxaliplatin IP injection	Tuesday-Saline mock/5-FU IP injection	

Table 8.1 Outline of NOD-SCID pilot study

A comprehensive overview of the mouse pilot study presented in chapter 5. Five were used per group, but one had to culled in the Meriva group for non-study related reasons and so was excluded from the study. The study ended on week 8 when the last mouse was culled.

Sample	Passage	Findings
P153	-	Moderately differentiated adenocarcinoma with cribriform pattern, odd mucin droplet and fibroblastic reaction in liver
	MP1	Similar tumour but associated with necrosis with zone of cellular fibroblastic reaction
	MP1	Similar tumour but associated with necrosis
P117	-	Moderately differentiated adenocarcinoma with cribriform pattern but abundant extracellular mucin, some fibrosis
	MP2	Similar with little extracellular mucin
	MP3	Similar with little extracellular mucin, some fibroblastic response
P114	-	Moderately well differentiated adenocarcinoma with moderate amounts of mucin and goblet cells, mild fibroblastic reaction
	MP1	Pattern like metastasis above - moderately well differentiated with mucin and goblet cells
	MP2	Pattern like metastasis above - moderately well differentiated with mucin and even more goblet cells
	MP2	Similar to above - moderately well differentiated with mucin and goblet cells
	MP3	Similar to above - moderately well differentiated with mucin and goblet cells
P107	-	Moderately differentiated adenocarcinoma with cribriform pattern with fibrosis and fibroblastic reaction in liver
	MP1	Moderately differentiated adenocarcinoma with cribriform pattern with small zone of fibroblastic reaction
	MP2	Similar with necrosis and cell debris
P104	-	Moderately differentiated adenocarcinoma with cribriform pattern with abundant fibrosis
	MP1	Moderately differentiated adenocarcinoma with cribriform pattern with necrosis and small zone of fibroblastic reaction
	MP2	Moderately differentiated adenocarcinoma with cribriform pattern with necrosis and small zone of fibroblastic reaction
	MP3	Moderately differentiated adenocarcinoma with cribriform pattern with necrosis and small zone of fibroblastic reaction
	MP4	Moderately differentiated adenocarcinoma with cribriform pattern with necrosis and small zone of fibroblastic reaction
P103	-	Scanty cribriform adenocarcinoma only
	-	Moderately differentiated adenocarcinoma with cribriform pattern with abundant fibrosis and fibroblastic reaction
	MP1	Similar with small zone of fibroblastic reaction
	MP2	Very cellular but similar with small zone of fibroblastic reaction
	MP2	Similar with small zone of fibroblastic reaction
	MP3	Very cellular but similar with small zone of fibroblastic reaction
	MP3	Very cellular but similar with small zone of fibroblastic reaction
P095	-	Moderately differentiated adenocarcinoma with glandular pattern with necrosis and abundant interstitial fibrosis
	MP1	Similar with necrosis and small amount of interstitial fibroblastic reaction
P093	-	Moderately differentiated adenocarcinoma with cribriform pattern with abundant interstitial fibrosis
	MP1	Similar with moderate fibroblastic reaction
	MP2	Similar with small zone of fibroblastic reaction
	MP2	Similar with small zone of fibroblastic reaction
	MP3	Similar with necrosis only
	MP3	Small fragment of similar tumour with necrosis only
	MP3	Small fragment of similar tumour with necrosis only
P088	-	Moderately differentiated adenocarcinoma with glandular pattern and abundant interstitial fibrosis
	MP1	Moderately differentiated adenocarcinoma with glandular pattern and small zones of fibroblastic reaction
	MP3	Moderately differentiated adenocarcinoma with glandular pattern and small zones of fibroblastic reaction
	MP4	Moderately differentiated adenocarcinoma with glandular pattern and small zones of fibroblastic reaction
	MP4	Moderately differentiated adenocarcinoma with glandular pattern and small zones of fibroblastic reaction
	MP5	Moderately differentiated adenocarcinoma with glandular pattern and small zones of fibroblastic reaction

P084	-	Moderately differentiated adenocarcinoma with glandular pattern and abundant interstitial fibrosis and fibroblastic proliferation
	MP1	Florid glandular pattern with minimal fibroblastic reaction
	MP2	Florid glandular pattern with minimal fibroblastic reaction

Table 8.2 The histological assessment of serially passaged CRLM in NOD-SCID mice

The full data, corresponding to the data presented and discussed in chapter 3.7. Patient CRLM tissue was serially passaged in NOD-SCID mice though implantation of small tissue pieces subcutaneously. From each passage some tissue was used for histological assessment by a trained pathologist. P=patient numbers, and MP=mouse passage with the number indicating which mouse passage the tissue was taken from. Histological assessment was undertaken by a trained pathologist.

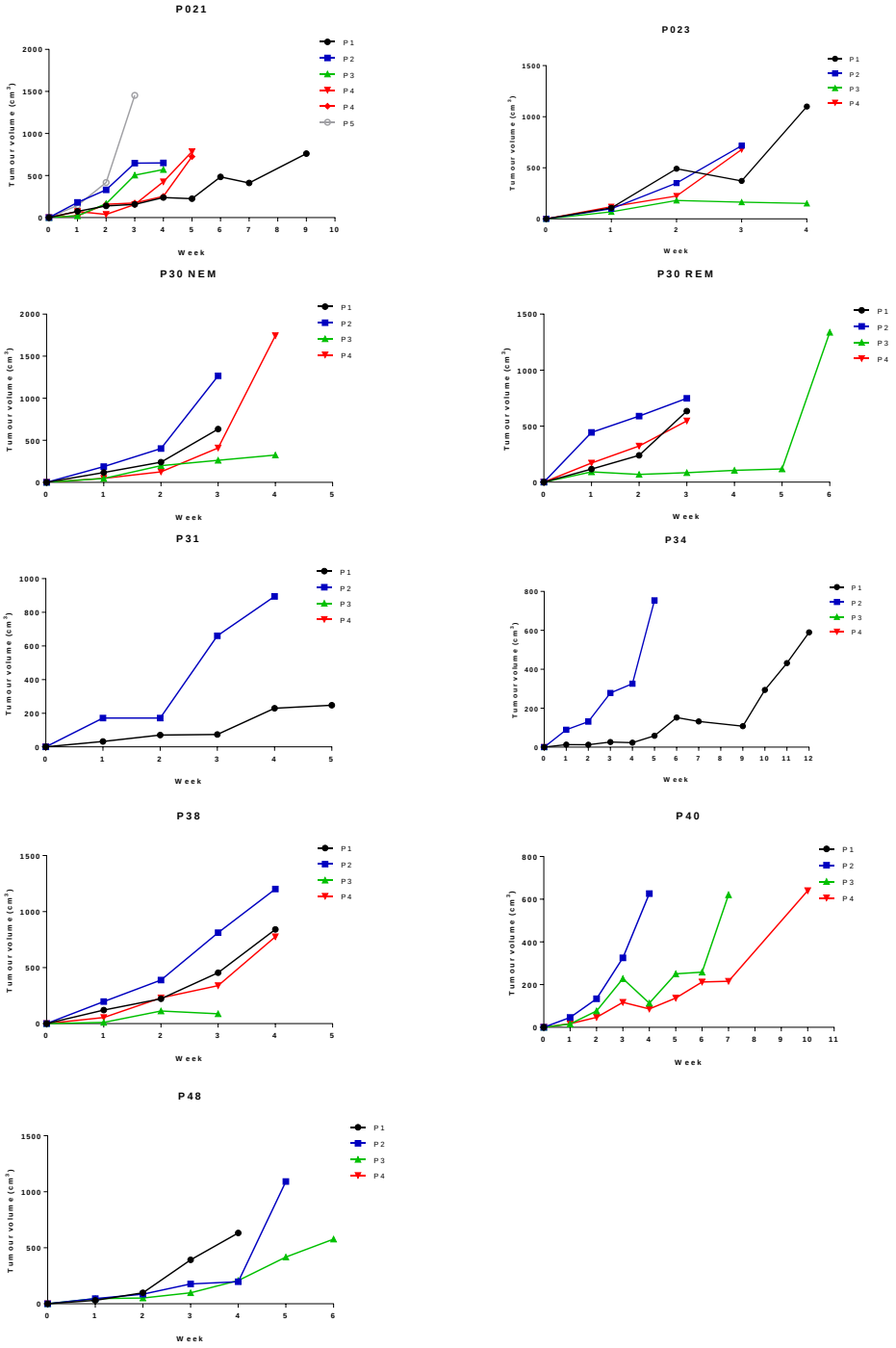

Figure 8.1 Individual NOD-SCID xenograft growth rates over serial passages

Measurements were taken once a week starting from the moment the tumours became palpable. One sample was carried out in two mice, P30.

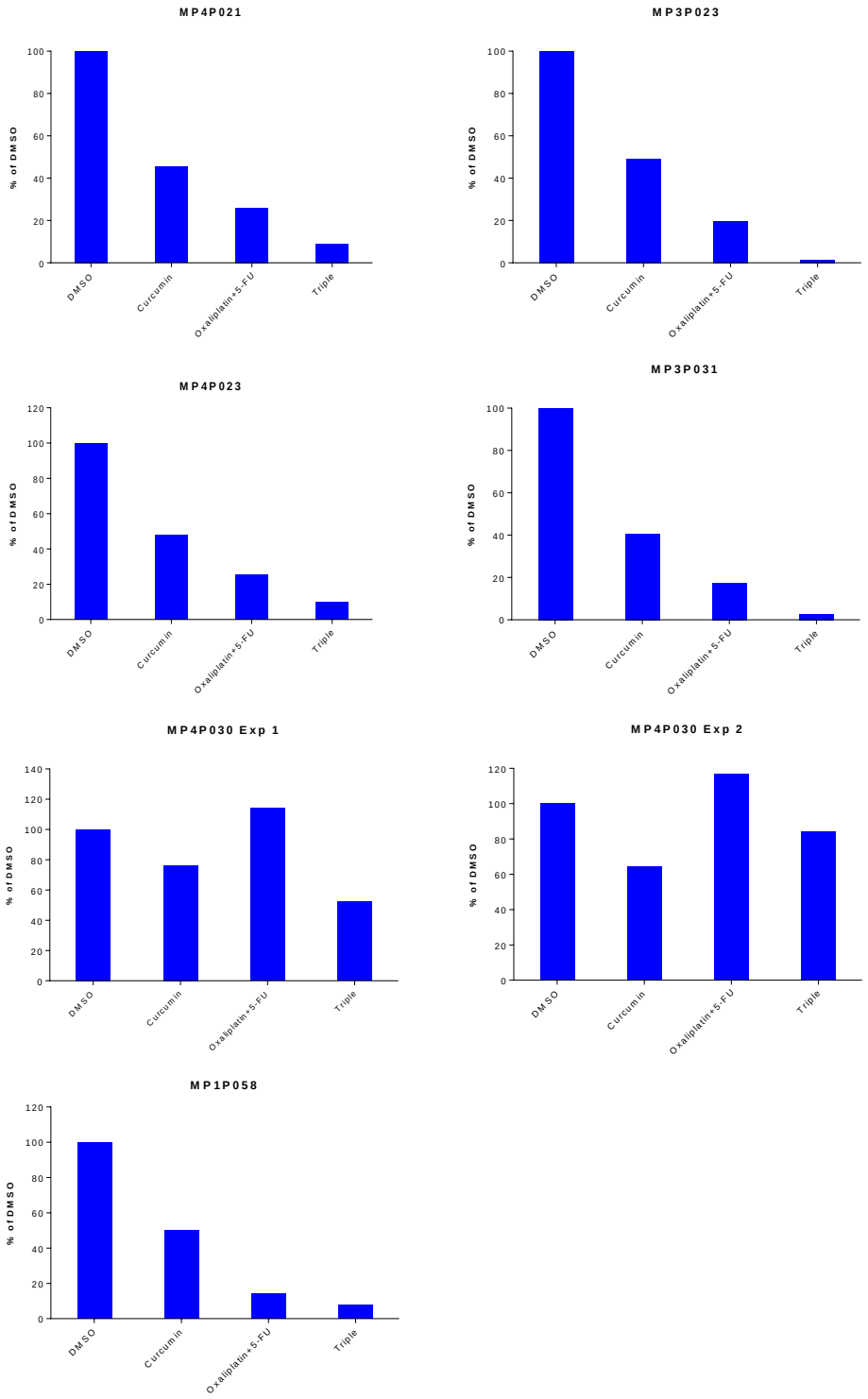

Figure 8.2 The number of spheroids produced after treatment with curcumin, oxaliplatin and 5-FU using xenograft derived CRLM tissue, displayed as individual samples

Freshly xenografts were processed and the cells used for spheroid growth, treated, and the number of spheroids counted after two weeks counted using a light microscopy. Each graph represents a different experiment using fresh xenograft material. The results are represented as a percentage of the DMSO.

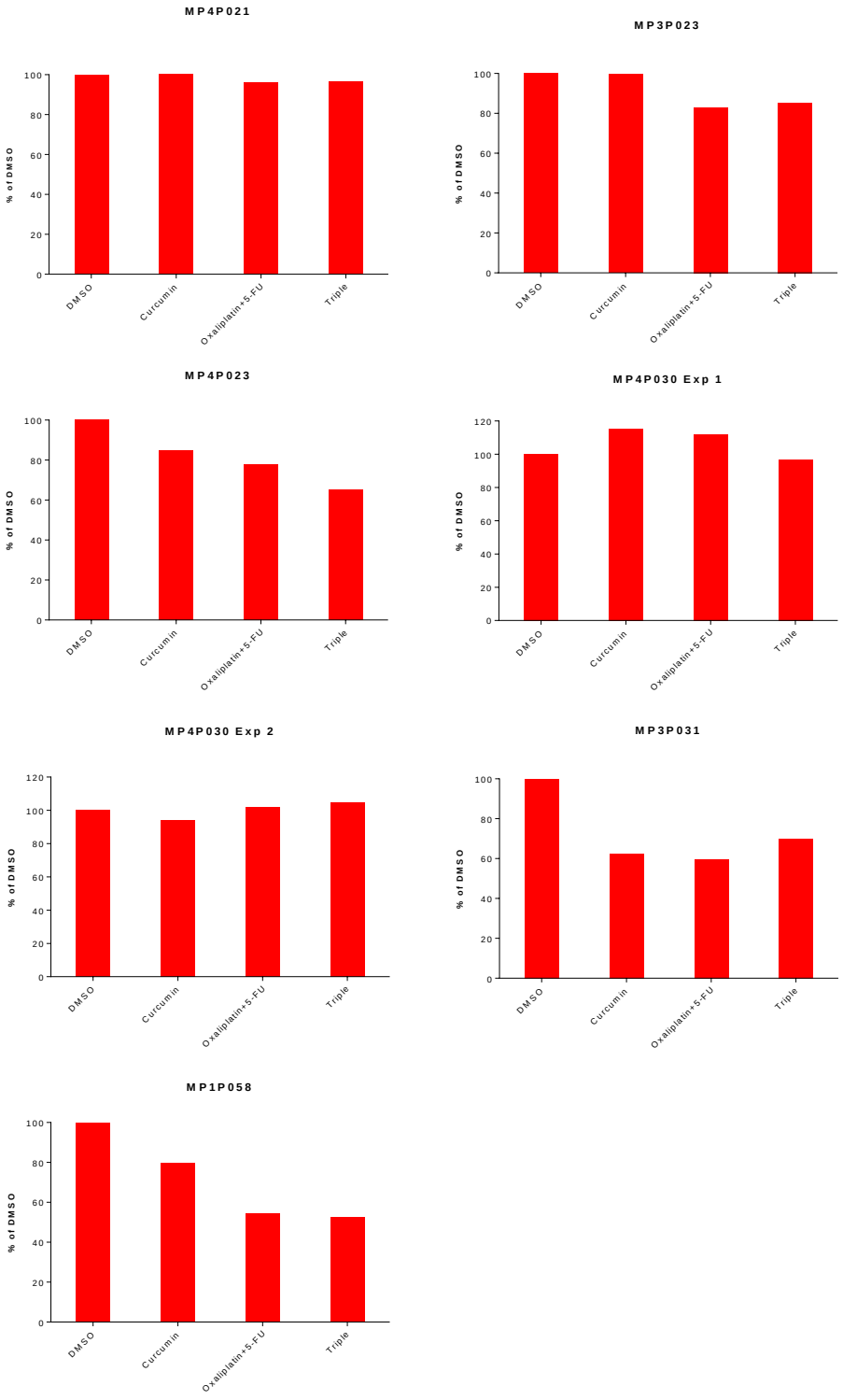

Figure 8.3 The size of spheroids after treatment with curcumin, oxaliplatin and 5-FU using xenograft derived CRLM tissue, displayed as individual samples.
During the same experiments as figure 7.2 the spheroids were measured. Each graph corresponds to the same patient spheroids treated in figure 7.2. Two measurements were taken/spheroid and averaged. Measurements were assessed using the ?? software attached to a microscope.

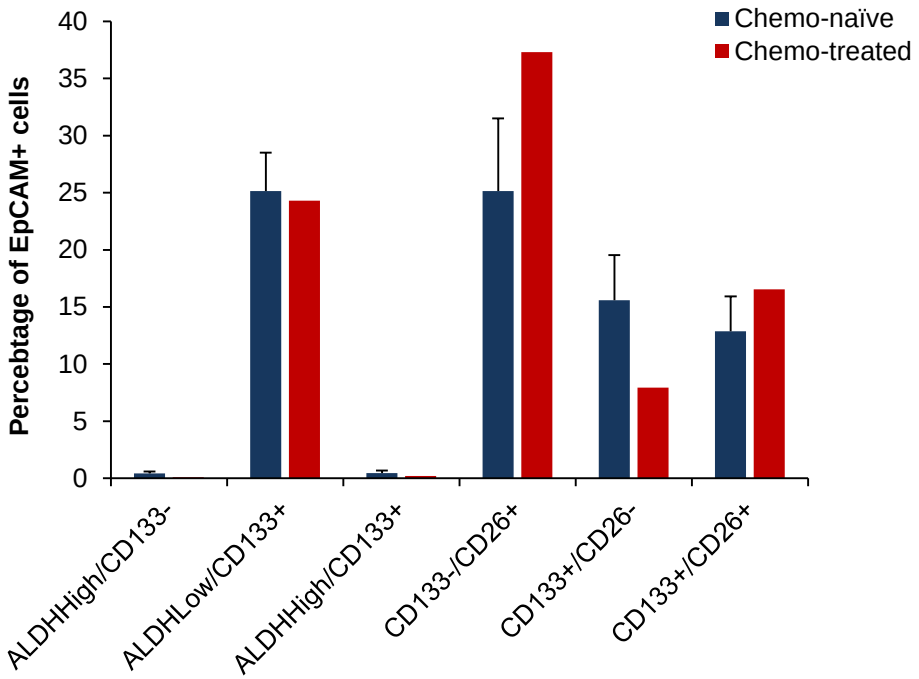

Figure 8.4 Expression of TIC markers between chemo-naïve and treated patients
A comparison between the expression of TIC markers between chemo-naïve (N=11) and chemo-treated patients (N=2) that were confirmed to have received therapy specifically for their metastasis. Error bars represent SEM.

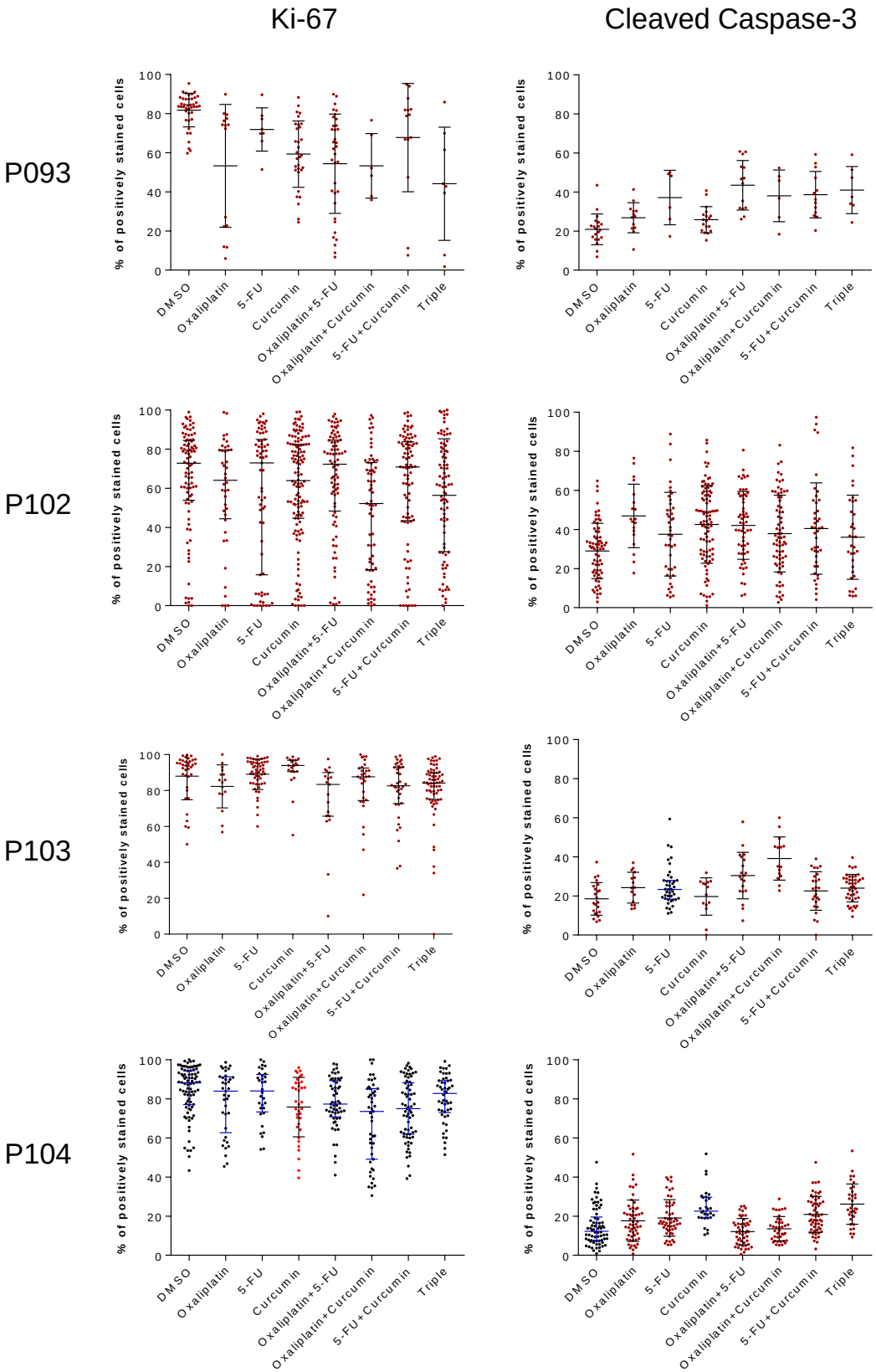

Figure 8.5 Individual results for explant ki67 and cleaved caspase-3, continued on the next page

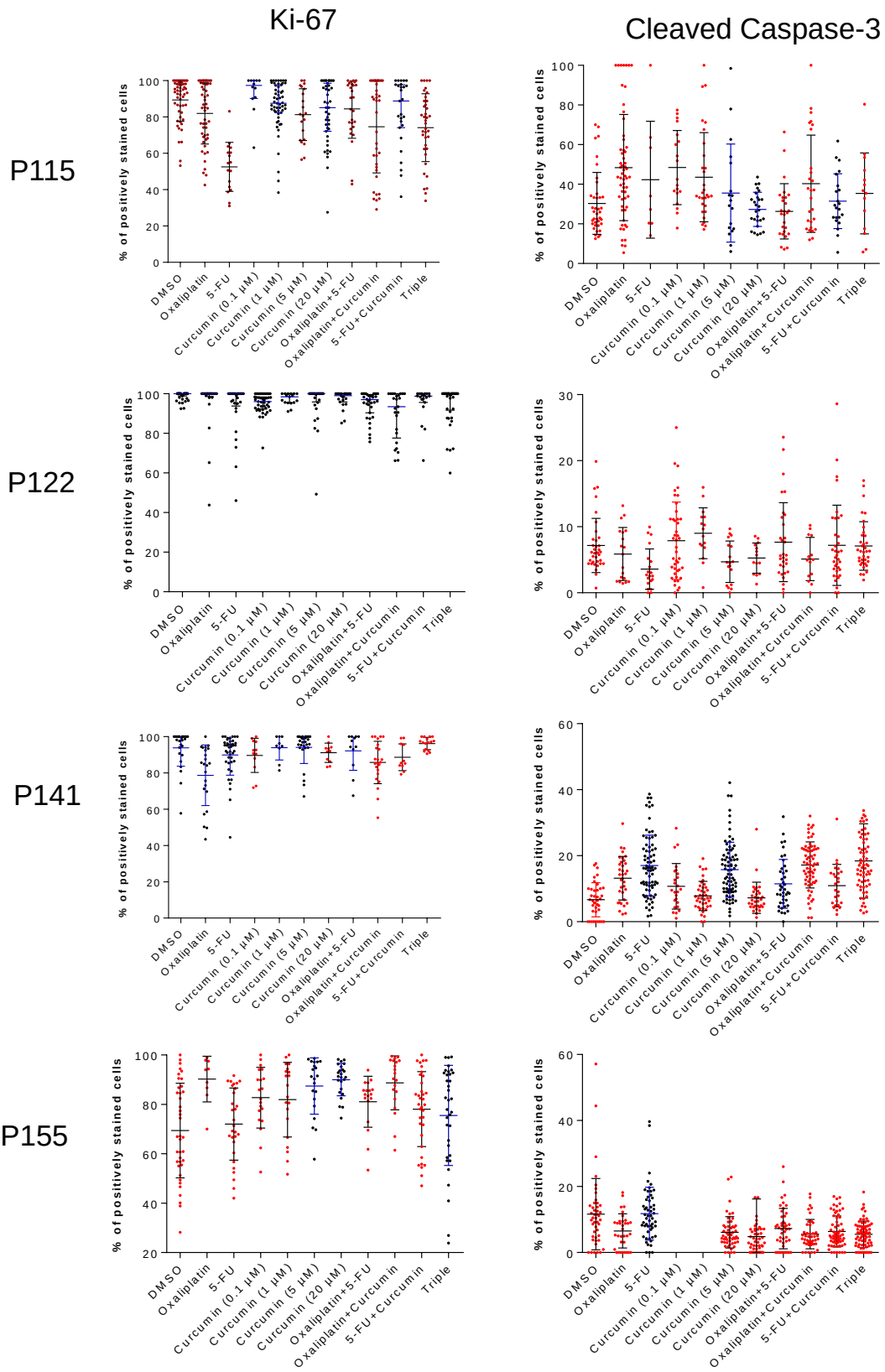

Figure 8.5 Individual results for explant ki67 and cleaved caspase-3, continued on the next page

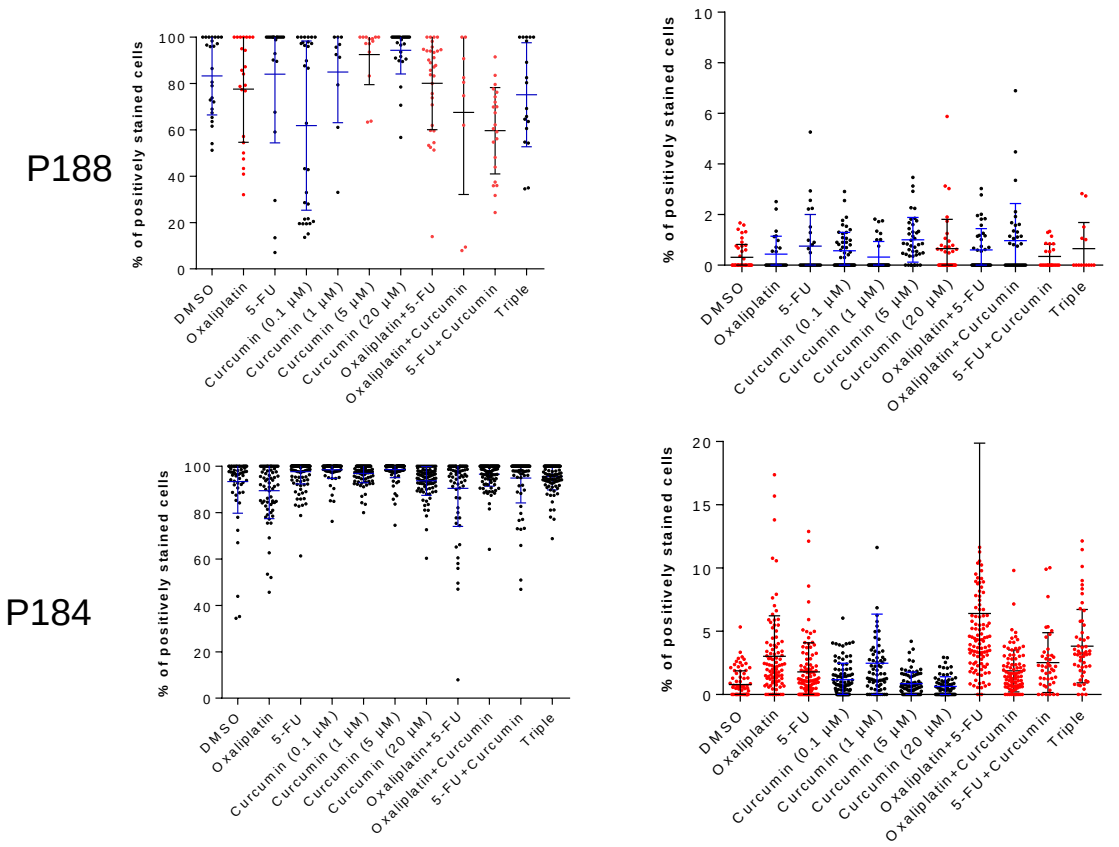

Figure 8.5 Individual results for explant ki67 and cleaved caspase-3

Explants were generated from fresh CRLM tissue and treated for 24 hours, and used for immunohistochemical assessment for ki67 and Cleaved-caspase 3 staining. Each dot represents the percentage of cells positive for that marker on a picture, with up to ten pictures taken/pieces of tissue and up to 9 pieces of tissue were treated/group. The counting was done blind by two people.

Explant culture: Statistical results

The following tables contain the corresponding statistical results for the data presented in Figure 7.5. Following advice from a biostatistician data was first tested for normality and then either a parametric (normally distributed data) or non-parametric (non-normally distributed data) paired sample t-test was applied. When comparing abnormal and normal data both parametric and non-parametric testes were applied and both results indicated in the table, and significant results are highlighted yellow.

P093 ki67

	Untreated	Oxaliplatin	5-FU	Curcumin	Oxaliplatin + 5-FU	Curcumin + Oxaliplatin	Curcumin + 5-FU	Triple
Untreated	-	0.001	0.006	0.000	0.000	0.003	0.041	0.003
Oxaliplatin	-	-	0.331	0.701	0.345	0.912	0.314	0.459
5-FU	-	-	-	0.036	0.743	0.043	0.862	0.016
Curcumin	-	-	-	-	0.536	0.896	0.053	0.531
Oxaliplatin + 5-FU	-	-	-	-	-	0.096	0.850	0.056
Oxaliplatin + Curcumin	-	-	-	-	-	-	0.472	0.484
Curcumin + 5-FU	-	-	-	-	-	-	-	0.182

P093 Cleaved caspase-3

	Untreated	Oxaliplatin	5-FU	Curcumin	Oxaliplatin + 5-FU	Curcumin + Oxaliplatin	Curcumin + 5-FU	Triple
Untreated	-	0.051	0.019	0.017	0.000	0.02	0.001	0.001
Oxaliplatin	-	-	0.072	0.865	0.002	0.077	0.003	0.024
5-FU	-	-	-	0.266	0.657	0.899	0.438	0.286
Curcumin	-	-	-	-	0.002	0.082	0.018	0.003
Oxaliplatin + 5-FU	-	-	-	-	-	0.577	0.154	0.135
Oxaliplatin + Curcumin	-	-	-	-	-	-	0.377	0.172
Curcumin + 5-FU	-	-	-	-	-	-	-	0.161

P102 ki67

	Untreated	Oxaliplatin	5-FU	Curcumin	Oxaliplatin + 5-FU	Curcumin + Oxaliplatin	Curcumin + 5-FU	Triple
Untreated	-	0.361	0.272	0.279	0.602	0.004	0.431	0.066 and 0.069
Oxaliplatin	-	-	0.402	0.420	0.347	0.288	0.872	0.957 and 0.816
5-FU	-	-	-	0.916	0.166	0.189	0.992	0.817 and 0.640
Curcumin	-	-	-	-	0.146	0.025	0.522	0.809 and 0.721
Oxaliplatin + 5-FU	-	-	-	-	-	0.001	0.568	0.078 and 0.09
Oxaliplatin + Curcumin	-	-	-	-	-	-	0.02	0.036 and 0.024
Curcumin + 5-FU	-	-	-	-	-	-	-	0.246 and 0.324

P102 Cleaved caspase-3

	Untreated	Oxaliplatin	5-FU	Curcumin	Oxaliplatin + 5-FU	Curcumin + Oxaliplatin	Curcumin + 5-FU	Triple
Untreated	-	0.000	0.008	0.000	0.000	0.001	0.005	0.064
Oxaliplatin	-	-	0.043	0.047	0.960	0.409	0.191	0.408
5-FU	-	-	-	0.225	0.147	0.937	0.368	0.485
Curcumin	-	-	-	-	0.932	0.132	0.669	0.385
Oxaliplatin + 5-FU	-	-	-	-	-	0.311	0.606	0.128
Oxaliplatin + Curcumin	-	-	-	-	-	-	0.497	0.424
Curcumin + 5-FU	-	-	-	-	-	-	-	0.730

P103 ki67

	Untreated	Oxaliplatin	5-FU	Curcumin	Oxaliplatin + 5-FU	Curcumin + Oxaliplatin	Curcumin + 5-FU	Triple
Untreated	-	0.782	0.999	0.242 and 0.086	0.072 and 0.064	0.104 and 0.072	0.008 and 0.008	0.022 and 0.027
Oxaliplatin	-	-	0.064	0.154 and 0.088	0.156 and 0.215	0.540 and 0.756	0.181 and 0.163	3.4 and 0.352
5-FU	-	-	-	0.284 and 0.067	0.025 and 0.024	0.315 and 0.329	0.013 and 0.018	0.000 and 0.000
Curcumin	-	-	-	-	0.002	0.003	0.002	0.007
Oxaliplatin + 5-FU	-	-	-	-	-	0.376	0.601	0.968
Oxaliplatin + Curcumin	-	-	-	-	-	-	0.111	0.141
Curcumin + 5-FU	-	-	-	-	-	-	-	0.313

P103 Cleaved caspase-3

	Untreated	Oxaliplatin	5-FU	Curcumin	Oxaliplatin + 5-FU	Curcumin + Oxaliplatin	Curcumin + 5-FU	Triple
Untreated	-	0.021	0.012 and 0.014	0.949	0.001	0.000	0.113	0.051
Oxaliplatin	-	-	0.340 and 0.352	0.157	0.235	0.002	0.791	0.897
5-FU	-	-	-	0.098 and 0.245	0.505 and 0.391	0.006 and 0.009	0.058 and 0.091	0.726 and 0.933
Curcumin	-	-	-	-	0.045	0.000	0.532	0.356
Oxaliplatin + 5-FU	-	-	-	-	-	0.012	0.043	0.024
Oxaliplatin + Curcumin	-	-	-	-	-	-	0.000	0.000
Curcumin + 5-FU	-	-		-	-	-	-	0.488

P104 ki67

	Untreated	Oxaliplatin	5-FU	Curcumin	Oxaliplatin + 5-FU	Curcumin + Oxaliplatin	Curcumin + 5-FU	Triple
Untreated	-	0.122	0.822	0.038 and 0.039	0.001	0.000	0.000	0.033
Oxaliplatin	-	-	0.525	0.509 and 0.522	0.689	0.033	0.213	0.551
5-FU	-	-	-	0.042 and 0.024	0.575	0.008	0.054	0.695
Curcumin	-	-	-	-	0.162 and 0.076	0.198 and 0.133	0.604 and 0.696	0.215 and 0.125
Oxaliplatin + 5-FU	-	-	-	-	-	0.005	0.264	0.515
Oxaliplatin + Curcumin	-	-	-	-	-	-	0.097	0.007
Curcumin + 5-FU	-	-		-	-	-	-	0.104

P104 Cleaved caspase-3

	Untreated	Oxaliplatin	5-FU	Curcumin	Oxaliplatin + 5-FU	Curcumin + Oxaliplatin	Curcumin + 5-FU	Triple
Untreated	-	.0.264 and 0.293	0.094 and 0.084	0.004 and 0.007	0.007 and 0.012	0.098 and 0.089	0.001 and 0.001	0.003 and 0.005
Oxaliplatin	-	-	0.575	0.022	0.002	0.143	0.097	0.000
5-FU	-	-	-	0.001	0.000	0.01	0.166	0.000
Curcumin	-	-	-	-	0.000 and 0.000	0.000 and 0.000	0.389 and 0.214	0.764 and 0.496
Oxaliplatin + 5-FU	-	-	-	-	-	0.810	0.000	0.000
Oxaliplatin + Curcumin	-	-	-	-	-	-	0.000	0.000
Curcumin + 5-FU	-	-		-	-	-	-	0.095

P115 ki67

	Untreated	Oxaliplatin	5-FU	Curcumin 0.1 µM	Curcumin 1 µM	Curcumin 5 µM	Curcumin 20 µM	Oxaliplatin + 5-FU	Curcumin + Oxaliplatin	Curcumin + 5-FU	Triple
Untreated	-	**0.014**	**0.000**	**0.87 (0.657)**	**0.333 (0.409)**	**0.002**	**0.011 (0.023)**	**0.177**	**0.004**	**0.098 (0.086)**	**0.000**
Oxaliplatin	-	-	**0.574**	**0.06 (0.110)**	**0.110 (0.112)**	**0.574**	**0.972 (0.812)**	**0.617**	**0.04**	**0.943 (0.882)**	**0.018**
5-FU	-	-	-	**0.000 (0.002)**	**0.000 (0.000)**	**0.000**	**0.000 (0.000)**	**0.000**	**0.035**	**0.000 (0.001)**	**0.000**
Curcumin 0.1 µM	-	-	-	-	**0.028**	**0.019 (0.023)**	**0.063**	**0.150 (0.182)**	**0.001 (0.006)**	**0.203**	**0.007 (0.008)**
Curcumin 1 µM	-	-	-	-	-	**0.514 (0.566)**	**0.247**	**0.975 (0.970)**	**0.013 (0.056)**	**0.848**	**0.001 (0.001)**
Curcumin 5 µM	-	-	-	-	-	-	**0.970 (0.852)**	**0.835**	**0.048**	**0.919 (0.903)**	**0.303**
Curcumin 20 µM	-	-	-	-	-	-	-	**0.526 (0.395)**	**0.134 (0.163)**	**0.904**	**0.085 (0.084)**
Oxaliplatin + 5-FU	-	-	-	-	-	-	-	-	**0.05**	**0.667 (0.737)**	**0.075**
Oxaliplatin + Curcumin	-	-	-	-	-	-	-	-	-	**0.130 (0.174)**	**0.920**
Curcumin + 5-FU	-	-	-	-	-	-	-	-	-	-	**0.157 (0.258)**

P115 Cleaved caspase-3

	Untreated	Oxaliplatin	5-FU	Curcumin 5 µM	Curcumin 20 µM	Oxaliplatin + 5-FU	Curcumin + Oxaliplatin	Curcumin + 5-FU	Triple
Untreated	-	0.019	0.998 (0.715)	0.053	0.455	0.219	0.003	0.195	0.214
Oxaliplatin	-	-	0.046 (0.013)	0.682	0.654	0.211	0.396	0.212	0.812
5-FU	-	-	-	0.053 (0.048)	0.000 (0.000)	0.189 (0.198)	0.011 (0.006)	0.001 (0.002)	0.005 (0.005)
Curcumin 5 µM	-	-	-	-	0.696	0.291	0.073	0.942	0.746
Curcumin 20 µM	-	-	-	-	-	0.782	0.400	0.845	0.628
Oxaliplatin + 5-FU	-	-	-	-	-	-	0.309	0.848	0.450
Oxaliplatin + Curcumin	-	-	-	-	-	-	-	0.016	0.001
Curcumin + 5-FU	-	-	-	-	-	-	-	-	0.514

P122 ki67

	Untreated	Oxaliplatin	5-FU	Curcumin 0.1 µM	Curcumin 1 µM	Curcumin 5 µM	Curcumin 20 µM	Oxaliplatin + 5-FU	Curcumin + Oxaliplatin	Curcumin + 5-FU	Triple
Untreated	-	**0.778**	**0.063**	**0.000**	**0.397**	**0.248**	**0.212**	**0.002**	**0.002**	**0.554**	**0.065**
Oxaliplatin	-	-	**0.307**	**0.108**	**0.347**	**0.638**	**0.256**	**0.053**	**0.014**	**0.140**	**0.861**
5-FU	-	-	-	**0.501**	**0.272**	**0.469**	**0.906**	**0.820**	**0.192**	**0.3**	**0.445**
Curcumin 0.1 µM	-	-	-	-	**0.281**	**0.285**	**0.031**	**0.926**	**0.11**	**0.868**	**0.908**
Curcumin 1 µM	-	-	-	-	-	**0.347**	**0.345**	**0.332**	**0.012**	**0.594**	**0.510**
Curcumin 5 µM	-	-	-	-	-	-	**1**	**0.153**	**0.044**	**0.191**	**0.339**
Curcumin 20 µM	-	-	-	-	-	-	-	**0.073**	**0.003**	**0.356**	**0.820**
Oxaliplatin + 5-FU	-	-	-	-	-	-	-	-	**0.171**	**0.601**	**0.782**
Oxaliplatin + Curcumin	-	-	-	-	-	-	-	-	-	**0.016**	**0.092**
Curcumin + 5-FU	-	-	-	-	-	-	-	-	-	-	**0.211**

P122 caspase 3

	Untreated	Oxaliplatin	5-FU	Curcumin 0.1 µM	Curcumin 1 µM	Curcumin 5 µM	Curcumin 20 µM	Oxaliplatin + 5-FU	Curcumin + Oxaliplatin	Curcumin + 5-FU	Triple
Untreated	-	**0.306**	**0.007**	**0.433**	**0.416**	**0.052**	**0.115**	**0.786**	**0.106**	**0.894**	**0.856**
Oxaliplatin	-	-	**0.119**	**0.278**	**0.025**	**0.302**	**0.434**	**0.329**	**0.448**	**0.02**	**0.319**
5-FU	-	-	-	**0.003**	**0.000**	**0.346**	**0.256**	**0.041**	**0.014**	**0.001**	**0.000**
Curcumin 0.1 µM	-	-	-	-	**0.950**	**0.028**	**0.03**	**0.519**	**0.11**	**0.519**	**0.323**
Curcumin 1 µM	-	-	-	-	-	**0.013**	**0.003**	**0.498**	**0.01**	**0.501**	**0.141**
Curcumin 5 µM	-	-	-	-	-	-	**0.704**	**0.143**	**0.619**	**0.002**	**0.008**
Curcumin 20 µM	-	-	-	-	-	-	-	**0.174**	**0.871**	**0.015**	**0.062**
Oxaliplatin + 5-FU	-	-	-	-	-	-	-	-	**0.187**	**0.954**	**0.762**
Oxaliplatin + Curcumin	-	-	-	-	-	-	-	-	-	**0.006**	**0.082**
Curcumin + 5-FU	-	-	-	-	-	-	-	-	-	-	**0.917**

P141 ki67

	Untreated	Oxaliplatin	5-FU	Curcumin 0.1 µM	Curcumin 1 µM	Curcumin 5 µM	Curcumin 20 µM	Oxaliplatin + 5-FU	Curcumin + Oxaliplatin	Curcumin + 5-FU	Triple
Untreated	-	0.001 (0.00)	0.064 (0.034)	0.155 (0.158)	0.923 (0.753)	0.948 (0.715)	0.241 (0.286)	0.456 (0.374)	0.014 (0.017)	0.046 (0.033)	0.423 (0.826)
Oxaliplatin	-	-	0.033 (0.012)	0.131 (0.158)	0.144 (0.086)	0.002 (0.012)	0.042 (0.033)	0.003 (0.002)	0.068 (0.072)	0.26 (0.657)	0.006 (0.001)
5-FU	-	-	-	0.617 (0.937)	0.346 (0.515)	0.036 (0.006)	0.334 (0.445)	0.325 (0.424)	0.346 (0.2)	0.601 (0.79)	0.048 (0.049)
Curcumin 0.1 µM	-	-	-	-	0.207	0.829 (0.875)	0.561	0.563 (0.657)	0.263	0.883	0.083
Curcumin 1 µM	-	-	-	-	-	0.334 (0.237)	0.442	0.789 (0.953)	0.102	0.15	0.502
Curcumin 5 µM	-	-	-	-	-	-	0.55 (0.859)	0.425 (0.583)	0.02 (0.021)	0.912 (0.929)	0.094 (0.158)
Curcumin 20 µM	-	-	-	-	-	-	-	0.893 (0.646)	0.15	0.47	0.048
Oxaliplatin + 5-FU	-	-	-	-	-	-	-	-	0.113 (0.117)	0.492 (0.374)	0.334 (0.695)
Oxaliplatin + Curcumin	-	-	-	-	-	-	-	-	-	0.65	0.003
Curcumin + 5-FU	-	-	-	-	-	-	-	-	-	-	0.004

P141 Cleaved caspase-3

	Untreated	Oxaliplatin	5-FU	Curcumin 0.1 µM	Curcumin 1 µM	Curcumin 5 µM	Curcumin 20 µM	Oxaliplatin + 5-FU	Curcumin + Oxaliplatin	Curcumin + 5-FU	Triple
Untreated	-	0.000	0.000	0.036	0.346	0.000 (0.000)	0.740 (0.513)	0.000	0.000	0.031 (0.043)	0.000
Oxaliplatin	-	-	0.028	0.063	0.000	0.137 (0.140)	0.000 (0.000)	0.059	0.001	0.053 (0.055)	0.070
5-FU	-	-	-	0.009	0.000	0.464 (0.344)	0.000 (0.000)	0.003	0.953	0.013 (0.023)	0.519
Curcumin 0.1 µM	-	-	-	-	0.099	0.028 (0.025)	0.027 (0.021)	0.813	0.001	0.821 (0.989)	0.001
Curcumin 1 µM	-	-	-	-	-	0.000 (0.000)	0.953 (0.908)	0.004	0.000	0.036 (0.049)	0.000
Curcumin 5 µM	-	-	-	-	-	-	0.000 (0.000)	0.008 (0.013)	0.594 (0.270)	0.006 (0.012)	0.157 (0.192)
Curcumin 20 µM	-	-	-	-	-	-	-	0.011 (0.018)	0.000 (0.000)	0.075 (0.038)	0.000 (0.000)
Oxaliplatin + 5-FU	-	-	-	-	-	-	-	-	0.000	0.749 (0.770)	0.007
Oxaliplatin + Curcumin	-	-	-	-	-	-	-	-	-	0.000 (0.001)	0.451
Curcumin + 5-FU	-	-	-	-	-	-	-	-	-	-	0.006 (0.002)

P155 ki67

	Untreated	Oxaliplatin	5-FU	Curcumin 0.1 µM	Curcumin 1 µM	Curcumin 5 µM	Curcumin 20 µM	Oxaliplatin + 5-FU	Curcumin + Oxaliplatin	Curcumin + 5-FU	Triple
Untreated	-	0.001	0.171	0.00	0.00	0.000 (0.00)	0.000 (0.000)	0.000	0.000	0.002	0.044 (0.062)
Oxaliplatin	-	-	0.000	0.034	0.038	0.608 (0.0678)	0.955 (0.678)	0.124	0.943	0.132	0.171 (0.139)
5-FU	-	-	-	0.007	0.026	0.001 (0.002)	0.000 (0.000)	0.022	0.000	0.028	0.364 (0.157)
Curcumin 0.1 µM	-	-	-	-	0.769	0.324 (0.269)	0.082 (0.126)	0.619	0.104	0.287	0.288 (0.575)
Curcumin 1 µM	-	-	-	-	-	0.269 (0.351)	0.09 (0.145)	0.847	0.095	0.427	0.523 (0.852)
Curcumin 5 µM	-	-	-	-	-	-	0.418 (0.455)	0.198 (0.133)	0.603 (0.709)	0.062 (0.03)	0.101 (0.122)
Curcumin 20 µM	-	-	-	-	-	-	-	0.037 (0.043)	0.847 (0.940)	0.01 (0.016)	0.004 (0.016)
Oxaliplatin + 5-FU	-	-	-	-	-	-	-	-	0.037	0.375	0.557 (0.777)
Oxaliplatin + Curcumin	-	-	-	-	-	-	-	-	-	0.007	0.037 (0.028)
Curcumin + 5-FU	-	-	-	-	-	-	-	-	-	-	0.557 (0.67)

P155 Cleaved caspase-3

	Untreated	Oxaliplatin	5-FU	Curcumin 5 µM	Curcumin 20 µM	Oxaliplatin + 5-FU	Curcumin + Oxaliplatin	Curcumin + 5-FU	Triple
Untreated	-	0.006	0.942 (0.557)	0.047	0.000	0.02	0.011	0.007	0.295
Oxaliplatin	-	-	0.007 (0.002)	0.295	0.654	0.3	0.688	0.648	0.087
5-FU	-	-	-	0.003 (0.003)	0.000 (0.000)	0.051 (0.07)	0.001 (0.001)	0.000 (0.000)	0.000 (0.000)
Curcumin 5 µM	-	-	-	-	0.696	0.057	0.864	0.726	0.561
Curcumin 20 µM	-	-	-	-	-	0.782	0.4	0.845	0.628
Oxaliplatin + 5-FU	-	-	-	-	-	-	0.410	0.676	0.370
Oxaliplatin + Curcumin	-	-	-	-	-	-	-	0.271	0.399
Curcumin + 5-FU	-	-	-	-	-	-	-	-	0.343

P184 ki67

	Untreated	Oxaliplatin	5-FU	Curcumin 0.1 µM	Curcumin 1 µM	Curcumin 5 µM	Curcumin 20 µM	Oxaliplatin + 5-FU	Curcumin + Oxaliplatin	Curcumin + 5-FU	Triple
Untreated	-	.411	.023	.003	.984	.004	.145	.197	.353	.334	.986
Oxaliplatin	-	-	.000	.000	.000	.000	.004	.431	.000	.003	.001
5-FU	-	-	-	.074	.062	.014	.000	0.000	0.412	0.056	0.027
Curcumin 0.1 µM	-	-	-	-	0.001	0.780	0.000	0.000	0.001	0.009	0.000
Curcumin 1 µM	-	-	-	-	-	0.000	0.000	0.031	0.872	0.325	267
Curcumin 5 µM	-	-	-	-	-	-	0.000	0.002	0.000	0.009	0.000
Curcumin 20 µM	-	-	-	-	-	-	-	0.448	0.007	0.019	0.015
Oxaliplatin + 5-FU	-	-	-	-	-	-	-	-	0.079	0.02	0.171
Oxaliplatin + Curcumin	-	-	-	-	-	-	-	-	-	0.926	0.022
Curcumin + 5-FU	-	-	-	-	-	-	-	-	-	-	0.878

P184 Caspase 3

	Untreated	Oxaliplatin	5-FU	Curc 0.1 µM	Curc 1 µM	Curc 5 µM	Curc 20 µM	Oxaliplatin + 5-FU	Curc + Oxaliplatin	Curc + 5-FU	Triple
Untreated	-	0.000	0.002	0.528	0.012	0.873	0.795	0.000	0.000	0.052	0.000
Oxaliplatin	-	-	0.000	0.000	0.516	0.000	0.000	0.008	0.381	0.167	0.273
5-FU	-	-	-	0.826	0.125	0.003	0.004	0.000	0.074	0.569	0.001
Curcumin 0.1 µM	-	-	-	-	0.014	0.005	0.000	0.002	0.000	0.220	0.001
Curcumin 1 µM	-	-	-	-	-	0.003	0.001	0.099	0.977	0.376	0.364
Curcumin 5 µM	-	-	-	-	-	-	0.426	0.000	0.000	0.005	0.000
Curcumin 20 µM	-	-	-	-	-	-	-	0.000	0.000	0.001	0.657
Oxaliplatin + 5-FU	-	-	-	-	-	-	-	-	0.001	0.001	0.407
Oxaliplatin + Curcumin	-	-	-	-	-	-	-	-	-	0.027	0.038
Curcumin + 5-FU	-	-	-	-	-	-	-	-	-	-	0.01.

P188 Ki67 stats

	Untreated	Oxaliplatin	5-FU	Curc 0.1 µM	Curc 1 µM	Curc 5 µM	Curc 20 µM	Oxaliplatin + 5-FU	Curc + Oxaliplatin	Curc + 5-FU	Triple
Untreated	-	0.302 0.570	0.22 0.036	0.009 0.031	0.531 0.374	0.306 0.79	0.033 0.058	0.366 0.279	0.144 0.263	0.003 0.009	0.076 0.088
Oxaliplatin	-	-	0.000 0.002	0 032 0.033	0.031 0.025	0.022 0.023	0.023 0.039	0.578 0.711	0.779 0.674	0.02 0.033	0.884 0.868
5-FU	-	-	-	0.02 0.03	0.438 0.6	0.988 0.753	0.298 0.05	0.708 0.463	0.149 0.116	0.000 0.001	0.434 0.345
Curcumin 0.1 µM	-	-	-	-	0.006 0.021	0.003 0.011	0.000 0.002	0.024 0.072	0.431 0.767	0.859 0.833	0.004 0.007
Curcumin 1 µM	-	-	-	-	-	0.191 0.123	0.104 0.086	0.095 0.086	0.240 0.176	0.007 0.015	0.883 0.612
Curcumin 5 µM	-	-	-	-	-	-	0.312 0.327	0.011 0.016	0.118 0.161	0.000 0.003	0.021 0.05
Curcumin 20 µM	-	-	-	-	-	-	-	0.007 0.016	0.096 0.128	0.000 0.000	0.003 0.008
Oxaliplatin + 5-FU	-	-	-	-	-	-	-	-	0.441	0.006 0.014	0.739 0.82
Oxaliplatin + Curcumin	-	-	-	-	-	-	-	-	-	0.444 0.441	0.263 0.263
Curcumin + 5-FU	-	-	-	-	-	-	-	-	-	-	0.052 0.063

P188 Caspase

	Untreated	Oxaliplatin	5-FU	Curc 0.1 µM	Curc 1 µM	Curc 5 µM	Curc 20 µM	Oxaliplatin + 5-FU	Curc + Oxaliplatin	Curc + 5-FU	Triple
Untreated	-	0.068 0.061	0.011 0.013	0.049 0.053	0.588 0.65	0.001 0.01	0.121 0.241	0.172 0.253	0.012 0.011	0.154 0.209	0.341 0.515
Oxaliplatin	-	-	0.124	0.396	0.733	0.006	0.17	0.494	0.150 0.136	0.950 0.875	0.310
5-FU	-	-	-	0.723	0.246	0.067	0.654	0.987	0.605 0.776	0.086 0.113	0.575
Curcumin 0.1 µM	-	-	-	-	0.074	0.031	0.871	0.804	0.286 0.500	0.128 0.163	0.859
Curcumin 1 µM	-	-	-	-	-	0.017	0.378	0.136	0.022 0.013	0.498 0.534	0.484
Curcumin 5 µM	-	-	-	-	-	-	0.098	0.172	0.901 0.966	0.014 0.021	0.209
Curcumin 20 µM	-	-	-	-	-	-	-	0.753	0.399 0.498	0.094 0.109	0.657
Oxaliplatin + 5-FU	-	-	-	-	-	-	-	-	0.526 0.527	0.084 0.3	0.678
Oxaliplatin + Curcumin	-	-	-	-	-	-	-	-	-	0.084 0.110	0.228 0.236
Curcumin + 5-FU	-	-	-	-	-	-	-	-	-	-	0.990 0.779

Treatment	P093	P102	P103	P104	P115	P122	P141	P155	P184	P188
DMSO	-	+++	-	++	+	++	+++	+	+++	-
Oxaliplatin	+	+		+	+	+	++	-	+++	+
5-FU	-	+	-	+	-	+	+++	+	+++	++
OX+5-FU	-	+++	-	+	-	++	+++	+	+++	+
Curcumin 0.1 µM					+	+	+++	-	+++	++
Curcumin 1 µM					+	+	+++	+	+++	+
Curcumin 5 µM	-	++	-	+	+	+	+++	-	+++	+
Curcumin 20 µM					+	+	+++	-	+++	+
Curcumin+oxaliplatin	-	++	-	+	+	-	+++	-	+++	+
Curcumin+5-FU	+	+	-	++	+	++	+++	+	+++	++
Triple	-	++	+	+	-	+	+++	+	+++	+

Table 8.3 The effect on ALDH1A1 expression when using 24-hour explant cultures to assess different treatment combinations
Staining intensity was assessed by a qualified pathologist. +++=most intense, ++=intermediate, +=low and a minus symbol indicates the sample was negative. No symbol indicates that the tissue was missing, or had no intact epithelial cells to score.

Treatment	P102	P103	P104	P122	P115	P184	P188	P141	P155
DMSO	++	++	+	-	-	+	+	++	+
Oxaliplatin	+	+	+	-	-	+	+	+	-
5-FU	+	++	+	+/-	-	++	++	++	++
OX+5-FU	++	++	-	-	+	+	+	+	-
Curcumin 0.1 µM						++	-	+	-
Curcumin 1 µM				-		+	+	++	-
Curcumin 5 µM	+	+	+	+	-	+	+	++	-
Curcumin 20 µM				+		+	+	-	-
Curcumin+oxaliplatin	+	+	-	-	-	+	-	+	+
Curcumin+5-FU	-	+		+	-	+	+	+	-
Triple		++	-	-		+	-	++	+

Table 8.4 The effect on CD133 expression when using 24-hour explant cultures to assess different treatment combinations
Staining intensity was assessed by a qualified pathologist. +++=most intense, ++=intermediate, +=low and a minus symbol indicates the sample was negative. No symbol indicates that the tissue was missing, or had no intact epithelial cells to score.

	P093	P102	P103	P104	P115	P122	P141	P155	P184	P188
DMSO	++	++	++	++	+	++	+++	+	++	+
Oxaliplatin	++	+++	++	++	+	++	+++	+	++	+
5-FU	++	+++	++	++	+	++	+++	+	++	+
Oxaliplatin+5-FU	++	+++	++	++	+	++	+++	+	+	+
Curcumin 0.1 µM					++	++	+++	+	Missing	++
Curcumin 1 µM					++	+++	+++	+	+	++
Curcumin 5 µM	++	+++		++	++	++	+++	+	+	++
Curcumin 20 µM					++	++	+++	+	+	+
Curcumin+oxaliplatin		+++	++	++	+	++	+++	+	+	+
Curcumin+5-FU	++	+++	++	++	+	++	+++	+	+	+
Triple	++	+++	++	++	+	+	+++	+	+	+

Table 8.5 The effect on CD26 expression when using 24-hour explant cultures to assess different treatment combinations
Staining intensity was assessed by a qualified pathologist. +++=most intense, ++=intermediate, +=low and a minus symbol indicates the sample was negative. No symbol indicates that the tissue was missing, or had no intact epithelial cells to score.

	P093	P102	P103	P104	P115	P122	P141	P155	P184	P188
DMSO	+	+++	+	++	+	+	++	+	+	++
Oxaliplatin	+	++	+	+	+	+	++	+	+	++
5-FU		+++	+	+		+	++	+	+	++
Oxaliplatin+5-FU	+	++	+	+	++	++	++	+	+	++
Curcumin 0.1 µM					+	+	+++	+	++	++
Curcumin 1 µM					+	+	+++	+	++	++
Curcumin 5 µM		++		+	+	+	++	+	+	++
Curcumin 20 µM					+	+	++	+	++	++
Curcumin+oxaliplatin		+++	++	+	+	+	++	+	++	++
Curcumin+5-FU	+	++	+	+	+	+	++	+	++	++
Triple		+++	+	+		+	+++	+	++	++

Table 8.6 The effect on nanog expression when using 24-hour explant cultures to assess different treatment combinations
Staining intensity was assessed by a qualified pathologist. +++=most intense, ++=intermediate, +=low and a minus symbol indicates the sample was negative. No symbol indicates that the tissue was missing, or had no intact epithelial cells to score.

Group	Number	Carcinoma	Comment
MLH1	833/1//11	> 90% stained nuclei, mostly moderate ++	About 30% smooth muscle and endothelial nuclei densely stained
	1024/11	> 90% stained nuclei, mostly moderate ++	Tumour only
	1089/1/11	> 90% stained nuclei, mostly marked +++	Reactive stroma shows positive nuclear staining
	1090/1/11	> 90% stained nuclei, mostly marked +++	About 30% smooth muscle and endothelial nuclei densely stained
	343/1/12	> 90% stained nuclei, moderately dense ++	Reactive stroma, liver negative
	728/12	> 90% stained nuclei, mostly marked +++	Reactive stroma negative
	1273/12	> 90% stained nuclei, mostly moderate ++	About 30% smooth muscle nuclei densely stained
	1419/12	> 90% stained nuclei, mostly marked +++	About 30% smooth muscle and endothelial nuclei densely stained
	521/13	> 90% stained nuclei, mostly marked +++	About 30% smooth muscle and stromal nuclei densely stained
	570/13	Variable staining some marked some weak ++ overall	About 30% smooth muscle and stromal nuclei densely stained
MSH2	833/1//11	> 90% stained nuclei, mostly marked +++	About 30% smooth muscle and endothelial nuclei densely stained
	1024/11	> 90% stained nuclei, mostly marked +++	Tumour only
	1089/1/11	> 90% stained nuclei, mostly marked +++	Reactive stroma shows positive nuclear staining
	1090/1/11	> 90% stained nuclei, mostly marked +++	About 30% smooth muscle and endothelial nuclei densely stained
	343/1/12	> 90% stained nuclei, a few marked, most moderate ++	Reactive stroma slightly positive
	728/12	> 90% stained nuclei, mostly marked +++	Reactive stroma negative
	1273/12	> 90% stained nuclei, mostly marked +++	About 30% smooth muscle nuclei and reactive stroma densely stained
	1419/12	> 90% stained nuclei, mostly marked +++	About 30% smooth muscle and endothelial nuclei densely stained
	521/13	> 90% stained nuclei, mostly marked +++	About 30% smooth muscle and stromal nuclei densely stained
	570/13	> 90% stained nuclei, mostly moderate ++	About 30% smooth muscle and stromal nuclei densely stained
MSH6	833/1//11	> 90% stained nuclei, mostly marked +++; some light cytoplasmic staining	> 90% smooth muscle, endothelium, stroma positive nuclei.
	1024/11	> 90% stained nuclei, mostly marked +++; some light cytoplasmic staining	> 90% smooth muscle, endothelium, stroma positive nuclei.
	1089/1/11	> 90% stained nuclei, mostly marked +++; some light cytoplasmic staining	> 90% smooth muscle, endothelium, stroma positive nuclei. Liver nuclei variably stained, light cytoplasmic staining of liver cells
	1090/1/11	> 90% stained nuclei, marked +++; some light cytoplasmic staining	> 90% smooth muscle, endothelium, stroma positive nuclei.
	343/1/12	> 90% stained nuclei, *but only 20% dense*; overall ++ some light cytoplasmic staining	50% stroma positive nuclei. Liver nuclei variably stained, light cytoplasmic staining of liver cells
	728/12	> 90% stained nuclei, mostly marked +++; some light cytoplasmic staining	> 90% stroma positive nuclei.
	1273/12	> 90% stained nuclei, mostly marked +++; some light cytoplasmic staining	> 90% smooth muscle, endothelium, stroma positive nuclei. Liver nuclei variably stained, light cytoplasmic staining of liver cells
	1419/12	> 90% stained nuclei, mostly marked +++; some light cytoplasmic staining	> 90% stroma positive nuclei.
	521/13	> 90% stained nuclei, *but only 20% dense*; overall ++ some light cytoplasmic staining	> 90% stroma positive nuclei.
	570/13	> 90% stained nuclei, variable some marked but overall ++; some light cytoplasmic staining	> 90% stroma positive nuclei.
ERCC1	833/1//11	> 90% stained nuclei, but only 20% dense; overall ++; some weak cytoplasmic stain	> 50% smooth muscle, endothelium, stroma positive nuclei.
	1024/11	> 90% stained nuclei, but weakly;	> 50% smooth muscle, endothelium, stroma positive

		overall ++; some weak cytoplasmic stain	nuclei.
	1089/1/11	Small fragment only, > 90% stained nuclei, mostly marked +++; some light cytoplasmic staining	> 50% smooth muscle, endothelium, stroma positive nuclei.
	1090/1/11	Small fragment only, > 90% stained nuclei, mostly marked +++; some light cytoplasmic staining	> 50% smooth muscle, endothelium, stroma positive nuclei.
	343/1/12	< 10% cell nuclei stained densely; overall + some weak cytoplasmic staining	> 50% smooth muscle, endothelium, stroma positive nuclei.
	728/12	> 90% stained nuclei, but weakly +; some weak cytoplasmic stain	> 50% smooth muscle, endothelium, stroma positive nuclei.
	1273/12	> 90% stained nuclei, but weakly +; some weak cytoplasmic stain	> 50% smooth muscle, endothelium, stroma positive nuclei.
	1419/12	> 90% stained nuclei, but moderately ++; some weak cytoplasmic stain	> 50% smooth muscle, endothelium, stroma positive nuclei.
	521/13	> 90% stained nuclei, but moderately ++; some weak cytoplasmic stain	> 50% smooth muscle, endothelium, stroma positive nuclei
	570/13	> 90% stained nuclei, but moderately ++; some weak cytoplasmic stain	> 50% smooth muscle, endothelium, stroma positive nuclei
XRCC1	833/1//11	> 90% marked stained nuclei +++,	> 90% smooth muscle/stroma and endothelial nuclei densely stained.
	1024/11	> 90% moderately ++ stained nuclei,	> 90% smooth muscle/stroma and endothelial nuclei densely stained.
	1089/1/11	> 90% marked +++ stained nuclei,	> 90% smooth muscle/stroma and endothelial nuclei densely stained. Liver nuclei strongly stained
	1090/1/11	> 90% marked +++ stained nuclei,	> 90% smooth muscle/stroma and endothelial nuclei densely stained.
	343/1/12	> 90% moderately ++ stained nuclei,	> 90% smooth muscle/stroma and endothelial nuclei densely stained.
	728/12	> 90% marked +++ stained nuclei,	> 90% smooth muscle/stroma and endothelial nuclei densely stained.
	1273/12	> 90% marked +++ stained nuclei,	> 90% smooth muscle/stroma and endothelial nuclei densely stained. Liver nuclei moderately stained
	1419/12	> 90% marked +++ stained nuclei,	> 90% smooth muscle/stroma and endothelial nuclei densely stained.
	521/13	> 90% marked +++ stained nuclei,	> 90% smooth muscle/stroma and endothelial nuclei densely stained.
	570/13	> 90% marked +++ stained nuclei,	> 90% smooth muscle/stroma and endothelial nuclei densely stained.

Table 8.7 Assessment for IHC staining intensity of DNA repair enzymes

The full data corresponding section 4.6. A trained pathologist assessed the staining intensity, grading on a four-tier system; -, +, ++, +++ with more "+" symbols indicating a higher staining intensity and "–" indicating no expression. The stroma was used as an internal positive control. All staining and scoring was carried on CRLM tissue taken directly from the patient and represent the same ten patients used for explant culture.